A Theoretical Analysis of the Spin Susceptibility Tensor and Quasiparticle Density of States for Quasi-one-dimensional Superconductors

A Thesis
Presented to
The Academic Faculty

by

Cawley D. Vaccarella

In Partial Fulfillment
of the Requirements for the Degree of
Doctor of Philosophy in Physics

Georgia Institute of Technology
November 2001

A Theoretical Analysis of the Spin Susceptibility Tensor and Quasiparticle Density of States for Quasi-one-dimensional Superconductors

Approved:

Carlos A. R. Sá de Melo, Chairman

Helmut J. Biritz

Walter A. de Heer

Mei-Xin Chan

Thomas Money
(G.I.T. Department of Mathematics)

Date Approved 11/15/01

to my Mother Brigitte

for her Faith and Support

in All my endeavors

I am indebted to my advisor Carlos Sá de Melo for the time spent in discussion of the many topics and ideas that needed to come together in order to make this a successful research. I would like to express thanks to Richard Duncan for his help on the numerical portion of this thesis. I would also like to thank Robert Cherng for his collaboration on the analysis of the critical frequencies of the density of states and spin susceptibility and his contribution in obtaining the energy gap.

Contents

List of Figures

SUMMARY

There is experimental evidence that the order parameter in $(TMTSF)_2X$ is of a gapped triplet variety. To aid in the experimental investigation of the possible gapped nature of the order parameter, the quasiparticle density of states (DOS) has been calculated. The quasiparticle density of states could in principle be measured using photoemission or STM. Since the DOS depends on the order parameter through the excitation energy, then an observed gap in the quasiparticle density of states at would reveal a gap in the excitation spectrum of the quasiparticles and implies that the order parameter of the system is itself gapped. On the other hand, should the measured DOS have no gap this would indicate that the order parameter has nodes on the Fermi surface. The low frequency dependence of the DOS has been calculated. The low frequency behavior of the DOS depends on the node structure of the order parameter and measurement of the low frequency dependence could be used to reveal the node structure of the order parameter. For a triplet superconductor, there is an associated order parameter vector which controls the behavior of tensor quantities such as the electron spin susceptibility tensor. Measurement of the electron spin susceptibility can be used to determine the direction of this vector in the crystalline lattice. In this case the uniform dynamical electron spin susceptibility tensor has been calculated for selected symmetries corresponding to the P-wave state.

Chapter I

Introduction

Both experimental and theoretical efforts in the search for triplet superconductivity have intensified since the discovery of superfluidity in liquid ^{3}He in the early 1970's. Although such materials as heavy fermion, organic, and oxide superconductors have been looked at as candidates for triplet superconductors, the focus here is on the Bechgaard Salt family of organic superconductors (*bitetramethyltetraselenafulvalene*) or $(TMTSF)_2X$, $X = [PF_6, ClO_4...]$.

The recent developments discussed in this section regarding the Bechgaard Salts were made after 1996. Before discussing any of these results the chief differences between $(TMTSF)_2X$ and liquid ^{3}He will be noted: $(TMTSF)_2X$ consists of charged fermions interacting on a lattice while liquid ^{3}He is a fluid consisting of neutral fermionic ^{3}He-atoms. In particular the way in which the high anisotropy of the lattice influences the superconducting state will be examined.

The introduction will proceed as follows: 1) some general background will be given about the Bechgaard Salts, 2) some of the experimental evidence supporting $(TMTSF)_2X$ as a candidate triplet superconductor will be discussed.

1.1 Background

The discovery of the first organic superconductor bitetramethyltetraselenafulvalene hexafluorophosphate $(TMTSF)_2PF_6$ in 1980 has lead to the search for superconductivity in other quasi-one-dimensional Bechgaard Salts $(TMTSF)_2X$ $[X = PF_6, ClO_4, ...]$.

This search lead to the discovery and investigation of metallic phases and spin density wave phases in addition to superconducting phases in these materials. The appearance of these phases depends on temperature, pressure, magnetic field and anion ordering.

The origin of many of these features can be ascribed to the extreme anisotropy of the crystal lattice which results from the weak coupling between the chain-like structures comprising the lattice. These chains of $(TMTSF)_2X$ can be thought of as runnig along the $\hat{\mathbf{a}}$-axis (i.e., the direction of highest electronic conductivity): The $(TMTSF)_2X$

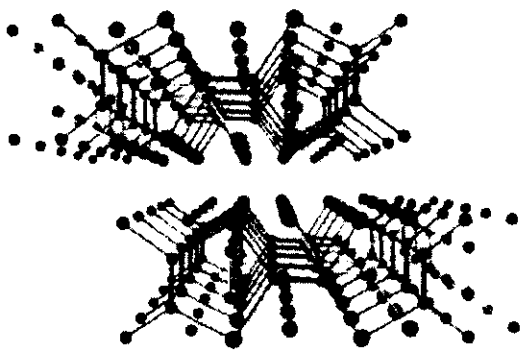

Figure 1: View of the crystal structure of $(TMTSF)_2ClO_4$ along the direction of highest conductivity ($\hat{\mathbf{a}}$-axis).

molecules stack along the $\hat{\mathbf{a}}$-axis (or x-axis) which is the direction of highest electronic conductivity. The $\hat{\mathbf{b}}'$-axis (y-axis) runs in the horizontal direction (across the figure) so that the molecules form sheets lying in the xy-plane [1]. The $\hat{\mathbf{c}}^*$-axis (z-axis) runs vertically (up and down the figure) and cuts through the $(TMTSF)_2X$-planes. The $\hat{\mathbf{c}}^*$-axis is the direction corresponding to smallest electronic conductivity so that for the electronic conductivities and transfer energies: $\sigma_x \gg \sigma_y \gg \sigma_z$ & $|t_x| \gg |t_y| \gg |t_z|$. Furthermore, the $(TMTSF)_2X$ molecules lying in the xy-plane are separated by anions lying in the z-axis.

The family of compounds comprising the Bechgaard Salt family, $(TMTSF)_2X$, is isostructural. They share a triclinic structure having similar lattice parameters and angles. Some typical values characterizing the lattice are: $a = 7.297\text{Å}, b' = 7.711\text{Å}, c^* = 13.522\text{Å}, \alpha = 83.39°, \beta = 86.27°, \gamma = 71.01°$:

The Selenium orbitals are principlely responsible for providing the conduction path-

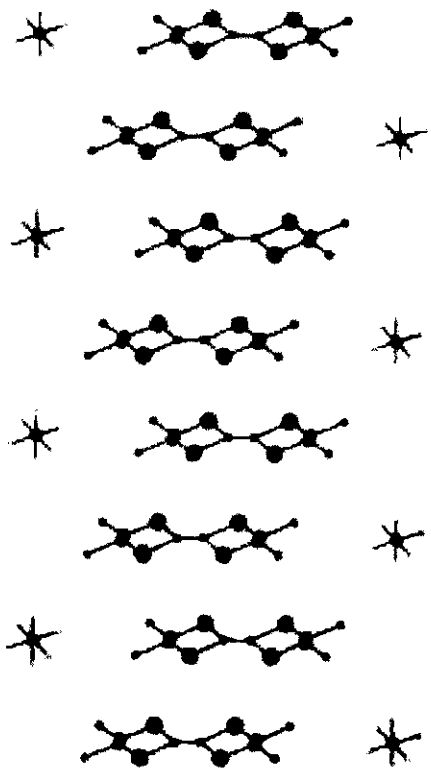

Figure 2: Diagram of the crystal structure of $(TMTSF)_2PF_6$ showing the principle directions $\hat{\mathbf{a}}$, $\hat{\mathbf{b}}'$ and $\hat{\mathbf{c}}^*$.

ways for the charge carriers in $(TMTSF)_2X$. Although the spacing between neighboring Se-atoms is comparable within the $\hat{\mathbf{a}} - \hat{\mathbf{b}}'$-plane, the overlap of Se-orbitals is greatest along the $\hat{\mathbf{a}}$-direction accounting for the anisotropy in the electronic transfer energies. These energies have estimated values on the order of 5800K, 1226K, 48K.

As a consequence of this anisotropy the electronic spectrum is quasi-one-dimensional.

The crystal energy dispersion is taken approximately to be:

$$\xi(\mathbf{k}) = t_x \cos(k_x a) + t_y \cos(k_y b) + t_z \cos(k_z c) - \mu, \tag{1}$$

where $\xi(\mathbf{k}) = \epsilon(\mathbf{k}) - \mu$ is referenced to the chemical potential $\mu \approx 5800K/\sqrt{2}$ (this value corresponds to quarter filling). In the later sections on the quasiparticle density of states and the uniform susceptibility it will become clear that the predominance of contributions to the aforementioned quantities comes from momentum states very near the Fermi Surface $\epsilon(\mathbf{k}) = \mu$. In view of this and the fact that $(TMTSF)_2X$ is quasi-one-dimensional owing to the high anisotropy in the transfer energies $|t_x| \gg |t_y| \gg |t_z|$, the Fermi Surface is no longer simply connected, but instead consists of two sheets that are centered on the Fermi wave vector in the x-direction and run over the full Brillouin zone in y and z

1.2 Recent Experiments on Quasi-one-dimensional Superconductors

This section describes three important experiments that were performed after 1997, which set the basis for unconventional superconductivity, most likely triplet, in quasi-one-dimensional superconductors of the Bechgaard salt family. Measurements of the upper critical field in $(TMTSF)_2PF_6$ performed by Lee *et. al.* [2] and the possible connections to triplet superconductivity are discussed. Then, the experimental work of Belin and Behnia (BB) [3]on the thermal conductivity of $(TMTSF)_2ClO_4$ is reviewed. Lastly, a review is made of the Knight shift experiments by Lee *et. al.* [4] in $(TMTSF)_2PF_6$. The analysis of these three experiments provides a picture of the unconventional nature of the quasi-one-dimensional organic superconductors of the Bechgaard salt family,$(TMTSF)_2X$.

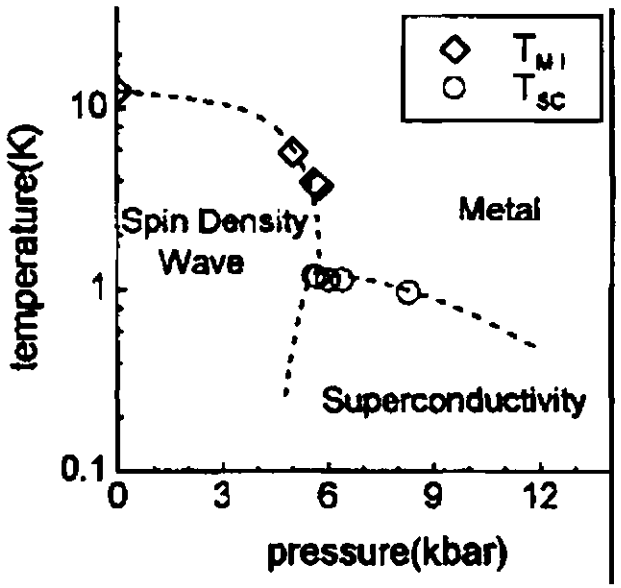

Figure 3: The temperature versus pressure phase diagram for $(TMTSF)_2PF_6$. Notice the proximity of the superconducting phase to the spin density wave (SDW) insulating phase.

1.2.1 Anisotropy of the Upper Critical Field in $(TMTSF)_2PF_6$

First the paper by Lee *et. al.* [2] where the upper critical field of the quasi-one-dimensional superconductor $(TMSTF)_2PF_6$ at pressure $P = 6.0$ kbar is reviewed. This pressure is large enough to suppress the nearby spin density wave phase (see phase diagram in Fig. 3) . From resistance measurements, Lee *et. al.* [2] extract the critical temperature as a function of magnetic field $T_c(H)$, for magnetic field aligned precisely with the three principle directions $\hat{\mathbf{a}}$, $\hat{\mathbf{b}}'$ and $\hat{\mathbf{c}}^*$. The data was collected for fields up to 6 T and temperatures down to 0.1 K.

Three new featureswere observed at low temperatures (see Fig. 4, p. 6). First, the upper critical field displays pronounced upward curvature without saturation for $\mathbf{H} \parallel \hat{\mathbf{a}}$ and $\mathbf{H} \parallel \hat{\mathbf{b}}'$; second, $H_{c_2}^{b'}$ becomes larger than $H_{c_2}^{a}$ at low temperatures; third, both $H_{c_2}^{a}$

and $H_{c_2}^{b'}$ exceed the Pauli paramagnetic limit, (i.e., the theoretical limit imposed by the paramagnetic effect of the applied magnetic field on the electronic spin susceptibility [5, 6]). pressure phase diagram (see Fig. 3). This experimental evidence combined points in the direction of unconventional pairing in quasi-one-dimensional superconductors. The upper critical field along these directions exceeds the Pauli paramagnetic

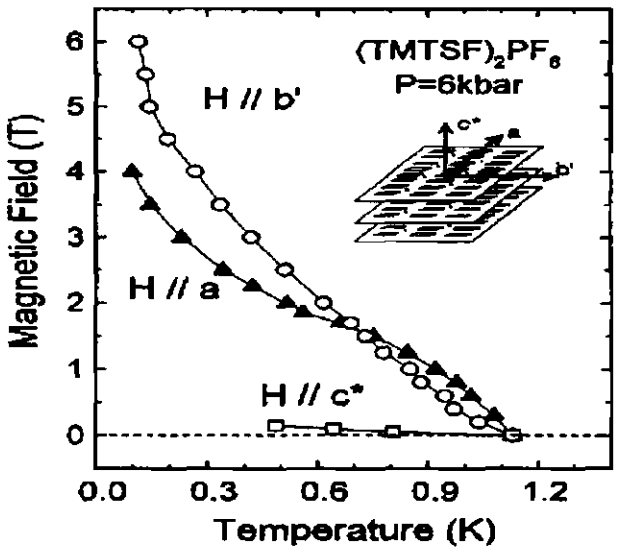

Figure 4: The magnetic field versus temperature ($H - T$) phase diagram for $(TMTSF)_2PF_6$ using the junction criterion for magnetic fields aligned along the three principle axis $\hat{\mathbf{a}}$, $\hat{\mathbf{b}}'$, and $\hat{\mathbf{c}}^*$.

limit for this compound by a factor of 2, at least. This paramagnetic limit (also known as the Clogston-Chandrasekhar limit [5, 6]) is given by $2\mu_B H_P(T=0) = 1.84 k_B T_c(0)$ (i.e., the zero temperature paramagnetic limiting field equals 1.84 $\times$ the zero field critical temperature) for an isotropic S wave system in the absence of spin-orbit scattering, or by $2\mu_B H_P(T=0) = 1.58 k_B T_c(0)$ for an anisotropic singlet pairing [7]. In the case of $(TMSTF)_2PF_6$ these estimates correspond to 2.1 T and 1.8 T. At low temperatures, however, it was observed that $H_{c_2}^{b'} > 3H_P$.

The other unusual feature is the anisotropy inversion that occurs above the characteristic field $H^* \approx 1.6\mathsf{T}$, where $H_{c_2}^{b'}$ becomes larger than $H_{c_2}^{a}$ above the characteristic field H^*. Lee *et. al.* extracted the phase diagram in Fig. 4 from measurement of the sample resistance vs. temperature for various applied magnetic fields (see Fig. 5). They defined five temperature criteria to extract the critical temperature as a function of magnetic field. These criteria are defined as follows: (a) an onset T_O, (b) a "junction" T_J, (c) a midpoint T_M, (d) a zero resistance extrapolation T_X (where the tail near $R = 0$ is ignored), and (e) a zero resistance point T_Z. Using this approach, they were able to connect the resulting curves $T_i(H)$ (for each criteria) with the physical upper critical field $H_{c_2}(T)$.

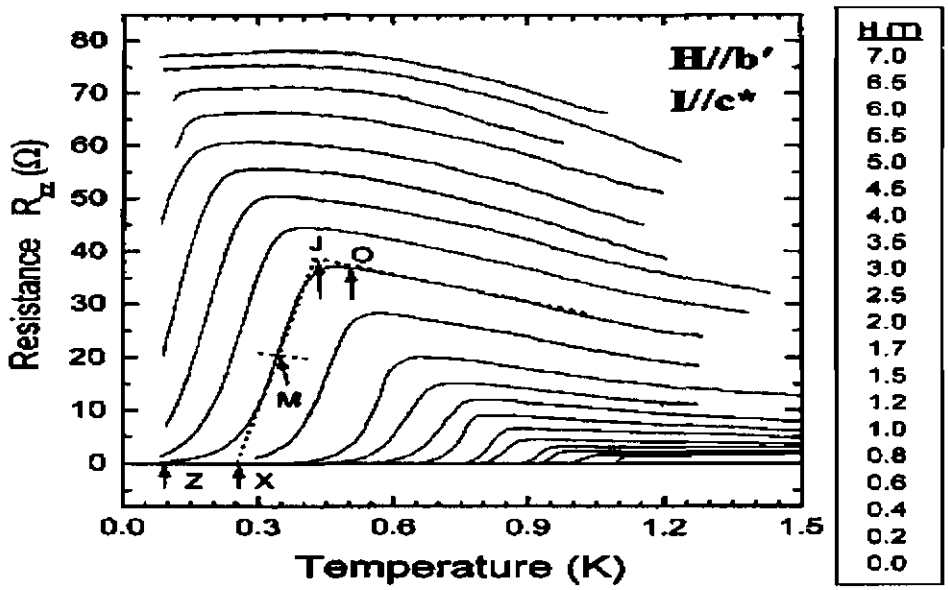

Figure 5: $(\mathsf{TMSTF})_2\mathsf{PF}_6$ interlayer resistance versus temperature for various magnetic fields $\mathbf{H} \parallel \hat{\mathbf{b}}'$ at $P = 6$ kbar. Five different criteria for the putative critical temperature $T_c(H)$ are indicated: O (onset), J (junction), M (midpoint), X ($R \to 0$), and Z ($R = 0$).

In Fig. 6 the anisotropy inversion is shown in detail under four different criteria

(T_0, T_J, T_M and T_X). Lee *et. al.* [2] had fewer data points for the $R = 0$ (T_Z) criterion, however they found that the anisotropy inversion still occurs at $T \approx 0.35$K. Notice in Fig. 6 that the data sets look very similar. The shift of the anisotropy inversion temperature is due to the width of the superconducting transition, however the anisotopry inversion field $H^* \approx 1.6$ T is largely insensitive to the criterion used. Furthermore, the superconducting state was more resilient for fields along $\hat{\mathbf{b}}'$ than along $\hat{\mathbf{a}}$, which suggested that the quasi-one-dimensional nature of the system was very important.

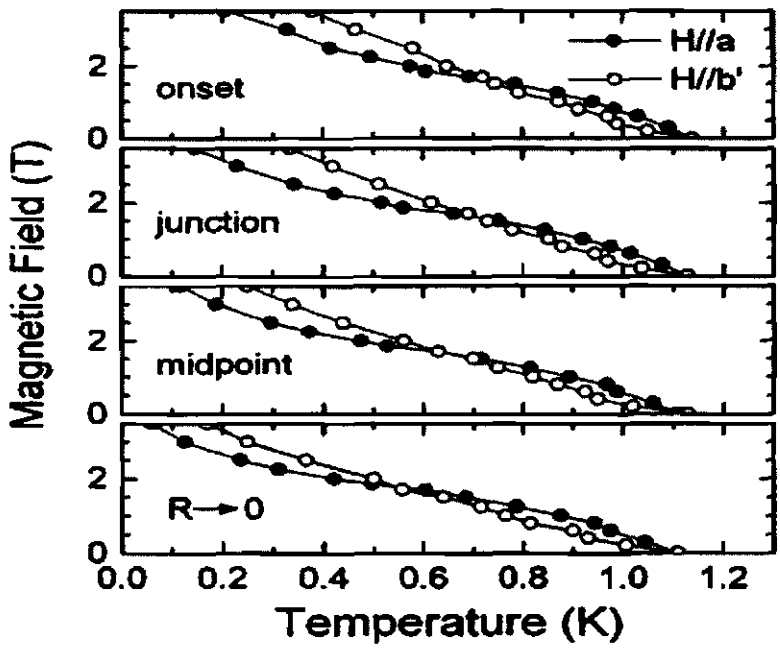

Figure 6: This figure shows the anisotropy inversion for $\mathbf{H}\|\hat{\mathbf{a}}$ and $\mathbf{H}\|\hat{\mathbf{b}}'$ for four different resistance criteria: onset, junction, midpoint and $R \to 0$.

Lee *et. al.* [2] have pointed out that several theoretical investigations concerning low-dimensional superconductors needed to be checked for consistency with their experimental data. They have checked their data against the ideas of Efetov and Larkin [8], who pointed out that superconductivity in quasi-one-dimensional systems

could survive in large magnetic fields, provided that electrons, in different chains, formed pairs in the triplet channel. It was also suggested by Abrikosov [9, 10] that the early observations of the upper critical fields of Bechgaard salts could be made consistent with triplet pairing, given that the critical temperature of these systems was strongly suppressed in the presence of non-magnetic disorder (impurities). Later, Lebed [11, 12] and Dupuis, Montambaux, and Sá de Melo [13] (DMS) have suggested a remarkable magnetic field induced reentrant phase in quasi-one-dimensional superconductors. This remarkable reentrance was not observed in the experiments of Lee *et. al.* [2], however many of the theoretical ideas put forth in the papers by Lebed [11, 12] and DMS [13] seem to be applicable to the experimental situation described here. For instance, the idea that there is a dimensional crossover that confines the electronic motion along $\hat{\mathbf{c}}^*$, when the magnetic field is applied along $\hat{\mathbf{b}}'$ leads to the suppression of the orbital frustration-induced pair breaking. In theory, there could also be a series of spectacular first order phase transitions separating different superconducting phases as the magnetic field is increased [13]. These first order phase transitions were not observed in the work by Lee *et. al.* [2]. However, in the scenario proposed by Lebed and DMS, the upper critical field would exceed the Pauli paramagnetic limit and show reentrant behavior for both singlet and triplet pairing. The reentrant behavior was predicted to be much more dramatic for the triplet case, but very sensitive to accurate alignment of the magnetic field with $\hat{\mathbf{b}}'$, as suggested by Lebed [11, 12] and DMS [13], and emphasized recently by Vaccarella and Sá de Melo [14], who calculated the angular dependence of the upper critical field in the field regime of the predicted reentrant phase.

One theory which remains consistent with most experimental facts discussed in Lee *et. al* [2] is that due to Lebed [11, 12] and DMS [13]. This theory predicts a *magnetic field-induced* dimensional crossover for $\mathbf{H} \parallel \hat{\mathbf{b}}'$. The interlayer motion δz is confined to $\pm z_0 t_z/\hbar\omega_c$, where z_0 is the layer spacing along $\hat{\mathbf{c}}^*$, t_z is the bandwidth along z,

and ω_c is the semiclassical Brillouin zone crossing frequency, $\omega_c = ez_0 v_F H/\hbar$. The dimensional crossover occurs when ω_c is comparable to t_z. Using a Fermi velocity $v_F = 2 \times 10^5$ m/s, interlayer spacing $z_0 = 1.3$ nm, and a bandwidth t_z between 5 K and 10 K [13], ω_c reaches t_z in a crossover field of 2 T to 4 T, the same magnitude as the anisotropy inversion field H^* shown in Fig. 4. At high magnetic fields, where $\omega_c \gg t_z$ and $\delta z \ll z_0$, the interlayer motion in inhibited. As a result, the orbital pair breaking effect is dramatically reduced and superconductivity survives at high magnetic fields.

1.2.2 Thermal Conductivity of Superconducting $(TMTSF)_2ClO_4$: Evidence for a Nodeless Gap

The experimental work of Belin and Behnia [3] (BB) on the thermal resistivity of superconducting $(TMTSF)_2ClO_4$ is discussed here. The main result of their work was that the electronic contribution to heat transport decreases rapidly below the critical temperature for superconductivity, thus indicating the absence of low-energy electronic excitations, (i.e., a nodeless gap).

Belin and Behnia measured both the electrical and the thermal conductivities of four $(TMTSF)_2ClO_4$ single crystals grown by standard electrochemical techniques. The sample size discussed by BB has dimensions $1.1 \times 0.23 \times 0.07 mm^3$.

In their paper [3] the observed temperature dependence of the thermal conductivity κ and of the electrical resistance R is shown at low temperatures. When the sample became superconducting they observed a sharp decrease in κ. More specifically, the sharp decrease occurred at $T \sim 1K$ which is coincident with the end of the resistive transition. This kink in $\kappa(T)$ disappears with the destruction of superconductivity under a small magnetic field along the $\hat{c}^*$-axis.

BB's goal was to observe the quasiparticle (electronic) component of the thermal conductivity. In general, the separation of lattice and quasiparticle components of thermal transport in superconductors is not a straightforward procedure, since the condensation of electrons in the superconducting state affects lattice contribution due to electron-phonon coupling. To gain insight on the effect of the superconducting instability on heat carriers, they analyzed the ratio $\Delta\kappa/T$ corresponding to the difference between the two experimental curves of κ/T (at $H = 0$ and $H = 5\mathsf{kOe}$), as a function of temperature. In BB's paper [3] a plot of $\Delta\kappa/T$ shows that it increases steadily with decreasing temperature before saturating at a temperature of about 0.4 K. This saturation was observed at the same temperature for all the samples studied in BB's work. The saturation value $(\Delta\kappa/T)|_{sat}$ was $3.7 \pm 0.4\mu\mathsf{WK}^{-2}$ in the sample studied. This value is very close to L_0/R_0 ($= 3.8 \pm 0.5\mu\mathsf{WK}^{-2}$, in the sample studied). The ratio L_0/R_0 is the expected maximum electronic contribution to heat transport according to the WF law.

BB argued that the saturation in $\Delta\kappa/T$ indicates the absence of low energy quasiparticle heat carriers. Neglecting the magnetoresistance (which was shown to be very small at $H = 5\mathsf{kOe}$ [3]) BB expressed $\Delta\kappa/T$ as

$$\frac{\Delta\kappa(T)}{T} = \left(\frac{\kappa^{\mathsf{n}}_{\mathsf{el}}(T)}{T} - \frac{\kappa^{\mathsf{s}}_{\mathsf{el}}(T)}{T}\right) + \left(\frac{\kappa^{\mathsf{n}}_{\mathsf{ph}}(T)}{T} - \frac{\kappa^{\mathsf{s}}_{\mathsf{ph}}(T)}{T}\right)$$

where subscripts $\{\mathsf{e}, \mathsf{ph}\}$ refer to electronic and lattice (phonon) components and superscripts $\{\mathsf{s}, \mathsf{n}\}$ refer to superconducting and normal states. A finite electron-phonon coupling typically leads to an *increase* in the lattice thermal conductivity in the superconducting state so that $\kappa^{\mathsf{n}}_{\mathsf{ph}}(T) \leq \kappa^{\mathsf{s}}_{\mathsf{ph}}(T)$ for the whole temperature range below T_c. This means that at finite temperature below T_c, $\Delta\kappa/T$ represents a lower bound to the difference between the electronic thermal conductivities of the normal and superconducting states. At zero temperature, however, this difference was observed to be equal to L_0/R_0. These two constraints allowed BB to extract the temperature dependence of the normalized electronic thermal conductivity $\kappa^{\mathsf{s}}_{\mathsf{el}}/\kappa^{\mathsf{n}}_{\mathsf{el}}$ from $\Delta\kappa/T$. The

experimental ratio of $\kappa^s_{el}/\kappa^n_{el}$ could then be compared with other experimental results (e.g., UPt_3), and with theoretical results for different gap symmetries.

BB considered two different scenarios for the temperature dependence of the thermal conductivity in the normal state, while neglecting the effect of electronic condensation on lattice thermal conductivity. In the first scenario they assumed a constant κ^n_{el}/T (equal to L_0/ρ_0). In the second scenario, they assumed that the thermal conductivity in the normal state followed the behavior imposed by the temperature dependence of electrical resistivity and the WF law (see [3]). The second scenario implies a difference of 27 percent in the geometric factor of the sample for electric and thermal transport. BB observed [3] that the normalized $\kappa^s_{el}/\kappa^n_{el}$ curves are not very different for the two possible scenarios. In addition, BB made a comparison [3] between data from $(TMTSF)_2ClO_4$ and the data from the unconventional superconductor UPt_3 [15]. A plot of these two curves [3] reveals that the decrease in $\kappa^s_{el}/\kappa^n_{el}$ is much faster in $(TMTSF)_2ClO_4$ than in UPt_3. The main conclusion from BB's work is clear: their data cannot be made consistent with a gap function that has nodes on the Fermi surface. Their analysis and their conclusion are a direct consequence of the apparent saturation of the quantity $\Delta\kappa/T$ [3], and are quite robust. In summary, Belin and Behnia [3] measured the thermal conductivity of $(TMTSF)_2ClO_4$ in the superconducting and metallic states, and concluded that their results were incompatible with the presence of nodes in the order parameter function.

The combined studies of the upper critical fields in $(TMTSF)_2PF_6$ [2] (discussed in section §1.2.1) and the thermal conductivity measurements of $(TMTSF)_2ClO_4$ discussed in this section suggest a fully gapped triplet state in the Bechgaard salts family $(TMTSF)_2X$.

1.2.3 Evidence for Triplet Superconductivity in $(TMSTF)_2PF_6$ from ^{77}Se Knight Shifts

This section briefly reviews some of the work of Lee *et. al.* [4], where ^{77}Se Knight shifts (K) and resistivity were measured simultaneously in $(TMTSF)_2PF_6$ under pressure. These experiments were performed with the goal of clarifying the ground state symmetry of this material. Knight shift experiments are the next natural candidate experiment to get detailed information about the order parameter symmetry of the superconducting state. The Knight shift is linearly proportional to the electron spin susceptibility, and is a direct measure of the spin polarization of the superconducting state. In the case of a singlet superconductor it is expected that the spin contribution K_s to the Knight shift is strongly suppressed at low temperatures below the superconducting transition temperature. This is particularly true when the measurements are performed at very low magnetic fields. However, the experiments of Lee *et. al.* indicated that there was no observable change in the Knight shift between the metallic and superconducting states of $(TMTSF)_2ClO_4$. Thus, their observation supports the hypothesis of triplet P wave superconductivity in this material.

In very small magnetic fields, a singlet superconducting ground state leads to a vanishing of the spin contribution, K_s, to the total K as $T \to 0$. The expected shifts for ^{77}Se are in the range 340-480 ppm for cooling from the normal phase to a singlet superconducting phase. However, Lee *et. al.* [4] concluded from their measured spectra that no change was observed ($\delta K_s = 0 \pm 20$ppm). To ensure that the pressurized sample was superconducting while acquiring the NMR data, they conducted transport measurements in parallel (synchronization) with the application of the radio-frequency pulses.

The observed NMR spectra were measured at temperatures above and below T_c. , Lee *et. al.* found no shift in the first moment to within the experimental error bars. The lack of any observable difference between the spectra as the temperature was

varied indicated that the system is not a singlet superconductor.

1.3 Summary

There is strong experimental evidence that the order parameter in $(TMTSF)_2X$ is of the triplet variety. This evidence includes work by Lee *et. al.* [2],[4] and Belin & Behnia [3]. First Lee *et. al.* measured the H vs. T phase diagram and observed that for $H\|\hat{\mathbf{a}}$ that the field exceeds the Pauli paramagnetic limit by factors of 2 and 3.

Further work done by Belin & Behnia [3] measured the thermal conductivity of $(TMTSF)_2ClO_4$ in the normal and superconducting states. Belin & Behnia's data show that as $T \to 0$, $\kappa_{el}^{s}(T)/\kappa_{el}^{n}(T) \to 0$. The apparent exponential dependence of the electron thermal conductivity with decreasing temperature in the superconducting state implies a gap in the response and a gapped symmetry for the order parameter.

The last experiment which supports $(TMTSF)_2X$ as a candidate for triplet superconductivity was a Knight shift measurement done by Lee *et. al.* [4]. The Knight shift measures the electron spin response of the system to applied field. For singlet spin pairing, the spin response is gapped and is diminished with decreasing temperature such that at low temperature $\chi(T) = \chi_0\, e^{-\beta\Delta_0}$.

For triplet spin pairing, the spin response is constant for special field directions, independent of temperature, and equal to the normal value $\chi(T) = \chi_N$. This is what is observed by Lee *et. al.* [4] for $H\|\hat{\mathbf{a}}$ where $\chi = \chi_N$. The measurement for $H\|\hat{\mathbf{b}}'$ gives results similar to the $H\|\hat{\mathbf{a}}$-measurement [4]. The measurement for $H\|\hat{\mathbf{c}}^*$ cannot be done since the magnitude of the applied field H necessary to perform the NMR experiment exceeds the upper critical field in that direction $H > H_{c_2}^{c^*}$.

These three experiments taken together point very strongly toward a gapped triplet

order parameter.

Chapter II

Background and Motivation for the Description of Cooper Pairs

2.1 Cooper Pairing

In order to study Cooper pairing on an introductory level in $(TMTSF)_2X$ it is beneficial to study the quantum mechanical problem of two-body bound pairs in a lattice. In this treatment a pair of electrons is added to the Fermi sea at $T = 0$. These electrons interact very weakly with each other and only interact with the other electron in the Fermi Sea under the Pauli exclusion principle [16].

The basic idea (due to Cooper [17]) is that even for a very weakly attractive interaction that the ground state of the Fermi sea of electrons is unstable against the formation of at least one bound pair. This will be demonstrated in the following by showing that the binding energy Δ of the pair is negative. As such the two body Schroedinger Equation is solved with central potential.

$$-\frac{\hbar^2}{2m}(\nabla_1^2 + \nabla_2^2)\Psi + V(\mathbf{r}_1 - \mathbf{r}_2)\Psi = (\Delta + 2\epsilon_F)\Psi. \tag{2}$$

Here the $2\epsilon_F$ term is the free particle energy for two unbound electrons at the Fermi surface in a degenerate electron gas. From above if the electrons are to be bound in a pair then, it must be that $\Delta < 0$ so that the bound pair has lower energy than the free electrons.

Solution of this equation can be simplified by transforming the problem first to the

center of mass coordinate frame:

$$-\frac{\hbar^2}{m}(\nabla_{\mathbf{r}}^2)\Psi + V(\mathbf{r})\Psi = (\Delta + 2\epsilon_F)\Psi$$

and then to the momentum representation:

$$\Psi(\mathbf{r}) = \frac{V_0}{(2\pi)^3}\int d^3k\, e^{i\mathbf{k}\cdot\mathbf{r}} g(\mathbf{k}).$$

The resulting integral equation is then multiplied by $e^{-i\mathbf{k}'\cdot\mathbf{r}}$ and integrated over real space:

$$\int d^3k d^3r \left[\frac{\hbar^2}{m}k^2 - 2\epsilon_F - \Delta\right] e^{i(\mathbf{k}-\mathbf{k}')\cdot\mathbf{r}} g(\mathbf{k}) + \int d^3k\, d^3r\, e^{i(\mathbf{k}-\mathbf{k}')\cdot\mathbf{r}} V(\mathbf{r}) g(\mathbf{k}) = 0. \quad (3)$$

Using the definition of the Fourier Transform

$$V(\mathbf{k}) = \frac{1}{V}\int d^3r\, e^{-i\mathbf{k}\cdot\mathbf{r}}\, V(\mathbf{r})$$

where V is the volume of the sample (and then switching dummy variables) one obtains:

$$(2\pi)^3\left[\frac{\hbar^2}{m}k^2 - 2\epsilon_F - \Delta\right] g(\mathbf{k}) + V\int d^3k' V(\mathbf{k}-\mathbf{k}') g(\mathbf{k}') = 0. \quad (4)$$

Next a model for the pair interaction is constructed. The potential is attractive in the vicinity of the Fermi surface (where the pair resides) and zero everywhere else. It is also assumed that the potential can be expanded with respect to a suitable basis in the lattice.

$$V(\mathbf{k}-\mathbf{k}') = V_{\mathsf{FS}}(\mathbf{k},\mathbf{k}') \sum_{j=1}^{d_\Gamma} \gamma_j\, \psi_j^\Gamma(\mathbf{k}) \psi_j^\Gamma(\mathbf{k}')^* \quad (5)$$

$$\text{where} \quad V_{\mathsf{FS}}(\mathbf{k},\mathbf{k}') = \begin{cases} -V_{\mathsf{FS}} < 0, & k_F < k, k' < k_F + \delta k \\ \\ 0, & \text{otherwise} \end{cases}$$

$$\text{with} \quad \frac{V}{(2\pi)^3}\int d^3k\psi_j^\Gamma(\mathbf{k})^*\psi_l^\Gamma(\mathbf{k}) = \mathsf{N}_{\Gamma,j}\delta_{jl}$$

and where $\delta k \ll k_F$ is a small variation of the wave vector of the bound electron pair near the Fermi surface. d_Γ is the dimension of the span of $\{\psi_j^\Gamma(\mathbf{k})\}$ and Γ labels the irreducible representation to which the basis functions belong. $\mathsf{N}_{\Gamma,j}$ is the normalization of the basis functions. By expanding the pair wave function in the basis

$$g^\Gamma(\mathbf{k}) = \sum_{j=1}^{d_\Gamma} \eta_j\, \psi_j^\Gamma(\mathbf{k}) \tag{6}$$

one can simplify the expression for the Schrödinger Eq. 4:

$$0 = g^\Gamma(\mathbf{k}) + \frac{V_0}{(2\pi)^3\,[2\xi - \Delta]}\int d^3k' V(\mathbf{k}-\mathbf{k}')g^\Gamma(\mathbf{k}') \qquad \xi \doteq \frac{\hbar^2k^2}{2m} - \epsilon_F.$$

Remember that the interaction potential is nonvanishing only on the Fermi surface. Therefore the integral above is performed over a thin shell region on the Fermi surface denoted by (FS).

$$0 = g^\Gamma(\mathbf{k}) - \frac{V_{\mathsf{FS}}}{[2\xi - \Delta]}\sum_{j=1}^{d_\Gamma}\mathsf{K}_j^\Gamma(\mathsf{FS})\psi_j^\Gamma(\mathbf{k}) \tag{7}$$

$$\text{where}\mathsf{K}_j^\Gamma(\mathsf{FS}) = \gamma_j\frac{V_0}{(2\pi)^3}\int_{\mathsf{FS}} d^3k\,\psi_j^\Gamma(\mathbf{k})^* g^\Gamma(\mathbf{k}).$$

$g^\Gamma(\mathbf{k})$ corresponds to the orbital piece of the pair wave function, $\psi_j^\Gamma(\mathbf{k})$ is the j^{th} basis function, V_{FS} is the interaction strength, ξ is the energy of motion for one of the members of the pair referenced to the Fermi energy ϵ_F, $\mathsf{K}_j^\Gamma(\mathsf{FS})$ is some constant and Δ is the binding energy we seek. Utilizing the expansion of $g^\Gamma(\mathbf{k})$ in the $\{\psi_j^\Gamma(\mathbf{k})\}$ basis one can simplify the expression further:

$$0 = \eta_j - \frac{V_{\mathsf{FS}}}{[2\xi - \Delta_j]}\mathsf{K}_j^\Gamma(\mathsf{FS}) \tag{8}$$

Each of the particles in the pair have an energy ϵ on the Fermi surface between ϵ_F and $\epsilon_F + \epsilon_l$ (or $0 < \xi < \epsilon_l$). Integrating the expression above over the allow range,

one may isolate the binding energy:

$$1 = \frac{1}{2}\ln\left(\frac{\Delta_j - 2\epsilon_l}{\Delta_j}\right)\frac{\mathsf{K}_j^\Gamma(\mathsf{FS})}{\eta_j}\frac{V_{\mathsf{FS}}}{\epsilon_l}. \tag{9}$$

$$\Delta_j = -2\epsilon_l \frac{1}{\exp\{2[\eta_j/\mathsf{K}_j^\Gamma(\mathsf{FS})]\cdot[\epsilon_l/V_{\mathsf{FS}}]\} - 1}$$

2.2 Spin Structure of Paired States

It was already shown that the pair Hamiltonian has solutions $g^\Gamma(\mathbf{k})$ that can be expanded in the basis $\{\psi_j^\Gamma(\mathbf{k})\}_{j=1}^{d_\Gamma}$. This basis forms a orthogonal set of solutions to the Schrödinger equation and reflects the symmetry of the lattice Γ. The solution $g^\Gamma(\mathbf{k})$ represents the orbital piece of the pair wave function. If we now include the spin component, the general state of a single pair is

$$\Psi_{\mathsf{pair}}(\mathbf{k}, \sigma_1, \sigma_2) = g^\Gamma(\mathbf{k})\chi(\sigma_1\sigma_2).$$

The two particle spinor $\chi(\sigma_1\sigma_2)$ expresses the spin of the pair as a function of the spin coordinates of the individual particles.

$\Psi_j^\Gamma(\mathbf{k}, \sigma_1, \sigma_2)$ is a Fermion wave function for a bound pair of electrons. It is therefore antisymmetric. For pairing in the spin triplet channel, the spinor $\chi(\sigma_1\sigma_2)$ $[= \chi(\sigma_2\,\sigma_1)]$ is even and consequently $g^\Gamma(\mathbf{k})$ is odd in the momentum index $[g^\Gamma(-\mathbf{k}) = -g^\Gamma(\mathbf{k})]$. The odd parity orbital component is customarily labeled by $\Gamma = \Gamma_u$ [19].

For pairing in the spin singlet channel, the spinor $\chi(\sigma_1\sigma_2)$ $[= -\chi(\sigma_2\,\sigma_1)]$ is odd and consequently $g^\Gamma(\mathbf{k})$ is even in the momentum index $[g^\Gamma(-\mathbf{k}) = g^\Gamma(\mathbf{k})]$. The even parity orbital component is customarily labeled by $\Gamma = \Gamma_g$ [19].

2.2.1 Triplet Pairing

Now consider the case of triplet spin pairing first. For this state we can have a mixture of spin pairing in the three different spin channels:

$$\widehat{\Delta}^{\Gamma}(\mathbf{k}) = g_1^{\Gamma}(\mathbf{k})|\uparrow\uparrow\rangle + g_2^{\Gamma}(\mathbf{k})(|\uparrow\downarrow\rangle + |\downarrow\uparrow\rangle) + g_3^{\Gamma}(\mathbf{k})|\downarrow\downarrow\rangle.$$

In this case the pair wave function is a linear superposition of states that each satisfy the Schrödinger equation separately. This solution can be cast in a more compact form by associating each of the four above kets with an entry in a 2×2 matrix:

$$|\uparrow\uparrow\rangle \Longleftrightarrow \begin{pmatrix} 1 & 0 \\ 0 & 0 \end{pmatrix} \quad |\uparrow\downarrow\rangle \Longleftrightarrow \begin{pmatrix} 0 & 1 \\ 0 & 0 \end{pmatrix} \quad |\downarrow\uparrow\rangle \Longleftrightarrow \begin{pmatrix} 0 & 0 \\ 1 & 0 \end{pmatrix} \quad |\downarrow\downarrow\rangle \Longleftrightarrow \begin{pmatrix} 0 & 0 \\ 0 & 1 \end{pmatrix}.$$

Then the triplet wave function can be represented as the matrix:

$$\widehat{\Delta}^{\Gamma}(\mathbf{k}) = \begin{pmatrix} g_1^{\Gamma}(\mathbf{k}) & g_2^{\Gamma}(\mathbf{k}) \\ g_2^{\Gamma}(\mathbf{k}) & g_3^{\Gamma}(\mathbf{k}) \end{pmatrix}.$$

Very plainly these are three orbital wave functions $g_n^{\Gamma}(\mathbf{k})$ written into the entries of an associated matrix. The importance of casting the wave function into this form will become clear later on when the excitation energy is obtained from the Hamilitonian for the many body case. In that case it will be seen that the order parameter $\Delta^{\Gamma}(\mathbf{k})$ will have the same symmetry properties in the indices as our 2-body bound pair wave function.

We can make a connection with the traditional Pauli spin matrices by writing each of the matrices associated with a ket, above, in terms of the Pauli matrices and factoring out $i\boldsymbol{\sigma}_2$ to the right yielding:

$$\widehat{\Delta}^{\Gamma}(\mathbf{k}) = \Delta_{\mathbf{0}} \left(d_1^{\Gamma}(\mathbf{k})\boldsymbol{\sigma}_1 + d_2^{\Gamma}(\mathbf{k})\boldsymbol{\sigma}_2 + d_3^{\Gamma}(\mathbf{k})\boldsymbol{\sigma}_3 \right) i\boldsymbol{\sigma}_{\hat{2}} = i\Delta_{\mathbf{0}} \left(\vec{\boldsymbol{\sigma}}\, \boldsymbol{\sigma}_{\hat{2}} \right) \cdot \mathbf{d}(\mathbf{k}) \qquad (10)$$

where the old and new orbital pieces are related by

$$g_1^\Gamma(\mathbf{k}) = \Delta_0[-d_1^\Gamma(\mathbf{k}) + id_2^\Gamma(\mathbf{k})]$$
$$g_2^\Gamma(\mathbf{k}) = \Delta_0 \quad d_3^\Gamma(\mathbf{k})$$
$$g_3^\Gamma(\mathbf{k}) = \Delta_0[\quad d_1^\Gamma(\mathbf{k}) + id_2^\Gamma(\mathbf{k})].$$

Here the $d_\alpha^\Gamma(\mathbf{k})$ contain the orbital information associated with the α-direction of the lattice and have the symmetry of the lattice Γ. $\mathbf{d}^\Gamma(\mathbf{k})$ corresponds to the orbital component of the pair wave function for pairing in the triplet channel. It is a 3-D vector whose components are constructed from the $g_n^\Gamma(\mathbf{k})$-orbitals. The $g_n^\Gamma(\mathbf{k})$-orbitals are themselves solutions to the Schrödinger equation and correspond to the three possible spin triplet pairing states. Δ_0 is a number containing amplitude information from the $g_n^\Gamma(\mathbf{k})$-orbitals (e.g., it may carry temperature dependent information) so that $\mathbf{d}^\Gamma(\mathbf{k})$ then contains just directional information plus orbital information (through its $\mathbf{k}$-dependence).

Eq. 10 is called the order parameter of the system and from its structure it is clear that the orientation of $\mathbf{d}^\Gamma(\mathbf{k})$ (also referred to as the order parameter) is intimately related to the spin components of the paired electrons (where the Pauli matrices contain the spin information). Clearly the order parameter is a matrix. It will be seen later that quantities like the tensor electron spin susceptibility have comonents that are related to the components of Eq. 10. Although, the precise relationship between the components of these quantities will be delineated in a later section, the tensor susceptibility can be probed by experiment to determine the orientation of vector order parameter $\mathbf{d}^\Gamma(\mathbf{k})$ relative to crystal lattice directions in real space.

The expansion of the vector order parameter in the lattice basis functions takes the form:

$$\mathbf{d}^\Gamma(\mathbf{k}) = \sum_{j=1}^{d_\Gamma} \boldsymbol{\eta}_j^\Gamma \psi_j^\Gamma(\mathbf{k}), \quad \alpha = \{1,2,3\}. \tag{11}$$

The vector $\boldsymbol{\eta}_j^\Gamma$ can be associated with a superconducting order parameter. When this vector has finite components it is associated with the presence of Cooper pairing in the triplet channel.

One point of interest whose relevance will become clear later on is what happens when $\widehat{\Delta}^\Gamma(\mathbf{k})$ is regarded as being proportional to a unitary matrix:

$$\widehat{\Delta}^\Gamma(\mathbf{k}) = \Delta_0 \begin{pmatrix} -d_1^\Gamma(\mathbf{k}) + id_2^\Gamma(\mathbf{k}) & d_3^\Gamma(\mathbf{k}) \\ d_3^\Gamma(\mathbf{k}) & d_1^\Gamma(\mathbf{k}) + id_2^\Gamma(\mathbf{k}) \end{pmatrix}.$$

In this case $\widehat{\Delta}^\Gamma(\mathbf{k})\widehat{\Delta}^\Gamma(\mathbf{k})^\dagger \propto \widehat{\sigma}_0$:

$$\widehat{\Delta}^\Gamma(\mathbf{k})\widehat{\Delta}^\Gamma(\mathbf{k})^\dagger =$$

$$\begin{pmatrix} |\Delta_0 \mathbf{d}^\Gamma(\mathbf{k})|^2 & 2|\Delta_0|^2 \Im\left\{[d_1^\Gamma(\mathbf{k}) + id_2^\Gamma(\mathbf{k})]d_3^\Gamma(\mathbf{k})^*\right\} \\ 2|\Delta_0|^2 \Im\left\{[d_1^\Gamma(\mathbf{k}) + id_2^\Gamma(\mathbf{k})]d_3^\Gamma(\mathbf{k})^*\right\} & |\Delta_0 \mathbf{d}^\Gamma(\mathbf{k})|^2 \end{pmatrix}$$

$$= |\Delta_0 \mathbf{d}^\Gamma(\mathbf{k})|^2 \widehat{\sigma}_0 \tag{12}$$

We obtain a condition on the $\mathbf{d}-$vector that if $\widehat{\Delta}^\Gamma(\mathbf{k})$ is unitary then

$$\Im\left\{[d_1^\Gamma(\mathbf{k}) + id_2^\Gamma(\mathbf{k})]d_3^\Gamma(\mathbf{k})^*\right\} = 0. \tag{13}$$

For the purposes of this discussion the $\mathbf{d}-$vector will in general be real so that this condition is satisfied.

Note the relation between the trace of $\widehat{\Delta}^\Gamma(\mathbf{k})\widehat{\Delta}^\Gamma(\mathbf{k})^\dagger$ and the $\mathbf{d}-$vector:

$$\mathsf{Tr}\left[\widehat{\Delta}^\Gamma(\mathbf{k})\widehat{\Delta}^\Gamma(\mathbf{k})^\dagger\right] = 2|\Delta_0 \mathbf{d}^\Gamma(\mathbf{k})|^2.$$

Lastly, it is worth noting that the triplet pair wave function inherits the symmetry properties:

$$\Delta_{\alpha\beta}^\Gamma(-\mathbf{k}) = -\Delta_{\alpha\beta}^\Gamma(\mathbf{k}) \tag{14}$$

$$\Delta_{\alpha\beta}^\Gamma(\mathbf{k}) = \quad \Delta_{\beta\alpha}^\Gamma(\mathbf{k}) \tag{15}$$

where the first line reflects the odd parity of the orbital component of the triplet and the second line reflects the even parity of the spin component. More simply one may write:

$$\widehat{\Delta}^{t}(-\mathbf{k}) = -\widehat{\Delta}^{t}(\mathbf{k}) \tag{16}$$

where t here means transpose.

2.2.2 Singlet Pairing

The singlet pairing state is much easier to recast. The wave function in this case has the form:

$$\widehat{\Delta}^{\Gamma}(\mathbf{k}) = \Delta_0 g^{\Gamma}(\mathbf{k})(|\uparrow\downarrow\rangle - |\downarrow\uparrow\rangle).$$

Making the same associations of ket with matrix yields:

$$\widehat{\Delta}^{\Gamma}(\mathbf{k}) = \Delta_0\, g^{\Gamma}(\mathbf{k}) \begin{pmatrix} 0 & 1 \\ -1 & 0 \end{pmatrix} = i\Delta_0\, g^{\Gamma}(\mathbf{k})\, \widehat{\sigma}_2$$

where $i\,\boldsymbol{\sigma}_2$ reflects the explicit antisymmetry of the spin part of the singlet state. Here $g^{\Gamma}(\mathbf{k})$ has been put on the same footing as $\mathbf{d}(\mathbf{k})$ in that information such as temperature dependence is carried by Δ_0.

For singlet pairing the wave function inherits the symmetry properties:

$$\widehat{\Delta}^{\Gamma}_{\alpha\beta}(-\mathbf{k}) = \widehat{\Delta}^{\Gamma}_{\alpha\beta}(\mathbf{k}) \tag{17}$$

$$\widehat{\Delta}^{\Gamma}_{\alpha\beta}(\mathbf{k}) = -\widehat{\Delta}^{\Gamma}_{\beta\alpha}(\mathbf{k}) \tag{18}$$

where the first line reflects the even parity of the orbital component of the singlet and the second line reflects the odd parity of the spin component. More simply one may write:

$$\widehat{\Delta}^{t}(-\mathbf{k}) = -\widehat{\Delta}^{t}(\mathbf{k}). \tag{19}$$

2.3 The Energy of Quasiparticle Excitations

This section provides a brief derivation of the diagonalization of the many body Hamiltonian and quasiparticle excitation energy for particles in a lattice. A more detailed treatment can be found in appendix §A. This section introduces the concept of quasiparticles as electron-hole combinations and demonstrates how the magnitude of the order parameter modifies the quasiparticle excitation energy.

2.3.1 The Diagonalization of the Hamiltonian

The purpose of this section is to derive the expression for the excitation energy $E_{\mathbf{k}}$ by diagonalizing the Hamiltonian in the many body problem for a general 2-body interaction in a lattice. The process of diagonalization will lead to introduction of quasiparticles which are composite particles consisting of electrons and electron holes in the superconductor. The system Hamiltonian to be diagonlized is:

$$\widehat{H} = \sum_{\mathbf{k}\alpha} \xi_{\mathbf{k}} a^{\dagger}_{\mathbf{k}\alpha} a_{\mathbf{k}\alpha} + \frac{1}{2} \sum_{\mathbf{k}\mathbf{k}'} \sum_{\alpha\beta\mu\lambda} V_{\alpha\beta,\lambda\mu}(\mathbf{k},\mathbf{k}') a^{\dagger}_{-\mathbf{k}\alpha} a^{\dagger}_{\mathbf{k}\beta} a_{\mathbf{k}'\lambda} a_{-\mathbf{k}'\mu}.$$

Note this is the most general form of the Hamiltonian for a two body interaction where $V_{\alpha\beta,\lambda\mu}(\mathbf{k},\mathbf{k}')$ is some general spin and momentum dependent interaction. The interaction can be shown to have the symmetry properties:

$$V_{\alpha\beta,\lambda\mu}(\mathbf{k},\mathbf{k}') = -V_{\beta\alpha,\lambda\mu}(-\mathbf{k},\mathbf{k}') = -V_{\alpha\beta,\mu\lambda}(\mathbf{k},-\mathbf{k}') = V_{\beta\alpha,\mu\lambda}(-\mathbf{k}',-\mathbf{k}) = V^{*}_{\alpha\beta,\lambda\mu}(\mathbf{k}',\mathbf{k}). \quad (20)$$

We now consider diagnolizing the Hamiltonian in order to find the eigen-energies of the system. Consider that in its present form the the interaction term is quartic in the electron operators. This makes it very difficult to put $\widehat{H}$ into a suitable form for diagonalization. Nevertheless, $\widehat{H}$ can be put into diagonal form if one considers replacing the operator products $a^{\dagger}_{-\mathbf{k}\alpha} a^{\dagger}_{\mathbf{k}\beta}$ and $a_{\mathbf{k}'\lambda} a_{-\mathbf{k}'\mu}$ with their respective average values:

$$F^{\dagger}_{\alpha\beta}(\mathbf{k}) = \langle a^{\dagger}_{-\mathbf{k}\alpha} a^{\dagger}_{\mathbf{k}\beta} \rangle \quad \text{and} \quad F_{\lambda\mu}(\mathbf{k}') = \langle a_{\mathbf{k}'\lambda} a_{-\mathbf{k}'\mu} \rangle. \quad (21)$$

Now the Hamiltonian is quadratic and therefore factorable under a suitable change of basis. The operator products can then be rewritten in terms of these averages according to:

$$a^\dagger_{-\mathbf{k}\alpha}a^\dagger_{\mathbf{k}\beta} = F^\dagger_{\alpha\beta}(\mathbf{k}) + (\, a^\dagger_{-\mathbf{k}\alpha}a^\dagger_{\mathbf{k}\beta} - F^\dagger_{\alpha\beta}(\mathbf{k})\,)$$

$$a_{\mathbf{k}'\lambda}a_{-\mathbf{k}'\mu} = F_{\lambda\mu}(\mathbf{k}') + (\, a_{\mathbf{k}'\lambda}a_{-\mathbf{k}'\mu} - F_{\lambda\mu}(\mathbf{k}')\,)$$

$$\begin{aligned} a^\dagger_{-\mathbf{k}\alpha}a^\dagger_{\mathbf{k}\beta}a_{\mathbf{k}'\lambda}a_{-\mathbf{k}'\mu} = {} & F^\dagger_{\alpha\beta}(\mathbf{k})F_{\lambda\mu}(\mathbf{k}') \\ & + F^\dagger_{\alpha\beta}(\mathbf{k})(a_{\mathbf{k}'\lambda}a_{-\mathbf{k}'\mu} - F_{\lambda\mu}(\mathbf{k}')) \\ & + (a^\dagger_{-\mathbf{k}\alpha}a^\dagger_{\mathbf{k}\beta} - F^\dagger_{\alpha\beta}(\mathbf{k}))F_{\lambda\mu}(\mathbf{k}') \\ & + (a^\dagger_{-\mathbf{k}\alpha}a^\dagger_{\mathbf{k}\beta} - F^\dagger_{\alpha\beta}(\mathbf{k}))(a_{\mathbf{k}'\lambda}a_{-\mathbf{k}'\mu} - F_{\lambda\mu}(\mathbf{k}')). \end{aligned}$$

Using the Mean Field Approximation the operators in terms of their average values is called the . The excitation energy can be found without knowing the exact form of the anomalous averages. So we'll forgo determining their explicit form. Since the last term is quadratic in the difference of the pair of operators average of the operator pair it's contribution is negligible and it is dropped.

Substituting this result back into the Hamiltonian and recognizing the F's as complex matrices indexed by the spin labels of the electron operators one obtains:

$$\begin{aligned} \widehat{H} = & \sum_{\mathbf{k}\alpha} \xi_{\mathbf{k}} a^\dagger_{\mathbf{k}\alpha}a_{\mathbf{k}\alpha} \\ & + \frac{1}{2}\sum_{\mathbf{k}\mathbf{k}'}\sum_{\alpha\beta\mu\lambda} V_{\alpha\beta,\lambda\mu}(\mathbf{k},\mathbf{k}')\left[-F^\dagger_{\alpha\beta}(\mathbf{k})F_{\lambda\mu}(\mathbf{k}') + F^\dagger_{\alpha\beta}(\mathbf{k})a_{\mathbf{k}'\lambda}a_{-\mathbf{k}'\mu} + F_{\lambda\mu}(\mathbf{k}')a^\dagger_{-\mathbf{k}\alpha}a^\dagger_{\mathbf{k}\beta}.\right] \end{aligned} \tag{22}$$

At this point it is convenient to consider functions of the form

$$\Delta_{\mathbf{k},\beta\alpha} = -\textstyle\sum_{\mathbf{k}',\lambda\mu} V_{\alpha\beta,\lambda\mu}(\mathbf{k},\mathbf{k}')F_{\lambda\mu}(\mathbf{k}') \tag{23}$$

which is known as the gap equation. $V_{\alpha\beta,\lambda\mu}(\mathbf{k},\mathbf{k}')$ models the interaction of the electrons bound in Cooper pairs. It's symmetry properties (Eq. 20) are consistent with those of a symmetrized function. The wave function of an N-body system of Fermions

is antisymmetrized and so is the potential that describes the interaction. Observe that $\Delta_{\mathbf{k},\beta\alpha}$ inherits the symmetry of the interaction potential. The general form of the pair wave function obtained in §2.2 is perfectly suited to *model* the antisymmetrized solution of the gap equation $\Delta_{\mathbf{k},\beta\alpha}$:

$$\Delta_{\alpha\beta}(\mathbf{k}) = \Delta_0\, g_l(\mathbf{k})\, (i\widehat{\sigma}_y)_{\alpha\beta}\,,$$

$$\Delta_{\alpha\beta}(\mathbf{k}) = \Delta_0\, (i\,\vec{\sigma}\cdot\widehat{\sigma}_y\cdot\mathbf{d}(\mathbf{k}))_{\alpha\beta}\,.$$

Writing the Hamiltonian in terms of the gap functions:

$$\widehat{H} = \frac{1}{2}\sum_{\mathbf{k}\alpha}\xi_{\mathbf{k}}(a^\dagger_{\mathbf{k}\alpha}a_{\mathbf{k}\alpha} - a_{\mathbf{k}\alpha}a^\dagger_{\mathbf{k}\alpha}) + \frac{1}{2}\sum_{\mathbf{k},\alpha\beta}\left[\Delta^\dagger_{\alpha\beta}(\mathbf{k})a_{-\mathbf{k}\alpha}a_{\mathbf{k}\beta} + \Delta_{\alpha\beta}(\mathbf{k})a^\dagger_{\mathbf{k}\alpha}a^\dagger_{-\mathbf{k}\beta}\right]$$
$$+\frac{1}{2}\sum_{\mathbf{k},\alpha\beta}\left[\xi_{\mathbf{k}} + F^\dagger_{\beta\alpha}(\mathbf{k})\Delta_{\alpha\beta}(\mathbf{k})\right]$$

$$\text{setting}\quad E_0 = \tfrac{1}{2}\textstyle\sum_{\mathbf{k},\alpha\beta}\left[\xi_{\mathbf{k}} + F^\dagger_{\beta\alpha}(\mathbf{k})\Delta_{\alpha\beta}(\mathbf{k})\right] \tag{24}$$

The Hamiltonian is diagonalized by the transformation:

$$\widehat{u}_{\mathbf{k}} = \frac{(E_{\mathbf{k}} + \xi_{\mathbf{k}})\widehat{\sigma}_0}{\sqrt{(E_{\mathbf{k}} + \xi_{\mathbf{k}})^2 + \frac{1}{2}\mathsf{Tr}[\widehat{\Delta}_{\mathbf{k}}\widehat{\Delta}^\dagger_{\mathbf{k}}]}} \tag{25}$$

$$\widehat{v}_{\mathbf{k}} = \frac{-\widehat{\Delta}_{\mathbf{k}}}{\sqrt{(E_{\mathbf{k}} + \xi_{\mathbf{k}})^2 + \frac{1}{2}\mathsf{Tr}[\widehat{\Delta}_{\mathbf{k}}\widehat{\Delta}^\dagger_{\mathbf{k}}]}}. \tag{26}$$

with eigen-energy excitation energy:

$$E_{\mathbf{k}} = \sqrt{\xi^2_{\mathbf{k}} + |\Delta_0|^2|\mathbf{d}(\mathbf{k})|^2} = \sqrt{\xi^2_{\mathbf{k}} + \tfrac{1}{2}\mathsf{Tr}[\widehat{\Delta}_{\mathbf{k}}\widehat{\Delta}^\dagger_{\mathbf{k}}]}. \tag{27}$$

E_0 is then the ground state energy. The Hamiltonian is diagonal in the new basis:

$$b_{\mathbf{k},\alpha} = \sum_\beta\left\{(E_{\mathbf{k}} + \xi_{\mathbf{k}})\delta_{\alpha\beta}a_{\mathbf{k},\beta} + \widehat{\Delta}_{\mathbf{k},\alpha\beta}a^\dagger_{\mathbf{k},\beta}\right\} \tag{28}$$

$$b^\dagger_{\mathbf{k},\alpha} = \sum_\beta\left\{-\widehat{\Delta}^\dagger_{\mathbf{k},\alpha\beta}a_{\mathbf{k},\beta} + (E_{\mathbf{k}} + \xi_{\mathbf{k}})\delta_{\alpha\beta}a^\dagger_{\mathbf{k},\beta}\right\}$$

where $\alpha, \beta = \{\uparrow, \downarrow\}$. The b-operators depend linearly on the original electron operators $\{a, a^\dagger\}$. They represent the creation and destruction of the quasiparticles mentioned earlier. As can be seen, the action of b (or $b^\dagger$) creates an electron (by the action of $a^\dagger$ and an electron hole by the action of a. The new b-operators form the *operator* basis which diagonalize the system Hamiltonian.

Chapter III

THE QUASIPARTICLE DENSITY OF STATES DOS

The primary motivation for calculating the DOS is to use it to obtain information about the presence (or absence) of nodes in the energy gap for low energy quasiparticles. In the case where the energy gap has no nodes the DOS vanishes for energies below a critical frequency ($|\hbar\omega| < |\hbar\omega_{\mathbf{gap}}| \Rightarrow \mathcal{N}(\omega) = 0$). In the case where nodes are present, $\mathcal{N}(\omega)$ remains finite for all frequencies $|\omega| > 0$.

The approach used in this section to calculate the quasiparticles density of states is compared with that of Mineev [19] for the isotropic. In this case the A-phase of superfluid ^{3}He is analyzed where the order parameter has the form $\mathbf{d}(\mathbf{k}) = (\hat{k}_x + i\hat{k}_y, 0, 0)$. The Fermi surface is spherical, characterized by the usual $\epsilon = \alpha k^2$ dispersion. Due to the form of the order parameter there is a node at the North and South poles of the Fermi surface. Mineev [19] shows that at very low frequency (excitation energy) the quasiparticle density of states should have a quadratic dependence on the excitation energy, $\hbar\omega$, given by:

$$N(\omega) = N_0 \left(\frac{\hbar\omega}{\Delta_0} \right)^2 \tag{29}$$

where N_0 is the density of states at the Fermi level. The goal of the next section is to compute the quasiparticle density of states, $N(\omega)$, by two separate methods. The first approach, that of Mineev, is compared with with the approach used in this work to characterize the dependence of the density of quasiparticle states at low frequency. The reason for considering two methods is two-fold: firstly in the case of a complicated energy dispersion a straight forward approach for calculating is $N(\omega)$ needed, secondly it is desirable to show that a more general method developed in this work

yields the correct result for a well known case.

In what follows the dependence of the quasiparticle density of states on the excitation energy is calculated by two different methods for the A-phase and k^2 energy dispersion. The results are then compared.

3.1 Comparison Calculation

We now calculate the quasiparticle density of states for low frequency $\hbar\omega$ (small excitation energy) by two separate methods. The method employed by Mineev is straight forward enough but relies on knowing exactly how the density of states disperses at the Fermi level with particle energy. One can find this energy dispersion for a D-dimensional system having momentum-energy dispersion $\epsilon(\mathbf{k}) = \alpha k^n$ by a simple transformation from $\mathbf{k}$-space coordinates to the energy representation:

$$\int d^{\mathsf{D}}k\, G(\mathbf{k}) = \int d\Omega dk\, k^{\mathsf{D}-1} G(\mathbf{k}) = \int d\Omega d\epsilon\, \rho(\epsilon)\widetilde{G}(\epsilon)$$
$$\rho(\epsilon) = \frac{1}{\alpha n}\left[\frac{\epsilon}{\alpha}\right]^{(\mathsf{D}/n)-1}. \tag{30}$$

In finding the momentum-energy density $\rho(\epsilon)$ one need be able to invert the momentum-energy dispersion to find $k(\epsilon)$. For more complicated dependencies, however, inverting the momentum dispersion to find $k(\epsilon)$ can be quite difficult. A more general approach to calculating the quasiparticle density of states will be needed.

3.1.1 Mineev's Approach

Beginning from the same starting point as Mineev, the definition of the quasiparticle density of states in the strict BCS limit is:

$$N(\omega) = \sum_{\mathbf{k}\alpha} \delta(\hbar\omega - E_{\mathbf{k},\alpha}) \quad \text{where,} \tag{31}$$

$$E_{\mathbf{k},\alpha} = \sqrt{\xi_{\mathbf{k}}^2 + |\Delta(\mathbf{k},\alpha)|^2},\ \xi_{\mathbf{k}} = \hbar^2k^2/2m - \mu \tag{32}$$

$$|\Delta(\mathbf{k},\alpha)|^2 = \Delta_0^2|\mathbf{d}(\mathbf{k})|^2 = \Delta_0^2|(\hat{k}_x + i\hat{k}_y, 0, 0)|^2 = \Delta_0^2\sin^2(\theta) \tag{33}$$

This is the excitation energy with gap $|\Delta(\mathbf{k},\alpha)|$ corresponding to the case of ^{3}He in the A-phase. The pairing of ^{3}He atoms in the A-phase is characterized by the angular momentum state:

$$\Psi^A_{\text{pair}} = Y_{1,1}(\widehat{\mathbf{k}})(|\uparrow\uparrow\rangle - |\downarrow\downarrow\rangle) \sim (k_x + ik_y)\boldsymbol{\sigma}_z \tag{34}$$

That is, pairing occurs in a spin triplet channel—with net spin $m_S = 0$—where each pair of atoms has orbital angular momentum $l = \hbar$, giving total angular momentum for N pairs equal to $N\hbar$. As it turns out , the gap function $|\Delta(\mathbf{k},\alpha)|$ contains all the information about the symmetry of the system that is contained in Ψ^A_{pair} [ref. section §2.2]. Therefore

$$|\Delta(\mathbf{k},\alpha)|^2 \sim \Delta_0^2|(\hat{k}_x + i\hat{k}_y, 0, 0)|^2(\delta_{\alpha,1} - \delta_{\alpha,-1})^2 = \Delta_0^2 \sin^2(\theta)|e^{i\phi}|^2.$$

Clearly the A-phase has nodes (i.e., the gap vanishes) near the polar regions at $\theta = 0, \pi$ implying that it is easy to excited pairs of ^{3}He atoms out of the superfluid ground state when the momentum of the pair lies near $\theta = 0$ or $\theta = \pi$. Utilizing this fact along with the spherical symmetry of the system a calculation of the DOS for ^{3}He proceeds as follows.

$N(\omega)$ is nonvanishing only when $\hbar\omega = E_{\mathbf{k}}$ (i.e., when there exists a state $\{\mathbf{k},\alpha\}$ of given energy $\hbar\omega$). Since the sum is over all orbital and spin quantum numbers then exactly all those states of energy $\hbar\omega$ are counted. Clearly, the sum is over a discrete set of states; however, in the case of many discrete states having the same or similar energy one can pass to the continuum limit (note the factor of 2 coming from the spin sum):

$$N(\omega) = 2V_0 \int \frac{d^3k}{(2\pi)^3}\delta(\hbar\omega - E(k,\theta)). \tag{35}$$

In a 3-dimensional system governed by a k^2 energy dispersion the density of states is

$$\rho(\epsilon) = \frac{1}{2\alpha}\left[\frac{\epsilon}{\alpha}\right]^{1/2} \quad \alpha = \frac{\hbar^2}{2m}.$$

and near the Fermi level:

$$\rho(\epsilon_F) = \frac{m}{\hbar^2}\sqrt{\frac{2m\mu}{\hbar^2}} = \frac{mk_F}{\hbar^2}.$$

With regard to Mineev's approach, one uses the fact that in the strict BCS limit only those states very near the Fermi surface contribute to the quasiparticle density of states (or equivalently only those energies near the Fermi level contribute so that $\rho \approx \rho(\epsilon_F)$). Then Eq. 35 becomes:

$$\begin{aligned} N(\omega) &= 2\frac{V_0}{(2\pi)^3}\int d\Omega k^2 dk\, \delta(\hbar\omega - E(k,\theta)) = 2\frac{V_0}{(2\pi)^3}\int d\Omega d\epsilon\, \rho(\epsilon)\delta(\hbar\omega - E(\epsilon,\theta)) \\ &= 2V_0 N_0 \int \frac{d\Omega}{4\pi} d\epsilon\, \delta(\hbar\omega - E(\epsilon,\theta)) \quad N_0 \doteq \frac{mk_F}{2\pi^2\hbar^2} = \frac{1}{2\pi^2}\rho(\epsilon_F) \end{aligned} \tag{36}$$

where N_0 is the quasiparticle density of states at the Fermi level. Using $E = \sqrt{\xi^2 + \Delta^2}$, $\xi = (\epsilon - \mu)$ one can show that $d\epsilon = (E/\xi)dE = (E/\sqrt{E^2 - \Delta^2})dE$

$$N(\omega) = 2N_0V_0 \int \frac{d\Omega}{4\pi}\int dE \frac{E\,\delta(\hbar\omega - E)}{\sqrt{E^2 - \Delta^2}} = N_0V_0 \int_0^{\pi} \sin(\theta)d\theta \frac{\hbar\omega}{\sqrt{(\hbar\omega)^2 - \Delta_0^2\sin^2(\theta)}}$$

Clearly, in the case of small energy $\hbar\omega$ the range of integration must be restricted such that $\sin^2\theta < (\hbar\omega)^2/\Delta_0^2$ (else, the density of states would be complex). For $\hbar\omega$ small enough $\sin(\theta)$ is approximately θ and one obtains:

$$N(\omega) = 2N_0V_0 \int_0^{\frac{\hbar\omega}{\Delta}} \theta d\theta \frac{\hbar\omega}{\sqrt{(\hbar\omega)^2 - \Delta_0^2\theta^2}} = 2N_0V_0\left(\frac{\hbar\omega}{\Delta_0}\right)^2. \tag{37}$$

The factor of 2 accounts for a contribution from the regions near the nodes at $\theta = 0$ and $\theta = \pi$. Notice that the quasiparticle density of states disperses as the square of the excitation energy $\hbar\omega$ normalized by the magnitude of the excitation energy gap.

Also, observe that the density of states vanishes for $\hbar\omega = 0$. However, arbitrarily small amounts of energy can create excitations in this system. This corresponds physically to the fact that quasiparticle excitations occur only when there is enough energy available to cause pair breaking and excite quasiparticles out of the superconducting ground state. Alternatively one may say that there are no zero energy

excitations.

With this result the task now is to perform the same calculation using a more general approach. The objective is to obtain the same dispersion for $N(\omega)$ with small frequency $\hbar\omega$.

3.1.2 A More General Approach

In this section a more general approach to calculating the DOS is developed. Here, $\mathcal{N}(\omega)$ is again calculated for the A-phase of ^{3}He. This approach does not rely on one's ability to invert the energy-momentum lattice dispersion (and subsequently find the density of states N_0 at the Fermi level) as is required by the previous method. The advantage gained is the ability to treat systems with lattice dispersions which are considerably more complicated than a simple power-law-type dispersion. The expectation is that this method will yield a more generalized result for $\mathcal{N}(\omega)$ and in the process recover the result from the previous section. Beginning with Eq. 35, the integration is performed by using the delta function identity:

$$\delta(F(k)) = \frac{1}{|F'(k)|}\sum_{k_j}\delta(k-k_j), \quad \text{where} \quad F(k_j)=0. \tag{38}$$

In Eq. 35 the argument of the delta function corresponds to $F(k)$:

$$F(k) = F(\omega,k,\theta) = \hbar\omega - [(\hbar^2k^2/2m-\mu)^2 + \Delta_0^2\sin^2\theta]^{1/2}.$$

Applying the identity to the delta function integrand of Eq. 35:

$$N(\omega) = \frac{V_0}{4\pi^3}\int k^2 dk d\Omega \frac{\sum_j \delta(k-k_j(\omega,\theta))}{|\partial F(\omega,k,\theta)/\partial k|}, \quad N(\omega)\in\Re. \tag{39}$$

The integration is first performed on k, holding $\hbar\omega$ and θ fixed. This requires one to find the $k_j(\omega,\theta)$ (i.e., the zeros of the argument of the delta function $F(\omega,k_j,\theta) = \hbar\omega - E(k_j,\theta) = 0$). Solving for the k_j and noting that they correspond

to magnitudes (i.e., nonnegative) one obtains:

$$(\hbar\omega)^2 = E^2(k,\theta) = (\xi_{\mathbf{k}})^2 + \Delta_0^2 \sin^2\theta \tag{40}$$

$$|\xi_{\mathbf{k}}| = \sqrt{(\hbar\omega)^2 - \Delta_0^2 \sin^2\theta} \tag{41}$$

$$\xi_{\mathbf{k}} = \hbar^2 k^2/2m - \mu = (-)^j \sqrt{(\hbar\omega)^2 - \Delta_0^2 \sin^2\theta} \tag{42}$$

$$k_j = \frac{1}{\hbar}\sqrt{2m\mu + (-)^j 2m[(\hbar\omega)^2 - \Delta_0^2 \sin^2\theta]}, \quad j = 1,2, \quad k \in \Re. \tag{43}$$

That k is real requires the integration on θ be such that $\sin^2\theta \leq (\hbar\omega/\Delta_0)^2$. Furthermore, it is seen from Eqs. 41 & 42

$$\begin{aligned} &\text{for } \; j = 1 \;\; \xi_{\mathbf{k}} < 0 \Rightarrow \quad k \leq \sqrt{2m\mu}/\hbar = k_F \\ &\text{for } \; j = 2 \;\; \xi_{\mathbf{k}} > 0 \Rightarrow \quad k \geq \sqrt{2m\mu}/\hbar = k_F. \end{aligned} \tag{44}$$

Clearly, the $j = 1$ root corresponds to k in the interval $[0, k_F]$ and the $j = 2$ root corresponds to k in the interval $[k_F, \infty)$. Putting all this back into the integral, keeping in mind the restrictions on the angular and k integrations:

$$N(\omega) = \frac{V_0}{4\pi^3}\int d\Omega \int_0^\infty k^2 dk\, \Theta\left(\left[\frac{\hbar\omega}{\Delta_0}\right]^2 - \sin^2\theta\right) \frac{\sum_j \delta(k-k_j)\,\Theta([-]^j(k-k_F))}{|\partial F(\omega,k,\theta)/\partial k|}$$

$$= \frac{V_0}{2\pi^2}\int_0^\pi \sin\theta d\theta\, \Theta\left(\left[\frac{\hbar\omega}{\Delta_0}\right]^2 - \sin^2\theta\right) \otimes$$

$$\otimes \left\{ \int_0^{k_F} k^2 dk \frac{\delta(k-k_1)}{|\partial F(\omega,k,\theta)/\partial k|} + \int_{k_F}^\infty k^2 dk \frac{\delta(k-k_2)}{|\partial F(\omega,k,\theta)/\partial k|} \right\}$$

$$= \frac{V_0}{2\pi^2}\int_0^\pi \sin\theta d\theta\, \Theta\left(\left[\frac{\hbar\omega}{\Delta_0}\right]^2 - \sin^2\theta\right) \left\{ \frac{k_1^2}{|\partial F(\omega,k,\theta)/\partial k|_{k_1}} + \frac{k_2^2}{|\partial F(\omega,k,\theta)/\partial k|_{k_2}} \right\} \tag{45}$$

Using the fact that $\left.\frac{\partial F}{\partial k}\right|_{k_j} = -\frac{[\hbar^2 k_j^2/2m - \mu](\hbar^2/m)k_j}{\hbar\omega}$ and substituting for k_j from (16) yields:

$$N(\omega) = V_0 \frac{m\hbar\omega}{2\pi^2\hbar^3} \int_0^\pi \sin\theta d\theta \, \Theta\left(\left[\frac{\hbar\omega}{\Delta_0}\right]^2 - \sin^2\theta\right) \otimes$$
$$\otimes \left\{ \frac{\sqrt{2m\mu - 2m((\hbar\omega)^2 - \Delta_0^2\sin^2\theta)^{1/2}}}{\sqrt{(\hbar\omega)^2 - \Delta_0^2\sin^2\theta}} + \frac{\sqrt{2m\mu + 2m((\hbar\omega)^2 - \Delta_0^2\sin^2\theta)^{1/2}}}{\sqrt{(\hbar\omega)^2 - \Delta_0^2\sin^2\theta}} \right\} \tag{46}$$

In the limit of small frequency, $\hbar\omega$, the theta function imposes the condition that $\sin\theta$ be small. In this case the only contribution to $N(\omega)$ comes from near the nodes at $\theta = 0, \pi$. Setting $\alpha = \Delta_0/\hbar\omega$, $\beta = \mu/\hbar\omega$, $x = \alpha\theta$ and factoring out $\sqrt{\frac{2m}{\hbar\omega}}$:

$$N(\omega) = 2V_0 \frac{m\hbar\omega}{2\pi^2\hbar^3}\sqrt{\frac{2m}{\hbar\omega}} \int_0^{\frac{1}{\alpha}} \theta d\theta \left\{ \frac{\sqrt{\beta - (1-\alpha^2\theta^2)^{1/2}}}{\sqrt{1-\alpha^2\theta^2}} + \frac{\sqrt{\beta + (1-\alpha^2\theta^2)^{1/2}}}{\sqrt{1-\alpha^2\theta^2}} \right\}$$
$$= V_0 \frac{m\hbar\omega}{\pi^2\hbar^3}\sqrt{\frac{2m}{\hbar\omega}}\frac{\sqrt{\beta}}{\alpha^2} \int_0^1 x dx (1-x^2)^{-1/2} \Big\{$$
$$\sqrt{1 - \beta^{-1}(1-x^2)^{1/2}} + \sqrt{1 + \beta^{-1}(1-x^2)^{1/2}} \Big\} \tag{47}$$

The theta function restricts the integration near $\theta = 0$ to be on $[0, \hbar\omega/\Delta_0]$. The factor of 2 in front of the first line accounts for the contribution from the nodes at $\theta = 0$ and $\theta = \pi$. Observe that typically $\hbar\omega < \mu$ and that x is integrated on $[0, 1]$. This implies that the two terms in brackets in Eq. 47 can be expanded in $y(x) = (1-x^2)^{1/2}$. One obtains:

$$N(\omega) = V_0 \frac{m(\hbar\omega)^2}{\pi^2\hbar^3}\frac{\sqrt{2m\mu}}{\Delta_0^2} \otimes \tag{48}$$
$$\otimes \int_0^1 \frac{x dx}{y(x)} \left\{ 2 - \sum_{n=2} \frac{(2n-3)!!}{n!} \left[\left(\frac{\beta^{-1}}{2}\right)^n + \left(\frac{-\beta^{-1}}{2}\right)^n \right] [y(x)]^n \right\}$$

where $\int_0^1 x dx [y(x)]^n = \int_0^1 x dx (1-x^2)^{n/2} = \frac{1}{n+2}$.

Notice that the odd terms cancel out. Upon integration one obtains:

$$N(\omega) = 2V_0 \frac{mk_F}{\pi^2\hbar^2} \left(\frac{\hbar\omega}{\Delta_0}\right)^2 \left\{ 1 - \sum_{n=1} \frac{(4n-3)!!}{(2n+1)!} \left[\frac{\hbar\omega}{2\mu}\right]^{2n} \right\} \tag{49}$$

For very small frequency the quadratic dependence of the quasiparticle density of states is recovered:

$$N(\omega) = 4V_0N_0\left(\frac{\hbar\omega}{\Delta_0}\right)^2 \tag{50}$$

Notice that this result is a factor of 2 larger than the one obtained by Mineev. Looking at Eq. 43 one sees that there are two sets of contributions to $\mathcal{N}(\omega)$ which are divided into states with $k \leq k_F$ and states with $k \geq k_F$. Apparently, the approximation $\rho(\epsilon) \rightarrow \rho(\epsilon_F)$ used to simplify the integration in §3.1.1 is too strong and misses some of the contributions.

Next we consider the DOS for the quasi-one-dimensional superconductor $(\mathsf{TMTSF})_2\mathsf{X}$.

3.2 The General DOS for a Lattice

The general definition of the quasiparticle density of states DOS is:

$$\mathcal{N}(\omega) = \sum_{\mathbf{k}}[u_{\mathbf{k}}^2\delta(\hbar\omega - E_{\mathbf{k}}) + v_{\mathbf{k}}^2\delta(\hbar\omega + E_{\mathbf{k}})] \tag{51}$$

where

$$E_{\mathbf{k}} = \sqrt{\xi_{\mathbf{k}}^2 + |\Delta(\mathbf{k})|^2} \tag{52}$$

$$\xi_{\mathbf{k}} = t_x\cos(a_1k_1) + t_y\cos(a_2k_2) + t_z\cos(a_3k_3) - \mu \tag{53}$$

$$u_{\mathbf{k}}^2 = \frac{1}{2}\left(1 + \frac{\xi_{\mathbf{k}}}{E_{\mathbf{k}}}\right) \quad v_{\mathbf{k}}^2 = \frac{1}{2}\left(1 - \frac{\xi_{\mathbf{k}}}{E_{\mathbf{k}}}\right) \tag{54}$$

In what follows the DOS for the S,P and D_{xy} symmetries will be discussed. The first and second terms contain the quasiparticle and quasihole coherence factors $u_{\mathbf{k}}^2$ & $v_{\mathbf{k}}^2$ and correspond to the density of states for the quasiparticles and quasiholes respectively. The quasiparticle term contribute to $\mathcal{N}(\omega)$ only for $\omega > 0$. This is because the excitation energy in the delta function is nonnegative. Similarly, the quasihole term contributes to $\mathcal{N}(\omega)$ only for $\omega < 0$. Using the definition of the coherence factors these two terms are written compactly as:

$$\mathsf{N}(\omega) = \frac{V_0}{(2\pi)^3}\int \frac{d^3\mathbf{r}}{V_0}\,\frac{1}{2}\left(1+\mathrm{sgn}(\omega)\frac{\xi_{\mathbf{r}}}{E_{\mathbf{r}}}\right)\delta(\hbar\omega-\mathrm{sgn}(\omega)E_{\mathbf{r}}) \tag{55}$$

This can be obtained by passing from the discrete to the continuous case $[\sum_{\mathbf{k}} \rightarrow (V_0/(2\pi)^3)\int d^3\mathbf{k}]$, converting to dimensionless variables $(a_j k_j \rightarrow x_j)$, $V_0 = a_1 a_2 a_3$ and taking account of the sign difference in the coherence factors. In general the quasiparticle density of states will differ in shape for quasiparticles and quasiholes; however, certain features such as the location of critical frequencies [see appendix §F] remain the same. The only contributions to the integral will come from momentum states $\mathbf{r}$ such that $F(\mathbf{r},\omega) = \hbar\omega - \mathrm{sgn}(\omega)E_{\mathbf{r}} = 0$.

The integration over momenta reduces to a $2D$-integration by applying the delta function identity

$$\delta(F(x)) = \sum_l \frac{\delta(x-x_l)}{|\partial F(x)/\partial x|} \quad F(x_l) = 0 \tag{56}$$

where l indexes the roots of $F(x)$. The DOS takes the form:

$$\mathsf{N}(\omega) = \frac{1}{2}\frac{1}{(2\pi)^3}\sum_l \int dydz\,\left(1+\mathrm{sgn}(\omega)\frac{\xi_{x_l}}{E_{x_l}}\right)\frac{1}{|\partial F(\mathbf{r},\omega)/\partial x|_{x_l}} \tag{57}$$

$$F(\mathbf{r},\omega) = \hbar\omega - \mathrm{sgn}(\omega)E_{\mathbf{r}}$$

where the quantities subscripted by x_l are to be evaluated at $x_l = x_l(y,z,\omega)$. To obtain the x_l one solves $F(\mathbf{r},\omega) = \hbar\omega - \mathrm{sgn}(\omega)E_{\mathbf{r}} = 0$ for x. The root x_l will be different for the various symmetries so that it is convenient at this point to treat the S, P, D_{xy} symmetries in separate sections.

In the following sections, the DOS is obtained for the singlet S & D symmetries and for the triplet P symmetries.

3.3 The DOS for the Singlet S Symmetry

The general form of the DOS in Eq. 57 was obtained above. To begin, $F(\mathbf{r},\omega) = \hbar\omega - \mathrm{sgn}(\omega)E_{\mathbf{r}} = 0$ is solved for the S symmetry. The order parameter of the S symmetries has the from:

$$\Delta(\mathbf{r}) = \Delta_0|\mathbf{d}(\mathbf{r})| = \Delta_0. \tag{58}$$

Putting this form of the gap into $\hbar\omega - -\hbar\omega = E_{\mathbf{r}} = 0$ and solving for x_l yields:

$$\cos(x_{js}) = \frac{-t_x f(y,z) + (-)^j \sqrt{D_{\mathsf{S}}(y,z,\omega)}}{t_x^2} \tag{59}$$

$$x_{js} = (-)^s \arccos\left[\frac{-t_x f(y,z) + (-)^j \sqrt{D_{\mathsf{S}}(y,z,\omega)}}{t_x^2}\right] \tag{60}$$

$$D_{\mathsf{S}}(y,z,\omega) = t_x^2\left((\hbar\omega)^2 - |\Delta_0|^2\right). \tag{61}$$

So the roots are indexed by two indices $l = \{js\}$, $(j,s = 1,2)$ and

$$\mathrm{sgn}(\omega)E_{x_{js}} = \hbar\omega$$

$$E_{x_{js}} = |\hbar\omega|$$

$$\begin{aligned}\xi_{x_{js}} &= t_x\cos(x_{js}) + f(y,z)\\ &= (-)^j\frac{\sqrt{D_{\mathsf{S}}(y,z,\omega)}}{t_x}\end{aligned}$$

$$\left.\frac{\partial F(\mathbf{r},\omega)}{\partial x}\right|_{x_{js}} = (-)^j\frac{\sin(x_{js})}{\hbar\omega}\sqrt{D_{\mathsf{S}}(y,z,\omega)} \tag{62}$$

Putting all these components together in Eq. 57 gives:

$$\mathsf{N}(\omega) = \frac{1}{2}\frac{1}{(2\pi)^3}\sum_{js}\int dydz\left(1+\mathrm{sgn}(\omega)\frac{\xi x_{js}}{|\hbar\omega|}\right)\frac{|\hbar\omega|\cdot\Theta(D_{\mathsf{S}}(y,z,\omega))}{|\sin(x_{js})\sqrt{D_{\mathsf{S}}(y,z,\omega)}|}$$

$$= \frac{1}{2}\frac{1}{(2\pi)^3}\sum_{js}\int dydz\left(|\hbar\omega|+\mathrm{sgn}(\omega)(-)^j\frac{\sqrt{D_{\mathsf{S}}(y,z,\omega)}}{t_x}\right)\frac{\Theta(D_{\mathsf{S}}(y,z,\omega))}{|\sin(x_{js})\sqrt{D_{\mathsf{S}}(y,z,\omega)}|}.$$

Since the second term is even in y, z it cancels out when the sum on j is performed:

$$\mathsf{N}(\omega) = \frac{1}{2}\frac{1}{(2\pi)^3}\frac{|\hbar\omega|}{\sqrt{t_x^2\left((\hbar\omega)^2-|\Delta_0|^2\right)}}\Theta([\hbar\omega]^2-|\Delta_0|^2)\sum_{js}\int\frac{dydz}{|\sin(x_{js})|}. \tag{63}$$

A plot for positive low frequency is given in Fig. 7.

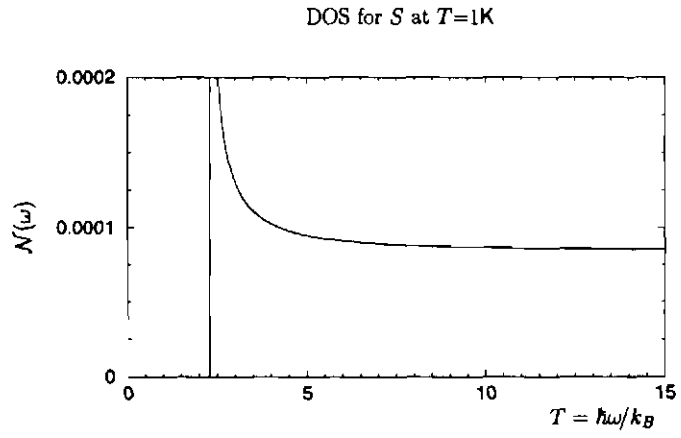

Figure 7: This figure shows the DOS for the S symmetry for positive frequency in units of temperature (1K) $[T = \hbar\omega/k_B]$. Notice the gap at $T = \Delta_0/k_B$. $[t_x = k_B(5800\mathsf{K}), t_y = k_B(1226\mathsf{K}), t_z = k_B(48\mathsf{K}), \mu = k_B(4003\mathsf{K}), \Delta_0 = k_B(2.281\mathsf{K})]$

In the low frequency limit $|\hbar\omega| \sim |\Delta_0|$ and $D_{\mathsf{S}}(y,z,\omega) \approx 0$. One can use that fact that $|t_x, \mu \gg t_y, t_z|$ to make the rough approximation $-f(y,z)/t_x \approx \mu/t_x$ so that $|\sin(x_{js})| \approx \sqrt{1-[\mu/t_x]^2}$ and the DOS for the S symmetry is approximately:

$$\mathsf{N}(\omega) = \frac{1}{\pi\sqrt{t_x^2-\mu^2}}\frac{|\hbar\omega|}{\sqrt{(\hbar\omega)^2-|\Delta_0|^2}}\Theta([\hbar\omega]^2-|\Delta_0|^2) \tag{64}$$

which reveals that the S symmetry is gapped and divergent at $|\omega| = |\Delta_0|$. The plot of the DOS for the S symmetry from Eq. 63 is seen to contain the singularity at $|\omega| = |\Delta_0|$ predicted in the approximation above; however, the approximation does not contain information about the cut-off frequencies lying at the top of the band $E_{\mathbf{r}}$ which occur [see appendix §F] at:

$$\hbar\omega_{\max,j=1} = \sqrt{(t_x + t_y + t_z + \mu)^2 + \Delta_0^2} \tag{65}$$

$$\hbar\omega_{\max,j=2} = \sqrt{(t_x + t_y + t_z - \mu)^2 + \Delta_0^2}. \tag{66}$$

These frequencies are obtained by considering the implicit definition of $|\sin(x_{js})|$ in terms of $\cos(x_{js})$ in Eq. 59. While cosine is bounded in magnitude to be no greater than 1, the right hand side is not. In fact, for a given value of $j = 1, 2$ there are frequencies $\omega_{\max,j}$ for which the right hand side exceeds the value 1 in magnitude. These frequencies define the cut-off values of ω corresponding to the top of the energy band $E_{\mathbf{r}}$ and depend on whether $j = 1$ or 2. An analysis is performed to determine these cut-offs in the index [see appendix §F].

3.4 The DOS for the Singlet D_{xy} Symmetry

Firstly, $F(\mathbf{r}, \omega) = \hbar\omega - \mathrm{sgn}(\omega)E_{\mathbf{r}} = 0$ is solved for the D_{xy} symmetry. The order parameter for this symmetry has the from:

$$\Delta(\mathbf{r}) = \Delta_0 \sin(x)\sin(y) \tag{67}$$

Putting this form of the gap into $\hbar\omega - \mathrm{sgn}(\omega)E_{\mathbf{r}} = 0$ and solving for x_l yields:

$$\cos(x_{js}) = \frac{-t_x f(y,z) + (-)^j \sqrt{D_{\mathrm{D_{xy}}}(y,z,\omega)}}{t_x^2 - \Delta_0^2 \sin^2(y)}$$

$$x_{js} = (-)^s \arccos\left[\frac{-t_x f(y,z) + (-)^j \sqrt{D_{\mathrm{D_{xy}}}(y,z,\omega)}}{t_x^2 - \Delta_0^2 \sin^2(y)}\right] \tag{68}$$

and

$$D_{\mathrm{D_{xy}}}(y,z,\omega) = |\Delta_0|^2 \sin^2(y) f^2(y,z) - \tag{69}$$

$$(t_x^2 - |\Delta_0|^2 \sin^2(y))\left[|\Delta_0|^2 \sin^2(y) - (\hbar\omega)^2\right]$$

where $l = \{js\}$ $(j, s = 1, 2)$ and

$$E_{x_{js}} = |\hbar\omega|$$

$$\begin{aligned}\xi_{x_{js}} &= t_x \cos(x_{js}) + f(y,z) \\ &= -\left[\frac{\Delta_0^2 \sin^2(y)}{t_x^2 - \Delta_0^2 \sin^2(y)}\right] f(y,z) + \frac{(-)^j t_x}{t_x^2 - \Delta_0^2 \sin^2(y)} \sqrt{D_{\mathsf{D}_{xy}}(y,z,\omega)}\end{aligned}$$

$$\left.\frac{\partial F(\mathbf{r},\omega)}{\partial x}\right|_{x_{js}} = (-)^j \frac{\sin(x_{js})}{\hbar\omega} \sqrt{D_{\mathsf{D}_{xy}}(y,z,\omega)}. \tag{70}$$

Putting all these components together in Eq. 57 gives:

$$\mathsf{N}(\omega) = \frac{1}{2}\frac{1}{(2\pi)^3} \sum_{js} \int dydz \left(1 + \mathrm{sgn}(\omega)\frac{\xi_{x_{js}}}{|\hbar\omega|}\right) \frac{|\hbar\omega| \cdot \Theta(D_{\mathsf{D}_{xy}}(y,z,\omega))}{|\sin(x_{js})\sqrt{D_{\mathsf{D}_{xy}}(y,z,\omega)}|}$$

$$\begin{aligned}= \frac{1}{2}\frac{1}{(2\pi)^3} \sum_{js} \int dydz \Bigg\{ &\left(|\hbar\omega| - \mathrm{sgn}(\omega)\left[\frac{\Delta_0^2 \sin^2(y)}{t_x^2 - \Delta_0^2 \sin^2(y)}\right] f(y,z)\right) \otimes \\ &\otimes \frac{\Theta(D_{\mathsf{D}_{xy}}(y,z,\omega))}{|\sin(x_{js})\sqrt{\mathsf{D}_{\mathsf{D}_{xy}}(\mathsf{y},\mathsf{z},\omega)}|}\Bigg\} \\ + \mathrm{sgn}(\omega)\frac{1}{2}\frac{1}{(2\pi)^3} \sum_{js} (-)^j \int dydz &\left(\frac{t_x}{t_x^2 - \Delta_0^2 \sin^2(y)}\right) \frac{\Theta(D_{\mathsf{D}_{xy}}(y,z,\omega))}{|\sin(x_{js})|}\end{aligned}$$

The integrand on the third line is even in y, z so that it vanishes when the sum on j is performed:

$$\mathsf{N}(\omega) = \frac{1}{2}\frac{1}{(2\pi)^3} \sum_{js} \int dydz \left(|\hbar\omega| - \left[\frac{\mathrm{sgn}(\omega)\Delta_0^2 \sin^2(y)}{t_x^2 - \Delta_0^2 \sin^2(y)}\right] f(y,z)\right) \frac{\Theta(D_{\mathsf{D}_{xy}}(y,z,\omega))}{|\sin(x_{js})\sqrt{D_{\mathsf{D}_{xy}}(y,z,\omega)}|} \tag{71}$$

The gap parameter vanishes for $y = 0, \pm\pi$ so that the D_{xy} symmetry is gapless. The

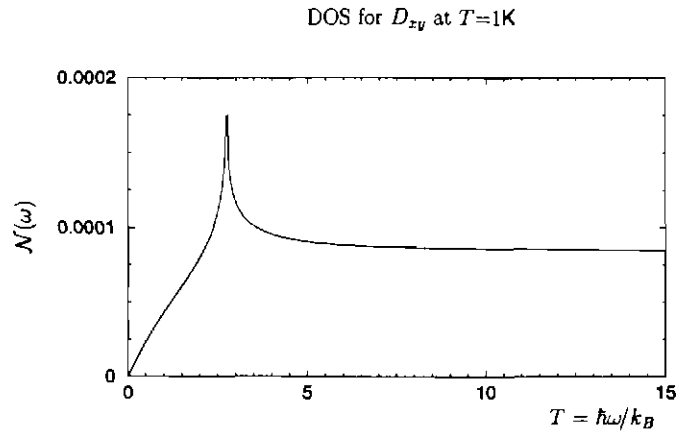

Figure 8: This figure shows the DOS for the D_{xy} symmetry for positive frequency in units of temperature (1K) $[T = \hbar\omega/k_B]$. Notice in contrast to the gapped S that there is no gap in $\mathcal{N}(\omega)$ in this case. $[t_x = k_B(5800\text{K}), t_y = k_B(1226\text{K}), t_z = k_B(48\text{K}), \mu = k_B(4003\text{K}), \Delta_0 = k_B(3.675\text{K})]$

plot of Eq. 71 shows the gapless response ($\omega_{\text{min}} = 0$) with critical frequencies at:

$$\omega_{\text{min}}{}^2 = 0 \tag{72}$$

$$\omega_1{}^2 = \Delta_0^2[1 - \cos^2(y_1)][1 - \{\alpha\cos(y_1) + \beta_1\}^2] \tag{73}$$

$$\omega_2{}^2 = \Delta_0^2[1 - \cos^2(y_2)][1 - \{\alpha\cos(y_2) + \beta_2\}^2] \tag{74}$$

$$\alpha = \frac{t_y}{t_x} \quad \beta_1 = \frac{t_z - \mu}{t_x} \quad \beta_2 = \frac{-t_z - \mu}{t_x}$$

$$\cos(\theta) = \beta_{\text{n}}(\alpha^2 - 1)\left(\frac{2 + 2\alpha^2 + \beta_{\text{n}}^2}{3}\right)^{\frac{3}{2}}$$

$$\cos(y_{\text{n}}) = \frac{1}{\alpha}\left[\sqrt{\frac{2 + 2\alpha^2 + \beta_{\text{n}}^2}{3}}\cos\left(\frac{\theta + 4\pi}{3}\right) - \frac{\beta_{\text{n}}}{2}\right] \quad \text{n} = 1, 2$$

Further analysis on $D_{\mathbf{D}_{xy}}(y, z, \omega)$ [see appendix §F] again reveals the cut-off frequencies:

$$\hbar\omega_{\text{max},j=1} = |t_x + t_y + t_z + \mu| \tag{75}$$

$$\hbar\omega_{\text{max},j=2} = |t_x + t_y + t_z - \mu|. \tag{76}$$

3.5 The DOS for the Triplet P Symmetries

Now one solves $F(\mathbf{r},\omega) = \hbar\omega - \mathrm{sgn}(\omega)E_{\mathbf{r}} = 0$ for the P symmetries. The order parameter of the gapped P symmetries has the following from:

$$\Delta(\mathbf{r}) = \Delta_0|\mathbf{d}(\mathbf{r})| = \Delta_0\left(A\sin(x), B\sin(y), C\sin(z)\right) \quad A \neq 0. \tag{77}$$

Putting $\Delta(\mathbf{r}) = \Delta_0\left(A\sin(x), B\sin(y), C\sin(z)\right)$ into $\hbar\omega - \mathrm{sgn}(\omega)E_{\mathbf{r}} = 0$ and solving for x_l yields:

$$\cos(x_{js}) = \frac{-t_x f(y,z) + (-)^j\sqrt{D_{\mathsf{P}}(y,z,\omega)}}{t_x^2 - A^2\Delta_0^2} \tag{78}$$

$$x_{js} = (-)^s \arccos\left[\frac{-t_x f(y,z) + (-)^j\sqrt{D_{\mathsf{P}}(y,z,\omega)}}{t_x^2 - A^2\Delta_0^2}\right] \tag{79}$$

and

$$\begin{aligned} D_{\mathsf{P}}(y,z,\omega) &= A^2|\Delta_0|^2 f^2(y,z) - \\ &(t_x^2 - A^2|\Delta_0|^2)\left[B^2|\Delta_0|^2\sin^2(y) + C^2|\Delta_0|^2\sin^2(z) + A^2|\Delta_0|^2 - (\hbar\omega)^2\right]. \end{aligned} \tag{80}$$

Now, $l = \{js\}$ $(j,s = 1,2)$ so one has:

$$E_{x_{js}} = |\hbar\omega|$$

$$\begin{aligned} \xi_{x_{js}} &= t_x\cos(x_{js}) + f(y,z) \\ &= -\left[\frac{A^2\Delta_0^2}{t_x^2 - A^2\Delta_0^2}\right] f(y,z) + \frac{(-)^j\, t_x}{t_x^2 - A^2\Delta_0^2}\sqrt{D_{\mathsf{P}}(y,z,\omega)} \end{aligned}$$

$$\left.\frac{\partial F(\mathbf{r},\omega)}{\partial x}\right|_{x_{js}} = (-)^j\,\frac{\sin(x_{js})}{\hbar\omega}\sqrt{D_{\mathsf{P}}(y,z,\omega)}. \tag{81}$$

Putting all these components together gives:

$$\mathsf{N}(\omega) = \frac{1}{2}\frac{1}{(2\pi)^3}\sum_{js}\int dydz\left(1+\mathrm{sgn}(\omega)\frac{\xi x_{js}}{|\hbar\omega|}\right)\frac{|\hbar\omega|\cdot\Theta(D_{\mathsf{P}}(y,z,\omega))}{|\sin(x_{js})\sqrt{D_{\mathsf{P}}(y,z,\omega)}|}$$

$$= \frac{1}{2}\frac{1}{(2\pi)^3}\sum_{js}\int dydz\left(|\hbar\omega| - \left[\frac{\mathrm{sgn}(\omega)A^2\Delta_0^2}{t_x^2 - A^2\Delta_0^2}\right]f(y,z)\right)\frac{\Theta(D_{\mathsf{P}}(y,z,\omega))}{|\sin(x_{js})\sqrt{D_{\mathsf{P}}(y,z,\omega)}|}$$
$$+\mathrm{sgn}(\omega)\frac{1}{2}\frac{1}{(2\pi)^3}\sum_{js}(-)^j\int dydz\left(\frac{t_x}{t_x^2 - A^2\Delta_0^2}\right)\frac{\Theta(D_{\mathsf{P}}(y,z,\omega))}{|\sin(x_{js})|}$$

The integrand on the third line is even in y, z. When the sum on j is performed, the contribution of the third line is canceled out:

$$\mathsf{N}(\omega) = \frac{1}{2}\frac{1}{(2\pi)^3}\sum_{js}\int dydz\left(|\hbar\omega| - \left[\frac{\mathrm{sgn}(\omega)A^2\Delta_0^2}{t_x^2 - A^2\Delta_0^2}\right]f(y,z)\right)\frac{\Theta(D_{\mathsf{P}}(y,z,\omega))}{|\sin(x_{js})\sqrt{D_{\mathsf{P}}(y,z,\omega)}|} \tag{82}$$

Plots for the various P symmetries are given below The critical frequency analysis

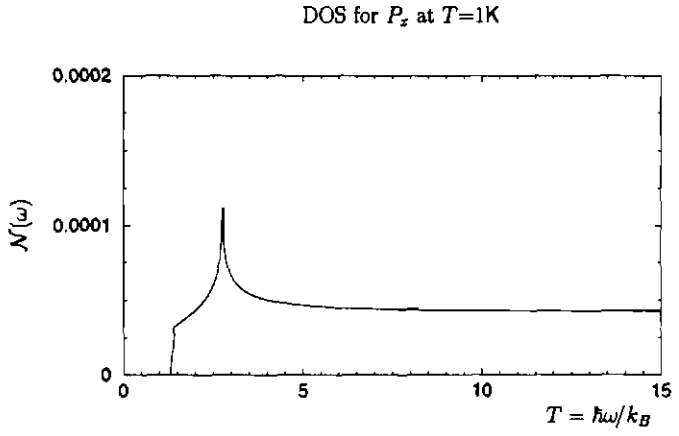

Figure 9: This figure shows the DOS for the P_x symmetry for positive frequency in units of temperature (1K), $T = \hbar\omega/k_B$. The gapped response begins at $T = \hbar\omega_{\mathsf{min}}/k_B = 1.301\mathsf{K}$. $[A = 1, B = 0, C = 0, t_x = k_B(5800\mathsf{K}), t_y = k_B(1226\mathsf{K}), t_z = k_B(48\mathsf{K}), \mu = k_B(4003\mathsf{K}), \Delta_0 = k_B(3.136\mathsf{K})]$

performed on $D_{\mathsf{P}}(y,z,\omega) > 0$ [see appendix §F] yields the critical frequencies for the

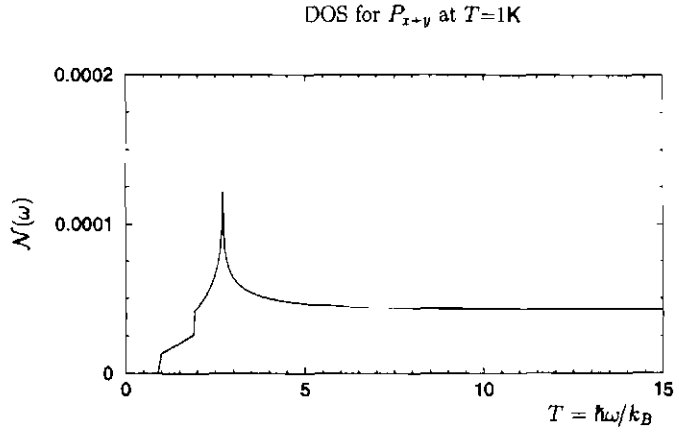

Figure 10: This figure shows the DOS for the P_{x+y} symmetry for positive frequency in units of temperature (1K), $T = \hbar\omega/k_B$. The gapped response begins at $T = \hbar\omega_{\mathsf{min}}/k_B = 0.897\mathsf{K}$. $[A = 1, B = 1, C = 0, t_x = k_B(5800\mathsf{K}), t_y = k_B(1226\mathsf{K}), t_z = k_B(48\mathsf{K}), \mu = k_B(4003\mathsf{K}), \Delta_0 = k_B(2.162\mathsf{K})]$

gapped symmetries (i.e., $A \neq 0$):

$$\omega_{\mathsf{min}}^2 = A^2\frac{{\Delta_0}^2}{\hbar^2}\left[1 - \frac{(\mu + t_y + t_z)^2}{t_x^2 - A^2{\Delta_0}^2}\right] \tag{83}$$

$$\omega_1^2 = A^2\frac{{\Delta_0}^2}{\hbar^2}\left[1 - \frac{(\mu + t_y - t_z)^2}{t_x^2 - A^2{\Delta_0}^2}\right] \tag{84}$$

$$\omega_2^2 = A^2\frac{{\Delta_0}^2}{\hbar^2}\left[1 - \frac{(\mu - t_y + t_z)^2}{t_x^2 - A^2{\Delta_0}^2}\right] \tag{85}$$

$$\omega_3^2 = A^2\frac{{\Delta_0}^2}{\hbar^2}\left[1 - \frac{(\mu - t_y - t_z)^2}{t_x^2 - A^2{\Delta_0}^2}\right]. \tag{86}$$

$$\omega_4^2 = \frac{{\Delta_0}^2}{\hbar^2}\left[[A^2 + B^2] - A^2B^2\frac{(\mu + t_z)^2}{A^2t_y^2 + KB^2}\right] \tag{87}$$

$$\omega_5^2 = \frac{{\Delta_0}^2}{\hbar^2}\left[[A^2 + B^2] - A^2B^2\frac{(\mu - t_z)^2}{A^2t_y^2 + KB^2}\right]. \tag{88}$$

$$\omega_6^2 = \frac{{\Delta_0}^2}{\hbar^2}\left[[A^2 + C^2] - A^2C^2\frac{(\mu + t_y)^2}{A^2t_z^2 + KC^2}\right] \tag{89}$$

$$\omega_7^2 = \frac{{\Delta_0}^2}{\hbar^2}\left[[A^2 + C^2] - A^2C^2\frac{(\mu - t_y)^2}{A^2t_z^2 + KC^2}\right]. \tag{90}$$

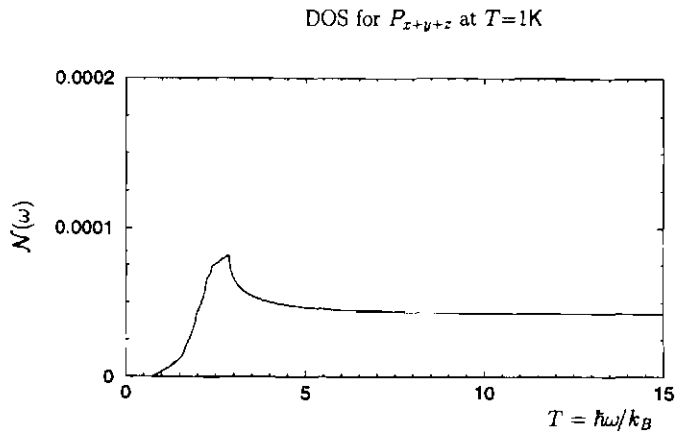

Figure 11: This figure shows the DOS for the P_{x+y+z} symmetry for positive frequency in units of temperature (1K), $T = \hbar\omega/k_B$. The gapped response begins at $T = \hbar\omega_{\rm min}/k_B = 0.745$K. $[A = B = C = \sqrt{2/3}, t_x = k_B(5800\text{K}), t_y = k_B(1226\text{K}), t_z = k_B(48\text{K}), \mu = k_B(4003\text{K}), \Delta_0 = k_B(2.199\text{K})]$

$$\omega_8^2 = \frac{{\Delta_0}^2}{\hbar^2}\left[[A^2+B^2+C^2] - A^2B^2C^2\frac{\mu^2}{A^2[t_z^2B^2+t_y^2C^2]+B^2C^2K}\right] \qquad (91)$$

$$K = t_x^2 - A^2\Delta_0^2$$

The frequencies $\{\omega_{\rm min}$—$\omega_3\}$ describe the P_x symmetry [Fig. 9]: the beginning of the gapped response, the location of the first kink, the locations of the leading and trailing edges of the peak respectively.

The P_{x+y} symmetry [Fig. 10] can be described in terms of $\{\omega_{\rm min}, ..., \omega_5\}$: the beginning of the gapped response, the location of leading and trailing edges of the first kink (step), the location of the leading edge of the second step and the locations of the leading and trailing edges of the peak. The P_{x+z} symmetry would have the same features except that $\{\omega_4$ & $\omega_5\}$ would be replaced by $\{\omega_6$ & $\omega_7\}$ corresponding to finite A & C and $B = 0$ instead of finite A & B and $C = 0$ as in the P_{x+y}.

The P_{x+y+z} symmetry [Fig. 11] is described in terms of $\{\omega_{\rm min}$—$\omega_8\}$: the beginning of the gapped response, the location of leading and trailing edges of the first two

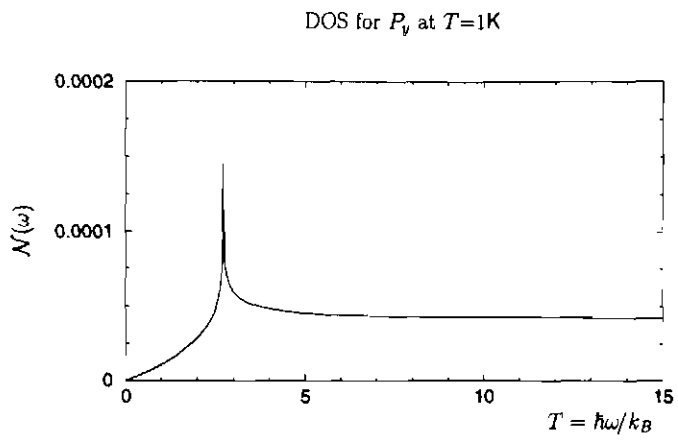

Figure 12: This figure shows the DOS for the P_y symmetry for positive frequency in units of temperature (1K), $T = \hbar\omega/k_B$. From the plot it is clear that this is a gapless symmetry. $[A = 0, B = 1, C = 0, t_x = k_B(5800\text{K}), t_y = k_B(1226\text{K}), t_z = k_B(48\text{K}), \mu = k_B(4003\text{K}), \Delta_0 = k_B(2.703\text{K})]$

kinks (steps), the location of the leading edge of the third step and the locations of the leading and trailing edges of the peak. In describing the P_{x+y+z} all nine frequencies are incorporated corresponding to finite A, B, C. Notice the *stubby* appearance of the plot. This is because all the special frequencies are located very near one another.

For the gapless symmetries (i.e., $A = 0$) [Figs. 12 & 13] the analysis performed on $D_P(y, z, \omega) > 0$ yields the critical frequencies:

$$\omega_{\text{min}}{}^2 = 0 \tag{92}$$

$$\omega_1{}^2 = \frac{|\Delta_0|^2}{\hbar^2} B^2 \tag{93}$$

$$\omega_2{}^2 = \frac{|\Delta_0|^2}{\hbar^2} C^2 \tag{94}$$

$$\omega_3{}^2 = \frac{|\Delta_0|^2}{\hbar^2} [B^2 + C^2]. \tag{95}$$

Further analysis [see appendix §F] reveals the cut-off frequencies

$$\hbar\omega_{\text{max},j=1} = |t_x + t_y + t_z + \mu| \tag{96}$$

$$\hbar\omega_{\text{max},j=2} = |t_x + t_y + t_z - \mu|. \tag{97}$$

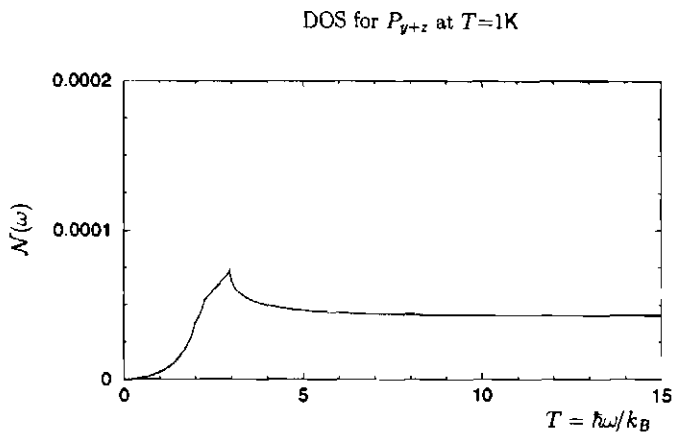

Figure 13: This figure shows the DOS for the P_{y+z} symmetry for positive frequency in units of temperature (1K), $T = \hbar\omega/k_B$. From the plot it is clear that this is a gapless symmetry. $[A = 0, B = 3\sqrt{2}/4, C = \sqrt{2 - B^2}, t_x = k_B(5800\text{K}), t_y = k_B(1226\text{K}), t_z = k_B(48\text{K}), \mu = k_B(4003\text{K}), \Delta_0 = k_B(2.091\text{K})]$

3.6 The Low Frequency Limit

The low frequency limit $|\omega| \sim \mathcal{O}(\omega_{\text{min}})$ of the quasiparticle density of states for selected symmetries $\text{sym} = \{D, P\}$ is discussed below (the low frequency limit for the S-symmetry has already been discussed) . In this limit one can exploit the fact that $|\omega| \sim \mathcal{O}(\omega_{\text{min}})$, which restricts the region of k-space in the 1^{st} Brillouin zone that can contribute to $\mathcal{N}(\omega)$. First we will look at the D_{xy}-symmetry and then selected P-symmetries.

3.6.1 Low Frequency D_{xy} Case

To find the low frequency limit observe that the largest contributions to the DOS, in Eq. 71, come from regions of the 1^{st} Brillouin zone where $\sqrt{D_{\text{D}_{xy}}(y, z, \omega)} \sim 0$. Contributing regions obey $D_{\text{D}_{xy}}(y, z, \omega) \geq 0$. Under the restriction $|\omega| \sim \mathcal{O}(\omega_{\text{min}})$ the contributing regions are bounded by the level curves $D_{\text{D}_{xy}}(y, z, \omega) = 0$ for a particular frequency ω.

These level curve shown below in figure 14 is for the gapless D_{xy}-symmetry. Observe

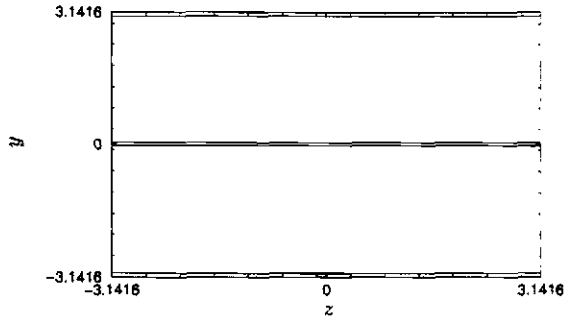

Figure 14: This figure shows the level curves corresponding to $D_{\mathsf{D}_{xy}} = 0$ for the gapless symmetry D_{xy}. $[t_x = k_B(5800\mathsf{K}), t_y = k_B(1226\mathsf{K}), t_z = k_B(48\mathsf{K}), \mu = k_B(4003\mathsf{K})]$

that when $\omega_{min} \leq |\omega| \leq \omega_1$ the contributing regions come from the edges and middle of the 1^{st} B.Z. Here $\omega = k_B(0.108\mathsf{K})/\hbar$ was used.

Expanding the numerator and denominator of Eq. 71 near the point $y = \pi$ and multiplying by four to pick up all the contributions (near $\pm\pi$ and above and below $y = 0$) reveals that at low frequency, the DOS for this symmetry has a linear dependence on frequency:

$$\mathcal{N}(\omega) = \frac{|\hbar\omega|}{\pi \sin(ak_F)}. \tag{98}$$

Next we look at the gapped P-symmetries.

3.6.2 Low Frequency Gapped P Cases

For the gapped P cases $\{P_x, P_{x+y}, P_{x+y+z}\}$ the level curves of $D_{\mathsf{P}} = 0$ are given in Fig. 15. For P_x $\omega = (\omega_1 + \omega_{\mathsf{min}})/2 = k_B(1.184\mathsf{K})/\hbar$ was used. For P_{x+y} $\omega = (\omega_1 + \omega_{\mathsf{min}})/2 = k_B(1.184\mathsf{K})/\hbar$ was used. For P_{x+y+z} $\omega = (\omega_1 + \omega_{\mathsf{min}})/2 = k_B(0.967\mathsf{K})/\hbar$ was used.

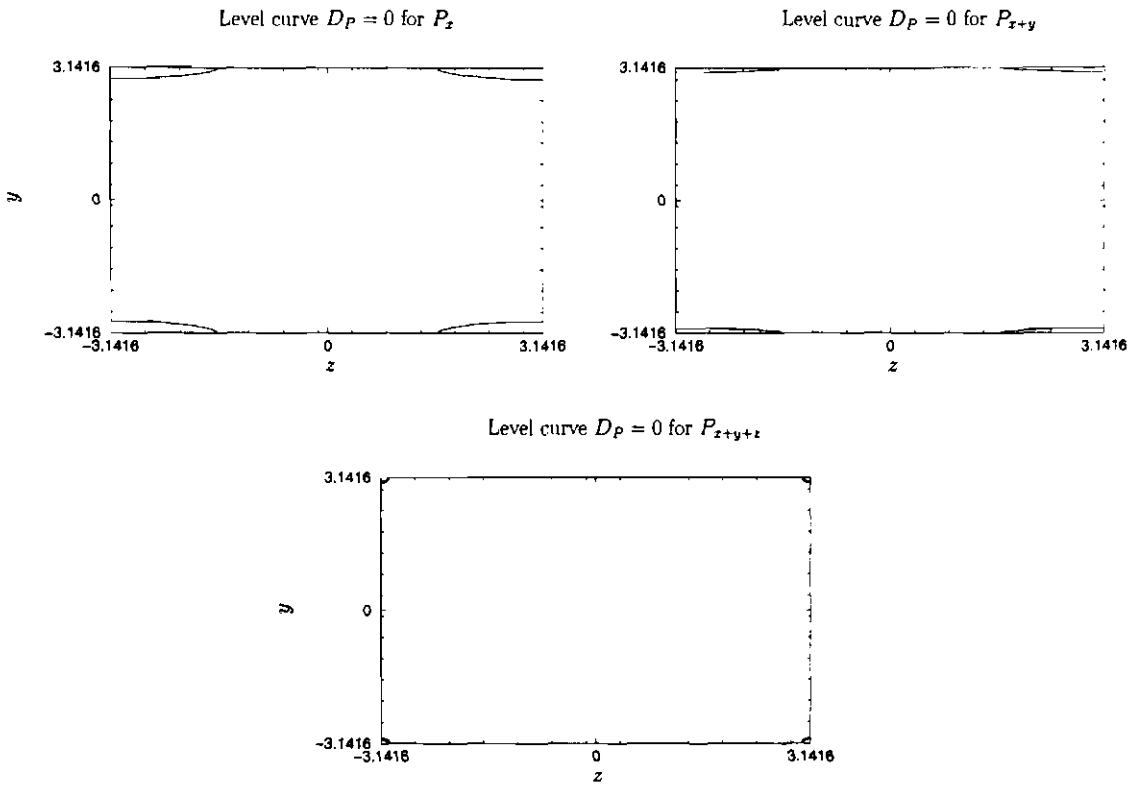

Figure 15: This figure shows the level curves corresponding to $D_{\mathsf{P}} = 0$ for the gapped symmetries P_x, P_{x+y}, P_{x+y+z} respectively. $[t_x = k_B(5800\mathsf{K}), t_y = k_B(1226\mathsf{K}), t_z = k_B(48\mathsf{K}), \mu = k_B(4003\mathsf{K})]$

Clearly there are four regions contributing to $\mathcal{N}(\omega)$ in low frequency. Expanding the integrand in Eq. 82 about the point $(y, z) = (\pi, \pi)$ and multiplying by four gives:

$$\mathcal{N}(\omega) = \frac{1}{2\pi^2 \sin(ak_F)} \sqrt{\frac{\Lambda_1}{\Lambda_2 \Lambda_3}} \Theta(\omega^2 - \omega_{\min}^2) \tag{99}$$
$$\times \left[|\hbar\omega| + \mathrm{sgn}(\omega) \frac{A^2 \Delta_0}{t_x^2 - A^2 \Delta_0^2} \left(t_y + t_z + \mu - \frac{t_y \Lambda_1}{6\Lambda_2} - \frac{t_z \Lambda_1}{6\Lambda_3} \right) \right]$$

where

$$\Lambda_1 = (t_x^2 - A^2|\Delta_0|^2)\hbar^2[\omega^2 - \omega_{\min}^2] \tag{100}$$

$$\Lambda_2 = |\Delta_0|^2[A^2 t_y(t_y + t_z + \mu) + B^2(t_x^2 - A^2|\Delta_0|^2)] \tag{101}$$

$$\Lambda_3 = |\Delta_0|^2[A^2 t_z(t_y + t_z + \mu) + C^2(t_x^2 - A^2|\Delta_0|^2)] \tag{102}$$

Clearly the DOS for the gapped symmetries has a rather complicated low frequency dependence. In very low frequency, though, the $|\hbar\omega|$ term is negligible compared to the second term and $\mathcal{N}(\omega) \propto [\omega^2 - \omega_{\min}^2]^{3/2}$.

Lastly, the gapless P-symmetries P_y & P_{y+z} are considered.

3.6.3 Low Frequency Gapless P Cases

For the gapless P cases $\{P_y, P_{y+z}\}$ the level curves of $D_{\mathsf{P}} = 0$ are given in Fig. 16.

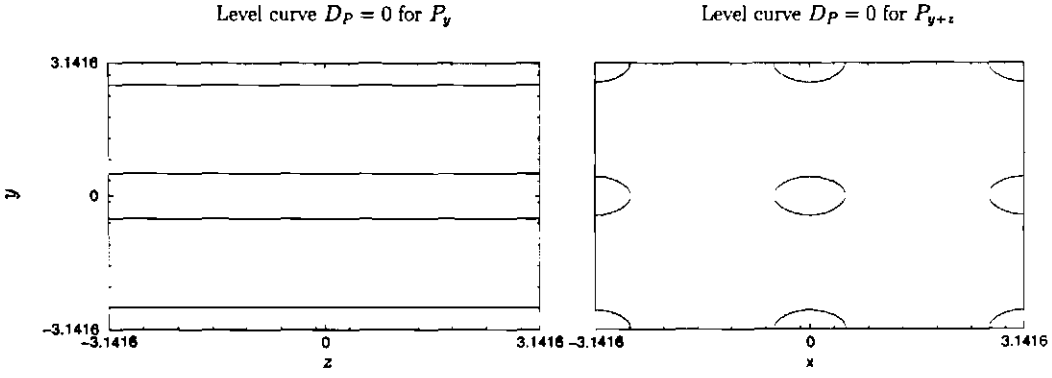

Figure 16: This figure shows the level curves corresponding to $D_{\mathsf{P}} = 0$ for the gapless symmetries P_y, P_{y+z} respectively. $[t_x = k_B(5800\mathrm{K}), t_y = k_B(1226\mathrm{K}), t_z = k_B(48\mathrm{K}), \mu = k_B(4003\mathrm{K})]$

For P_y $\omega = (\omega_1 + \omega_{\mathsf{min}})/2 = k_B(1.5\mathrm{K})/\hbar$ was used. For P_{y+z} $\omega = (\omega_1 + \omega_{\mathsf{min}})/2 = k_B(1.403\mathrm{K})/\hbar$ was used.

Clearly there are four regions contributing to $\mathcal{N}(\omega)$ in low frequency for the P_y case. Expanding the integrand in Eq. 82 near $y, = \pi$ and multiplying by four gives:

$$\mathcal{N}(\omega) = \frac{|\hbar\omega|}{\pi|\Delta_0 B\, t_x| \sin(ak_F)}. \tag{103}$$

Observe that for the P_{y+z} case there are nine contributing regions or equivalenty sixteen *quarter* sized regions. Expanding the integrand in Eq. 82 near the point $(y, z) = (\pi, \pi)$ and multiplying by 16 gives are result similar to the gapped case except that now $A = 0$. We get:

$$\mathcal{N}(\omega) = \frac{2(\hbar\omega)^2}{\pi^2|\Delta_0|^2|BCt_x|}. \tag{104}$$

Note the difference in the low frequency dependencies of the two gapless symmetries. The difference can be ascribed to the fact that for the P_y-symmetry the order parameter has line nodes on the Fermi surface while for the P_{y+z}-symmetry the order parameter has point nodes on the Fermi surface. Recall the calculation in §3.1 for the A-phase of ^{3}He. The order parameter for the A-phase had point nodes (at $\theta = 0, \pi$); consequently the low frequency density of states for ^{3}He in the A-phase had a quadratic dependence on ω.

Evidently, then a linear low frequency dependence implies a line of nodes on the Fermi surface.

3.7 Summary

In this section the quasiparticle density of states has been determined for various symmetries of the order parameter. Gapped and gapless symmetries have been explored for both the spin singlet and spin triplet pairing. The quasiparticle density of states depends on the magnitude of the order parameter so that it can be used only to determine whether the order parameter has nodes. It can provide good qualitative

and quantitative information about the k-dependence of the order parameter. However, it cannot provide information about orientation dependence since it depends on the magnitude of the order parameter:

$$\tfrac{1}{2}\mathrm{Tr}[\widehat{\Delta}_{\mathbf{k}}\widehat{\Delta}_{\mathbf{k}}^{\dagger}] = |\Delta_0 \mathbf{d}(\mathbf{k})|^2 \tag{105}$$

$$\text{where } \widehat{\Delta}_{\mathbf{k},\alpha\beta} = i\left[(\vec{\sigma}\sigma_2)\cdot\mathbf{d}(\mathbf{k})\right]_{\alpha\beta}.$$

The DOS could be measured with either an STM or photoemission experiment.

One can see that the energy gap is independent of the direction of the order parameter $\mathbf{d}(\mathbf{k})$. Since the DOS depends on just the magnitude of the order parameter through the energy gap, we will need to consider yet another quantity (e.g., a tensor susceptibility) if we are to study the directional aspect of the triplet superconducting order parameter. In this case the electron spin susceptibility can be used to provide information about the spin response of the system. In particular it can be used to specify whether pairing occurs in the spin singlet channel or the spin triplet channels.

Chapter IV

THE ELECTRON SPIN SUSCEPTIBILITY

The electron spin susceptibility can be used to provide information about the spin response of the system. The shape of the various tensor components depend on the symmetry and orientation of the order parameter in the lattice so that it can be used to determine the direction of the order parameter. It is useful to employ the trick of working in imaginary time $\tau = it$ so that when we analytically continue to real time (by Wick's rotation) we will acquire both time dependent and thermal information about the susceptibility.

4.1 Some Conventions

The local electron spin operator has the form

$$\mathsf{s}_n(\mathbf{r}_i,\tau) = \mathcal{N}_n \sum_{\alpha\beta} \Psi^\dagger_\alpha(\mathbf{r}_i,\tau)[\boldsymbol{\sigma}_n]_{\alpha\beta}\Psi_\beta(\mathbf{r}_i,\tau) \quad n = 1,2,3. \tag{106}$$

where

$$\boldsymbol{\sigma}_1 = \begin{pmatrix} 0 & 1 \\ 1 & 0 \end{pmatrix} \quad \boldsymbol{\sigma}_2 = \begin{pmatrix} 0 & -i \\ i & 0 \end{pmatrix} \quad \boldsymbol{\sigma}_3 = \begin{pmatrix} 1 & 0 \\ 0 & -1 \end{pmatrix}$$

are the usual Pauli spin matrices. These matrices can be put in a more compact form:

$$[\boldsymbol{\sigma}_n]_{\alpha\beta} = \begin{bmatrix} \eta_{n,2} & \eta_{n,3} \\ \eta_{n,1} & -\eta_{n,2} \end{bmatrix}_{\alpha\beta}$$

$$\eta_{n,1} = \delta_{n1} + i\delta_{n2}$$

$$\eta_{n,2} = \delta_{n3}$$

$$\eta_{n,3} = \delta_{n1} - i\delta_{n2}. \tag{107}$$

This is the generalized Pauli spin matrix in direction $n = \{1, 2, 3\}$. $\mathcal{N}_n$ is a normalization factor to be determined. $\mathbf{s}_n(\mathbf{r}_i, \tau)$ is the local electron spin operator in the lattice and describes an electron spin at position $\mathbf{r}_i$ and time τ. The sum is over the spin indices α, β.

All sums are indicated by an explicit sum-symbol $\sum$ with the correspondence between the discrete and continuous cases given by:

$$\sum_{\mathbf{k}} \longleftrightarrow \frac{V_0}{(2\pi)^3} \int \mathrm{d}^3 k$$
$$\sum_{\mathbf{r}} \longleftrightarrow \frac{1}{V} \int \mathrm{d}^3 r \tag{108}$$

where V is the volume of the unit cell. The Fourier Transformations in space and imaginary time are given by:

$$B_m(\mathbf{r}_i) = \sum_{\mathbf{k}} e^{i\mathbf{k}\cdot\mathbf{r}_i} B_m(\mathbf{k}) \tag{109}$$

$$B_m(\mathbf{k}) = \frac{1}{N_0} \sum_{\mathbf{r}_i} e^{-i\mathbf{k}\cdot\mathbf{r}_i} B_m(\mathbf{r}_i) \quad N_0 = \text{no. lattice sights} \tag{110}$$

$$D_m(\tau) = \frac{1}{\hbar\beta_0} \sum_{i\omega_n} e^{-i\omega_n \tau} D_m(i\omega_n) \tag{111}$$

$$D_m(i\omega_n) = \int_0^{\hbar\beta_0} \mathrm{d}\tau e^{i\omega_n \tau} D_m(\tau) \qquad \frac{1}{\beta_0} \doteq k_B T \tag{112}$$

The frequency expansion is valid whether one is considering Fermions or Bosons. In this case we are interested in Fermions so that the frequencies ω_n are the Fermion frequencies:

$$\hbar\omega_n = \frac{(2n+1)\pi}{\beta_0} \quad n \in \mathbf{I}. \tag{113}$$

For Bosons one would have $\hbar\omega_n = 2n\pi/\beta_0$. With these conventions we'll next consider the calculation of the susceptibility using the Kubo Formula.

4.2 The Kubo Formula: Linear Response Theory

The Kubo formula for the correlation between a pair of electron spins will be used to calculate the magnetic susceptibility for the superconducting systems we are interested in. First it is necessary to transform the Kubo formula to the momentum – and ultimately to the frequency – domain. The transformed correlation function (given below in terms of the electron magnetic moment m_a) will allow us to investigate the spin response of the system to an applied field of wave number $\mathbf{q}$ and frequency ω.

$$\begin{aligned}\chi_{mn}(\mathbf{r}_i, \mathbf{r}_j, \tau) &= \langle \mathsf{T}\mathcal{M}_m(\mathbf{r}_i, \tau)\mathcal{M}_n(\mathbf{r}_j, 0)\rangle \\ &= \sum_{\mathbf{k},\mathbf{k}'} e^{i\mathbf{k}\cdot\mathbf{r}_i + i\mathbf{k}'\cdot\mathbf{r}_j}\langle \mathsf{T}\mathcal{M}_m(\mathbf{k}, \tau)\mathcal{M}_n(\mathbf{k}', 0)\rangle. \qquad (114)\end{aligned}$$

$$\mathcal{M}_m = \sum_n \frac{\mu_B}{2} g_{mn}\mathsf{s}_n = \sum_n g_{mn}\frac{e}{mc}\left(\frac{\hbar}{2}\mathsf{s}_n\right) \qquad (115)$$

Note that the bare electron Lande g-factor can in general be a tensor. This is because it can be renormalized when there is spin-orbit coupling present. In an orthogonal crystal is diagonal $g_{mn} = g_m\delta_{mn}$. It is convenient to write $\chi_{mn}(\mathbf{Q}, \mathbf{q}, \tau)$ in terms of relative and center of mass coordinates:

$$\begin{aligned}\tilde{\mathbf{r}}_s &= \frac{1}{2}(\mathbf{r}_i - \mathbf{r}_j) \\ \mathbf{R}_l &= \frac{1}{2}(\mathbf{r}_i + \mathbf{r}_j).\end{aligned}$$

Observe that $\mathbf{R}$ and $\tilde{\mathbf{r}}$, being comprised of the discrete $\mathbf{r}_i$ and $\mathbf{r}_j$, also take discrete values and so are labeled with the discrete indices $\{l, s\}$ so that:

$$\chi_{mn}(\mathbf{R}_l, \tilde{\mathbf{r}}_s, \tau) = \sum_{\mathbf{k},\mathbf{k}'}\langle \mathsf{T}\mathcal{M}_m(\mathbf{k}, \tau)\mathcal{M}_n(\mathbf{k}', 0)\rangle \exp\left\{\frac{i}{2}[(\mathbf{k} - \mathbf{k}')\cdot\tilde{\mathbf{r}}_s + (\mathbf{k} + \mathbf{k}')\cdot\mathbf{R}_l]\right\} \qquad (116)$$

Note that in Eq. 114, $\mathbf{r}_j$ is the position of the electron *spin* at lattice site j. In Eq. 116, $\tilde{\mathbf{r}}_s$ is the relative coordinate between two electrons and specifies the relative position of two spins; in this case the index s ranges over all the possible relative displacements

of two electrons spins in the lattice.

Applying the Fourier transformation Eq. 110 to the relative and center of mass coordinates in Eq. 116 we obtain:

$$\begin{aligned}
\chi_{mn}(\mathbf{Q},\mathbf{q},\tau) &= N_0^{-2}\sum_{ls}\chi_{mn}(\mathbf{R}_l,\tilde{\mathbf{r}}_s,\tau)e^{-i\mathbf{Q}\cdot\mathbf{R}_l}e^{-i\mathbf{q}\cdot\mathbf{r}_s} \\
&= N_0^{-2}\sum_{\mathbf{k},\mathbf{k}'}\sum_{ls}\langle \mathsf{T}\mathcal{M}_m(\mathbf{k},\tau)\mathcal{M}_n(\mathbf{k}',0)\rangle e^{\left\{i[(\mathbf{k}-\mathbf{k}'-2\mathbf{q})\cdot\tilde{\mathbf{r}}_s+(\mathbf{k}+\mathbf{k}'-2\mathbf{Q})\cdot\mathbf{R}_l]/2\right\}} \\
&= N_0^{-2}\sum_{\mathbf{k},\mathbf{k}'}\langle \mathsf{T}\mathcal{M}_m(\mathbf{k},\tau)\mathcal{M}_n(\mathbf{k}',0)\rangle\,\delta_{\frac{\mathbf{k}-\mathbf{k}'}{2}-\mathbf{q},0}\,\delta_{\frac{\mathbf{k}+\mathbf{k}'}{2}-\mathbf{Q},0}\,N_0^2 \\
\chi_{mn}(\mathbf{Q},\mathbf{q},\tau) &= \langle \mathsf{T}\mathcal{M}_m(\mathbf{Q}+\mathbf{q},\tau)\mathcal{M}_n(\mathbf{Q}-\mathbf{q},0)\rangle. \qquad (117)
\end{aligned}$$

When the system in translationally invariant, only relative motions within the lattice are relevant so that the center of mass momentum can be set equal to zero $\mathbf{Q}=\mathbf{0}$. Using the relation between the magnetic moment $\mathcal{M}$ and the electron spin operator expressed in Eq. 115 we obtain:

$$\chi_{mn}(\mathbf{q},\tau) = \mathbb{G}_{mn}\langle \mathsf{T}\mathbf{s}_m(\mathbf{q},\tau)\mathbf{s}_n(-\mathbf{q},0)\rangle, \qquad (118)$$

where

$$\mathbb{G}_{mn} \doteq \left(\frac{\mu_B}{2}\right)^2 g_m g_n. \qquad (119)$$

This expression is known as the Kubo formula and will be used in the calculation of the electron spin susceptibility to be discussed in the next section.

4.3 Electron Spin Susceptibility Tensor

In this section the calculation of the susceptibility will follow from an application of the Kubo Formula, Eq. 118. The form of the local spin operator in real space is given above. In order to calculate $\chi_{mn}(\mathbf{q},\omega)$ it is useful to transform the local spin operator

into its reciprocal space form:

$$\begin{aligned} \mathsf{s}_m(\mathbf{q},\tau) &= N_0^{-1}\sum_j e^{-i\mathbf{q}\cdot\mathbf{r}_j}\mathsf{s}_m(\mathbf{r}_j,\tau) \\ &= N_0^{-1}\mathcal{N}_m\sum_j e^{-i\mathbf{q}\cdot\mathbf{r}_j}\sum_{\alpha\beta}\Psi_\alpha^\dagger(\mathbf{r}_j,\tau)[\boldsymbol{\sigma}_m]_{\alpha\beta}\Psi_\beta(\mathbf{r}_j,\tau) \\ &= N_0^{-1}\mathcal{N}_m\sum_{\alpha\beta j} e^{(-\mathbf{q}+\mathbf{k}-\mathbf{k}')\cdot\mathbf{r}_j}\Psi_\alpha^\dagger(\mathbf{k}',\tau)[\boldsymbol{\sigma}_m]_{\alpha\beta}\Psi_\beta(\mathbf{k},\tau). \end{aligned} \tag{120}$$

Because we are considering electrons moving in a superconductor, {**k**,**q**} take on the interpretation of momenta. Again $\Psi_\alpha(\mathbf{r}_i,\tau) = \sum_{\mathbf{k}} e^{i\mathbf{k}\cdot\mathbf{r}_i}\Psi_\alpha(\mathbf{k},\tau)$ and asserting the connection between Ψ_α & $\Psi_\alpha^\dagger$: $\Psi_\alpha^\dagger(\mathbf{r}_i,\tau) = \sum_{\mathbf{k}} e^{-i\mathbf{k}\cdot\mathbf{r}_i}\Psi_\alpha^\dagger(\mathbf{k},\tau)$ with an accompanying sign change with the conjugation of the phase. Summing the phase over all $\mathbf{r}_j$ gives a factor of $N_0\delta_{-\mathbf{q}+\mathbf{k}-\mathbf{k}',0}$. Finally, summing on $\mathbf{k}'$ gives:

$$\mathsf{s}_m(\mathbf{q},\tau) = \mathcal{N}_m\sum_{\mathbf{k}\alpha\beta}\Psi_\alpha^\dagger(\mathbf{k}-\mathbf{q},\tau)[\boldsymbol{\sigma}_m]_{\alpha\beta}\Psi_\beta(\mathbf{k},\tau). \tag{121}$$

Substituting Eq. 121 into Eq. 118 leads to:

$$\chi_{mn}(\mathbf{q},\tau) \;=\; \mathcal{N}_m\mathcal{N}_n\mathbb{G}_{mn}\sum_{\mathbf{k},\mathbf{k}'}\sum_{\alpha\beta\gamma\delta}[\boldsymbol{\sigma}_m]_{\alpha\beta}[\boldsymbol{\sigma}_n]_{\gamma\delta}\,\mathcal{C}_{\alpha\beta\gamma\delta}(\mathbf{k},\mathbf{k}',\mathbf{q},\tau), \tag{122}$$

where

$$\mathcal{C}_{\alpha\beta\gamma\delta}(\mathbf{k},\mathbf{k}',\mathbf{q},\tau) \;=\; \langle \mathsf{T}\Psi_\alpha^\dagger(\mathbf{k}-\mathbf{q},\tau)\Psi_\beta(\mathbf{k},\tau)\Psi_\gamma^\dagger(\mathbf{k}'+\mathbf{q},0)\Psi_\delta(\mathbf{k}',0)\rangle. \tag{123}$$

In the next step the tensor $\mathcal{C}_{\alpha\beta\gamma\delta}(\mathbf{k},\mathbf{k}',\mathbf{q},\tau)$ is contracted out using Wick's Theorem [18]. Observe that there are two sets of contractions. Performing contractions between the $\Psi_\alpha(\mathbf{k},\tau)$ evaluated at different times:

<u>First contraction</u>:

$$\begin{aligned} &= -\langle \mathsf{T}\Psi_\delta(\mathbf{k}',0)\Psi_\alpha^\dagger(\mathbf{k}-\mathbf{q},\tau)\rangle\langle \mathsf{T}\Psi_\beta(\mathbf{k},\tau)\Psi_\gamma^\dagger(\mathbf{k}'+\mathbf{q},0)\rangle \\ &= -G_{\delta\alpha}(\mathbf{k}',0;\mathbf{k}-\mathbf{q},\tau)G_{\beta\gamma}(\mathbf{k},\tau;\mathbf{k}'+\mathbf{q},0) \\ &= -G_{\delta\alpha}(\mathbf{k}-\mathbf{q},-\tau)G_{\beta\gamma}(\mathbf{k},\tau)\delta_{\mathbf{k}',\mathbf{k}-\mathbf{q}}\delta_{\mathbf{k},\mathbf{k}'+\mathbf{q}}\delta_{\alpha\delta}\delta_{\beta\gamma} \end{aligned} \tag{124}$$

Second contraction:

$$
\begin{aligned}
&= -\langle \mathsf{T}\Psi^{\dagger}_{\alpha}(\mathbf{k}-\mathbf{q},\tau)\Psi^{\dagger}_{\gamma}(\mathbf{k}'+\mathbf{q},0)\rangle\langle \mathsf{T}\Psi_{\beta}(\mathbf{k},\tau)\Psi_{\delta}(\mathbf{k}',0)\rangle \\
&= -F^{\dagger}_{\alpha\gamma}(-\mathbf{k}+\mathbf{q},\tau;\mathbf{k}'+\mathbf{q},0)F_{\beta\delta}(\mathbf{k},\tau;-\mathbf{k}',0) \\
&= -F^{\dagger}_{\alpha\gamma}(-\mathbf{k}+\mathbf{q},\tau)F_{\beta\delta}(\mathbf{k},\tau)\delta_{-\mathbf{k}+\mathbf{q},\mathbf{k}'+\mathbf{q}}\delta_{\mathbf{k},-\mathbf{k}'} \qquad (125)
\end{aligned}
$$

where the definitions

$$-\langle \mathsf{T}\Psi_{\alpha}(\mathbf{k},\tau)\Psi^{\dagger}_{\beta}(\mathbf{k}',\tau_0)\rangle \doteq G_{\alpha\beta}(\mathbf{k},\tau-\tau_0)\delta_{\mathbf{k},\mathbf{k}'}\delta_{\alpha\beta} \qquad (126)$$

$$\langle \mathsf{T}\Psi_{\alpha}(\mathbf{k},\tau)\Psi_{\beta}(\mathbf{k}',\tau_0)\rangle \doteq F_{\alpha\beta}(\mathbf{k},\tau-\tau_0)\delta_{\mathbf{k},-\mathbf{k}'} \qquad (127)$$

$$\langle \mathsf{T}\Psi^{\dagger}_{\alpha}(\mathbf{k},\tau)\Psi^{\dagger}_{\beta}(\mathbf{k}',\tau_0)\rangle \doteq F^{\dagger}_{\alpha\beta}(-\mathbf{k},\tau-\tau_0)\delta_{-\mathbf{k},\mathbf{k}'} \qquad (128)$$

have been applied. The first contraction (Eqs. 124) represent single particle propagation. In this case, the momentum and spin of the particle are conserved. The Kronecker deltas appearing in the third line then, reflect the conservation of momentum and spin for a single particle.

The second contraction represents pairing. It accounts for the existence of pairs of fermions in the ground state (at $T = 0$) and at finite temperature. The pair propagator F depends on the momentum of the individual electrons that make the Fermion pair and the time interval $\tau = \tau_2 - \tau_1$ over which the pair propagates. In the pair propagator, F, the labels $(\mathbf{k}-\mathbf{q})$ and $(\mathbf{k}'+\mathbf{q})$ are the respective momenta of the individual fermions forming the paired state. Assuming that the ground state contains only pairs of particles with opposite momentum one has $(\mathbf{k}-\mathbf{q}) = -(\mathbf{k}'+\mathbf{q})$.

In the third line F is then labeled with the momentum of one of the constituent particles (the other pair member necessarily has opposite momentum). In passing to the third line the redundant momentum label is discarded, but the pairing of opposite momenta is still accounted for by the appearance of the Kronecker deltas.

In what follows the nonuniform dynamical susceptibility tensor $\chi_{mn}(\mathbf{q},\tau)$ is developed. Putting all the pieces together the susceptibility becomes:

$$\chi_{mn}(\mathbf{q},\tau) = -\mathcal{N}_m\mathcal{N}_n\mathbb{G}_{mn}\sum_{\mathbf{k},\mathbf{k}'}\sum_{\alpha\beta\gamma\delta}[\boldsymbol{\sigma}_m]_{\alpha\beta}[\boldsymbol{\sigma}_n]_{\gamma\delta}\otimes$$
$$\otimes\left[G_{\delta\alpha}(\mathbf{k}-\mathbf{q},-\tau)\,G_{\beta\gamma}(\mathbf{k},\tau)\delta_{\mathbf{k}',\mathbf{k}-\mathbf{q}}\delta_{\mathbf{k},\mathbf{k}'+\mathbf{q}}\delta_{\alpha\delta}\delta_{\beta\gamma}\right.$$
$$\left.+F^{\dagger}_{\alpha\gamma}(-\mathbf{k}+\mathbf{q},\tau)\,F_{\beta\delta}(\mathbf{k},\tau)\delta_{-\mathbf{k}+\mathbf{q},\mathbf{k}'+\mathbf{q}}\delta_{\mathbf{k},-\mathbf{k}'}\right]$$

and summing on $\mathbf{k}'$:

$$\chi_{mn}(\mathbf{q},\tau) = -\mathcal{N}_m\mathcal{N}_n\mathbb{G}_{mn}\sum_{\mathbf{k}}\sum_{\alpha\beta\gamma\delta}[\boldsymbol{\sigma}_m]_{\alpha\beta}[\boldsymbol{\sigma}_n]_{\gamma\delta}\left[G_{\delta\alpha}(\mathbf{k}-\mathbf{q},-\tau)\,G_{\beta\gamma}(\mathbf{k},\tau)\delta_{\alpha\delta}\delta_{\beta\gamma}\right.$$
$$\left.+\,F^{\dagger}_{\alpha\gamma}(-\mathbf{k}+\mathbf{q},\tau)\,F_{\beta\delta}(\mathbf{k},\tau)\right]. \quad (129)$$

Next the susceptibility is transformed to the frequency domain by first writing the propagators in terms of an expansion over Matsubara frequencies. Writing the G and F functions in a frequency expansion using Eq. 111:

$$\chi_{mn}(\mathbf{q},\tau) = -\mathcal{N}_m\mathcal{N}_n\mathbb{G}_{mn}\left(\frac{1}{\hbar\beta_0}\right)^2\sum_{\mathbf{k}}\sum_{\alpha\beta\gamma\delta}\sum_{i\omega_S i\omega_P}[\boldsymbol{\sigma}_m]_{\alpha\beta}[\boldsymbol{\sigma}_n]_{\gamma\delta}\otimes$$
$$\otimes\left[+e^{i\omega_S\tau}e^{-i\omega_P\tau}G_{\delta\alpha}(\mathbf{k}-\mathbf{q},i\omega_S)\,G_{\beta\gamma}(\mathbf{k},i\omega_P)\right.$$
$$\left.+e^{-i\omega_S\tau}e^{-i\omega_P\tau}F^{\dagger}_{\alpha\gamma}(-\mathbf{k}+\mathbf{q},i\omega_S)\,F_{\beta\delta}(\mathbf{k},i\omega_P)\right]. \quad (130)$$

Performing the frequency transformation

$$\chi_{mn}(\mathbf{q},i\omega) = \int_0^{\hbar\beta_0} d\tau\, e^{i\omega\tau}\chi_{mn}(\mathbf{q},\tau) \quad (131)$$

and using the fact that $\int_0^{\hbar\beta_0} d\tau\, e^{i\omega\tau}e^{\pm i\nu\tau} = \hbar\beta_0\delta_{\omega\pm\nu}$ Eq. 130 becomes

$$\chi_{mn}(\mathbf{q},i\omega) = -\mathcal{N}_m\mathcal{N}_n\mathbb{G}_{mn}\left(\frac{1}{\hbar\beta_0}\right)^2\sum_{\mathbf{k}}\sum_{\alpha\beta\gamma\delta}\sum_{i\omega_S i\omega_P}[\boldsymbol{\sigma}_m]_{\alpha\beta}[\boldsymbol{\sigma}_n]_{\gamma\delta}\otimes$$
$$\otimes\hbar\beta_0\left[\delta_{\omega+\omega_S-\omega_P}G_{\delta\alpha}(\mathbf{k}-\mathbf{q},i\omega_S)\,G_{\beta\gamma}(\mathbf{k},i\omega_P)\right.$$
$$\left.+\delta_{\omega-\omega_S-\omega_P}F^{\dagger}_{\alpha\gamma}(-\mathbf{k}+\mathbf{q},i\omega_S)\,F_{\beta\delta}(\mathbf{k},i\omega_P)\right]. \quad (132)$$

upon integration over τ. Further summation over $i\omega_S$ leads to

$$\chi_{mn}(\mathbf{q}, i\omega) = -\mathcal{N}_m\mathcal{N}_n\mathbb{G}_{mn}\left(\frac{1}{\hbar\beta_0}\right)\sum_{\mathbf{k}}\sum_{\alpha\beta\gamma\delta}\sum_{i\omega_P}[\boldsymbol{\sigma}_m]_{\alpha\beta}[\boldsymbol{\sigma}_n]_{\gamma\delta}\otimes \tag{133}$$

$$\otimes\left[G_{\delta\alpha}(\mathbf{k}-\mathbf{q}, i\omega - i\omega_P)\, G_{\beta\gamma}(\mathbf{k}, i\omega_P) + F^{\dagger}_{\alpha\gamma}(-\mathbf{k}+\mathbf{q}, i\omega - i\omega_P)\, F_{\beta\delta}(\mathbf{k}, i\omega_P)\right].$$

Observe that to obtain the susceptibility as a function of wave vector $\mathbf{q}$ and frequency there are eight summations left to be performed: three from the $\mathbf{k}$ summation, four from the spin index summation and one remaining frequency summation.

In the next section the form of the Green functions will be specified at which point the frequency summation is performed first using a trick from complex analysis [see appendix §B]. We can then consider the sum on the spin indices $\{\alpha, \beta, \gamma, \delta\}$. The result of the spin sum will be seen to depend on whether we consider pairing in the spin singlet or spin triplet channel. Lastly, the sum on $\mathbf{k}$ is performed.

Consideration of $\chi(\mathbf{q}, \omega, T)$ is made for the unitary case in the next section.

4.4 The Unitary Electron Spin Susceptibility

The unitary electron spin susceptibility characterizes the spin response of electrons paired in a unitary state (i.e., a state that preserves time reversal symmetry). The order parameter, corresponding to a unitary pairing state, obeys a unitary condition:

$$\widehat{\Delta}(\mathbf{k})\widehat{\Delta}(\mathbf{k})^{\dagger} \propto \mathbb{I}. \tag{134}$$

This is significant for the case of triplet pairing, where in principle, pairs could exist in a nonunitary triplet pairing state that breaks time reversal symmetry. Accordingly the order parameter then would not obey the unitary condition.

Beginning with the form of the Green functions for the unitary case we have:

$$G_{\lambda\mu}(\mathbf{k}, i\omega) = -\frac{i\hbar\omega - \xi_{\mathbf{k}}}{\hbar^2\omega^2 + \xi_{\mathbf{k}}^2 + \frac{1}{2}\mathsf{Tr}|\widehat{\Delta}_{\mathbf{k}}|^2}\delta_{\lambda,\mu} \tag{135}$$

$$F_{\lambda\mu}(\mathbf{k}, i\omega) = \frac{\Delta_{\lambda\mu}(\mathbf{k})}{\hbar^2\omega^2 + \xi_{\mathbf{k}}^2 + \frac{1}{2}\mathsf{Tr}|\widehat{\Delta}_{\mathbf{k}}|^2} \tag{136}$$

which can be derived from the equations of motion for the Green functions:

$$\frac{\partial G_{\alpha\beta}(\mathbf{k}, \tau - \tau_0)}{\partial\tau} = -\frac{\partial}{\partial\tau}\langle \mathsf{T}\Psi_\alpha(\mathbf{k}, \tau)\Psi_\beta^\dagger(\mathbf{k}, \tau_0)\rangle \tag{137}$$

$$\frac{\partial F_{\alpha\beta}(\mathbf{k}, \tau - \tau_0)}{\partial\tau} = \frac{\partial}{\partial\tau}\langle \mathsf{T}\Psi_\alpha(\mathbf{k}, \tau)\Psi_\beta(-\mathbf{k}, \tau_0)\rangle \tag{138}$$

$$\frac{\partial F_{\alpha\beta}^\dagger(\mathbf{k}, \tau - \tau_0)}{\partial\tau} = \frac{\partial}{\partial\tau}\langle \mathsf{T}\Psi_\alpha^\dagger(-\mathbf{k}, \tau)\Psi_\beta^\dagger(\mathbf{k}, \tau_0)\rangle. \tag{139}$$

The derivation is outlined in the book by Mahan [18] and in the paper by Sigrist and Ueda [20]. Expanding the Green functions by partial fraction (in anticipation of performing the frequency sum) we have for the single particle propagator

$$G_{\lambda\mu}(\mathbf{k}, i\omega) = \left[\frac{u_{\mathbf{k}}^2}{i\hbar\omega - E_{\mathbf{k}}} + \frac{v_{\mathbf{k}}^2}{i\hbar\omega + E_{\mathbf{k}}}\right] \tag{140}$$

and for the pair propagator

$$F_{\lambda\mu}(\mathbf{k}, i\omega) = \frac{\Delta_{\lambda\mu}(\mathbf{k})}{2E_{\mathbf{k}}}\left[\frac{1}{i\hbar\omega + E_{\mathbf{k}}} - \frac{1}{i\hbar\omega - E_{\mathbf{k}}}\right] \tag{141}$$

where the quasiparticle & quasihole coherence factors are given

$$u_{\mathbf{k}}^2 = \frac{1}{2}\left(1 + \frac{\xi_{\mathbf{k}}}{E_{\mathbf{k}}}\right) \tag{142}$$

$$v_{\mathbf{k}}^2 = \frac{1}{2}\left(1 - \frac{\xi_{\mathbf{k}}}{E_{\mathbf{k}}}\right). \tag{143}$$

The order parameter for the singlet and triplet pairing channels we have

$$\Delta_{\lambda\mu}^{\mathsf{S}}(\mathbf{k}) = i\Delta_0 g(\mathbf{k})[\boldsymbol{\sigma}_2]_{\lambda\mu} \tag{144}$$

and

$$\Delta_{\lambda\mu}^{\mathsf{T}}(\mathbf{k}) = i\Delta_0[\vec{\boldsymbol{\sigma}}\boldsymbol{\sigma}_2 \cdot \mathbf{d}(\mathbf{k})]_{\lambda\mu} \tag{145}$$

respectively. The quasiparticle excitation energy is given by [see §2.2 and §A]

$$E_{\mathbf{k}}^{i} = \sqrt{\xi_{\mathbf{k}}^2 + \tfrac{1}{2}\mathsf{Tr}\{\widehat{\Delta}^{i\,\dagger}(\mathbf{k})\widehat{\Delta}^{i}(\mathbf{k})\}} \doteq \sqrt{\xi_{\mathbf{k}}^2 + \tfrac{1}{2}\mathsf{Tr}|\widehat{\Delta}^{i}(\mathbf{k})|^2} \quad i = \mathsf{S},\mathsf{T} \tag{146}$$

where for singlet

$$\frac{1}{2}\mathsf{Tr}|\widehat{\Delta}^{\mathsf{S}}(\mathbf{k})|^2 = |\Delta_0 g(\mathbf{k})|^2$$

and for triplet

$$\frac{1}{2}\mathsf{Tr}|\widehat{\Delta}^{\mathsf{T}}(\mathbf{k})|^2 = |\Delta_0 \mathbf{d}(\mathbf{k})|^2.$$

Note that in performing partial fractions on the Green Functions that the coherence factors $u_{\mathbf{k}}^2$ and $v_{\mathbf{k}}^2$ were obtained. From BCS theory $u_{\mathbf{k}}^2$ is interpreted as a measure how much of the quasiparticle is particle (electron) and $v_{\mathbf{k}}^2$ specifies how much is (hole). These quantities differ from the case of the nonunitary susceptibility worked out in the appendix [see appendix §D.3].

Also recall from the discussion of the spin structure of paired states [see section §2.2] that the gap function has two distinct general forms that are symmetry dependent. Eq. 144 is the order parameter for the singlet case and depends on a scalar order parameter (called $g(\mathbf{k})$ here) multiplied by an antisymmetric matrix. Eq. 145 is the order parameter for the triplet case and depends on a vector order parameter $\mathbf{d}(\mathbf{k})$ multiplied by a symmetric matrix. The matrices in both expressions account for particle exchange under the spin indices: antisymmetric in indices for singlet; symmetric for triplet.

Lastly, note the use of the trace symbol (Tr) in the expression for the energy dispersion. This is to emphasize the fact that the energy gap intrinsically depends on a nonscalar quantity.

The expanded form of the Green functions can be used to write χ_{mn} in Eq. 133 as

$$\chi_{mn}(\mathbf{q}, i\omega) = \tag{147}$$
$$-\mathcal{N}_m\mathcal{N}_n\mathbb{G}_{mn}\sum_{\mathbf{k}}\sum_{\alpha\beta\gamma\delta}[\boldsymbol{\sigma}_m]_{\alpha\beta}[\boldsymbol{\sigma}_n]_{\gamma\delta}\left[\Pi^I_{\alpha\beta\gamma\delta}(\mathbf{k},\mathbf{q},i\omega)+\Pi^{II}_{\alpha\beta\gamma\delta}(\mathbf{k},\mathbf{q},i\omega)\right].$$

Π^I and Π^{II} come from the single particle and pair propagators in Eq. 133 respectively. These functions are then defined to be

$$\Pi^I_{\alpha\beta\gamma\delta}(\mathbf{k},\mathbf{q},i\omega) \doteq \frac{1}{\hbar\beta}\sum_{i\omega_P}G_{\delta\alpha}(\mathbf{k}-\mathbf{q},i\omega-i\omega_P)G_{\beta\gamma}(\mathbf{k},i\omega_P) \tag{148}$$
$$= \frac{1}{\hbar\beta}\sum_{i\omega_P}\left[\frac{u^2_{\mathbf{k}-\mathbf{q}}}{i\hbar\omega_P - i\hbar\omega - E_{-\mathbf{k}+\mathbf{q}}} - \frac{v^2_{\mathbf{k}-\mathbf{q}}}{i\hbar\omega_P - i\hbar\omega + E_{-\mathbf{k}+\mathbf{q}}}\right]\otimes$$
$$\otimes\left[\frac{u^2_{\mathbf{k}}}{i\hbar\omega_P - E_{\mathbf{k}}} - \frac{v^2_{\mathbf{k}}}{i\hbar\omega_P + E_{\mathbf{k}}}\right]\delta_{\alpha\delta}\delta_{\beta\gamma}$$

coming from the single particle propagators and

$$\Pi^{II}_{\alpha\beta\gamma\delta}(\mathbf{k},\mathbf{q},i\omega) \doteq \frac{1}{\hbar\beta}\sum_{i\omega_P}F^{\dagger}_{\alpha\gamma}(-\mathbf{k}+\mathbf{q},i\omega-i\omega_P)F_{\beta\delta}(\mathbf{k},i\omega_P) \tag{149}$$
$$=\frac{1}{\hbar\beta}\frac{\Delta^{\dagger}_{\alpha\gamma}(-\mathbf{k}+\mathbf{q})\Delta_{\beta\delta}(\mathbf{k})}{4E_{-\mathbf{k}+\mathbf{q}}E_{\mathbf{k}}}\otimes$$
$$\otimes\sum_{i\omega_P}\left[\frac{1}{i\hbar\omega_P - i\hbar\omega + E_{-\mathbf{k}+\mathbf{q}}} - \frac{1}{i\hbar\omega_P - i\hbar\omega - E_{-\mathbf{k}+\mathbf{q}}}\right]\left[\frac{1}{i\hbar\omega_P + E_{\mathbf{k}}} - \frac{1}{i\hbar\omega_P - E_{\mathbf{k}}}\right]$$

coming from the pair propagators. Using the expanded form simplifies the summation over Matsubara frequencies [see appendix §B]. We obtain:

$$\Pi^I_{\alpha\beta\gamma\delta}(\mathbf{k},\mathbf{q},i\omega) = \delta_{\alpha\delta}\delta_{\beta\gamma}\Bigg\{$$
$$(1-f(E_{\mathbf{k}-\mathbf{q}})-f(E_{\mathbf{k}}))\left[\frac{u^2_{\mathbf{k}}v^2_{\mathbf{k}-\mathbf{q}}}{i\hbar\omega - E_{\mathbf{k}-\mathbf{q}} - E_{\mathbf{k}}} - \frac{u^2_{\mathbf{k}-\mathbf{q}}v^2_{\mathbf{k}}}{i\hbar\omega + E_{\mathbf{k}-\mathbf{q}} + E_{\mathbf{k}}}\right]$$
$$+(f(E_{\mathbf{k}-\mathbf{q}})-f(E_{\mathbf{k}}))\left[\frac{u^2_{\mathbf{k}-\mathbf{q}}u^2_{\mathbf{k}}}{i\hbar\omega + E_{\mathbf{k}-\mathbf{q}} - E_{\mathbf{k}}} - \frac{v^2_{\mathbf{k}-\mathbf{q}}v^2_{\mathbf{k}}}{i\hbar\omega - E_{\mathbf{k}-\mathbf{q}} + E_{\mathbf{k}}}\right]\Bigg\} \tag{150}$$

and

$$\Pi^{II}_{\alpha\beta\gamma\delta}(\mathbf{k},\mathbf{q},i\omega) = \frac{\Delta^{\dagger}_{\alpha\gamma}(-\mathbf{k}+\mathbf{q})\Delta_{\beta\delta}(\mathbf{k})}{4E_{-\mathbf{k}+\mathbf{q}}E_{\mathbf{k}}}\Bigg\{$$
$$(1-f(E_{-\mathbf{k}+\mathbf{q}})-f(E_{\mathbf{k}}))\left[\frac{1}{i\hbar\omega+E_{-\mathbf{k}+\mathbf{q}}+E_{\mathbf{k}}}-\frac{1}{i\hbar\omega-E_{-\mathbf{k}+\mathbf{q}}-E_{\mathbf{k}}}\right]$$
$$+(f(E_{-\mathbf{k}+\mathbf{q}})-f(E_{\mathbf{k}}))\left[\frac{1}{i\hbar\omega+E_{-\mathbf{k}+\mathbf{q}}-E_{\mathbf{k}}}-\frac{1}{i\hbar\omega-E_{-\mathbf{k}+\mathbf{q}}+E_{\mathbf{k}}}\right]\Bigg\}. \quad (151)$$

Observe the appearance of the Fermi functions after the frequency sums were performed. In substituting $\Pi^{I}_{\alpha\beta\gamma\delta}(\mathbf{k},\mathbf{q},i\omega)$ and $\Pi^{II}_{\alpha\beta\gamma\delta}(\mathbf{k},\mathbf{q},i\omega)$ into Eq. 147 spin sums arise having the form:

$$\sum_{\alpha\beta\gamma\delta}[\boldsymbol{\sigma}_m]_{\alpha\beta}[\boldsymbol{\sigma}_n]_{\gamma\delta}\,\delta_{\alpha\delta}\delta_{\beta\gamma} \quad (152)$$

$$\sum_{\alpha\beta\gamma\delta}[\boldsymbol{\sigma}_m]_{\alpha\beta}[\boldsymbol{\sigma}_n]_{\gamma\delta}\,\Delta^{\dagger}_{\alpha\gamma}(-\mathbf{k}+\mathbf{q})\Delta_{\beta\delta}(\mathbf{k}) \quad (153)$$

The first sum is independent of whether one is considering pairing in the singlet or triplet channel. Referring to appendix §C the first sum evaluates to:

$$\sum_{\alpha\beta\gamma\delta}[\boldsymbol{\sigma}_m]_{\alpha\beta}[\boldsymbol{\sigma}_n]_{\gamma\delta}\,\delta_{\alpha\delta}\delta_{\beta\gamma} = 2\delta_{mn}. \quad (154)$$

Due to the appearance of the spin dependent order parameter in the second sum, the spin symmetry of the system (either singlet or triplet) needs to be accounted for. Referring to the appendix §C for the singlet case one obtains:

$$\sum_{\alpha\beta\gamma\delta}[\boldsymbol{\sigma}_m]_{\alpha\beta}[\boldsymbol{\sigma}_n]_{\gamma\delta}\,\Delta^{\dagger}_{\alpha\gamma}(-\mathbf{k}+\mathbf{q})\Delta_{\beta\delta}(\mathbf{k}) = 2\delta_{mn}|\Delta_0|^2 g^*(-\mathbf{k}+\mathbf{q})g(\mathbf{k}). \quad (155)$$

For the unitary triplet case one obtains:

$$\sum_{\alpha\beta\gamma\delta}[\boldsymbol{\sigma}_m]_{\alpha\beta}[\boldsymbol{\sigma}_n]_{\gamma\delta}\,\Delta^{\dagger}_{\alpha\gamma}(-\mathbf{k}+\mathbf{q})\Delta_{\beta\delta}(\mathbf{k}) =$$
$$2|\Delta_0|^2\Big\{\mathbf{d}^*(-\mathbf{k}+\mathbf{q})\cdot\mathbf{d}(\mathbf{k})\delta_{mn}-[d^*_{\alpha}(-\mathbf{k}+\mathbf{q})\,d_{\beta}(\mathbf{k})+d^*_{\beta}(-\mathbf{k}+\mathbf{q})\,d_{\alpha}(\mathbf{k})]\Big\}. \quad (156)$$

After some simplification [see appendix §D] the singlet susceptibility tensor becomes:

$$\chi^{\mathsf{S}}_{mn}(\mathbf{q},i\omega) = -2\delta_{mn}\,\mathcal{N}_m\mathcal{N}_n\mathbb{G}_{mn}\sum_{\mathbf{k}}\Bigg\{\frac{|\Delta_0|^2 g^*(\mathbf{k}+\mathbf{q})g(\mathbf{k})}{4E_{\mathbf{k}+\mathbf{q}}E_{\mathbf{k}}}\otimes \tag{157}$$

$$\otimes\Bigg(\left(1-f(E_{\mathbf{k}+\mathbf{q}})-f(E_{\mathbf{k}})\right)\left[\frac{1}{i\hbar\omega+E_{\mathbf{k}+\mathbf{q}}+E_{\mathbf{k}}}-\frac{1}{i\hbar\omega-E_{\mathbf{k}+\mathbf{q}}-E_{\mathbf{k}}}\right]$$

$$+\left(f(E_{\mathbf{k}+\mathbf{q}})-f(E_{\mathbf{k}})\right)\left[\frac{1}{i\hbar\omega+E_{\mathbf{k}+\mathbf{q}}-E_{\mathbf{k}}}-\frac{1}{i\hbar\omega-E_{\mathbf{k}+\mathbf{q}}+E_{\mathbf{k}}}\right]\Bigg)$$

$$+\Bigg(\left(1-f(E_{\mathbf{k}+\mathbf{q}})-f(E_{\mathbf{k}})\right)\left[\frac{u^2_{\mathbf{k}}v^2_{\mathbf{k}+\mathbf{q}}}{i\hbar\omega-E_{\mathbf{k}+\mathbf{q}}-E_{\mathbf{k}}}-\frac{u^2_{\mathbf{k}+\mathbf{q}}v^2_{\mathbf{k}}}{i\hbar\omega+E_{\mathbf{k}+\mathbf{q}}+E_{\mathbf{k}}}\right]$$

$$+\left(f(E_{\mathbf{k}+\mathbf{q}})-f(E_{\mathbf{k}})\right)\left[\frac{u^2_{\mathbf{k}+\mathbf{q}}u^2_{\mathbf{k}}}{i\hbar\omega+E_{\mathbf{k}+\mathbf{q}}-E_{\mathbf{k}}}-\frac{v^2_{\mathbf{k}+\mathbf{q}}v^2_{\mathbf{k}}}{i\hbar\omega-E_{\mathbf{k}+\mathbf{q}}+E_{\mathbf{k}}}\right]\Bigg)\Bigg\}.$$

Notice χ^{S} is diagonal. In the case of no spin-orbit coupling χ^{S} will also have the same components in all directions (i.e., $\mathbb{G}_{mn}$ will be isotropic). The triplet susceptibility tensor takes the form:

$$\chi^{\mathsf{T}}_{mn}(\mathbf{q},i\omega) = \frac{1}{2}\mathcal{N}_m\mathcal{N}_n\mathbb{G}_{mn}\sum_{\mathbf{k}}\Bigg\{\frac{|\Delta_0|^2}{E_{\mathbf{k}+\mathbf{q}}E_{\mathbf{k}}}\mathcal{D}_{mn}(\mathbf{k},\mathbf{q})\otimes \tag{158}$$

$$\otimes\Bigg(\left(1-f(E_{\mathbf{k}+\mathbf{q}})-f(E_{\mathbf{k}})\right)\left[\frac{1}{i\hbar\omega+E_{\mathbf{k}+\mathbf{q}}+E_{\mathbf{k}}}-\frac{1}{i\hbar\omega-E_{\mathbf{k}+\mathbf{q}}-E_{\mathbf{k}}}\right]$$

$$+\left(f(E_{\mathbf{k}+\mathbf{q}})-f(E_{\mathbf{k}})\right)\left[\frac{1}{i\hbar\omega+E_{\mathbf{k}+\mathbf{q}}-E_{\mathbf{k}}}-\frac{1}{i\hbar\omega-E_{\mathbf{k}+\mathbf{q}}+E_{\mathbf{k}}}\right]\Bigg)$$

$$-4\delta_{mn}\Bigg(\left(1-f(E_{\mathbf{k}+\mathbf{q}})-f(E_{\mathbf{k}})\right)\left[\frac{u^2_{\mathbf{k}}v^2_{\mathbf{k}+\mathbf{q}}}{i\hbar\omega-E_{\mathbf{k}+\mathbf{q}}-E_{\mathbf{k}}}-\frac{u^2_{\mathbf{k}+\mathbf{q}}v^2_{\mathbf{k}}}{i\hbar\omega+E_{\mathbf{k}+\mathbf{q}}+E_{\mathbf{k}}}\right]$$

$$+\left(f(E_{\mathbf{k}+\mathbf{q}})-f(E_{\mathbf{k}})\right)\left[\frac{u^2_{\mathbf{k}+\mathbf{q}}u^2_{\mathbf{k}}}{i\hbar\omega+E_{\mathbf{k}+\mathbf{q}}-E_{\mathbf{k}}}-\frac{v^2_{\mathbf{k}+\mathbf{q}}v^2_{\mathbf{k}}}{i\hbar\omega-E_{\mathbf{k}+\mathbf{q}}+E_{\mathbf{k}}}\right]\Bigg)\Bigg\}$$

where

$$\mathcal{D}_{mn}(\mathbf{k},\mathbf{q}) \doteq \mathbf{d}^*(\mathbf{k}+\mathbf{q})\cdot\mathbf{d}(\mathbf{k})\delta_{mn} - [d_m^*(\mathbf{k}+\mathbf{q})d_n(\mathbf{k}) + d_n^*(\mathbf{k}+\mathbf{q})d_m(\mathbf{k})] \qquad (159)$$

and where f is the Fermi function

$$f(E_{\mathbf{k}}) = \frac{1}{e^{\beta E_{\mathbf{k}}}+1}. \qquad (160)$$

Generally, this tensor (derived under the condition that the order parameter is unitary) is symmetric having six independent components. Observe the dependence of the real and imaginary parts of $\chi^{\mathsf{T}}_{mn}(\mathbf{q},i\omega)$ on the orientation of the order parameter $\mathbf{d}(\mathbf{k})$ through $\mathcal{D}_{mn}(\mathbf{k},\mathbf{q})$. This dependence arises from the pair-propagator-F functions in $\Pi^{II}_{\alpha\beta\gamma\delta}(\mathbf{k},\mathbf{q},i\omega)$.

The response, $\chi^{\mathsf{T}}_{mn}(\mathbf{q},i\omega)$, will vary according to the spatial orientation of the order parameter. Recall that the order parameter is constructed out of three orbital components $[g_1^\Gamma(\mathbf{k}), g_2^\Gamma(\mathbf{k}), g_3^\Gamma(\mathbf{k})]$ each corresponding to one of the three possible triplet spin channels [see sections §2.1 & §2.2] and spin components $\{|\uparrow\uparrow\rangle, (|\uparrow\downarrow\rangle+|\downarrow\uparrow\rangle), |\downarrow\downarrow\rangle\}$. The $g_1^\Gamma(\mathbf{k})$ component is associated with the $|\uparrow\uparrow\rangle$ spin state, $g_3^\Gamma(\mathbf{k})$ with the $|\downarrow\downarrow\rangle$ spin state and $g_2^\Gamma(\mathbf{k})$ with the $(|\uparrow\downarrow\rangle + |\downarrow\uparrow\rangle)/\sqrt{2}$ spin state.

Performing the Wick's rotation (i.e., letting $i\hbar\omega \to \hbar\omega + i\delta$), then passing to the limit of $\delta \to 0$ and collecting the real and imaginary parts [see appendix §B] we obtain for the case of the singlet susceptibility the real part:

$$\Re\Big[\chi^{\mathsf{S}}_{mn}(\mathbf{q},\omega)\Big] = -2\,\delta_{mn}\,\mathbb{G}_{mn}\sum_{\mathbf{k}}\Bigg\{ \tag{161}$$
$$\frac{(u^2_{\mathbf{k}}u^2_{\mathbf{k+q}} + u_{\mathbf{k}}v_{\mathbf{k}}u_{\mathbf{k+q}}v_{\mathbf{k+q}})[f(E_{\mathbf{k+q}}) - f(E_{\mathbf{k}})]}{\hbar\omega + E_{\mathbf{k+q}} - E_{\mathbf{k}}}$$
$$-\frac{(v^2_{\mathbf{k}}v^2_{\mathbf{k+q}} + u_{\mathbf{k}}v_{\mathbf{k}}u_{\mathbf{k+q}}v_{\mathbf{k+q}})[f(E_{\mathbf{k+q}}) - f(E_{\mathbf{k}})]}{\hbar\omega - E_{\mathbf{k+q}} + E_{\mathbf{k}}}$$
$$+\frac{(u^2_{\mathbf{k}}v^2_{\mathbf{k+q}} - u_{\mathbf{k}}v_{\mathbf{k}}u_{\mathbf{k+q}}v_{\mathbf{k+q}})[1 - f(E_{\mathbf{k+q}}) - f(E_{\mathbf{k}})]}{\hbar\omega - E_{\mathbf{k+q}} - E_{\mathbf{k}}}$$
$$-\frac{(u^2_{\mathbf{k+q}}v^2_{\mathbf{k}} - u_{\mathbf{k}}v_{\mathbf{k}}u_{\mathbf{k+q}}v_{\mathbf{k+q}})[1 - f(E_{\mathbf{k+q}}) - f(E_{\mathbf{k}})]}{\hbar\omega + E_{\mathbf{k+q}} + E_{\mathbf{k}}}\Bigg\}$$

and for the imaginary part

$$\Im\Big[\chi^{\mathsf{S}}_{mn}(\mathbf{q},\omega)\Big] = 2\pi\,\delta_{mn}\,\mathbb{G}_{mn}\sum_{\mathbf{k}}\Bigg\{ \tag{162}$$
$$(u^2_{\mathbf{k}}u^2_{\mathbf{k+q}} + u_{\mathbf{k}}v_{\mathbf{k}}u_{\mathbf{k+q}}v_{\mathbf{k+q}})[f(E_{\mathbf{k+q}}) - f(E_{\mathbf{k}})]\delta(\hbar\omega + E_{\mathbf{k+q}} - E_{\mathbf{k}})$$
$$-(v^2_{\mathbf{k}}v^2_{\mathbf{k+q}} + u_{\mathbf{k}}v_{\mathbf{k}}u_{\mathbf{k+q}}v_{\mathbf{k+q}})[f(E_{\mathbf{k+q}}) - f(E_{\mathbf{k}})]\delta(\hbar\omega - E_{\mathbf{k+q}} + E_{\mathbf{k}})$$
$$+(u^2_{\mathbf{k}}v^2_{\mathbf{k+q}} - u_{\mathbf{k}}v_{\mathbf{k}}u_{\mathbf{k+q}}v_{\mathbf{k+q}})[1 - f(E_{\mathbf{k+q}}) - f(E_{\mathbf{k}})]\delta(\hbar\omega - E_{\mathbf{k+q}} - E_{\mathbf{k}})$$
$$-(u^2_{\mathbf{k+q}}v^2_{\mathbf{k}} - u_{\mathbf{k}}v_{\mathbf{k}}u_{\mathbf{k+q}}v_{\mathbf{k+q}})[1 - f(E_{\mathbf{k+q}}) - f(E_{\mathbf{k}})]\delta(\hbar\omega + E_{\mathbf{k+q}} + E_{\mathbf{k}})\Bigg\}.$$

For the triplet case the real part of the susceptibility is found to be

$$
\begin{aligned}
\Re\Big[\chi^{\mathsf{T}}_{mn}(\mathbf{q},\omega)\Big] = \frac{1}{2}\mathbb{G}_{mn}\sum_{\mathbf{k}}\Bigg\{ & \qquad (163)\\
& |\Delta_0|^2\frac{[f(E_{\mathbf{k}+\mathbf{q}})-f(E_{\mathbf{k}})]}{E_{\mathbf{k}+\mathbf{q}}E_{\mathbf{k}}}\Bigg(\\
& \qquad \frac{\Re\Big[\mathcal{D}_{mn}(\mathbf{k},\mathbf{q})\Big]}{\hbar\omega+E_{\mathbf{k}+\mathbf{q}}-E_{\mathbf{k}}}+\pi\Im\Big[\mathcal{D}_{mn}(\mathbf{k},\mathbf{q})\Big]\delta(\hbar\omega+E_{\mathbf{k}+\mathbf{q}}-E_{\mathbf{k}})\\
& \qquad -\frac{\Re\Big[\mathcal{D}_{mn}(\mathbf{k},\mathbf{q})\Big]}{\hbar\omega-E_{\mathbf{k}+\mathbf{q}}+E_{\mathbf{k}}}-\pi\Im\Big[\mathcal{D}_{mn}(\mathbf{k},\mathbf{q})\Big]\delta(\hbar\omega-E_{\mathbf{k}+\mathbf{q}}+E_{\mathbf{k}})\Bigg)\\
& +|\Delta_0|^2\frac{[1-f(E_{\mathbf{k}+\mathbf{q}})-f(E_{\mathbf{k}})]}{E_{\mathbf{k}+\mathbf{q}}E_{\mathbf{k}}}\Bigg(\\
& \qquad \frac{\Re\Big[\mathcal{D}_{mn}(\mathbf{k},\mathbf{q})\Big]}{\hbar\omega+E_{\mathbf{k}+\mathbf{q}}+E_{\mathbf{k}}}+\pi\Im\Big[\mathcal{D}_{mn}(\mathbf{k},\mathbf{q})\Big]\delta(\hbar\omega+E_{\mathbf{k}+\mathbf{q}}+E_{\mathbf{k}})\\
& \qquad -\frac{\Re\Big[\mathcal{D}_{mn}(\mathbf{k},\mathbf{q})\Big]}{\hbar\omega-E_{\mathbf{k}+\mathbf{q}}-E_{\mathbf{k}}}-\pi\Im\Big[\mathcal{D}_{mn}(\mathbf{k},\mathbf{q})\Big]\delta(\hbar\omega-E_{\mathbf{k}+\mathbf{q}}-E_{\mathbf{k}})\Bigg)\\
& -4\delta_{mn}\Bigg((1-f(E_{\mathbf{k}+\mathbf{q}})-f(E_{\mathbf{k}}))\left[\frac{u^2_{\mathbf{k}}v^2_{\mathbf{k}+\mathbf{q}}}{\hbar\omega-E_{\mathbf{k}+\mathbf{q}}-E_{\mathbf{k}}}-\frac{u^2_{\mathbf{k}+\mathbf{q}}v^2_{\mathbf{k}}}{\hbar\omega+E_{\mathbf{k}+\mathbf{q}}+E_{\mathbf{k}}}\right]\\
& \qquad +(f(E_{\mathbf{k}+\mathbf{q}})-f(E_{\mathbf{k}}))\left[\frac{u^2_{\mathbf{k}+\mathbf{q}}u^2_{\mathbf{k}}}{\hbar\omega+E_{\mathbf{k}+\mathbf{q}}-E_{\mathbf{k}}}-\frac{v^2_{\mathbf{k}+\mathbf{q}}v^2_{\mathbf{k}}}{\hbar\omega-E_{\mathbf{k}+\mathbf{q}}+E_{\mathbf{k}}}\right]\Bigg)\quad\Bigg\}
\end{aligned}
$$

and for the imaginary part we have

$$\Im\Big[\chi^{\mathsf{T}}_{mn}(\mathbf{q},\omega)\Big] = \frac{1}{2}\mathbb{G}_{mn}\sum_{\mathbf{k}}\Big\{ \tag{164}$$

$$|\Delta_0|^2\frac{[f(E_{\mathbf{k}+\mathbf{q}})-f(E_{\mathbf{k}})]}{E_{\mathbf{k}+\mathbf{q}}E_{\mathbf{k}}}\Bigg($$

$$\frac{\Im\Big[\mathcal{D}_{mn}(\mathbf{k},\mathbf{q})\Big]}{\hbar\omega+E_{\mathbf{k}+\mathbf{q}}-E_{\mathbf{k}}} - \pi\Re\Big[\mathcal{D}_{mn}(\mathbf{k},\mathbf{q})\Big]\delta(\hbar\omega+E_{\mathbf{k}+\mathbf{q}}-E_{\mathbf{k}})$$

$$-\frac{\Im\Big[\mathcal{D}_{mn}(\mathbf{k},\mathbf{q})\Big]}{\hbar\omega-E_{\mathbf{k}+\mathbf{q}}+E_{\mathbf{k}}} + \pi\Re\Big[\mathcal{D}_{mn}(\mathbf{k},\mathbf{q})\Big]\delta(\hbar\omega-E_{\mathbf{k}+\mathbf{q}}+E_{\mathbf{k}})\Bigg)$$

$$+|\Delta_0|^2\frac{[1-f(E_{\mathbf{k}+\mathbf{q}})-f(E_{\mathbf{k}})]}{E_{\mathbf{k}+\mathbf{q}}E_{\mathbf{k}}}\Bigg($$

$$\frac{\Im\Big[\mathcal{D}_{mn}(\mathbf{k},\mathbf{q})\Big]}{\hbar\omega+E_{\mathbf{k}+\mathbf{q}}+E_{\mathbf{k}}} - \pi\Re\Big[\mathcal{D}_{mn}(\mathbf{k},\mathbf{q})\Big]\delta(\hbar\omega+E_{\mathbf{k}+\mathbf{q}}+E_{\mathbf{k}})$$

$$-\frac{\Im\Big[\mathcal{D}_{mn}(\mathbf{k},\mathbf{q})\Big]}{\hbar\omega-E_{\mathbf{k}+\mathbf{q}}-E_{\mathbf{k}}} + \pi\Re\Big[\mathcal{D}_{mn}(\mathbf{k},\mathbf{q})\Big]\delta(\hbar\omega-E_{\mathbf{k}+\mathbf{q}}-E_{\mathbf{k}})\Bigg)$$

$$-4\pi\delta_{mn}\Bigg((1-f(E_{\mathbf{k}+\mathbf{q}})-f(E_{\mathbf{k}}))\otimes$$

$$\otimes\Big[-u^2_{\mathbf{k}}v^2_{\mathbf{k}+\mathbf{q}}\delta(\hbar\omega-E_{\mathbf{k}+\mathbf{q}}-E_{\mathbf{k}})+u^2_{\mathbf{k}+\mathbf{q}}v^2_{\mathbf{k}}\delta(\hbar\omega+E_{\mathbf{k}+\mathbf{q}}+E_{\mathbf{k}})\Big]$$

$$+(f(E_{\mathbf{k}+\mathbf{q}})-f(E_{\mathbf{k}}))\otimes$$

$$\otimes\Big[-u^2_{\mathbf{k}+\mathbf{q}}u^2_{\mathbf{k}}\delta(\hbar\omega+E_{\mathbf{k}+\mathbf{q}}-E_{\mathbf{k}})+v^2_{\mathbf{k}+\mathbf{q}}v^2_{\mathbf{k}}\delta(\hbar\omega-E_{\mathbf{k}+\mathbf{q}}+E_{\mathbf{k}})\Big]\Bigg)\quad\Big\}.$$

Special limits of the unitary susceptibility are considered in appendix E. Note that the uniform spin susceptibility tensor vansishes for the singlet case:

$$\lim_{\mathbf{q}\to\mathbf{0}}\chi^{\mathsf{S}}_{mn}(\mathbf{q},\omega)\to 0. \tag{165}$$

This implies that electrons paired in the spin singlet channel can respond only to nonuniform fields of finite $\mathbf{q}$ and ω. However, the triplet spin susceptibility does not

vanish in the uniform limit $\mathbf{q} \to \mathbf{0}$ (finite frequency) [see appendix E]. This case is considered for the P-wave state in the next section. The imaginary part of the susceptibility is easily obtained and will be discussed in the next section (note the real part is related to the imaginary part by the Kramers-Kronig relations [21]).

4.5 Uniform Spin Susceptibility Tensor for the Unitary Triplet P-wave State

We'll discuss here only the imaginary part of the susceptibility $\Im[\chi_{mn}]$ (the real part being related to it by the Kramers-Kronig relations [21] and is discussed in appendix E). Then in this section some of the properties of the imaginary part of the triplet susceptibility tensor are examined in the uniform limit

$$\Im\Big[\chi^{\mathsf{T}}_{mn}(\mathbf{0},\omega)\Big] = \frac{\pi}{2}\mathbb{G}_{mn}|\Delta_0|^2\sum_{\mathbf{k}}\Bigg\{[1-2f(E_{\mathbf{k}})]\otimes$$
$$\otimes\frac{2|\mathbf{d}(\mathbf{k})|^2\delta_{mn}-[d^*_m(\mathbf{k})d_n(\mathbf{k})+d^*_n(\mathbf{k})d_m(\mathbf{k})]}{E^2_{\mathbf{k}}}\Big(\delta(\hbar\omega-2E_{\mathbf{k}})-\delta(\hbar\omega+2E_{\mathbf{k}})\Big)\quad\Bigg\}. \tag{166}$$

The sum is taken over all wave vectors $\mathbf{k}$. Passing to the continuum limit:

$$\Im\Big[\chi^{\mathsf{T}}_{mn}(\mathbf{0},\omega)\Big] = \frac{\pi}{2}\mathbb{G}_{mn}|\Delta_0|^2\frac{N_0}{(2\pi)^3}\int d^3r\Bigg\{[1-2f(E_{\mathbf{r}})]\otimes \tag{167}$$
$$\otimes\frac{2|\mathbf{d}(\mathbf{r})|^2\delta_{mn}-[d^*_m(\mathbf{r})d_n(\mathbf{r})+d^*_n(\mathbf{r})d_m(\mathbf{r})]}{E^2_{\mathbf{r}}}\Big(\delta(\hbar\omega-2E_{\mathbf{r}})-\delta(\hbar\omega+2E_{\mathbf{r}})\Big)\quad\Bigg\}$$

where a transformation to a dimensionless variable has been performed: $x_j = a_j k_j$, $a_1a_2a_3 = V_0$, a_j is the lattice constant in direction j. We may exploit the fact that the excitation energy $E_{\mathbf{r}}$ and the order parameter $\Delta_{\mathbf{r}} = \vec{\sigma}\sigma_2\cdot\mathbf{d}(\mathbf{r})$ are periodic over the 1^{st} B.Z. Using this fact, N_0 is the number of unit cells in the reciprocal lattice and the integration is performed over just the 1^{st} Brillouin zone.

In order to integrate the susceptibility first observe the first delta function $\delta(\hbar\omega-2E_{\mathbf{r}})$

contributes when $\hbar\omega = 2E_{\mathbf{r}} \geq 0$. In this case $E_{\mathbf{r}} \to \hbar\omega/2 > 0$. The second delta function $\delta(\hbar\omega + 2E_{\mathbf{r}})$ contributes when $\hbar\omega = -2E_{\mathbf{r}} \leq 0$. In this case $E_{\mathbf{r}} \to -\hbar\omega/2 > 0$. In what follows the sign of the integral in Eq. 167 is seen to have the sign of ω while the magnitude of $\Im\left[\chi^{\mathsf{T}}_{mn}(\mathbf{0},\omega)\right]$ is the same for both positive and negative ω. Now recall the form of the excitation energy:

$$E_{\mathbf{r}} = \sqrt{\xi^2_{\mathbf{r}} + |\Delta_0 \mathbf{d}(\mathbf{r})|^2} \tag{168}$$

where the fact that $\frac{1}{2}\mathsf{Tr}|\widehat{\Delta}(\mathbf{k})|^2 = |\Delta_0 \mathbf{d}(\mathbf{k})|^2$ was used. The lattice dispersion is given by

$$\xi_{\mathbf{r}} = t_x \cos(x) + t_y \cos(y) + t_z \cos(z) - \mu \tag{169}$$

and trace of the order parameter in the chosen triplet P-wave state is given by

$$|\mathbf{d}(\mathbf{r})|^2 = A^2 \sin^2(x) + B^2 \sin^2(y) + C^2 \sin^2(z). \tag{170}$$

To compute $\chi_{mn}(\mathbf{0},\omega)$ we can apply the delta function identity:

$$\delta(F(x)) = \frac{\sum_l \delta(x - x_l)}{|\partial F/\partial x|} \quad \text{where} \quad F(x_l) = 0. \tag{171}$$

Here $F(x) \longleftrightarrow \hbar\omega \pm 2E_{\mathbf{r}}$. Solving for the zeros x_l corresponds to solving for the zeros of the expression:

$$\hbar\omega \pm 2E_{\mathbf{r}} = 0. \tag{172}$$

Squaring this expression leads to

$$\left(\frac{\hbar\omega}{2}\right)^2 = E^2_{\mathbf{r}} = \xi^2_{\mathbf{r}} + |\Delta_0 \mathbf{d}(\mathbf{r})|^2.$$

Note that in obtaining Eq. 173 from Eq. 172 the relative sign $\pm$ in $\delta(\hbar\omega \pm E_{\mathbf{r}})$ was lost. Thus, when the quadratic equation is applied to find the roots $\cos(x_l)$ of Eq. 173 the two solutions $\cos(x_l)$, $l = 1, 2$ will contribute regardless of the relative sign in the delta function.

Now, substituting into the above expression the explicit forms of ξ and $|\Delta_0 \mathbf{d}(\mathbf{r})|^2$ leads to

$$[t_x^2 - A^2|\Delta_0|^2]\cos^2(x) + 2t_x f(y,z)\cos(x) + A^2|\Delta_0|^2 - \left(\frac{\hbar\omega}{2}\right)^2 + f^2(y,z) + B^2|\Delta_0|^2\sin^2(y) + C^2|\Delta_0|^2\sin^2(z) = 0 \tag{173}$$

where

$$f(y,z) = t_y\cos(y) + t_z\cos(z) - \mu. \tag{174}$$

Solving first for the roots $\cos(x_l)$ and then inverting for x_l:

$$\cos(x) = -\frac{t_x f(y,z)}{t_x^2 - A^2|\Delta_0|^2} + \frac{(-)^j\sqrt{D_P(y,z,\omega)}}{t_x^2 - A^2|\Delta_0|^2} \tag{175}$$

$$x_{js}(y,z,\omega) = (-)^s \arccos\left[-\frac{t_x f(y,z)}{t_x^2 - A^2|\Delta_0|^2} + \frac{(-)^j\sqrt{D_P(y,z,\omega)}}{t_x^2 - A^2|\Delta_0|^2}\right] \tag{176}$$

where

$$D_P(y,z,\omega) = A^2|\Delta_0|^2 f^2(y,z) - (t_x^2 - A^2|\Delta_0|^2)\left[B^2|\Delta_0|^2\sin^2(y) + C^2|\Delta_0|^2\sin^2(z) + A^2|\Delta_0|^2 - \left(\frac{\hbar\omega}{2}\right)^2\right]. \tag{177}$$

Now, the arccosine in Eq. 176 is nonnegative, while x can range over positive and negative values (i.e., x is the dimensionless form of the momentum in the 1-direction, k_1). Therefore, after taking arccosine the result is multiplied by $\pm = (-)^s$ to account for both positive and negative x_{js}, which is then indexed by $s = 1, 2$. The index $j = 1, 2$ label the two solutions from the quadratic equation.

As mentioned earlier, the Fermi surface is separated into a two sheet structure due to the anisotropy of the transfer integrals: $|t_x| \gg |t_y| \gg |t_z|$. In fact the two sheets are located in a region very near

$$k_1 = \frac{1}{a}\arccos\left[\frac{\mu}{t_x} - \frac{t_y}{t_x}\cos(bk_2) - \frac{t_z}{t_x}\cos(ck_3)\right] \approx \frac{1}{a}\arccos\left[\frac{\mu}{t_x}\right] \approx \pm k_F. \tag{178}$$

In this particular case it can be seen that s indexes the solutions corresponding to the right and left hand sheets of the Fermi surface respectively. To each set of solutions labeled by a given value of s there are two solutions $j = 1, 2$ bringing to the total solutions to 4.

There are the 4 solutions, x_{js}, of the expression $(\hbar\omega/2)^2 = E_{\mathbf{r}}^2$ that contribute to the integral:

$$\Im\left[\chi^{\mathrm{T}}_{mn}(\mathbf{0},\omega)\right] = \frac{\pi}{2}\mathrm{sgn}(\omega)\mathbb{G}_{mn}|\Delta_0|^2\frac{N_0}{(2\pi)^3}\frac{[1-2f(|\hbar\omega|/2)]}{(|\hbar\omega|/2)^2}\otimes$$
$$\otimes\int d^3r\left(2|\mathbf{d}(\mathbf{r})|^2\delta_{mn} - [d^*_m(\mathbf{r})d_n(\mathbf{r}) + d^*_n(\mathbf{r})d_m(\mathbf{r})]\right)\frac{\sum_{js}\delta(x-x_{js})}{|\partial F(\mathbf{r},\omega)/\partial x|} \tag{179}$$

with

$$F(\mathbf{r},\omega) = \hbar\omega \pm E_{\mathbf{r}} \tag{180}$$

and

$$\begin{aligned}\frac{\partial F(\mathbf{r},\omega)}{\partial x} &= \mathrm{sgn}(\omega)\frac{2\sin(x)}{E_{\mathbf{r}}}[(t_x^2 - A^2|\Delta|_0^2)\cos(x) + t_x f(y,z)] \\ \left.\frac{\partial F(\mathbf{r},\omega)}{\partial x}\right|_{x_{js}} &= \mathrm{sgn}(\omega)\frac{4(-)^j\sin(x_{js})}{\hbar\omega}\sqrt{D_P(y,z,\omega)}\end{aligned} \tag{181}$$

where the last line above is $\partial F/\partial x$ evaluated at x_{js}. Here the form of $\cos(x_{js})$ from Eq. 176 was used as well as the fact that $E_{\mathbf{r}} = \hbar\omega/2$ when evaluated at x_{js}. $D_P(y,z,\omega)$ and $f(y,z)$ are even in y, z, ω so that $x_{js}(y,z,\omega)$ and $|\partial F(\mathbf{r},\omega)/\partial x|$ are also even in these variables. In fact $|\partial F(\mathbf{r},\omega)/\partial x|$ is even in both the *variable* x_{js} and the index s, which determines the sign of x_{js} and $\sin(x_{js})$. Therefore the index s can be summed over $[s = 1, 2]$ resulting in a factor of 2. The same argument does not apply to the index $j = 1, 2$. The parity of the integrand components becomes important when considering the dependence of the integral on the order parameter:

$$d_m(\mathbf{r}) = A\sin(x)\delta_{m1} + B\sin(y)\delta_{m2} + C\sin(z)\delta_{m3}. \tag{182}$$

This is the component form of the order parameter for the chosen P-wave case. It is a real quantity so that

$$2|\mathbf{d}(\mathbf{r})|^2\delta_{mn} - [d_m^*(\mathbf{r})d_n(\mathbf{r}) + d_n^*(\mathbf{r})d_m(\mathbf{r})] \rightarrow 2[|\mathbf{d}(\mathbf{r})|^2\delta_{mn} - d_m(\mathbf{r})d_n(\mathbf{r})]$$

where

$$|\mathbf{d}(\mathbf{r})|^2\delta_{mn} - d_m(\mathbf{r})d_n(\mathbf{r}) = \mathbb{D}_{mn} + \mathbb{Q}_{mn} \tag{183}$$

with

$$\mathbb{D}_{mn} = A^2\sin^2(x)[\delta_{mn} - \delta_{m1}\delta_{n1}] + B^2\sin^2(y)[\delta_{mn} - \delta_{m2}\delta_{n2}] + C^2\sin^2(z)[\delta_{mn} - \delta_{m3}\delta_{n3}] \tag{184}$$

$$\begin{aligned}\mathbb{Q}_{mn} = &-AB\sin(x)\sin(y)[\delta_{m1}\delta_{n2} + \delta_{m2}\delta_{n1}] - AC\sin(x)\sin(z)[\delta_{m1}\delta_{n3} + \delta_{m3}\delta_{n1}] \\ &-BC\sin(y)\sin(z)[\delta_{m2}\delta_{n3} + \delta_{m3}\delta_{n2}]\end{aligned} \tag{185}$$

Notice that the off diagonal term $\mathbb{Q}_{mn}$ has odd parity in x, y, z. Since the other factors in the integral, Eq. 179, are even, as previously discussed, this means that the off diagonal terms will vanish upon integration over the 1^{st} Brillouin zone. This has a very important implication for the structure of the uniform spin susceptibility tensor for the P-wave symmetry being discussed: $\chi_{mn}(\mathbf{0}, \omega)$ has no off diagonal elements (i.e., it is purely diagonal in form).

In addition note in $\mathbb{D}_{mn}$ that the first term vanishes when $m, n = 1$ while the other two terms (coming from the $m = 2, 3$ components of the order parameter) contribute. That is the susceptibility along the m-direction receives contributions from those components of the order parameter pointing perpendicular to the m-direction.

Putting the previous considerations together and noting the overall factor of 2 coming from the sum on s leads to:

$$\Im\Big[\chi^{\mathsf{T}}_{mn}(\mathbf{0},\omega)\Big] = 2\hbar|\omega|\mathrm{sgn}(\omega)N_0\frac{\pi|\Delta_0|^2}{(2\pi)^3}\mathbb{G}_{mn}\frac{[1-2f(|\hbar\omega|/2)]}{(\hbar\omega)^2}\otimes$$
$$\otimes\sum_{j\,=\,1,\,2}\int dydz\Big(A^2\sin^2(x_j)[\delta_{mn}-\delta_{m1}\delta_{n1}]+B^2\sin^2(y)[\delta_{mn}-\delta_{m2}\delta_{n2}]$$
$$+C^2\sin^2(z)[\delta_{mn}-\delta_{m3}\delta_{n3}]\Big)\frac{\Theta(D_P(y,z,\omega))}{\Big|\sin(x_j)\sqrt{D_P(y,z,\omega)}\Big|} \quad (186)$$

upon integrating on x. At this point one can make very general observations about the expected shape of the components of the susceptibility. Note that the imaginary part of the uniform susceptibility is the same magnitude but different sign for $\omega > 0$ and $\omega < 0$.

First note that in anticipation of some results of the next section it is useful to discuss qualitatively the relative strengths of the tensor components $\Im[\chi_{11}], \Im[\chi_{22}], \Im[\chi_{33}]$. For this purpose we analyze Eq. 186 and note that due to the quasi-one-dimensional condition $t_x \gg t_y \gg t_z$, $\sin(x_j)$ does not vary much over the 1^{st} B.Z. for low frequency.

Second note the function $D_P(y,z,\omega)$ in the denominator: since it appears under a radical the region of integration is restricted to points in the 1^{st} Brillouin zone where $D_P(y,z,\omega) \geq 0$. This set of allowed points includes regions in **k**-space where $D_P(y,z,\omega) \to 0$. These regions will, therefore, contribute most to the shape of the susceptibility.

Third note that as a variable, x_j corresponds to the k_x component of the momentum **k**. As a function, $x_j = x_j(y,z,\omega)$ gives the k_x component of the dimensionless momentum in the 1^{st} B.Z.

Because the $\Im[\chi_{22}]$ and $\Im[\chi_{33}]$ components contain the nearly constant term $A^2\sin^2(x_j)$, their shape will be dominated by regions in **k**-space where $\sqrt{D_P(y,z,\omega)} \sim 0$. This is in contrast to $\Im[\chi_{11}]$. Contributions to this term also come from terms in the numerator, $B^2\sin^2(y)$ and $C^2\sin^2(z)$, which vary between 0 and 1 over the 1^{st} Brillouin zone and which tend to wash out the features contributed by the denominator.

For A, B, C all of comparable value, one would expect $\Im[\chi_{11}]$ to have a smaller amplitude than $\Im[\chi_{22}]$ and $\Im[\chi_{33}]$ for most $|\omega|$. This difference in amplitudes is observed in the discussion on the P_{x+y} in section §4.5.1.

There is considerable structure in the shape of the susceptibility in this regime. In particular, since $\Im[\chi^{\mathsf{T}}_{mn}(\mathbf{0},\omega > \omega_{\max})]$, the imaginary component of the susceptibility, is a real quantity $\Im[\chi^{\mathsf{T}}_{mn}(\mathbf{0},\omega > \omega_{\max})] \in \Re$, the quantity $D_P(y,z,\omega)$ under the integral must be nonnegative for given y, z, ω. Solving $D_P(y,z,\omega) \geq 0$ for frequency

$$\omega^2 \geq 4A^2\frac{|\Delta_0|^2}{\hbar^2}\left[1 - \frac{f^2(y,z)}{t_x^2 - A^2|\Delta_0|^2}\right] + 4\frac{|\Delta_0|^2}{\hbar^2}\left(B^2\sin^2(y) + C^2\sin^2(z)\right) \qquad (187)$$

upon minimizing gives the smallest frequency of the susceptibility ($|y|, |z| \to \pi$):

$$\omega_{\min}{}^2 = 4A^2\frac{|\Delta_0|^2}{\hbar^2}\left[1 - \frac{(t_y + t_z + \mu)^2}{t_x^2 - A^2|\Delta_0|^2}\right]. \qquad (188)$$

For $|\omega| < \omega_{\min}$ the susceptibility will vanish. The vanishing of the susceptibility corresponds to the case where energy, $\hbar\omega$, of the perturbing magnetic field H is too small to cause the electron spins to respond in the superconducting state. When $\omega_{\min}$ has finite value for a given symmetry, $\Im[\chi_{mn}]$ is gapped. When $\omega_{\min} = 0$ for a given symmetry, $\Im[\chi_{mn}]$ is gapless. Whether $\Im[\chi_{mn}]$ gapped or gapless is related to whether the 1-component of the order parameter is present (i.e., whether A is finite in Eq. 170) for the P-wave state under consideration.

As a side note another important point about Eq. 186 that is hidden but clearly seen in expression Eq. 167 is the fact that there is an upper limit in the frequency,

$\omega_{\max}$, for $\Im[\chi_{mn}(\mathbf{0},\omega]$. $E_{\mathbf{r}}$ is a bounded function of $\mathbf{r}$ so that $E_{\mathbf{r}} \leq \max\{E_{\mathbf{r}}\}$. Then the maximum frequency is then $|\hbar\omega_{\max}| = 2\max\{E_{\mathbf{r}}\}$.

Regarding the integral form of the susceptibility, Eq. 186, if the 1-component, $A\sin(x)$, is present then the order parameter does not vanish anywhere. Recall the coordinate x is the dimensionless momentum $x = a_1 k_1 \approx \pm a k_F$. As discussed in appendix §F.1, $|x|$ is restricted to be near ak_F in the low frequency limit (i.e., finite in value) so that $A\sin(x)$ is finite and slowly varying over the entire Brillouin zone. This fact is exploited in the calculation of $\Im[\chi_{mn}]$ in the following sections.

Next it is convenient to divide the discussion between the gapped and gapless P-symmetries.

4.5.1 Kinks in the Gapped P-Symmetry

In this section the structure of $\Im[\chi_{mn}(\mathbf{0},\omega]$ is discussed for selected gapped P-symmetries. For this purpose recall that the Fermi surface is implicitly defined by the expression

$$\xi_{\mathbf{r}} = \epsilon_{\mathbf{r}} - \mu = 0. \tag{189}$$

where

$$\epsilon_{\mathbf{r}} = t_x\cos(x) + t_y\cos(y) + t_z\cos(z) \quad |t_x| \gg |t_y| \gg |t_z|. \tag{190}$$

Due to the anisotropy of the transfer integrals (i.e., $t_x \gg t_y \gg t_z$) and the fact that $\mu \approx t_x/\sqrt{2} \sim \mathcal{O}(t_x)$ (which corresponds to quarter filling) the x-momentum is restricted to be very near

$$|x| = a_1 k_F = \arccos\left[\frac{\mu - t_y\cos(y) - t_z\cos(z)}{t_x}\right] \approx \arccos\left[\frac{\mu}{t_x}\right] \approx \frac{\pi}{4}. \tag{191}$$

Therefore if the 1-component of $\mathbf{d}(\mathbf{k})$ $A\sin(x)$ is present (i.e., $A \neq 0$) then the order parameter does not vanish anywhere on the Fermi surface and the excitation energy

$$E_{\mathbf{r}} = \sqrt{\xi_{\mathbf{r}}^2 + |\Delta_0 \mathbf{d}(\mathbf{r})|^2} \tag{192}$$

$$\mathbf{d}(\mathbf{r}) = (A\sin(x), B\sin(y), C\sin(z)) \tag{193}$$

is said to be gapped since it is finite everywhere on the Fermi surface. A plot of the imaginary part of the suscpeptibility tensor

$$\Im\Big[\chi^{\mathsf{T}}_{mn}(\mathbf{0},\omega)\Big] = 2\hbar|\omega|\mathrm{sgn}(\omega)N_0\frac{\pi|\Delta_0|^2}{(2\pi)^3}\mathbb{G}_{mn}\frac{[1-2f(\hbar\omega/2)]}{(\hbar\omega)^2}\otimes$$
$$\otimes \sum_{j=1,2}\int dydz\Big(A^2\sin^2(x_j)[\delta_{mn}-\delta_{m1}\delta_{n1}] + B^2\sin^2(y)[\delta_{mn}-\delta_{m2}\delta_{n2}]$$
$$+ C^2\sin^2(z)[\delta_{mn}-\delta_{m3}\delta_{n3}]\Big)\frac{\Theta(D_P(y,z,\omega))}{\Big|\sin(x_j)\sqrt{D_P(y,z,\omega)}\Big|} \tag{194}$$

for $\omega \geq 0$ for the P_x ($A \neq 0; B, C = 0$) and P_{x+y} ($A, B \neq 0; C = 0$) symmetries reveals [see Figs. 17,19,20,21] characteristic structures that are slightly different for the two symmetries. Note that for P_x, $\Im[\chi_{11}] \equiv 0$ and $\Im[\chi_{22}] = \Im[\chi_{33}]$. An analysis

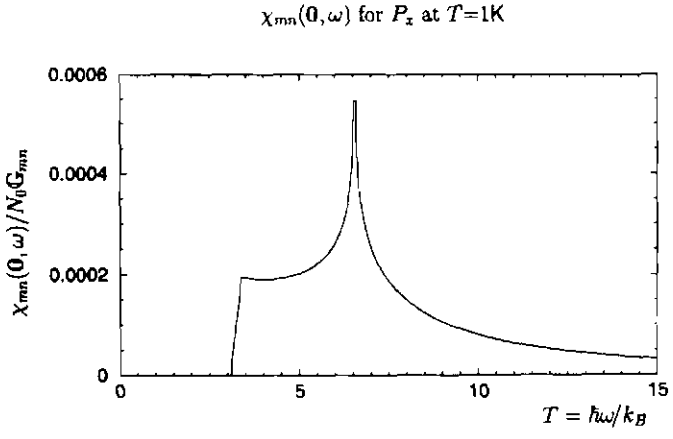

Figure 17: This figure shows the susceptibility $\Im\{\chi_{22}\} = \Im\{\chi_{33}\}$ for the P_x symmetry for positive frequency in units of temperature (1K), $T = \hbar\omega/k_B$. $[A = 1, B = 0, C = 0, t_x = k_B(5800\mathsf{K}), t_y = k_B(1226\mathsf{K}), t_z = k_B(48\mathsf{K}), \mu = k_B(4003\mathsf{K}), \Delta_{\mathbf{0}} = k_B(3.136\mathsf{K})]$

of the function $D_P(y,z,\omega)$ [see appendix §F] for the P_x symmetry the reveals the

special points:

$$\omega_{\min}^2 = 4A^2\frac{{\Delta_0}^2}{\hbar^2}\left[1-\frac{(\mu+t_y+t_z)^2}{t_x^2-A^2{\Delta_0}^2}\right] \quad (195)$$

$$\omega_1^2 = 4A^2\frac{{\Delta_0}^2}{\hbar^2}\left[1-\frac{(\mu+t_y-t_z)^2}{t_x^2-A^2{\Delta_0}^2}\right] \quad (196)$$

$$\omega_2^2 = 4A^2\frac{{\Delta_0}^2}{\hbar^2}\left[1-\frac{(\mu-t_y+t_z)^2}{t_x^2-A^2{\Delta_0}^2}\right] \quad (197)$$

$$\omega_3^2 = 4A^2\frac{{\Delta_0}^2}{\hbar^2}\left[1-\frac{(\mu-t_y-t_z)^2}{t_x^2-A^2{\Delta_0}^2}\right]. \quad (198)$$

The first point is of course the frequency minimum. The next point ${\omega_1}^2$ is the *step* in the graph for the P_x symmetry. Here the susceptibility undergoes a change in behavior from rapid growth to a very slow growth. Then it grows until it reaches a peak with leading edge at ${\omega_2}^2$ and trailing edge at ${\omega_3}^2$. Between these points the peak is relatively *flat* [see Fig. 18] and does not diverge.

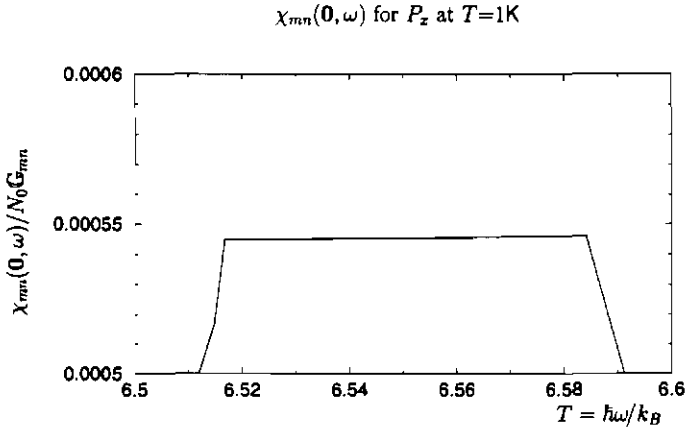

Figure 18: This figure shows the structure of the peak in the susceptibility for the P_x symmetry.

For P_{x+y}, the susceptibility tensor has the form $\chi_{11} \neq \chi_{22}$, $\chi_{33} = \chi_{11} + \chi_{22}$ [Figs. 19,20,21 respectively]. The susceptibility in this case has 6 critical frequencies. These

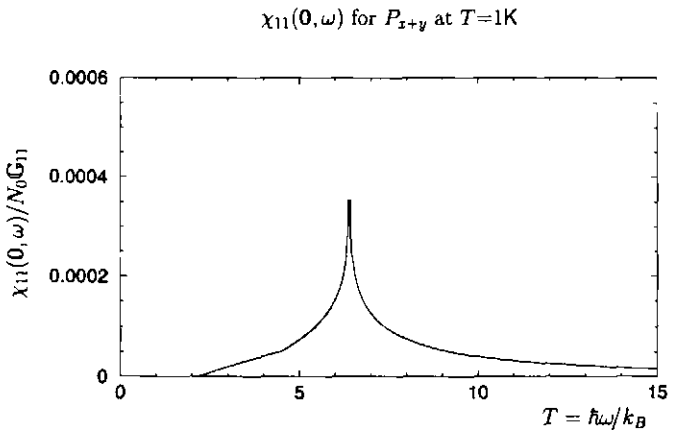

Figure 19: This figure shows the susceptibility $\Im\{\chi_{11}\}$ for the P_{x+y} symmetry. From the plot it is clear that this is a gapless symmetry. $[A = 1, B = 1, C = 0, t_x = k_B(5800\text{K}), t_y = k_B(1226\text{K}), t_z = k_B(48\text{K}), \mu = k_B(4003\text{K}), \Delta_0 = k_B(2.162\text{K})]$

include the first 4 already mentioned in the P_x case plus two more:

$$\omega_4^2 = 4\frac{{\Delta_0}^2}{\hbar^2}\left[[A^2+B^2] - A^2B^2\frac{(\mu+t_z)^2}{A^2t_y^2+KB^2}\right] \tag{199}$$

$$\omega_5^2 = 4\frac{{\Delta_0}^2}{\hbar^2}\left[[A^2+B^2] - A^2B^2\frac{(\mu-t_z)^2}{A^2t_y^2+KB^2}\right]. \tag{200}$$

In this case ${\omega_{\text{min}}}^2$ is still the beginning of the gapped response; however, the roles of the frequencies ${\omega_1}^2, {\omega_2}^2, {\omega_3}^2$ change for the P_{x+y}. They become the edges of the two steps seen in the graphs of $\Im[\chi_{mm}]$. The two new frequencies ${\omega_4}^2$ and ${\omega_5}^2$ locate the edges of the peak of the $\Im[\chi_{mm}]$.

Observe the apparent contrast in the shape between $\Im[\chi_{11}]$ and $\Im[\chi_{22}]$. The features at the critical frequencies apparent in $\Im[\chi_{22}]$ seem to be missing from $\Im[\chi_{11}]$. This is a bit deceptive. In fact what has happened is simply that this structure is latent but still present in $\Im[\chi_{11}]$.

Recall the 1-component, $A\sin(x)$, of the order parameter vector $\mathbf{d}(\mathbf{k})$ from Eq. 170 contributes only to the $\Im[\chi_{22}]$ and $\Im[\chi_{33}]$. $A^2\sin^2(x)$ is relatively constant over the

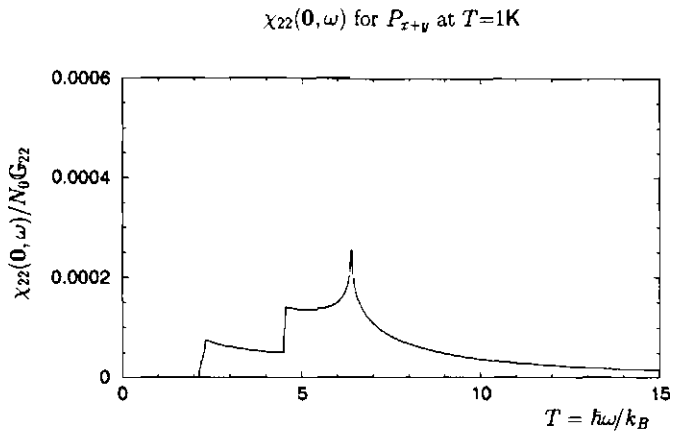

Figure 20: This figure shows the susceptibility $\Im\{\chi_{22}\}$ for the P_{x+y} symmetry.

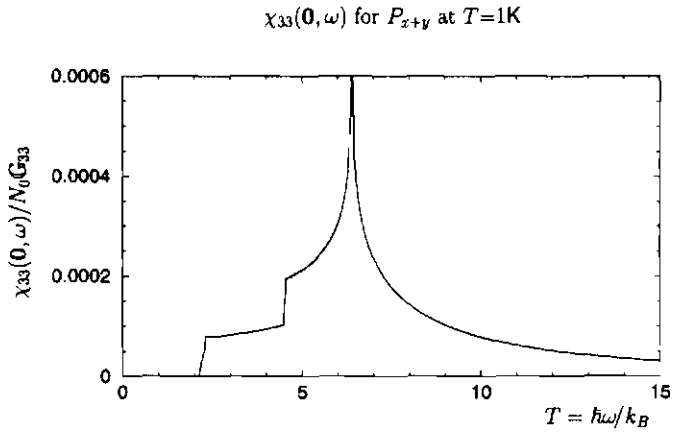

Figure 21: This figure shows the susceptibility $\Im\{\chi_{33}\}$ for the P_{x+y} symmetry.

1^{st} Brillouin zone so that the integral in $\Im[\chi(\mathbf{q}=\mathbf{0},\omega)]$ is dominated only by the $D_P(y,z,\omega)$ function which gives $\Im[\chi_{22}]$ and $\Im[\chi_{33}]$ their characteristic kinks and peaks. However, in $\Im[\chi_{11}]$ these features are dramatically reduced by the presence of the $B^2\sin^2(y)$ and $C^2\sin^2(z)$ terms in the integral which vary between 0 and 1 over the entire 1^{st} Brillouin zone.

In the case of the P_{x+z} symmetry (instead of the P_{x+y} symmetry) the frequencies

${\omega_4}^2$ and ${\omega_5}^2$ would be replace by:

$$\omega_6^2 = 4\frac{{\Delta_0}^2}{\hbar^2}\left[[A^2+C^2] - A^2C^2\frac{(\mu+t_y)^2}{A^2t_z^2+KC^2}\right] \quad (201)$$

$$\omega_7^2 = 4\frac{{\Delta_0}^2}{\hbar^2}\left[[A^2+C^2] - A^2C^2\frac{(\mu-t_y)^2}{A^2t_z^2+KC^2}\right]. \quad (202)$$

Finally the P_{x+y+z} symmetry has all the above mentioned frequencies as special points including:

$$\omega_8^2 = 4\frac{{\Delta_0}^2}{\hbar^2}\left[[A^2+B^2+C^2] - A^2B^2C^2\frac{\mu^2}{A^2[t_z^2B^2+t_y^2C^2]+B^2C^2K}\right]. \quad (203)$$

4.5.2 Kinks in the Gapless P-Symmetry

In this section the imaginary part of the uniform spin susceptibility $\Im[\chi_{mn}(\mathbf{0},\omega)]$ is analyzed for selected gapless P-wave states. An analysis of the function $D_P(y,z,\omega)$ for the gapless symmetries reveals for the P_y case the special frequencies:

which indicates the beginning of the gapless response

$${\omega_{\min}}^2 = 0 \quad (204)$$

and the location of the peak in the plot

$${\omega_1}^2 = 4\frac{|\Delta_0|^2}{\hbar^2}B^2. \quad (205)$$

The order parameter vector was chosen to be

$$\mathbf{d}(\mathbf{k}) = (0,0,1)B\sin(y). \quad (206)$$

The corresponding plot of the susceptibility for the P_y-symmetry is then
For P_z

$${\omega_{\min}}^2 = 0 \quad (207)$$

$${\omega_2}^2 = 4\frac{|\Delta_0|^2}{\hbar^2}C^2 \quad (208)$$

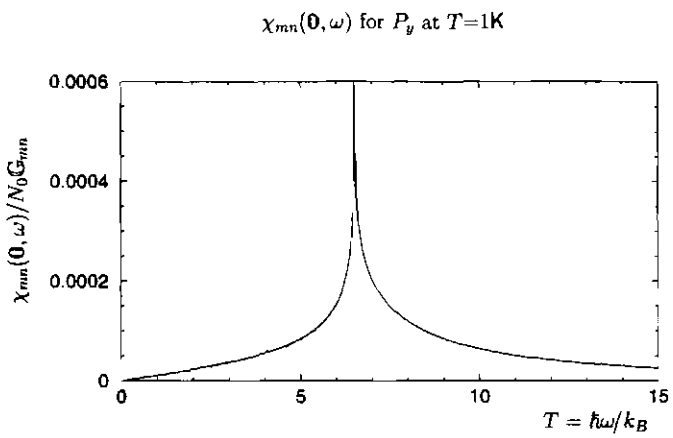

Figure 22: This figure shows the susceptibility $\Im\{\chi_{11}\}, \Im\{\chi_{22}\}, \Im\{\chi_{33} \equiv 0\}$ for the P_y symmetry. $[A = 0, B = 1, C = 0, t_x = k_B(5800\mathsf{K}), t_y = k_B(1226\mathsf{K}), t_z = k_B(48\mathsf{K}), \mu = k_B(4003\mathsf{K}), \Delta_\mathbf{0} = k_B(2.703\mathsf{K})]$

with order parameter vector given by

$$\mathbf{d}(\mathbf{k}) = (0, 0, 1)C\sin(z). \tag{209}$$

Finally for the P_{y+z} symmetry there are four critical frequencies:

the beginning of the gapless response

$$\omega_{\mathrm{min}}{}^2 = 0 \tag{210}$$

and the remaining frequencies which give the location of kinks and peaks:

$$\omega_1{}^2 = 4\frac{|\Delta_0|^2}{\hbar^2}B^2 \tag{211}$$

$$\omega_2{}^2 = 4\frac{|\Delta_0|^2}{\hbar^2}C^2 \tag{212}$$

$$\omega_3{}^2 = 4\frac{|\Delta_0|^2}{\hbar^2}[B^2 + C^2] \tag{213}$$

Next we perform an analytical calculation for the low frequency behavior of $\Im[\chi_{mn}(\mathbf{0},\omega)]$ for selected P-wave states.

4.5.3 The Low Frequency Limit

The low frequency limit $|\omega| \sim \mathcal{O}(\omega_{\min})$ of the uniform susceptibility for the general P_{x+y+z} and P_{y+z} cases (i.e., gapped and gapless symmetries) is discussed below. In this limit one can exploit the fact that $|\omega| \sim \mathcal{O}(\omega_{\min})$, which restricts the region of **k**-space in the 1^{st} Brillouin zone that can contribute to $\Im\left[\chi_{mn}(\mathbf{0},\omega)\right]$.

As discussed above the largest contributions to the susceptibility, as seen in Eq. 186, come from regions of the 1^{st} Brillouin zone where $\sqrt{D_P(y,z,\omega)} \sim 0$. Contributing regions obey $D_P(y,z,\omega) \geq 0$. Under the restriction $|\omega| \sim \mathcal{O}(\omega_{\min})$ the contributing regions are bounded by the level curves $D_P(y,z,\omega) = 0$ for a particular frequency ω.

These level curves are shown below beginning in figure 23 for the gapped case and figure 24 for the gapless case. Observe for the gapped cases [see Fig. 23] that when $\omega_{min} \leq |\omega| \leq \omega_1$ the contributing regions come from the corners of the 1^{st} B.Z. For P_x $\omega = (\omega_1 + \omega_{\min})/2 = k_B(2.369\mathrm{K})/\hbar$ was used. For P_{x+y} $\omega = (\omega_1 + \omega_{\min})/2 = k_B(2.369\mathrm{K})/\hbar$ was used. For P_{x+y+z} $\omega = (\omega_1 + \omega_{\min})/2 = k_B(1.934\mathrm{K})/\hbar$ was used.

Expanding the numerator and denominator of Eq. 186 about the point $(y,z) = (\pi,\pi)$ and multiplying by four to pick up all the contributions reveals that at low frequency, the imaginary part of the susceptibility has a square root dependence on frequency:

$$\Im\left[\chi_{mn}(\mathbf{0},\omega)\right] = \mathrm{sgn}(\omega)\frac{|\Delta_0|^2\mathbb{G}_{mn}[1-2f(\hbar\omega_{\min}/2)]}{\pi\hbar\omega_{\min}|\sin(ak_F)|}\Theta(\omega^2-\omega_{\min}^2)$$

$$\times\sqrt{\frac{\Lambda_0}{\Lambda_2\Lambda_3}}\left[\kappa_{A,mn}\sin^2(ak_F)+\frac{\Lambda_0}{3}\left(\frac{\kappa_{B,mn}}{\Lambda_2}+\frac{\kappa_{C,mn}}{\Lambda_3}\right)\right] \qquad (214)$$

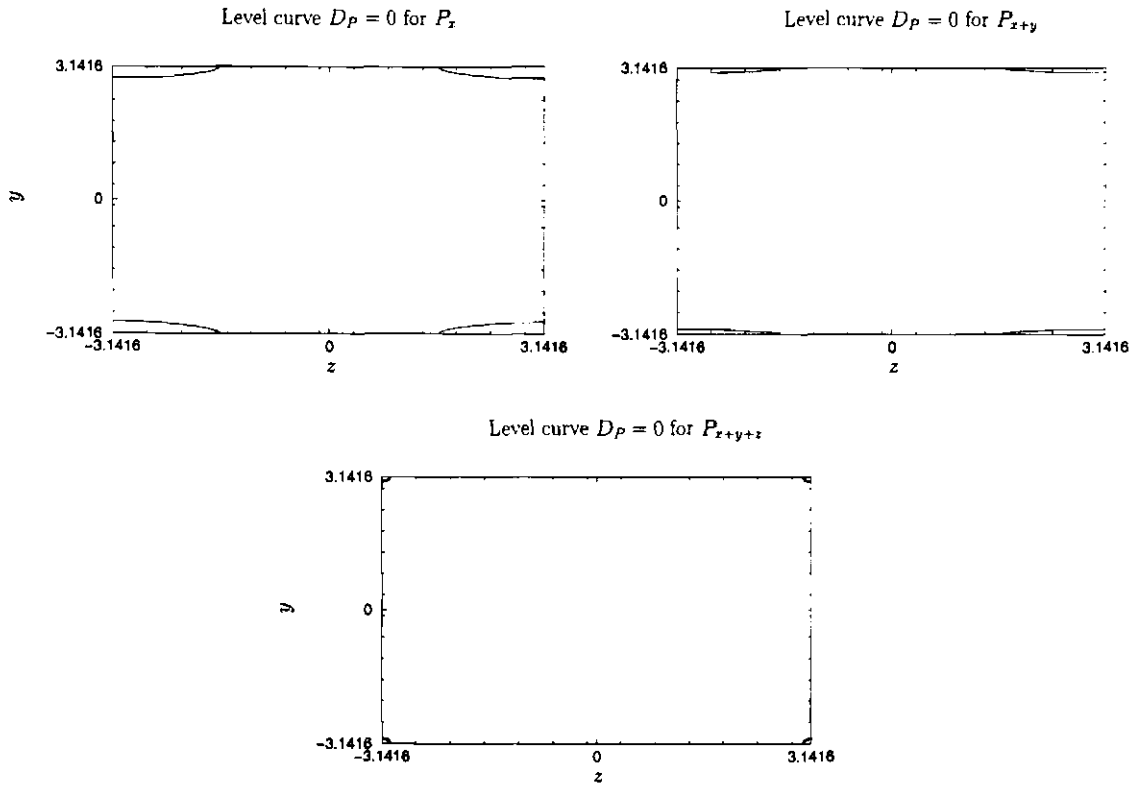

Figure 23: This figure shows the level curves corresponding to $D_P = 0$ for the gapped symmetries P_x, P_{x+y}, P_{x+y+z} respectively. $[t_x = k_B(5800\text{K}), t_y = k_B(1226\text{K}), t_z = k_B(48\text{K}), \mu = k_B(4003\text{K})]$

where

$$\Lambda_0 = (t_x^2 - A^2|\Delta_0|^2)\left(\frac{\hbar}{2}\right)^2[\omega^2 - \omega_{\min}^2] \tag{215}$$

$$\Lambda_2 = |\Delta_0|^2[A^2 t_y(t_y + t_z + \mu) + B^2(t_x^2 - A^2|\Delta_0|^2)] \tag{216}$$

$$\Lambda_3 = |\Delta_0|^2[A^2 t_z(t_y + t_z + \mu) + C^2(t_x^2 - A^2|\Delta_0|^2)] \tag{217}$$

and the tensors

$$\kappa_{A,mn} = A^2[\delta_{mn} - \delta_{m1}\delta_{n1}] \tag{218}$$

$$\kappa_{B,mn} = B^2[\delta_{mn} - \delta_{m2}\delta_{n2}] \tag{219}$$

$$\kappa_{C,mn} = C^2[\delta_{mn} - \delta_{m3}\delta_{n3}]. \tag{220}$$

contain information about the orientation of the **d**-vector.

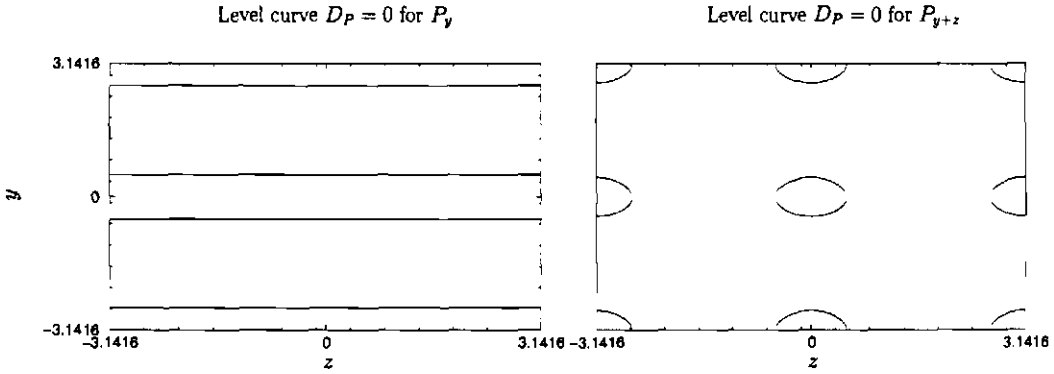

Figure 24: This figure shows the level curves corresponding to $D_P = 0$ for the gapped symmetries P_y, P_{y+z} respectively.

Next the low frequency dependence of $\Im[\chi_{mn}(\mathbf{0},\omega)]$ is analyzed for the gapless P_y and P_{y+z} cases. For the plots of the level curves in Fig. 24 for P_y $\omega = (\omega_1 + \omega_{\mathsf{min}})/2 = k_B(3\mathsf{K})/\hbar$ was used. For the plots of the level curves for P_{y+z} $\omega = (\omega_1 + \omega_{\mathsf{min}})/2 = k_B(2.806\mathsf{K})/\hbar$ was used.

The low frequency dependence of the gapless P_y and P_{y+z} cases can be obtained by setting $A = 0$, leaving B, C finite in Eq. 186. The minimum frequency from Eq. 187 is:

$$\omega^2 \geq 4\frac{|\Delta_0|^2}{\hbar^2}\left(B^2\sin^2(y) + C^2\sin^2(z)\right). \tag{221}$$

At $y, z = 0, \pm\pi$ $\omega^2 = {\omega_{\min}}^2 = 0$ and there are nine contributing regions in the low frequency limit. At (π, π) the contributing region is $1/4$ the size of the largest region at $(0, 0)$. There are 16 such *quarter*-sized regions. Therefore, one can expand the terms in Eq. 186 about (π, π) and multiply the result by 16 to get:

$$\Im\left[\chi_{mn}(\mathbf{0}, \omega)\right] = \mathrm{sgn}(\omega)\frac{4|\Delta_0|^2 \mathbb{G}_{mn}[1 - 2f(\hbar\omega/2)]}{\pi\hbar\omega|\sin(ak_F)|}\Theta(\omega^2) \times\sqrt{\frac{\Lambda_0}{\Lambda_2\Lambda_3}}\frac{\Lambda_0}{3}\left(\frac{\kappa_{B,mn}}{\Lambda_2} + \frac{\kappa_{C,mn}}{\Lambda_3}\right) \tag{222}$$

for the P_{y+z}-symmetry have order parameter

$$\mathbf{d}(\mathbf{k}) = (0, B\sin(y), C\sin(z)). \tag{223}$$

Using the fact that $A = 0$ and substituting in the explicit forms of the Λ's and the κ's gives:

$$\Im\left[\chi_{mn}(\mathbf{0}, \omega)\right] = \mathrm{sgn}(\omega)\frac{\mathbb{G}_{mn}[1 - 2f(\hbar\omega/2)]}{6\pi|t_x BC\sin(ak_F)|}\left|\frac{\hbar\omega}{\Delta_0}\right|^2 (2\delta_{mn} - \delta_{m2}\delta_{n2} - \delta_{m3}\delta_{n3}). \tag{224}$$

In the limit where $|\beta\hbar\omega/2| \ll 1$ ($|\hbar\omega| \ll 2k_B T$) one can Taylor expand $[1 - 2f(\hbar\omega/2)]$ about zero frequency

$$1 - 2f(\hbar\omega/2) \to \frac{\beta\hbar\omega}{4}$$

so that in this limit the P_{y+z} susceptibility has a cubic dependence in low frequency. In the very low temperature limit where $|\beta\hbar\omega/2| \gg 1$, $f(\hbar\omega/2) \to 0$ and the susceptibility has a quadratic low frequency dependence. This is in contrast to the gapless P_y, P_z cases analyzed below.

In the P_y case (setting $A, C = 0$) the integrand in Eq. 186 depends only on the y coordinate; consequently the contributing regions are bands near $y = 0, \pm\pi$–a feature that is topologically different from the P_{y+z} case. In fact, expanding the integrand

near $y = \pi$ (and multiplying by four to pick up all contributions) shows that in low frequency the P_y-susceptibility disperses linearly:

$$\Im\left[\chi_{mn}(\mathbf{0},\omega)\right] = \mathrm{sgn}(\omega)\frac{\mathbb{G}_{mn}[1-2f(\hbar\omega/2)]}{4|t_x B\sin(ak_F)|}\left|\frac{\hbar\omega}{\Delta_0}\right|(\delta_{mn}-\delta_{m2}\delta_{n2}). \tag{225}$$

In the very low frequency limit $|\beta\hbar\omega/2| \ll 1$ the P_y and P_z symmetries have a quadratic dependence on ω.

The power law for the P_{y+z} case is different from the P_y and P_z symmetries since P_{y+z} has point nodes while the P_y and P_z symmetries have line nodes on the Fermi surface. Next the general for of the electron spin susceptibility for the nonunitary case is considered.

4.6 Calculation of the General Nonunitary Electron Spin Susceptibility

Again the calculation begins with the definition of the appropriate Green Functions. According to Sigrist and Ueda [20] the Green Functions for the nonunitary triplet case are:

$$\widehat{G}(\mathbf{k},i\omega) = -\frac{\left[\omega^2+\xi^2+|\Delta_0\mathbf{d}(\mathbf{k})|^2\right]\boldsymbol{\sigma}_0+\mathbf{m}(\mathbf{k})\cdot\vec{\boldsymbol{\sigma}}}{(\omega^2+E_{\mathbf{k}+}^2)(\omega^2+E_{\mathbf{k}-}^2)}[i\omega+\xi_{\mathbf{k}}] \tag{226}$$

$$\widehat{F}(\mathbf{k},i\omega) = \frac{\left[\omega^2+\xi^2+|\Delta_0\mathbf{d}(\mathbf{k})|^2\right]\Delta_0\mathbf{d}(\mathbf{k})-i\Delta_0\,\mathbf{m}(\mathbf{k})\times\mathbf{d}(\mathbf{k})}{(\omega^2+E_{\mathbf{k}+}^2)(\omega^2+E_{\mathbf{k}-}^2)}\cdot(i\boldsymbol{\sigma}\boldsymbol{\sigma}_2) \tag{227}$$

$$\mathbf{m}(\mathbf{k}) = i|\Delta_0|^2\mathbf{d}(\mathbf{k})\times\mathbf{d}^*(\mathbf{k}). \tag{228}$$

Observe that these Green functions are written in matrix form whereas in the unitary case the Green functions (actually Green matrices) were written in an equivalent

matrix-component form. Also note that $\mathbf{m}(\mathbf{k})$ is real and even in its argument:

$$\mathbf{m}^*(\mathbf{k}) = -i|\Delta_0|^2\mathbf{d}^*(\mathbf{k}) \times \mathbf{d}(\mathbf{k}) = -i|\Delta_0|^2(-\mathbf{d}(\mathbf{k}) \times \mathbf{d}^*(\mathbf{k})) = \mathbf{m}(\mathbf{k}) \tag{229}$$

$$\mathbf{m}(-\mathbf{k}) = i|\Delta_0|^2\mathbf{d}(-\mathbf{k}) \times \mathbf{d}^*(-\mathbf{k}) = (-)^2 i|\Delta_0|^2\mathbf{d}(\mathbf{k}) \times \mathbf{d}^*(\mathbf{k}) = \mathbf{m}(\mathbf{k}). \tag{230}$$

Expanding the Green functions by partial fraction (in anticipation of performing the frequency sum) one obtains:

$$\widehat{G}(\mathbf{k}, i\omega) = \frac{1}{2|\mathbf{m}(\mathbf{k})|} \sum_{\mathsf{J}=\pm} \widehat{\Delta}^{\mathsf{G}}_{\mathsf{J}}(\mathbf{k}) \left\{ \frac{u^2_{\mathbf{k},\mathsf{J}}}{i\omega - E_{\mathbf{k},\mathsf{J}}} + \frac{v^2_{\mathbf{k},\mathsf{J}}}{i\omega + E_{\mathbf{k},\mathsf{J}}} \right\} \tag{231}$$

$$\widehat{F}(\mathbf{k}, i\omega) = \frac{1}{2|\mathbf{m}(\mathbf{k})|} \sum_{\mathsf{J}=\pm} \widehat{\Delta}^{\mathsf{F}}_{\mathsf{J}}(\mathbf{k}) \left[\quad \frac{1}{2E_{\mathbf{k},\mathsf{J}}} \left\{ \frac{1}{i\omega + E_{\mathbf{k},\mathsf{J}}} - \frac{1}{i\omega - E_{\mathbf{k},\mathsf{J}}} \right\} \quad \right] \tag{232}$$

where

$$u^2_{\mathbf{k},\mathsf{J}} = \frac{1}{2}\left(1 + \frac{\xi_{\mathbf{k}}}{E_{\mathbf{k},\mathsf{J}}}\right) \tag{233}$$

$$v^2_{\mathbf{k},\mathsf{J}} = \frac{1}{2}\left(1 - \frac{\xi_{\mathbf{k}}}{E_{\mathbf{k},\mathsf{J}}}\right) \tag{234}$$

are the quasiparticle and quasihole coherence factors and where

$$\widehat{\Delta}^{\mathsf{G}}_{\mathsf{J}}(\mathbf{k}) = \Big|\mathbf{m}(\mathbf{k})\Big|\boldsymbol{\sigma}_0 - \mathsf{J}\,\mathbf{m}(\mathbf{k}) \cdot \vec{\boldsymbol{\sigma}} \tag{235}$$

$$\widehat{\Delta}^{\mathsf{F}}_{\mathsf{J}}(\mathbf{k}) = i\Delta_0[\mathring{\mathbf{D}}_{\mathsf{J}}(\mathbf{k}) \cdot \vec{\boldsymbol{\sigma}}\boldsymbol{\sigma}_2] \tag{236}$$

are matrices similar in form to the order parameter matrix $\widehat{\Delta}_{\mathbf{k}}$. The vector

$$\mathring{\mathbf{D}}_{\mathsf{J}}(\mathbf{k}) \doteq \Delta_0 \left[\Big|\mathbf{m}(\mathbf{k})\Big| \mathbf{d}(\mathbf{k}) + i\mathsf{J}\,\mathbf{m}(\mathbf{k}) \times \mathbf{d}(\mathbf{k}) \right] \tag{237}$$

is another quantity that is similar to the order parameter vector $\mathbf{d}(\mathbf{k})$. The excitation energy in the nonunitary case is given by

$$E_{\mathbf{k},\mathsf{J}} = \sqrt{\xi^2_{\mathbf{k}} + |\Delta_0\mathbf{d}(\mathbf{k})|^2 + \mathsf{J}|\mathbf{m}(\mathbf{k})|} \quad \mathsf{J} = \pm. \tag{238}$$

First note that these are the nonunitary Green function matrices and correspond to a nonunitary order parameter:

$$\widehat{\Delta}_{\mathbf{k}}\widehat{\Delta}^{\dagger}_{\mathbf{k}} \not\propto \mathbb{I}. \tag{239}$$

Second observe that in performing partial fractions on the Green Functions that the coherence factors were again obtained but this time they carry a new index, J: $u^2_{\mathbf{k},\mathsf{J}}$, $v^2_{\mathbf{k},\mathsf{J}}$. This new index corresponds to a lifting of the degeneracy of the excitation energy: $E_{\mathbf{k}} \rightarrow E_{\mathbf{k},\mathsf{J}}$. According to Sigrist and Ueda [20] the term, $\mathbf{m}(\mathbf{k})$, corresponding to this new index, has the physical interpretation that it:

> "denotes a net spin average...of the pairing state for $\mathbf{k}$. From that one should not simply conclude that the total spin average [the average of $\mathbf{m}(\mathbf{k})$ over the whole Fermi surface] is finite. In many cases its average over the Fermi surface is zero. The meaning of a finite vector $\mathbf{m}(\mathbf{k})$ is more that the structure of the pair correlation is different for up- and down-spins in different directions of $\mathbf{k}$. Clearly, this can only occur if time-reversal symmetry is broken."

In other words, $\mathbf{m}(\mathbf{k})$ weights each $\mathbf{k}$-state with a combination of *up-up,down-down* and $m_s = 0$ spin state. Therefore, a net spin (finite $\mathbf{m}(\mathbf{k})$) implies that there is an unequal weighting of the three spin states $|\uparrow\uparrow\rangle$, $|\downarrow\downarrow\rangle$ and $|\uparrow\downarrow\rangle + |\downarrow\uparrow\rangle$ used to describe the spin of a Fermion pair in momentum state $\mathbf{k}$. So one pairing channel is preferred over the other two channels for a Fermion pair in a given $\mathbf{k}$-state.

This preference can be different for different $\mathbf{k}$-states so that $\mathbf{m}(\mathbf{k})$ changes over the Fermi surface. Additionally, the net spin of the ground state can still be zero. That is, $\mathbf{m}(\mathbf{k})$ can have an average value of zero over the Fermi surface, implying that sum of all the spins from each $\mathbf{k}$-state adds to zero.

Third note the introduction of parameters $\mathring{\mathbf{D}}_{\mathsf{J}}(\mathbf{k})$, $\widehat{\Delta}^{\mathsf{G}}_{\mathsf{J}}(\mathbf{k})$, $\widehat{\Delta}^{\mathsf{F}}_{\mathsf{J}}(\mathbf{k})$ in Eqns. 235,236,237; these forms make the Green functions for the nonunitary case appear aesthetically similar to the functions for the unitary case. The aesthetic similarity allows one to use results from the unitary case to simplify the analysis. It should be emphasized that $\mathbf{d}(\mathbf{k})$, and not $\mathring{\mathbf{D}}_{\mathsf{J}}(\mathbf{k})$, is still the order parameter of the system. $\mathring{\mathbf{D}}_{\mathsf{J}}(\mathbf{k})$ should be

regarded as an aesthetic artifice used to simplify consideration of the nonunitary case.

The general form of the nonunitary susceptibility is arrived at by performing the same sets of contraction on electron operators as was done in §. The form of the nonunitary susceptibility is then

$$\chi_{mn}(\mathbf{q}, i\omega) = \tag{240}$$
$$-\mathcal{N}_m\mathcal{N}_n\mathbb{G}_{mn}\sum_{\mathbf{k}}\sum_{\alpha\beta\gamma\delta}[\boldsymbol{\sigma}_m]_{\alpha\beta}[\boldsymbol{\sigma}_n]_{\gamma\delta}[\Pi^{I}_{\alpha\beta\gamma\delta}(\mathbf{k},\mathbf{q},i\omega)+\Pi^{II}_{\alpha\beta\gamma\delta}(\mathbf{k},\mathbf{q},i\omega)]$$

where from the single particle propagators one obtains

$$\begin{aligned}\Pi^{I}_{\alpha\beta\gamma\delta}(\mathbf{k},\mathbf{q},i\omega) =& \frac{1}{\beta}\sum_{i\omega_P} G_{\delta\alpha}(\mathbf{k}-\mathbf{q}, i\omega - i\omega_P)G_{\beta\gamma}(\mathbf{k}, i\omega_P)\\ =& \frac{1}{\beta}\sum_{\mathsf{J},\mathsf{H}=\pm}\frac{\Delta^{\mathsf{G}}_{\mathsf{J},\delta\alpha}(-\mathbf{k}+\mathbf{q})\Delta^{\mathsf{G}}_{\mathsf{H},\beta\gamma}(\mathbf{k})}{4|\mathbf{m}(-\mathbf{k}+\mathbf{q})|\cdot|\mathbf{m}(\mathbf{k})|}\otimes\\ &\otimes\sum_{i\omega_P}\left[\frac{u^2_{\mathbf{k}-\mathbf{q},\mathsf{J}}}{i\hbar\omega_P - i\hbar\omega - E_{\mathbf{k}-\mathbf{q},\mathsf{J}}} - \frac{v^2_{\mathbf{k}-\mathbf{q},\mathsf{J}}}{i\hbar\omega_P - i\hbar\omega + E_{\mathbf{k}-\mathbf{q},\mathsf{J}}}\right]\otimes\\ &\otimes\left[\frac{u^2_{\mathbf{k},\mathsf{H}}}{i\hbar\omega_P - E_{\mathbf{k},\mathsf{H}}} - \frac{v^2_{\mathbf{k},\mathsf{H}}}{i\hbar\omega_P + E_{\mathbf{k},\mathsf{H}}}\right]\end{aligned} \tag{241}$$

and from the pair propagators one has

$$\begin{aligned}\Pi^{II}_{\alpha\beta\gamma\delta}(\mathbf{k},\mathbf{q},i\omega) =& \frac{1}{\beta}\sum_{i\omega_P} F^{\dagger}_{\alpha\gamma}(-\mathbf{k}+\mathbf{q}, i\omega - i\omega_P)F_{\beta\delta}(\mathbf{k}, i\omega_P)\\ =& \frac{1}{\beta}\sum_{\mathsf{J},\mathsf{H}=\pm}\frac{\Delta^{\mathsf{F}\dagger}_{\mathsf{J},\alpha\gamma}(-\mathbf{k}+\mathbf{q})\Delta^{\mathsf{F}}_{\mathsf{H},\beta\delta}(\mathbf{k})}{16|\mathbf{m}(-\mathbf{k}+\mathbf{q})|\cdot|\mathbf{m}(\mathbf{k})|E_{-\mathbf{k}+\mathbf{q},\mathsf{J}}E_{\mathbf{k},\mathsf{H}}}\otimes\\ &\otimes\sum_{i\omega_P}\left[\frac{1}{i\hbar\omega_P - i\hbar\omega + E_{-\mathbf{k}+\mathbf{q},\mathsf{J}}} - \frac{1}{i\hbar\omega_P - i\hbar\omega - E_{-\mathbf{k}+\mathbf{q},\mathsf{J}}}\right]\otimes\\ &\otimes\left[\frac{1}{i\hbar\omega_P + E_{\mathbf{k},\mathsf{H}}} - \frac{1}{i\hbar\omega_P - E_{\mathbf{k},\mathsf{H}}}\right].\end{aligned} \tag{242}$$

In performing the frequency summations observe that the Green functions, Eqns. 226 and 227, have the same frequency dependencies as the Green functions for the unitary case. Therefore the summations can be performed immediately using the results from

the unitary case. Upon multiplying together all the frequency terms in square brackets and performing the frequency summation over Matsubara frequencies [see appendix §B] one obtains:

$$\Pi^{I}_{\alpha\beta\gamma\delta}(\mathbf{k},\mathbf{q},i\omega) = \sum_{\mathsf{J},\mathsf{H}=\pm 1} \frac{\Delta^{\mathsf{G}}_{\mathsf{J},\delta\alpha}(\mathbf{k}-\mathbf{q})\Delta^{\mathsf{G}}_{\mathsf{H},\beta\gamma}(\mathbf{k})}{4|\mathbf{m}(\mathbf{k}-\mathbf{q})|\cdot|\mathbf{m}(\mathbf{k})|}\otimes$$
$$\otimes\Bigg\{(1-f(E_{\mathbf{k}-\mathbf{q},\mathsf{J}})-f(E_{\mathbf{k},\mathsf{H}}))\left[\frac{u^2_{\mathbf{k},\mathsf{H}}v^2_{\mathbf{k}-\mathbf{q},\mathsf{J}}}{i\hbar\omega-E_{\mathbf{k}-\mathbf{q},\mathsf{J}}-E_{\mathbf{k},\mathsf{H}}}-\frac{u^2_{\mathbf{k}-\mathbf{q},\mathsf{J}}v^2_{\mathbf{k},\mathsf{H}}}{i\hbar\omega+E_{\mathbf{k}-\mathbf{q},\mathsf{J}}+E_{\mathbf{k},\mathsf{H}}}\right]$$
$$+(f(E_{\mathbf{k}-\mathbf{q},\mathsf{J}})-f(E_{\mathbf{k},\mathsf{H}}))\left[\frac{u^2_{\mathbf{k}-\mathbf{q},\mathsf{J}}u^2_{\mathbf{k},\mathsf{H}}}{i\hbar\omega+E_{\mathbf{k}-\mathbf{q},\mathsf{J}}-E_{\mathbf{k},\mathsf{H}}}-\frac{v^2_{\mathbf{k}-\mathbf{q},\mathsf{J}}v^2_{\mathbf{k},\mathsf{H}}}{i\hbar\omega-E_{\mathbf{k}-\mathbf{q},\mathsf{J}}+E_{\mathbf{k},\mathsf{H}}}\right]\Bigg\} \quad (243)$$

and

$$\Pi^{II}_{\alpha\beta\gamma\delta}(\mathbf{k},\mathbf{q},i\omega) = \sum_{\mathsf{J},\mathsf{H}=\pm} \frac{\Delta^{\mathsf{F}\dagger}_{\mathsf{J},\alpha\gamma}(-\mathbf{k}+\mathbf{q})\Delta^{\mathsf{F}}_{\mathsf{H},\beta\delta}(\mathbf{k})}{16|\mathbf{m}(-\mathbf{k}+\mathbf{q})|\cdot|\mathbf{m}(\mathbf{k})|E_{-\mathbf{k}+\mathbf{q},\mathsf{J}}E_{\mathbf{k},\mathsf{H}}}\otimes$$
$$\otimes\Bigg\{(1-f(E_{-\mathbf{k}+\mathbf{q},\mathsf{J}})-f(E_{\mathbf{k},\mathsf{H}}))\left[\frac{1}{i\hbar\omega+E_{-\mathbf{k}+\mathbf{q},\mathsf{J}}+E_{\mathbf{k},\mathsf{H}}}-\frac{1}{i\hbar\omega-E_{-\mathbf{k}+\mathbf{q},\mathsf{J}}-E_{\mathbf{k},\mathsf{H}}}\right]$$
$$+(f(E_{-\mathbf{k}+\mathbf{q}})-f(E_{\mathbf{k}}))\left[\frac{1}{i\hbar\omega+E_{-\mathbf{k}+\mathbf{q},\mathsf{J}}-E_{\mathbf{k},\mathsf{H}}}-\frac{1}{i\hbar\omega-E_{-\mathbf{k}+\mathbf{q},\mathsf{J}}+E_{\mathbf{k},\mathsf{H}}}\right]\Bigg\}. \quad (244)$$

Under the sum on $\mathbf{k}$ the tensors $\Pi^{I}_{\alpha\beta\gamma\delta}(\mathbf{k},\mathbf{q},i\omega)$ and $\Pi^{II}_{\alpha\beta\gamma\delta}(\mathbf{k},\mathbf{q},i\omega)$ may be written [see appendix §D] as:

$$\sum_{\mathbf{k}}\Pi^{I}_{\alpha\beta\gamma\delta}(\mathbf{k},\mathbf{q},i\omega) = \sum_{\mathbf{k}}\sum_{\mathsf{J},\mathsf{H}=\pm 1} \frac{\Delta^{\mathsf{G}}_{\mathsf{J},\delta\alpha}(\mathbf{k}+\mathbf{q})\Delta^{\mathsf{G}}_{\mathsf{H},\beta\gamma}(\mathbf{k})}{4|\mathbf{m}(\mathbf{k}+\mathbf{q})|\cdot|\mathbf{m}(\mathbf{k})|}\otimes$$
$$\otimes\Bigg\{(1-f(E_{\mathbf{k}+\mathbf{q},\mathsf{J}})-f(E_{\mathbf{k},\mathsf{H}}))\left[\frac{u^2_{\mathbf{k},\mathsf{H}}v^2_{\mathbf{k}+\mathbf{q},\mathsf{J}}}{i\hbar\omega-E_{\mathbf{k}+\mathbf{q},\mathsf{J}}-E_{\mathbf{k},\mathsf{H}}}-\frac{u^2_{\mathbf{k}+\mathbf{q},\mathsf{J}}v^2_{\mathbf{k},\mathsf{H}}}{i\hbar\omega+E_{\mathbf{k}+\mathbf{q},\mathsf{J}}+E_{\mathbf{k},\mathsf{H}}}\right]$$
$$+(f(E_{\mathbf{k}+\mathbf{q},\mathsf{J}})-f(E_{\mathbf{k},\mathsf{H}}))\left[\frac{u^2_{\mathbf{k}+\mathbf{q},\mathsf{J}}u^2_{\mathbf{k},\mathsf{H}}}{i\hbar\omega+E_{\mathbf{k}+\mathbf{q},\mathsf{J}}-E_{\mathbf{k},\mathsf{H}}}-\frac{v^2_{\mathbf{k}+\mathbf{q},\mathsf{J}}v^2_{\mathbf{k},\mathsf{H}}}{i\hbar\omega-E_{\mathbf{k}+\mathbf{q},\mathsf{J}}+E_{\mathbf{k},\mathsf{H}}}\right]\Bigg\} \quad (245)$$

where the fact that $\widehat{\Delta}^{\mathsf{G}}_{\mathsf{J},\delta\alpha}(\mathbf{k})$ and $E_{\mathsf{J},\mathsf{k}}$ have even parity in $\mathbf{k}$ was used. For $\Pi^{II}_{\alpha\beta\gamma\delta}(\mathbf{k},\mathbf{q},i\omega)$ the odd parity of $\widehat{\Delta}^{\mathsf{F}}_{\mathsf{J},\beta\gamma}(\mathbf{k})$ and even parity of $E_{\mathsf{J},\mathsf{k}}$ in $\mathbf{k}$ is used:

$$\sum_{\mathbf{k}} \Pi^{II}_{\alpha\beta\gamma\delta}(\mathbf{k},\mathbf{q},i\omega) = -\sum_{\mathbf{k}} \sum_{\mathsf{J},\mathsf{H}=\pm 1} \frac{\Delta^{\mathsf{F}\dagger}_{\mathsf{J},\alpha\gamma}(\mathbf{k}+\mathbf{q})\Delta^{\mathsf{F}}_{\mathsf{H},\beta\delta}(\mathbf{k})}{16|\mathbf{m}(\mathbf{k}+\mathbf{q})|\cdot|\mathbf{m}(\mathbf{k})|E_{\mathbf{k}+\mathbf{q},\mathsf{J}}E_{\mathbf{k},\mathsf{H}}} \otimes$$
$$\otimes\Bigg\{(1-f(E_{\mathbf{k}+\mathbf{q},\mathsf{J}})-f(E_{\mathbf{k},\mathsf{H}}))\left[\frac{1}{i\hbar\omega+E_{\mathbf{k}+\mathbf{q},\mathsf{J}}+E_{\mathbf{k},\mathsf{H}}}-\frac{1}{i\hbar\omega-E_{\mathbf{k}+\mathbf{q},\mathsf{J}}-E_{\mathbf{k},\mathsf{H}}}\right]$$
$$+(f(E_{\mathbf{k}+\mathbf{q},\mathsf{J}})-f(E_{\mathbf{k},\mathsf{H}}))\left[\frac{1}{i\hbar\omega+E_{\mathbf{k}+\mathbf{q},\mathsf{J}}-E_{\mathbf{k},\mathsf{H}}}-\frac{1}{i\hbar\omega-E_{\mathbf{k}+\mathbf{q},\mathsf{J}}+E_{\mathbf{k},\mathsf{H}}}\right]\Bigg\}. \tag{246}$$

The only change to the tensors is the removal of the minus sign from the argument of the functions $\widehat{\Delta}^{\mathsf{G}}_{\mathsf{J},\delta\alpha}(\mathbf{k})$ and $\widehat{\Delta}^{\mathsf{F}}_{\mathsf{J},\beta\gamma}(\mathbf{k})$ and the appearance of an explicit minus sign before the sum on $\mathbf{k}$ in $\sum_{\mathbf{k}}\Pi^{II}_{\alpha\beta\gamma\delta}(\mathbf{k},\mathbf{q},i\omega)$. Next the spin sums in Eq. 240 must be dealt with. These spin sums have the form:

$$\sum_{\alpha\beta\gamma\delta}[\boldsymbol{\sigma}_m]_{\alpha\beta}[\boldsymbol{\sigma}_n]_{\gamma\delta}\,\widehat{\Delta}^{\mathsf{G}}_{\mathsf{J},\delta\alpha}(\mathbf{k}+\mathbf{q})\widehat{\Delta}^{\mathsf{G}}_{\mathsf{H},\beta\gamma}(\mathbf{k}) \doteq \mathsf{S}^{\mathsf{G}}_{\mathsf{mn},\mathsf{JH}}(\mathbf{k},\mathbf{q}) \tag{247}$$

$$\sum_{\alpha\beta\gamma\delta}[\boldsymbol{\sigma}_m]_{\alpha\beta}[\boldsymbol{\sigma}_n]_{\gamma\delta}\,\widehat{\Delta}^{\mathsf{F}\,\dagger}_{\mathsf{J},\alpha\gamma}(\mathbf{k}+\mathbf{q})\widehat{\Delta}^{\mathsf{F}}_{\mathsf{H},\beta\delta}(\mathbf{k}) \doteq \mathsf{S}^{\mathsf{F}}_{\mathsf{mn},\mathsf{JH}}(\mathbf{k},\mathbf{q}). \tag{248}$$

It should also be noted that the matrix $\widehat{\Delta}^{\mathsf{G}}_{\mathsf{J}}(\mathbf{k})$ is neither symmetric nor antisymmetric. It is, however, strictly hermitian consisting of a real, symmetric contribution from the $|\mathbf{m}(\mathbf{k})|\boldsymbol{\sigma}_0$ term and an Hermitian contribution from the $-\mathsf{J}\mathbf{m}(\mathbf{k})\cdot\vec{\boldsymbol{\sigma}}$ term. Therefore, the spin sum containing this matrix must be handled separately from the spin index summations already considered [see appendix §C].

So the first sum is evaluated in the appendix [see appendix §C]. Observe that this sum arises from the $\Pi^{I}_{\alpha\beta\gamma\delta}(\mathbf{k},\mathbf{q},i\omega)$ tensor which contains the single-particle propagator piece of the susceptibility. Note that this part of the susceptibility is related to the Green functions describing single particle motion and that these matrices are neither strictly symmetric nor antisymmetric. This asymmetry corresponds to the

breaking of time reversal symmetry.

The second sum can be evaluated by analogy to the unitary case. It should be emphasized that the vector $\mathring{\mathbf{D}}_{\mathsf{J}}(\mathbf{k})$ is a complex vector similar to the actual order parameter $\mathbf{d}(\mathbf{k})$. The matrix $\widehat{\Delta}^{\mathsf{F}}_{\mathsf{J}}(\mathbf{k})$ (for the nonunitary case) is constructed in the same way as the unitary triplet gap, $\widehat{\Delta}^{\mathsf{T}}(\mathbf{k})$ [Eq. 145], by taking the inner product of the vector matrix $i\boldsymbol{\sigma}\boldsymbol{\sigma}_2$ with the complex vector $\mathring{\mathbf{D}}_{\mathsf{J}}(\mathbf{k})$. It follows that $\widehat{\Delta}^{\mathsf{F}}_{\mathsf{J}}(\mathbf{k})$ is a symmetric matrix just like $\widehat{\Delta}^{\mathsf{T}}(\mathbf{k})$.

Consequently, the spin sum in Eq. 248 is

$$\mathsf{S}^{\mathsf{F}}_{\mathsf{mn,JH}}(\mathbf{k},\mathbf{q}) \doteq \sum_{\alpha\beta\gamma\delta} [\boldsymbol{\sigma}_m]_{\alpha\beta}[\boldsymbol{\sigma}_n]_{\gamma\delta}\, \widehat{\Delta}^{\mathsf{F}\,\dagger}_{\mathsf{J},\alpha\gamma}(\mathbf{k}+\mathbf{q})\widehat{\Delta}^{\mathsf{F}}_{\mathsf{H},\beta\delta}(\mathbf{k}) =$$
$$2|\Delta_0|^2\Big\{\mathring{\mathbf{D}}^*_{\mathsf{J}}(\mathbf{k}+\mathbf{q})\cdot\mathring{\mathbf{D}}_{\mathsf{H}}(\mathbf{k})\delta_{mn} - [\mathring{\mathbf{D}}^*_{\mathsf{J},m}(\mathbf{k}+\mathbf{q})\,\mathring{\mathbf{D}}_{\mathsf{H},n}(\mathbf{k}) + \mathring{\mathbf{D}}^*_{\mathsf{J},n}(\mathbf{k}+\mathbf{q})\,\mathring{\mathbf{D}}_{\mathsf{H},m}(\mathbf{k})]\Big\} \tag{249}$$

In this case the associations $d_i \doteq \mathring{D}_i(\mathbf{k})$ and $\widetilde{d}_j \doteq \mathring{D}^*_j(\mathbf{k}+\mathbf{q})$ are made [see appendix §C].

After a lengthy and unpleasant ordeal (and switching indices $\mathsf{m},\mathsf{n} \to \mu,\nu$ the first

sum in Eq. 247 evaluates to:

$$\sum_{\alpha\beta\gamma\delta} [\boldsymbol{\sigma}_\mu]_{\alpha\beta}[\boldsymbol{\sigma}_\nu]_{\gamma\delta}\, \widehat{\Delta}^{\mathsf{G}}_{\mathsf{J},\delta\alpha}(\mathbf{k}+\mathbf{q})\widehat{\Delta}^{\mathsf{G}}_{\mathsf{H},\beta\gamma}(\mathbf{k}) =$$

$$2\Big\{\delta_{\mu\nu}\Big[m(\mathbf{k}+\mathbf{q})m(\mathbf{k}) - \mathsf{JH}\mathbf{m}(\mathbf{k}+\mathbf{q})\cdot\mathbf{m}(\mathbf{k})\Big]$$

$$+\mathsf{JH}\Big[m_\mu(\mathbf{k}+\mathbf{q})m_\nu(\mathbf{k}) + m_\nu(\mathbf{k}+\mathbf{q})m_\mu(\mathbf{k})\Big]$$

$$-i(\boldsymbol{\delta}_\mu \times \boldsymbol{\delta}_\nu)\cdot\Big[\mathsf{J}m(\mathbf{k})\mathbf{m}(\mathbf{k}+\mathbf{q}) - \mathsf{H}m(\mathbf{k}+\mathbf{q})\mathbf{m}(\mathbf{k})\Big]\Big\}$$

$$= \mathsf{S}^{\mathsf{G}}_{\mu\nu,\mathsf{JH}}(\mathbf{k},\mathbf{q}) \tag{250}$$

where

$$\boldsymbol{\delta}_\mu = (\delta_{\mu,1}, \delta_{\mu,2}, \delta_{\mu,3})$$

is a vector containing Kronecker deltas

$$m(\mathbf{k}) \doteq |\mathbf{m}(\mathbf{k})|$$

is the magnitude of the vector $\mathbf{m}(\mathbf{k})$

$$\mu, \nu = 1, 2, 3$$

are numbers which index the directions in three dimensional space.

The first and last terms contribute only to the diagonal and off-diagonal components of the susceptibility respectively. The middle term contributes to both. Also, since $\mathbf{m}(\mathbf{k})$ is a real vector, the first two terms are explicitly real while the last term is purely imaginary. One has for the real part

$$\Re\Big[\mathsf{S}^{\mathsf{G}}_{\mu\nu,\mathsf{JH}}(\mathbf{k},\mathbf{q})\Big] = 2\Big\{\delta_{\mu\nu}\Big[m(\mathbf{k}+\mathbf{q})m(\mathbf{k}) - \mathsf{JH}\mathbf{m}(\mathbf{k}+\mathbf{q})\cdot\mathbf{m}(\mathbf{k})\Big]$$

$$+\mathsf{JH}\Big[m_\mu(\mathbf{k}+\mathbf{q})m_\nu(\mathbf{k}) + m_\nu(\mathbf{k}+\mathbf{q})m_\mu(\mathbf{k})\Big]\Big\} \tag{251}$$

while for the imaginary part

$$\Im\left[\mathsf{S}^{\mathsf{G}}_{\mu\nu,\mathsf{JH}}(\mathbf{k},\mathbf{q})\right] = -2(\boldsymbol{\delta}_\mu \times \boldsymbol{\delta}_\nu)\cdot\left[\mathsf{J}m(\mathbf{k})\mathbf{m}(\mathbf{k}+\mathbf{q}) - \mathsf{H}m(\mathbf{k}+\mathbf{q})\mathbf{m}(\mathbf{k})\right] \quad (252)$$

After summing over spin indices, the susceptibility, Eq. 240, can be written as a sum of two terms:

$$\chi^{\text{nonunitary}}_{\mu\nu}(\mathbf{q},i\omega) = \chi^{\mathsf{G}}_{\mu\nu}(\mathbf{q},i\omega) + \chi^{\mathsf{F}}_{\mu\nu}(\mathbf{q},i\omega) \quad (253)$$

where

$$\chi^{\mathsf{G}}_{\mu\nu}(\mathbf{q},i\omega)$$

contains the contributions coming from the single-particle propagators and is given by

$$\begin{aligned}\chi^{\mathsf{G}}_{\mu\nu}(\mathbf{q},i\omega) = -\mathcal{N}_\mu\mathcal{N}_\nu\mathbb{G}_{\mu\nu}\sum_{\mathbf{k}}\sum_{\mathsf{J},\mathsf{H}=\pm}\frac{\mathsf{S}^{\mathsf{G}}_{\mu\nu,\mathsf{JH}}(\mathbf{k},\mathbf{q})}{4|\mathbf{m}(\mathbf{k}+\mathbf{q})|\cdot|\mathbf{m}(\mathbf{k})|}\otimes \\ \otimes\Bigg\{(1-f(E_{\mathbf{k}+\mathbf{q},\mathsf{J}})-f(E_{\mathbf{k},\mathsf{H}}))\left[\frac{u^2_{\mathbf{k},\mathsf{H}}v^2_{\mathbf{k}+\mathbf{q},\mathsf{J}}}{i\hbar\omega - E_{\mathbf{k}+\mathbf{q},\mathsf{J}} - E_{\mathbf{k},\mathsf{H}}} - \frac{u^2_{\mathbf{k}+\mathbf{q},\mathsf{J}}v^2_{\mathbf{k},\mathsf{H}}}{i\hbar\omega + E_{\mathbf{k}+\mathbf{q},\mathsf{J}} + E_{\mathbf{k},\mathsf{H}}}\right] \\ +(f(E_{\mathbf{k}+\mathbf{q},\mathsf{J}})-f(E_{\mathbf{k},\mathsf{H}}))\left[\frac{u^2_{\mathbf{k}+\mathbf{q},\mathsf{J}}u^2_{\mathbf{k},\mathsf{H}}}{i\hbar\omega + E_{\mathbf{k}+\mathbf{q},\mathsf{J}} - E_{\mathbf{k},\mathsf{H}}} - \frac{v^2_{\mathbf{k}+\mathbf{q},\mathsf{J}}v^2_{\mathbf{k},\mathsf{H}}}{i\hbar\omega - E_{\mathbf{k}+\mathbf{q},\mathsf{J}} + E_{\mathbf{k},\mathsf{H}}}\right]\Bigg\} \quad (254)\end{aligned}$$

and where

$$\chi^{\mathsf{F}}_{\mu\nu}(\mathbf{q},i\omega)$$

contains the contributions coming from the pair propagators and has the form

$$\chi^{\mathsf{F}}_{\mu\nu}(\mathbf{q},i\omega) = \quad \mathcal{N}_\mu\mathcal{N}_\nu\mathbb{G}_{\mu\nu}\sum_{\mathbf{k}}\sum_{\mathsf{J},\mathsf{H}=\pm}\frac{\mathsf{S}^{\mathsf{F}}_{\mu\nu,\mathsf{J}\mathsf{H}}(\mathbf{k},\mathbf{q})}{16|\mathbf{m}(\mathbf{k}+\mathbf{q})|\cdot|\mathbf{m}(\mathbf{k})|E_{\mathbf{k}+\mathbf{q},\mathsf{J}}E_{\mathbf{k},\mathsf{H}}}\otimes$$

$$\otimes\Bigg\{(1-f(E_{\mathbf{k}+\mathbf{q},\mathsf{J}})-f(E_{\mathbf{k},\mathsf{H}}))\left[\frac{1}{i\hbar\omega+E_{\mathbf{k}+\mathbf{q},\mathsf{J}}+E_{\mathbf{k},\mathsf{H}}}-\frac{1}{i\hbar\omega-E_{\mathbf{k}+\mathbf{q},\mathsf{J}}-E_{\mathbf{k},\mathsf{H}}}\right]$$

$$+(f(E_{\mathbf{k}+\mathbf{q},\mathsf{J}})-f(E_{\mathbf{k},\mathsf{H}}))\left[\frac{1}{i\hbar\omega+E_{\mathbf{k}+\mathbf{q},\mathsf{J}}-E_{\mathbf{k},\mathsf{H}}}-\frac{1}{i\hbar\omega-E_{\mathbf{k}+\mathbf{q},\mathsf{J}}+E_{\mathbf{k},\mathsf{H}}}\right]\Bigg\}. \quad (255)$$

Observe the cancellation of the explicit minus sign in front of terms in $\chi^{\mathsf{F}}_{\mu\nu}(\mathbf{q},i\omega)$ against a second minus sign which came from $\sum_{\mathbf{k}}\Pi_{\alpha\beta\gamma\delta}(\mathbf{k},\mathbf{q},i\omega)$ when it was rewritten above in Eq. 246. Next the Wick's rotation is performed (i.e., letting $i\hbar\omega\rightarrow\hbar\omega+i\delta$), and the limit of $\delta\rightarrow 0$ is taken.

Notice that the frequency terms of $\chi^{\mathsf{G}}_{\mu\nu}(\mathbf{q},i\omega)$ look exactly like the last four terms of $\chi^{\mathsf{S}}_{mn}(\mathbf{q},i\omega)$ in Eq. 157 which came from the single particle propagator terms. One can perform the Wick's rotation on these terms (simply use the results from the unitary singlet case) and multiply the real and imaginary parts with the real and imaginary parts of $\mathsf{S}^{\mathsf{G}}_{\mu\nu,\mathsf{J}\mathsf{H}}(\mathbf{k},\mathbf{q})$ (already obtained above). Collecting the real and imaginary parts:

for the single particle component

$$\Re\Big[\chi^{\mathsf{G}}_{\mu\nu}(\mathbf{q},\omega)\Big] = -\mathbb{G}_{\mu\nu}\sum_{\mathbf{k}}\sum_{\mathsf{J},\mathsf{H}=\pm}\frac{1}{4|\mathbf{m}(\mathbf{k}+\mathbf{q})|\cdot|\mathbf{m}(\mathbf{k})|}\Bigg\{$$

$$u^2_{\mathbf{k},\mathsf{H}}u^2_{\mathbf{k}+\mathbf{q},\mathsf{J}}[f(E_{\mathbf{k}+\mathbf{q},\mathsf{J}})-f(E_{\mathbf{k},\mathsf{H}})]\Bigg(\frac{\Re\Big[\mathsf{S}^{\mathsf{G}}_{\mu\nu,\mathsf{JH}}(\mathbf{k},\mathbf{q})\Big]}{\hbar\omega+E_{\mathbf{k}+\mathbf{q},\mathsf{J}}-E_{\mathbf{k},\mathsf{H}}}$$

$$+\pi\Im\Big[\mathsf{S}^{\mathsf{G}}_{\mu\nu,\mathsf{JH}}(\mathbf{k},\mathbf{q})\Big]\delta(\hbar\omega+E_{\mathbf{k}+\mathbf{q},\mathsf{J}}-E_{\mathbf{k},\mathsf{H}})\Bigg)$$

$$-v^2_{\mathbf{k},\mathsf{H}}v^2_{\mathbf{k}+\mathbf{q},\mathsf{J}}[f(E_{\mathbf{k}+\mathbf{q},\mathsf{J}})-f(E_{\mathbf{k},\mathsf{H}})]\Bigg(\frac{\Re\Big[\mathsf{S}^{\mathsf{G}}_{\mu\nu,\mathsf{JH}}(\mathbf{k},\mathbf{q})\Big]}{\hbar\omega-E_{\mathbf{k}+\mathbf{q},\mathsf{J}}+E_{\mathbf{k},\mathsf{H}}}$$

$$+\pi\Im\Big[\mathsf{S}^{\mathsf{G}}_{\mu\nu,\mathsf{JH}}(\mathbf{k},\mathbf{q})\Big]\delta(\hbar\omega-E_{\mathbf{k}+\mathbf{q},\mathsf{J}}+E_{\mathbf{k},\mathsf{H}})\Bigg)$$

$$+u^2_{\mathbf{k},\mathsf{H}}v^2_{\mathbf{k}+\mathbf{q},\mathsf{J}}[1-f(E_{\mathbf{k}+\mathbf{q},\mathsf{J}})-f(E_{\mathbf{k},\mathsf{H}})]\Bigg(\frac{\Re\Big[\mathsf{S}^{\mathsf{G}}_{\mu\nu,\mathsf{JH}}(\mathbf{k},\mathbf{q})\Big]}{\hbar\omega-E_{\mathbf{k}+\mathbf{q},\mathsf{J}}-E_{\mathbf{k},\mathsf{H}}}$$

$$+\pi\Im\Big[\mathsf{S}^{\mathsf{G}}_{\mu\nu,\mathsf{JH}}(\mathbf{k},\mathbf{q})\Big]\delta(\hbar\omega-E_{\mathbf{k}+\mathbf{q},\mathsf{J}}-E_{\mathbf{k},\mathsf{H}})\Bigg)$$

$$-u^2_{\mathbf{k}+\mathbf{q},\mathsf{J}}v^2_{\mathbf{k},\mathsf{H}}[1-f(E_{\mathbf{k}+\mathbf{q},\mathsf{J}})-f(E_{\mathbf{k},\mathsf{H}})]\Bigg(\frac{\Re\Big[\mathsf{S}^{\mathsf{G}}_{\mu\nu,\mathsf{JH}}(\mathbf{k},\mathbf{q})\Big]}{\hbar\omega+E_{\mathbf{k}+\mathbf{q},\mathsf{J}}+E_{\mathbf{k},\mathsf{H}}}$$

$$+\pi\Im\Big[\mathsf{S}^{\mathsf{G}}_{\mu\nu,\mathsf{JH}}(\mathbf{k},\mathbf{q})\Big]\delta(\hbar\omega+E_{\mathbf{k}+\mathbf{q},\mathsf{J}}+E_{\mathbf{k},\mathsf{H}})\Bigg)\Bigg\} \tag{256}$$

and

$$\Im\Big[\chi^{\mathsf{G}}_{\mu\nu}(\mathbf{q},\omega)\Big] = -\mathbb{G}_{\mu\nu}\sum_{\mathbf{k}}\sum_{\mathsf{J},\mathsf{H}=\pm}\frac{1}{4|\mathbf{m}(\mathbf{k}+\mathbf{q})|\cdot|\mathbf{m}(\mathbf{k})|}\Bigg\{$$

$$u^2_{\mathbf{k},\mathsf{H}}u^2_{\mathbf{k}+\mathbf{q},\mathsf{J}}[f(E_{\mathbf{k}+\mathbf{q},\mathsf{J}})-f(E_{\mathbf{k},\mathsf{H}})]\Bigg(\frac{\Im\Big[\mathsf{S}^{\mathsf{G}}_{\mu\nu,\mathsf{JH}}(\mathbf{k},\mathbf{q})\Big]}{\hbar\omega+E_{\mathbf{k}+\mathbf{q},\mathsf{J}}-E_{\mathbf{k},\mathsf{H}}}$$

$$-\pi\Re\Big[\mathsf{S}^{\mathsf{G}}_{\mu\nu,\mathsf{JH}}(\mathbf{k},\mathbf{q})\Big]\delta(\hbar\omega+E_{\mathbf{k}+\mathbf{q},\mathsf{J}}-E_{\mathbf{k},\mathsf{H}})\Bigg)$$

$$-v^2_{\mathbf{k},\mathsf{H}}v^2_{\mathbf{k}+\mathbf{q},\mathsf{J}}[f(E_{\mathbf{k}+\mathbf{q},\mathsf{J}})-f(E_{\mathbf{k},\mathsf{H}})]\Bigg(\frac{\Im\Big[\mathsf{S}^{\mathsf{G}}_{\mu\nu,\mathsf{JH}}(\mathbf{k},\mathbf{q})\Big]}{\hbar\omega-E_{\mathbf{k}+\mathbf{q},\mathsf{J}}+E_{\mathbf{k},\mathsf{H}}}$$

$$-\pi\Re\Big[\mathsf{S}^{\mathsf{G}}_{\mu\nu,\mathsf{JH}}(\mathbf{k},\mathbf{q})\Big]\delta(\hbar\omega-E_{\mathbf{k}+\mathbf{q},\mathsf{J}}+E_{\mathbf{k},\mathsf{H}})\Bigg)$$

$$+u^2_{\mathbf{k},\mathsf{H}}v^2_{\mathbf{k}+\mathbf{q},\mathsf{J}}[1-f(E_{\mathbf{k}+\mathbf{q},\mathsf{J}})-f(E_{\mathbf{k},\mathsf{H}})]\Bigg(\frac{\Im\Big[\mathsf{S}^{\mathsf{G}}_{\mu\nu,\mathsf{JH}}(\mathbf{k},\mathbf{q})\Big]}{\hbar\omega-E_{\mathbf{k}+\mathbf{q},\mathsf{J}}-E_{\mathbf{k},\mathsf{H}}}$$

$$-\pi\Re\Big[\mathsf{S}^{\mathsf{G}}_{\mu\nu,\mathsf{JH}}(\mathbf{k},\mathbf{q})\Big]\delta(\hbar\omega-E_{\mathbf{k}+\mathbf{q},\mathsf{J}}-E_{\mathbf{k},\mathsf{H}})\Bigg)$$

$$-u^2_{\mathbf{k}+\mathbf{q},\mathsf{J}}v^2_{\mathbf{k},\mathsf{H}}[1-f(E_{\mathbf{k}+\mathbf{q},\mathsf{J}})-f(E_{\mathbf{k},\mathsf{H}})]\Bigg(\frac{\Im\Big[\mathsf{S}^{\mathsf{G}}_{\mu\nu,\mathsf{JH}}(\mathbf{k},\mathbf{q})\Big]}{\hbar\omega+E_{\mathbf{k}+\mathbf{q},\mathsf{J}}+E_{\mathbf{k},\mathsf{H}}}$$

$$-\pi\Re\Big[\mathsf{S}^{\mathsf{G}}_{\mu\nu,\mathsf{JH}}(\mathbf{k},\mathbf{q})\Big]\delta(\hbar\omega+E_{\mathbf{k}+\mathbf{q},\mathsf{J}}+E_{\mathbf{k},\mathsf{H}})\Bigg)\Bigg\} \tag{257}$$

Notice that the frequency terms of $\chi^{\mathsf{F}}_{\mu\nu}(\mathbf{q},i\omega)$ look exactly like the first four terms of $\chi^{\mathsf{T}}_{mn}(\mathbf{q},i\omega)$ (which came from the pair propagators in Eq. 158). By making the association

$$\frac{1}{2}\frac{1}{E_{\mathbf{k}+\mathbf{q}}E_{\mathbf{k}}}|\Delta_0|^2\Big[\mathbf{d}^*(\mathbf{k}+\mathbf{q})\cdot\mathbf{d}(\mathbf{k})\delta_{mn}-[d^*_m(\mathbf{k}+\mathbf{q})d_n(\mathbf{k})+d^*_n(\mathbf{k}+\mathbf{q})d_m(\mathbf{k})]\Big]$$

$$=\frac{1}{2}\frac{|\Delta_0|^2\mathcal{D}_{mn}(\mathbf{k},\mathbf{q})}{E_{\mathbf{k}+\mathbf{q}}E_{\mathbf{k}}}\xrightarrow{m\to\mu\ \ n\to\nu}\sum_{\mathsf{J},\mathsf{H}=\pm}\frac{\mathsf{S}^{\mathsf{F}}_{\mu\nu,\mathsf{JH}}(\mathbf{k},\mathbf{q})}{16|\mathbf{m}(\mathbf{k}+\mathbf{q})|\cdot|\mathbf{m}(\mathbf{k})|E_{\mathbf{k}+\mathbf{q},\mathsf{J}}E_{\mathbf{k},\mathsf{H}}}$$

between the triplet unitary and nonunitary cases one can perform the Wick's rotation on these terms (simply use the results from the unitary triplet case, recall $\mathcal{D}_{mn}(\mathbf{k},\mathbf{q})$

was defined in Eq. 159) and collect the real and imaginary parts by making the appropriate substitutions in Eqs. 163 and 164:

for the particle pair component

$$\begin{aligned}
\Re\Big[\chi^{\mathsf{F}}_{\mu\nu}(\mathbf{q},\omega)\Big] = \mathbb{G}_{\mu\nu} \sum_{\mathbf{k}} \sum_{\mathsf{J},\mathsf{H}=\pm} \Bigg\{ & \frac{1}{16|\mathbf{m}(\mathbf{k}+\mathbf{q})|\cdot|\mathbf{m}(\mathbf{k})| E_{\mathbf{k}+\mathbf{q},\mathsf{J}} E_{\mathbf{k},\mathsf{H}}} \\
& [f(E_{\mathbf{k}+\mathbf{q}}) - f(E_{\mathbf{k}})] \Bigg(\frac{\Re\Big[\mathsf{S}^{\mathsf{F}}_{\mu\nu,\mathsf{JH}}(\mathbf{k},\mathbf{q})\Big]}{\hbar\omega + E_{\mathbf{k}+\mathbf{q}} - E_{\mathbf{k}}} \\
& \qquad + \pi\Im\Big[\mathsf{S}^{\mathsf{F}}_{\mu\nu,\mathsf{JH}}(\mathbf{k},\mathbf{q})\Big]\delta(\hbar\omega + E_{\mathbf{k}+\mathbf{q}} - E_{\mathbf{k}}) \\
& - \frac{\Re\Big[\mathsf{S}^{\mathsf{F}}_{\mu\nu,\mathsf{JH}}(\mathbf{k},\mathbf{q})\Big]}{\hbar\omega - E_{\mathbf{k}+\mathbf{q}} + E_{\mathbf{k}}} - \pi\Im\Big[\mathsf{S}^{\mathsf{F}}_{\mu\nu,\mathsf{JH}}(\mathbf{k},\mathbf{q})\Big]\delta(\hbar\omega - E_{\mathbf{k}+\mathbf{q}} + E_{\mathbf{k}}) \Bigg) \\
& [1 - f(E_{\mathbf{k}+\mathbf{q}}) - f(E_{\mathbf{k}})] \Bigg(\frac{\Re\Big[\mathsf{S}^{\mathsf{F}}_{\mu\nu,\mathsf{JH}}(\mathbf{k},\mathbf{q})\Big]}{\hbar\omega + E_{\mathbf{k}+\mathbf{q}} + E_{\mathbf{k}}} \\
& \qquad + \pi\Im\Big[\mathsf{S}^{\mathsf{F}}_{\mu\nu,\mathsf{JH}}(\mathbf{k},\mathbf{q})\Big]\delta(\hbar\omega + E_{\mathbf{k}+\mathbf{q}} + E_{\mathbf{k}}) \\
& - \frac{\Re\Big[\mathsf{S}^{\mathsf{F}}_{\mu\nu,\mathsf{JH}}(\mathbf{k},\mathbf{q})\Big]}{\hbar\omega - E_{\mathbf{k}+\mathbf{q}} - E_{\mathbf{k}}} - \pi\Im\Big[\mathsf{S}^{\mathsf{F}}_{\mu\nu,\mathsf{JH}}(\mathbf{k},\mathbf{q})\Big]\delta(\hbar\omega - E_{\mathbf{k}+\mathbf{q}} - E_{\mathbf{k}}) \Bigg) \Bigg\}
\end{aligned} \tag{258}$$

and

$$\Im\Big[\chi^{\mathsf{F}}_{\mu\nu}(\mathbf{q},\omega)\Big] = \mathbb{G}_{\mu\nu}\sum_{\mathbf{k}}\sum_{\mathsf{J},\mathsf{H}=\pm}\Bigg\{\frac{1}{16|\mathbf{m}(\mathbf{k}+\mathbf{q})|\cdot|\mathbf{m}(\mathbf{k})|E_{\mathbf{k}+\mathbf{q},\mathsf{J}}E_{\mathbf{k},\mathsf{H}}}$$
$$[f(E_{\mathbf{k}+\mathbf{q}})-f(E_{\mathbf{k}})]\Bigg(\frac{\Im\Big[\mathsf{S}^{\mathsf{F}}_{\mu\nu,\mathsf{JH}}(\mathbf{k},\mathbf{q})\Big]}{\hbar\omega+E_{\mathbf{k}+\mathbf{q}}-E_{\mathbf{k}}}$$
$$-\pi\Re\Big[\mathsf{S}^{\mathsf{F}}_{\mu\nu,\mathsf{JH}}(\mathbf{k},\mathbf{q})\Big]\delta(\hbar\omega+E_{\mathbf{k}+\mathbf{q}}-E_{\mathbf{k}})$$
$$-\frac{\Im\Big[\mathsf{S}^{\mathsf{F}}_{\mu\nu,\mathsf{JH}}(\mathbf{k},\mathbf{q})\Big]}{\hbar\omega-E_{\mathbf{k}+\mathbf{q}}+E_{\mathbf{k}}}+\pi\Re\Big[\mathsf{S}^{\mathsf{F}}_{\mu\nu,\mathsf{JH}}(\mathbf{k},\mathbf{q})\Big]\delta(\hbar\omega-E_{\mathbf{k}+\mathbf{q}}+E_{\mathbf{k}})\Bigg)$$
$$+[1-f(E_{\mathbf{k}+\mathbf{q}})-f(E_{\mathbf{k}})]\Bigg(\frac{\Im\Big[\mathsf{S}^{\mathsf{F}}_{\mu\nu,\mathsf{JH}}(\mathbf{k},\mathbf{q})\Big]}{\hbar\omega+E_{\mathbf{k}+\mathbf{q}}+E_{\mathbf{k}}}$$
$$-\pi\Re\Big[\mathsf{S}^{\mathsf{F}}_{\mu\nu,\mathsf{JH}}(\mathbf{k},\mathbf{q})\Big]\delta(\hbar\omega+E_{\mathbf{k}+\mathbf{q}}+E_{\mathbf{k}})$$
$$-\frac{\Im\Big[\mathsf{S}^{\mathsf{F}}_{\mu\nu,\mathsf{JH}}(\mathbf{k},\mathbf{q})\Big]}{\hbar\omega-E_{\mathbf{k}+\mathbf{q}}-E_{\mathbf{k}}}+\pi\Re\Big[\mathsf{S}^{\mathsf{F}}_{\mu\nu,\mathsf{JH}}(\mathbf{k},\mathbf{q})\Big]\delta(\hbar\omega-E_{\mathbf{k}+\mathbf{q}}-E_{\mathbf{k}})\Bigg)\Bigg\} \tag{259}$$

To reiterate the nonunitary electron spin susceptibility has the general form

$$\chi^{\mathsf{nonunitary}}_{\mu\nu}(\mathbf{q},\omega) = \chi^{\mathsf{G}}_{\mu\nu}(\mathbf{q},\omega)+\chi^{\mathsf{F}}_{\mu\nu}(\mathbf{q},\omega). \tag{260}$$

It should be noted that the unitary case can be obtained from the more general form of the nonunitary case by taking the careful limit $\mathbf{m}(\mathbf{k})\rightarrow\mathbf{0}$.

Chapter V

Conclusion

There is strong experimental evidence that the order parameter in $(TMTSF)_2X$ is of the triplet variety. This evidence includes work by Lee *et. al.* [2],[4] and Belin & Behnia [3]. First Lee *et. al.* [2] measured the H vs. T phase diagram and observed that for $H\|\hat{\mathbf{a}}$ & $H\|\hat{\mathbf{b}}'$ that the field exceeds the Pauli paramagnetic limit by factors of 3 or 4. Lee *et. al.* [2] also observed an anisotropy inversion where the plot of $H\|\hat{\mathbf{b}}'$ vs. T crosses over and exceeds the plot of $H\|\hat{\mathbf{a}}$ vs. T at low enough temperatures.

Further work done by Belin & Behnia [3] measured the thermal conductivity of $(TMTSF)_2ClO_4$ in the normal and superconducting states. Belin & Behnia's data show that as $T \to 0$, $\kappa^s_{el}(T)/\kappa^n_{el}(T) \to 0$. The apparent exponential dependence of the electron thermal conductivity at low temperature in the superconducting state implies inciates a gap in the response and a gapped symmetry for the order parameter.

The last experiment which supports $(TMTSF)_2X$ as a candidate for triplet superconductivity was a Knight shift measurement done by Lee *et. al.* [4]. The Knight shift measures the electron spin response of the system to applied field. For triplet spin pairing the spin response will be constant, independent of temperature, and equal to the normal value $\chi(T) = \chi_N$ for $\mathbf{H} \perp \mathbf{d}$. This is what is observed by Lee *et. al.* [4] for $\mathbf{H}\|\hat{a}, \hat{b}'$ and points very strongly toward pairing in the triplet channel.

The combined results of Lee *et. al.* and Belin & Behnia suggest the existence of a gapped triplet state in $(TMTSF)_2X$. In order to distinguish between different triplet states the quasiparticle density of states and electron spin susceptibility for several

triplet states.

The quasiparticle density of states has been determined for several gapped and gapless symmetries for both spin singlet and spin triplet pairing. The intent here was to study a quantity which depends on the magnitude of the order parameter: $|\mathbf{d}(\mathbf{k})|$. This provides a picture of the response coming from the orbital component of the Cooper pairs. This response can be gapped, in which case there are very few excitations at energies on the order of the energy gap $\hbar\omega \sim \Delta_0$. Or it can be gapless, in which case there are excitations for finite energy $\hbar\omega$ down to but not including zero frequency (where $\mathcal{N}(\omega)$=0).

For low energy, one may extract the frequency dependence of the DOS which will depend on the node structure of the order parameter at the Fermi Surface. The low frequency dependence of $\mathcal{N}(\omega)$ at low energy could in principle then be used to test whether the order parameter is gapped or gapless symmetry and furthermore it can be used to determine if the order parameter has point nodes or line nodes at the Fermi surface.

One could in principle measure the quasiparticle density of states using photoemission spectroscopy. This would provide a picture revealing information about node structure of the order parameter of the superconductor. Unfortunately, the organic compound $(\mathsf{TMTSF})_2\mathsf{X}$ is rather sensitive to X-ray radiation. A sample being measured by this technique is susceptible to degradation and might not provide good results. Another technique to measure the DOS is STM which probes the I-V characteristic of the sample which can be related to the DOS.

Because the DOS has a mathematically similar (though simpler) structure to the imaginary part of the uniform dynamical spin susceptibility ($\Im[\chi_{mn}]$), it was studied

in anticipaiton of the calculation for $\Im[\chi_{mn}]$. An approach was developed to obtain the DOS using the delta function identity $\delta(F(x)) = \sum_j \delta(x-x_j)/|dF/dx| \;\; F(x_j) = 0$. This approach was first applied to the solution of the density of states for ^{3}He in the A-phase. A solution containing the accepted result for ^{3}He was obtained.

For more complicated problems (e.g., the solution of the DOS for various symmetries of $(\mathsf{TMTSF})_2\mathsf{X}$) one can use this approach to reduce a three dimensional numerical integration over the 1^{st} Brillouin zone to a two dimensional numerical integration. The advantage, of course, is a gain in computational speed and a corresponding reduction in computing time.

The next step was to determine the imaginary part of the uniform dynamical spin susceptibility tensor. The intent here was to gain insight into spin degrees of freedom of Cooper pairs and excitations in a quasi-one-dimensional superconductor. The study of the spin susceptibility at low frequency also reveals information about the node structure which can be used to characterize the symmetry of the order parameter. This is because both the node structure and the low frequency dependence of $\Im[\chi_{mn}(\mathbf{q} = \mathbf{0}, \omega)]$ are symmetry dependent. By measuring the low frequency dependence, the node structure of the order parameter becomes known. In the case of weak spin-orbit coupling the node structure arises from orbital information carried in the order parameter and not from the spin information; however, the susceptibility is a tensor and it also depends on the the order parameter vector orientation. The vector nature of the order parameter is intimately tide into the spin degrees of freedom. By measuring the various components of the susceptibility one may learn about the orientation of the order parameter in the crystalline lattice and probe the spin degrees of freedom.

One could in principle measure the uniform dynamical spin susceptibility with a neutron scattering experiment. A beam of uniform, plane spin polarized neutrons could be used to investigate the spin response in the uniform dynamical limit $\chi(\mathbf{q} \to \mathbf{0}, \omega)$. One drawback to this approach is the sample size itself being on the order of less than 1mm^3. Samples sizes much larger than 1mm^3 would make better samples for such a measurement, though.

A drawback to using neutron scattering is that, currently it can only be used to measure the high frequency limit (corresponding to energies greater than $k_B 1\text{K}$); however, we are interested in the spin response at much lower energies. Alternatively, it may be possible to measure the low frequency spin response using ESR in the μ-wave range.

Appendix A

The Energy of Quasiparticle Excitations

A.1 The Hamiltonian and Symmetry Properties

The purpose of this section is to derive the expression for the excitation energy $E_{\mathbf{k}}$ by diagonalizing the Hamiltonian in the many body problem for a general 2-body interaction in a lattice. The process of diagonalization will lead to introduction of quasiparticles which are composite particles consisting of electrons and electron holes in the superconductor. The system Hamiltonian to be diagonlized is:

$$\widehat{H} = \sum_{\mathbf{k}\alpha} \xi_{\mathbf{k}} a^{\dagger}_{\mathbf{k}\alpha} a_{\mathbf{k}\alpha} + \frac{1}{2} \sum_{\mathbf{k}\mathbf{k}'} \sum_{\alpha\beta\mu\lambda} V_{\alpha\beta,\lambda\mu}(\mathbf{k},\mathbf{k}') a^{\dagger}_{-\mathbf{k}\alpha} a^{\dagger}_{\mathbf{k}\beta} a_{\mathbf{k}'\lambda} a_{-\mathbf{k}'\mu}.$$

Note this is the most general form of the Hamiltonian for a two body interaction where $V_{\alpha\beta,\lambda\mu}(\mathbf{k},\mathbf{k}')$ is some general spin and momentum dependent interaction. We can derive the symmetry properties for the interaction term by imposing the property of hermiticity on the interaction term. $V_{\alpha\beta,\lambda\mu}(\mathbf{k},\mathbf{k}')$ is just a complex number so that $\widehat{V}^{\dagger} = \widehat{V}$ yields:

$$\sum_{\mathbf{k}\mathbf{k}'} \sum_{\alpha\beta\mu\lambda} \left[V_{\alpha\beta,\lambda\mu}(\mathbf{k},\mathbf{k}')\, a^{\dagger}_{-\mathbf{k}\alpha} a^{\dagger}_{\mathbf{k}\beta} a_{\mathbf{k}'\lambda} a_{-\mathbf{k}'\mu} \right]^{\dagger} =$$

$$\sum_{\mathbf{k}\mathbf{k}'} \sum_{\alpha\beta\mu\lambda} V^{*}_{\mu\lambda,\beta\alpha}(\mathbf{k},\mathbf{k}')\, a^{\dagger}_{-\mathbf{k}'\mu} a^{\dagger}_{\mathbf{k}'\lambda} a_{\mathbf{k}\beta} a_{-\mathbf{k}\alpha} = \sum_{\mathbf{k}\mathbf{k}'} \sum_{\alpha\beta\mu\lambda} V_{\alpha\beta,\lambda\mu}(\mathbf{k},\mathbf{k}')\, a^{\dagger}_{-\mathbf{k}\alpha} a^{\dagger}_{\mathbf{k}\beta} a_{\mathbf{k}'\lambda} a_{-\mathbf{k}'\mu}$$

Now permuting the dummy spin and momentum indices under the sum on the left to put the left-hand-side operators into the same form as on the right yields

$$V^*_{\alpha\beta,\lambda\mu}(\mathbf{k}',\mathbf{k}) = V_{\alpha\beta,\lambda\mu}(\mathbf{k},\mathbf{k}') \tag{261}$$

Other symmetry properties may be obtained by permuting dummy indices under the sum:

$$\begin{aligned}\sum_{\mathbf{k}\mathbf{k}'}\sum_{\alpha\beta\mu\lambda} V_{\alpha\beta,\lambda\mu}(\mathbf{k},\mathbf{k}')a^\dagger_{-\mathbf{k}\alpha}a^\dagger_{\mathbf{k}\beta}a_{\mathbf{k}'\lambda}a_{-\mathbf{k}'\mu} &= \sum_{\{\cdots\}} V_{\beta\alpha,\lambda\mu}(\mathbf{k},\mathbf{k}')a^\dagger_{-\mathbf{k}\beta}a^\dagger_{\mathbf{k}\alpha}a_{\mathbf{k}'\lambda}a_{-\mathbf{k}'\mu} \\ &= \sum_{\{\cdots\}} -V_{\beta\alpha,\lambda\mu}(\mathbf{k},\mathbf{k}')a^\dagger_{\mathbf{k}\alpha}a^\dagger_{-\mathbf{k}\beta}a_{\mathbf{k}'\lambda}a_{-\mathbf{k}'\mu} \\ &= \sum_{\{\cdots\}} -V_{\beta\alpha,\lambda\mu}(-\mathbf{k},\mathbf{k}')a^\dagger_{-\mathbf{k}\alpha}a^\dagger_{\mathbf{k}\beta}a_{\mathbf{k}'\lambda}a_{-\mathbf{k}'\mu}\end{aligned}$$

so that

$$V_{\alpha\beta,\lambda\mu}(\mathbf{k},\mathbf{k}') = -V_{\beta\alpha,\lambda\mu}(-\mathbf{k},\mathbf{k}') \tag{262}$$

and similarly by permuting λ & μ

$$V_{\alpha\beta,\lambda\mu}(\mathbf{k},\mathbf{k}') = -V_{\alpha\beta,\mu\lambda}(\mathbf{k},-\mathbf{k}'). \tag{263}$$

Permuting all the spin indices:

$$\begin{aligned}\sum_{\mathbf{k}\mathbf{k}'}\sum_{\alpha\beta\mu\lambda} V_{\alpha\beta,\lambda\mu}(\mathbf{k},\mathbf{k}')a^\dagger_{-\mathbf{k}\alpha}a^\dagger_{\mathbf{k}\beta}a_{\mathbf{k}'\lambda}a_{-\mathbf{k}'\mu} &= \sum_{\{\cdots\}} V_{\beta\alpha,\mu\lambda}(\mathbf{k},\mathbf{k}')a^\dagger_{-\mathbf{k}\beta}a^\dagger_{\mathbf{k}\alpha}a_{\mathbf{k}'\mu}a_{-\mathbf{k}'\lambda} \\ &= \sum_{\{\cdots\}} V_{\beta\alpha,\mu\lambda}(\mathbf{k}',\mathbf{k})a^\dagger_{\mathbf{k}\alpha}a^\dagger_{-\mathbf{k}\beta}a_{-\mathbf{k}'\lambda}a_{\mathbf{k}'\mu} \\ &\quad \sum_{\{\cdots\}} V_{\beta\alpha,\mu\lambda}(-\mathbf{k}',-\mathbf{k})a^\dagger_{-\mathbf{k}\alpha}a^\dagger_{\mathbf{k}\beta}a_{\mathbf{k}'\lambda}a_{-\mathbf{k}'\mu}\end{aligned}$$

so that

$$V_{\alpha\beta,\lambda\mu}(\mathbf{k},\mathbf{k}') = V_{\beta\alpha,\mu\lambda}(-\mathbf{k}',-\mathbf{k}) \tag{264}$$

and

$$V_{\alpha\beta,\lambda\mu}(\mathbf{k},\mathbf{k}') = -V_{\beta\alpha,\lambda\mu}(-\mathbf{k},\mathbf{k}') = -V_{\alpha\beta,\mu\lambda}(\mathbf{k},-\mathbf{k}') = V_{\beta\alpha,\mu\lambda}(-\mathbf{k}',-\mathbf{k}) = V^*_{\alpha\beta,\lambda\mu}(\mathbf{k}',\mathbf{k}) \tag{265}$$

A.2 Mean Field Theory and Hamiltonian Diagonalization

We now consider diagnolizing the Hamiltonian in order to find the eigen-energies of the system for the general interaction $V_{\alpha\beta,\lambda\mu}(\mathbf{k},\mathbf{k}')$. To do this one must first consider that in its present form the Hamiltonian is quartic in the interaction (i.e., contains four operators). This makes it very difficult to put $\widehat{H}$ into a suitable form for diagonalization. Nevertheless, $\widehat{H}$ can be put into diagonal form if one considers replacing the operator products $a^\dagger_{-\mathbf{k}\alpha}a^\dagger_{\mathbf{k}\beta}$ and $a_{\mathbf{k}'\lambda}a_{-\mathbf{k}'\mu}$ with their respective average values:

$$F^\dagger_{\alpha\beta}(\mathbf{k}) = \langle a^\dagger_{-\mathbf{k}\alpha}a^\dagger_{\mathbf{k}\beta}\rangle \quad \text{and} \quad F_{\lambda\mu}(\mathbf{k}') = \langle a_{\mathbf{k}'\lambda}a_{-\mathbf{k}'\mu}\rangle. \tag{266}$$

This recasts the Hamiltonian in quadratic form so that it becomes factorable under a suitable change of basis. The operator products can then be rewritten in terms of these averages according to:

$$a^\dagger_{-\mathbf{k}\alpha}a^\dagger_{\mathbf{k}\beta} = F^\dagger_{\alpha\beta}(\mathbf{k}) + \left(a^\dagger_{-\mathbf{k}\alpha}a^\dagger_{\mathbf{k}\beta} - F^\dagger_{\alpha\beta}(\mathbf{k}) \right)$$

$$a_{\mathbf{k}'\lambda}a_{-\mathbf{k}'\mu} = F_{\lambda\mu}(\mathbf{k}') + \left(a_{\mathbf{k}'\lambda}a_{-\mathbf{k}'\mu} - F_{\lambda\mu}(\mathbf{k}') \right)$$

$$\begin{aligned} a^\dagger_{-\mathbf{k}\alpha}a^\dagger_{\mathbf{k}\beta}a_{\mathbf{k}'\lambda}a_{-\mathbf{k}'\mu} = {} & F^\dagger_{\alpha\beta}(\mathbf{k})F_{\lambda\mu}(\mathbf{k}') \\ & + F^\dagger_{\alpha\beta}(\mathbf{k})(a_{\mathbf{k}'\lambda}a_{-\mathbf{k}'\mu} - F_{\lambda\mu}(\mathbf{k}')) \\ & + (a^\dagger_{-\mathbf{k}\alpha}a^\dagger_{\mathbf{k}\beta} - F^\dagger_{\alpha\beta}(\mathbf{k}))F_{\lambda\mu}(\mathbf{k}') \\ & + (a^\dagger_{-\mathbf{k}\alpha}a^\dagger_{\mathbf{k}\beta} - F^\dagger_{\alpha\beta}(\mathbf{k}))(a_{\mathbf{k}'\lambda}a_{-\mathbf{k}'\mu} - F_{\lambda\mu}(\mathbf{k}')). \end{aligned}$$

Explicit expressions for the anomalous averages can be found from solving the equations of motion simultaneously for the Green Function and anamolous average [see the text by Mahan [18] or the paper by Sigrist and Ueda [20]:

$$\begin{aligned} \frac{\partial F_{\alpha\beta}(\mathbf{k},\tau)}{\partial\tau} &= \frac{\partial}{\partial\tau}\ \langle \mathsf{T}_\tau a_{\mathbf{k},\alpha}(\tau)a_{-\mathbf{k},\beta}(0)\rangle \\ \frac{\partial G_{\alpha\beta}(\mathbf{k},\tau)}{\partial\tau} &= \frac{\partial}{\partial\tau} -\langle \mathsf{T}_\tau a_{\mathbf{k},\alpha}(\tau)a^\dagger_{\mathbf{k},\beta}(0)\rangle. \end{aligned}$$

Note that knowledge of the explicit form of the anamolous average is not necessary for the purposes of finding the excitation energy. Rewriting the operators in terms of their average values is called the Mean Field Approximation. Since the last term is quadratic in the difference of a pair of operators and average of the operator pair it's contribution is neglible and it is dropped.

Substituting this result back into the Hamiltonian and recognizing the F's as complex matrices indexed by the spin labels of the electron operators one obtains:

$$\widehat{H} = \sum_{\mathbf{k}\alpha} \xi_{\mathbf{k}} a^{\dagger}_{\mathbf{k}\alpha} a_{\mathbf{k}\alpha} \tag{267}$$
$$+\frac{1}{2} \sum_{\mathbf{k}\mathbf{k}'} \sum_{\alpha\beta\mu\lambda} V_{\alpha\beta,\lambda\mu}(\mathbf{k},\mathbf{k}') \left[-F^{\dagger}_{\alpha\beta}(\mathbf{k}) F_{\lambda\mu}(\mathbf{k}') + F^{\dagger}_{\alpha\beta}(\mathbf{k}) a_{\mathbf{k}'\lambda} a_{-\mathbf{k}'\mu} + F_{\lambda\mu}(\mathbf{k}') a^{\dagger}_{-\mathbf{k}\alpha} a^{\dagger}_{\mathbf{k}\beta} \cdot \right]$$

At this point it is convenient to consider functions of the form

$$\Delta_{\mathbf{k},\beta\alpha} = -\sum_{\mathbf{k}',\lambda\mu} V_{\alpha\beta,\lambda\mu}(\mathbf{k},\mathbf{k}') F_{\lambda\mu}(\mathbf{k}') \tag{268}$$

In what follows the excitation energy will be seen to depend on the lattice energy dispersion $\xi_{\mathbf{k}}$ and the energy function $\Delta_{\mathbf{k},\beta\alpha}$. In rough terms this function corresponds to the binding energy that appeared in case of two body pairing treated earlier at the beginning of §2.1. It will be noted that this function inherits the symmetry of the interaction potential which, in turn, has the same symmetry properties as the pair wave function obtained in §2.2.

One may solve explicitly for the value of $\Delta_{\mathbf{k},\beta\alpha}$ (called the gap function). In principle this is done by first solving explicitly for the form of the anomalous average (which will contain an explicit dependence on the gap function). The above equation (called the gap equation) is then solved self consistently for $\Delta_{\mathbf{k},\beta\alpha}$.

Recall from §2.1 that in describing Cooper Pairs one must consider antisymmetrized wave functions that are either symmetric in the momentum index and antisymmetric

in the spin indices (singlet pairing) or vice versa (triplet pairing). This leads to the following symmetry properties of the wave function which are independent of whether one considers singlet or triplet pairing:

$$\begin{aligned}\widehat{\Delta}(\mathbf{k}) &= -\widehat{\Delta}^T(-\mathbf{k}) = -\widehat{\Delta}^{\dagger *}(-\mathbf{k}) \\ \widehat{\Delta}^*(\mathbf{k}) &= -\widehat{\Delta}^\dagger(-\mathbf{k}) \\ -\widehat{\Delta}^*(-\mathbf{k}) &= \widehat{\Delta}^\dagger(\mathbf{k}).\end{aligned}$$

For now observe that the interaction potential has the same symmetry properties as the pair wave function discussed earlier. Writing the Hamiltonian in terms of the gap functions:

$$\widehat{H} = \sum_{\mathbf{k}\alpha} \xi_{\mathbf{k}} a^\dagger_{\mathbf{k}\alpha} a_{\mathbf{k}\alpha} + \frac{1}{2}\left[\sum_{\mathbf{k}}\sum_{\alpha\beta} F^\dagger_{\alpha\beta}(\mathbf{k})\Delta_{\beta\alpha}(\mathbf{k}) - \sum_{\mathbf{k}'}\sum_{\mu\lambda}\Delta^\dagger_{\mu\lambda}(\mathbf{k}')a_{\mathbf{k}'\lambda}a_{-\mathbf{k}'\mu} - \sum_{\mathbf{k}}\sum_{\alpha\beta}\Delta_{\beta\alpha}(\mathbf{k})a^\dagger_{-\mathbf{k}\alpha}a^\dagger_{\mathbf{k}\beta}\right].$$

Rewriting the expression by switching the dummy variables α & β and applying $\widehat{\Delta}(\mathbf{k}) = -\widehat{\Delta}^T(-\mathbf{k})$ to the second and third terms (and letting $\mathbf{k}' \to \mathbf{k}$, $\lambda \to \alpha$, $\mu \to \beta$ in the second term) one obtains:

$$\widehat{H} = \sum_{\mathbf{k}\alpha} \xi_{\mathbf{k}} a^\dagger_{\mathbf{k}\alpha} a_{\mathbf{k}\alpha} + \frac{1}{2}\sum_{\mathbf{k},\alpha\beta}\left[F^\dagger_{\beta\alpha}(\mathbf{k})\Delta_{\alpha\beta}(\mathbf{k}) + \Delta^\dagger_{\alpha\beta}(-\mathbf{k})a_{\mathbf{k}\alpha}a_{-\mathbf{k}\beta} + \Delta_{\alpha\beta}(-\mathbf{k})a^\dagger_{-\mathbf{k}\alpha}a^\dagger_{\mathbf{k}\beta}\right].$$

Putting $\mathbf{k} \to -\mathbf{k}$ in the last two terms and using the commutation property, $\{a, a^\dagger\} = 1$, of the creation/annihilation operators to rewrite the kinetic energy term, the diagonalizable form of the Hamiltonian is obtained:

$$\widehat{H} = \frac{1}{2}\sum_{\mathbf{k}\alpha}\xi_{\mathbf{k}}(a^\dagger_{\mathbf{k}\alpha}a_{\mathbf{k}\alpha} - a_{\mathbf{k}\alpha}a^\dagger_{\mathbf{k}\alpha}) + \frac{1}{2}\sum_{\mathbf{k},\alpha\beta}\left[\Delta^\dagger_{\alpha\beta}(\mathbf{k})a_{-\mathbf{k}\alpha}a_{\mathbf{k}\beta} + \Delta_{\alpha\beta}(\mathbf{k})a^\dagger_{\mathbf{k}\alpha}a^\dagger_{-\mathbf{k}\beta}\right] + \frac{1}{2}\sum_{\mathbf{k},\alpha\beta}\left[\xi_{\mathbf{k}} + F^\dagger_{\beta\alpha}(\mathbf{k})\Delta_{\alpha\beta}(\mathbf{k})\right].$$

$\Delta_{\mathbf{k},\alpha\beta}$ has the same symmetry with respect to indices as the pair wave funciton discussed in section §2.2. Using the matrices obtained in §2.2 to express $\Delta_{\mathbf{k},\alpha\beta}$:

$$\Delta_{\alpha\beta}(\mathbf{k}) = \Delta_0\, g_l(\mathbf{k})\,(i\widehat{\sigma}_y)_{\alpha\beta},$$

$$\Delta_{\alpha\beta}(\mathbf{k}) = \Delta_0 \left(i\,\vec{\sigma}\cdot\widehat{\sigma}_y\cdot\mathbf{d}(\mathbf{k})\right)_{\alpha\beta}.$$

Expanding out the spin sum in $\widehat{H}$ yields:

$$\begin{aligned}\widehat{H} = E_0 + \frac{1}{2}\sum_{\mathbf{k}}\xi_{\mathbf{k}}(a^\dagger_{\mathbf{k}\uparrow}a_{\mathbf{k}\uparrow} - a_{-\mathbf{k}\uparrow}a^\dagger_{-\mathbf{k}\uparrow} + a^\dagger_{\mathbf{k}\downarrow}a_{\mathbf{k}\downarrow} - a_{-\mathbf{k}\downarrow}a^\dagger_{-\mathbf{k}\downarrow}) \\ + \frac{1}{2}\sum_{\mathbf{k}}\Big[\Delta_{\mathbf{k}\uparrow\uparrow}a^\dagger_{\mathbf{k}\uparrow}a^\dagger_{-\mathbf{k}\uparrow} + \Delta^\dagger_{\mathbf{k}\uparrow\uparrow}a_{-\mathbf{k}\uparrow}a_{\mathbf{k}\uparrow} \\ + \Delta_{\mathbf{k}\downarrow\downarrow}a^\dagger_{\mathbf{k}\downarrow}a^\dagger_{-\mathbf{k}\downarrow} + \Delta^\dagger_{\mathbf{k}\downarrow\downarrow}a_{-\mathbf{k}\downarrow}a_{\mathbf{k}\downarrow} \\ + \Delta_{\mathbf{k}\uparrow\downarrow}a^\dagger_{\mathbf{k}\uparrow}a^\dagger_{-\mathbf{k}\downarrow} + \Delta^\dagger_{\mathbf{k}\uparrow\downarrow}a_{-\mathbf{k}\uparrow}a_{\mathbf{k}\downarrow} \\ + \Delta_{\mathbf{k}\downarrow\uparrow}a^\dagger_{\mathbf{k}\downarrow}a^\dagger_{-\mathbf{k}\uparrow} + \Delta^\dagger_{\mathbf{k}\downarrow\uparrow}a_{-\mathbf{k}\downarrow}a_{\mathbf{k}\uparrow}\Big].\end{aligned}$$

We took the liberty of taking $\mathbf{k} \to -\mathbf{k}$ in the $aa^\dagger$ operators of the kinetic energy piece. This can be done since we are summing over all $\mathbf{k}$ and will enable us to group the operators in a special way such that the Hamiltonian may be written in terms of matrices and its diagonalization may be considered with greater ease [also note $\Delta_{\mathbf{k},\alpha\beta} \Leftrightarrow \Delta_{\alpha\beta}(\mathbf{k})$].

The kinetic energy piece is already diagonal and can be written in terms of matrices as follows:

$$t \equiv \begin{bmatrix} a^\dagger_{\mathbf{k}\uparrow}, a^\dagger_{\mathbf{k}\downarrow}, a_{-\mathbf{k}\uparrow}, a_{-\mathbf{k}\downarrow}\end{bmatrix}\begin{pmatrix} \xi_{\mathbf{k}} & 0 & 0 & 0 \\ 0 & \xi_{\mathbf{k}} & 0 & 0 \\ 0 & 0 & -\xi_{\mathbf{k}} & 0 \\ 0 & 0 & 0 & -\xi_{\mathbf{k}}\end{pmatrix}\begin{bmatrix} a_{\mathbf{k}\uparrow}, \\ a_{\mathbf{k}\downarrow}, \\ a^\dagger_{-\mathbf{k}\uparrow}, \\ a^\dagger_{-\mathbf{k}\downarrow}\end{bmatrix} = A^\dagger_{\mathbf{k}}\mathbf{T}_{\mathbf{k}}A_{\mathbf{k}}$$

$$\textit{where}\ \ A_{\mathbf{k}} \equiv \begin{bmatrix} a_{\mathbf{k}\uparrow}, \\ a_{\mathbf{k}\downarrow}, \\ a^\dagger_{-\mathbf{k}\uparrow}, \\ a^\dagger_{-\mathbf{k}\downarrow}\end{bmatrix}\ \textit{and}\ \ \mathbf{T}_{\mathbf{k}} \equiv \begin{pmatrix} \xi_{\mathbf{k}}\widehat{\sigma}_0 & \widehat{0} \\ \widehat{0} & -\xi_{\mathbf{k}}\widehat{\sigma}_0\end{pmatrix}.$$

The non-diagonal piece can be written in terms of the same $A_{\mathbf{k}}$-vector also so that $w = A_{\mathbf{k}}^{\dagger}\mathbf{W}_{\mathbf{k}}A_{\mathbf{k}}$ is equal to the sum of all the interaction terms in the Hamiltonian where:

$$\mathbf{W}_{\mathbf{k}} \equiv \begin{pmatrix} w_{11} & w_{12} & w_{13} & w_{14} \\ w_{21} & w_{22} & w_{23} & w_{24} \\ w_{31} & w_{32} & w_{33} & w_{34} \\ w_{41} & w_{42} & w_{43} & w_{44} \end{pmatrix}.$$

After multiplying out $w = A_{\mathbf{k}}^{\dagger}\mathbf{W}_{\mathbf{k}}A_{\mathbf{k}}$ and setting terms equal we find:

$$\mathbf{W}_{\mathbf{k}} \equiv \begin{pmatrix} 0 & 0 & \Delta_{\mathbf{k}\uparrow\uparrow} & \Delta_{\mathbf{k}\uparrow\downarrow} \\ 0 & 0 & \Delta_{\mathbf{k}\downarrow\uparrow} & \Delta_{\mathbf{k}\downarrow\downarrow} \\ \Delta_{\mathbf{k}\uparrow\uparrow}^{\dagger} & \Delta_{\mathbf{k}\uparrow\downarrow}^{\dagger} & 0 & 0 \\ \Delta_{\mathbf{k}\downarrow\uparrow}^{\dagger} & \Delta_{\mathbf{k}\downarrow\downarrow}^{\dagger} & 0 & 0 \end{pmatrix}.$$

Using the antisymmetry property of the gap function that $[-\widehat{\Delta}_{-\mathbf{k}}^{*}]_{\alpha\beta} = [\widehat{\Delta}_{\mathbf{k}}^{\dagger}]_{\alpha\beta}$ the interaction piece can be cast in its final form before diagonalization:

$$\mathbf{W}_{\mathbf{k}} \equiv \begin{pmatrix} 0 & 0 & \Delta_{\mathbf{k}\uparrow\uparrow} & \Delta_{\mathbf{k}\uparrow\downarrow} \\ 0 & 0 & \Delta_{\mathbf{k}\downarrow\uparrow} & \Delta_{\mathbf{k}\downarrow\downarrow} \\ -\Delta_{-\mathbf{k}\uparrow\uparrow}^{*} & -\Delta_{-\mathbf{k}\uparrow\downarrow}^{*} & 0 & 0 \\ -\Delta_{-\mathbf{k}\downarrow\uparrow}^{*} & -\Delta_{-\mathbf{k}\downarrow\downarrow}^{*} & 0 & 0 \end{pmatrix} = \begin{pmatrix} \widehat{0} & \widehat{\Delta}_{\mathbf{k}} \\ -\widehat{\Delta}_{-\mathbf{k}}^{*} & \widehat{0} \end{pmatrix} \Leftrightarrow \begin{pmatrix} \widehat{0} & \widehat{\Delta}_{\mathbf{k}} \\ \widehat{\Delta}_{\mathbf{k}}^{\dagger} & \widehat{0} \end{pmatrix}.$$

The full Hamiltonian becomes:

$$\widehat{H} = E_0 + \frac{1}{2}\sum_{\mathbf{k}} \left[a_{\mathbf{k}\uparrow}^{\dagger}, a_{\mathbf{k}\downarrow}^{\dagger}, a_{-\mathbf{k}\uparrow}, a_{-\mathbf{k}\downarrow}\right] \begin{pmatrix} \xi_{\mathbf{k}} & 0 & \Delta_{\mathbf{k}\uparrow\uparrow} & \Delta_{\mathbf{k}\uparrow\downarrow} \\ 0 & \xi_{\mathbf{k}} & \Delta_{\mathbf{k}\downarrow\uparrow} & \Delta_{\mathbf{k}\downarrow\downarrow} \\ -\Delta_{-\mathbf{k}\uparrow\uparrow}^{*} & -\Delta_{-\mathbf{k}\uparrow\downarrow}^{*} & -\xi_{\mathbf{k}} & 0 \\ -\Delta_{-\mathbf{k}\downarrow\uparrow}^{*} & -\Delta_{-\mathbf{k}\downarrow\downarrow}^{*} & 0 & -\xi_{\mathbf{k}} \end{pmatrix} \begin{bmatrix} a_{\mathbf{k}\uparrow}, \\ a_{\mathbf{k}\downarrow}, \\ a_{-\mathbf{k}\uparrow}^{\dagger}, \\ a_{-\mathbf{k}\downarrow}^{\dagger} \end{bmatrix}$$

$$\widehat{H} = E_0 + \frac{1}{2}\sum_{\mathbf{k}} A_{\mathbf{k}}^{\dagger}(\mathbf{T}_{\mathbf{k}} + \mathbf{W}_{\mathbf{k}})A_{\mathbf{k}} = E_0 + \frac{1}{2}\sum_{\mathbf{k}} A_{\mathbf{k}}^{\dagger}\mathbf{h}_{\mathbf{k}}A_{\mathbf{k}}.$$

The goal now is to affect a transformation on the Hamiltonian such that it is diagonalized and takes the form:

$$\widehat{H} = E_0 + \sum_{\mathbf{k}} \left[b^{\dagger}_{\mathbf{k}\uparrow}, b^{\dagger}_{\mathbf{k}\downarrow}, b_{-\mathbf{k}\uparrow}, b_{-\mathbf{k}\downarrow} \right] \begin{pmatrix} E_{\mathbf{k}} & 0 & 0 & 0 \\ 0 & E_{\mathbf{k}} & 0 & 0 \\ 0 & 0 & -E_{\mathbf{k}} & 0 \\ 0 & 0 & 0 & -E_{\mathbf{k}} \end{pmatrix} \begin{bmatrix} b_{\mathbf{k}\uparrow}, \\ b_{\mathbf{k}\downarrow}, \\ b^{\dagger}_{-\mathbf{k}\uparrow}, \\ b^{\dagger}_{-\mathbf{k}\downarrow} \end{bmatrix}$$

where $A_{\mathbf{k}} = \mathbf{U}_{\mathbf{k}} B_{\mathbf{k}}$ and $\mathbf{U}_{\mathbf{k}}$ is a 4×4 matrix that transforms $A_{\mathbf{k}}$ to the diagonal basis and is given by:

$$\mathbf{U}_{\mathbf{k}} = \begin{pmatrix} \widehat{u}_{\mathbf{k}} & \widehat{v}_{\mathbf{k}} \\ \widehat{v}^{*}_{-\mathbf{k}} & \widehat{u}^{*}_{-\mathbf{k}} \end{pmatrix}.$$

The $\widehat{u}_{\mathbf{k}}$ & $\widehat{v}_{\mathbf{k}}$ are 2×2 matrices to be determined. The Hamiltonian will be diagonalized under the assumption that $\Delta_{\mathbf{k},\alpha\beta}$ is proportional to a unitary matrix. As such, the eigen-state in the diagonal basis corresponding to a unitary gap function is called a unitary state. With this in mind $\mathbf{U}_{\mathbf{k}}$ is a unitary rotation that diagonalizes $\widehat{H}$. So far we have:

$$\widehat{H} = E_0 + \frac{1}{2} \sum_{\mathbf{k}} A^{\dagger}_{\mathbf{k}} \mathbf{h}_{\mathbf{k}} A_{\mathbf{k}} = E_0 + \frac{1}{2} \sum_{\mathbf{k}} B^{\dagger}_{\mathbf{k}} \mathbf{E}_{\mathbf{k}} B_{\mathbf{k}}.$$

Using $A_{\mathbf{k}} = \mathbf{U}_{\mathbf{k}} B_{\mathbf{k}}$ we obtain

$$B^{\dagger}_{\mathbf{k}} U^{\dagger}_{\mathbf{k}} \mathbf{h}_{\mathbf{k}} U_{\mathbf{k}} B_{\mathbf{k}} = B^{\dagger}_{\mathbf{k}} \mathbf{E}_{\mathbf{k}} B_{\mathbf{k}} \longrightarrow U_{\mathbf{k}} \mathbf{E}_{\mathbf{k}} = \mathbf{h}_{\mathbf{k}} U_{\mathbf{k}}.$$

From the expression $U_{\mathbf{k}} \mathbf{E}_{\mathbf{k}} = \mathbf{h}_{\mathbf{k}} U_{\mathbf{k}}$ four equations of constraint for $\widehat{u}_{\mathbf{k}}$ and $\widehat{v}_{\mathbf{k}}$ are obtained. After a little rearranging they are:

$$\begin{aligned} \widehat{u}_{\mathbf{k}}(E_{\mathbf{k}} - \xi_{\mathbf{k}}) &= \widehat{\Delta}_{\mathbf{k}} \widehat{v}^{*}_{-\mathbf{k}} \\ \widehat{v}_{\mathbf{k}}(E_{\mathbf{k}} + \xi_{\mathbf{k}}) &= -\widehat{\Delta}_{\mathbf{k}} \widehat{u}^{*}_{-\mathbf{k}} \\ \widehat{v}^{*}_{-\mathbf{k}}(E_{\mathbf{k}} + \xi_{\mathbf{k}}) &= -\widehat{\Delta}^{*}_{-\mathbf{k}} \widehat{u}_{\mathbf{k}} \\ \widehat{u}^{*}_{-\mathbf{k}}(E_{\mathbf{k}} - \xi_{\mathbf{k}}) &= \widehat{\Delta}^{*}_{\mathbf{k}} \widehat{v}_{\mathbf{k}}. \end{aligned} \tag{269}$$

A further constraint is imposed from the unitary of $\mathbf{U_k}$ that $\mathbf{U_k}\mathbf{U_k^\dagger} = \hat{\sigma}_0$. We then obtain a condition on $\hat{u}_\mathbf{k}$ and $\hat{v}_\mathbf{k}$ that:

$$\hat{u}_\mathbf{k}\hat{u}_\mathbf{k}^\dagger + \hat{v}_\mathbf{k}\hat{v}_\mathbf{k}^\dagger = \hat{\sigma}_0.$$

Combining the first and third expressions in Eq. 269 we get a relation for $\hat{u}_\mathbf{k}$:

$$\hat{u}_\mathbf{k}(E_\mathbf{k}^2 - \xi_\mathbf{k}^2) = -\hat{\Delta}_\mathbf{k}\hat{\Delta}^*_{-\mathbf{k}}\hat{u}_\mathbf{k} = \hat{\Delta}_\mathbf{k}\hat{\Delta}_\mathbf{k}^\dagger\hat{u}_\mathbf{k}.$$

The only constraint on $\hat{u}_\mathbf{k}$ is that it be unitary and obey the five equations of constraint above. So we are free to choose $\hat{u}_\mathbf{k}$ to be any 2×2 unitary matrix that obeys these conditions. This choice will then specify $\hat{v}_\mathbf{k}$. Making the simplest choice possible we choose $\hat{u}_\mathbf{k} = u_0\hat{\sigma}_0$ [$\hat{u}_\mathbf{k}$ is proportional to the identity]. With $\hat{\Delta}_\mathbf{k}$ proportional to a unitary matrix $\hat{\Delta}_\mathbf{k}\hat{\Delta}_\mathbf{k}^\dagger = |\Delta_0\mathbf{d}(\mathbf{k})|^2\hat{\sigma}_0$ then:

$$\hat{u}_\mathbf{k}(E_\mathbf{k}^2 - \xi_\mathbf{k}^2) = \hat{\Delta}_\mathbf{k}\hat{\Delta}_\mathbf{k}^\dagger\hat{u}_\mathbf{k} \longrightarrow (E_\mathbf{k}^2 - \xi_\mathbf{k}^2)\hat{\sigma}_0 = |\Delta_0\mathbf{d}(\mathbf{k})|^2\hat{\sigma}_0$$

and we obtain the expression for the new excitation spectrum in the diagonal basis

$$E_\mathbf{k} = \sqrt{\xi_\mathbf{k}^2 + |\Delta_0|^2|\mathbf{d}(\mathbf{k})|^2} = \sqrt{\xi_\mathbf{k}^2 + \frac{1}{2}\mathrm{Tr}[\hat{\Delta}_\mathbf{k}\hat{\Delta}_\mathbf{k}^\dagger]}.$$

Where we have used that fact from the discussion of section §2.2 that when $\hat{\Delta}_\mathbf{k}$ is proportional to a unitary matrix that $\mathrm{Tr}[\hat{\Delta}_\mathbf{k}\hat{\Delta}_\mathbf{k}^\dagger] = 2|\Delta_0\mathbf{d}(\mathbf{k})|^2$. From the second expression in Eq. 269 and the unitary condition on $\hat{u}_\mathbf{k}$ & $\hat{v}_\mathbf{k}$ u_0 and $\hat{v}_\mathbf{k}$ are determined:

$$\begin{aligned}
\hat{v}_\mathbf{k}(E_\mathbf{k} + \xi_\mathbf{k}) &= -\hat{\Delta}_\mathbf{k}\hat{u}^*_{-\mathbf{k}} \\
\Rightarrow \hat{v}_\mathbf{k} &= \frac{-\hat{\Delta}_\mathbf{k}}{E_\mathbf{k} + \xi_\mathbf{k}}u_0 \\
\hat{u}_\mathbf{k}\hat{u}_\mathbf{k}^\dagger + \hat{v}_\mathbf{k}\hat{v}_\mathbf{k}^\dagger &= \hat{\sigma}_0 \\
\Rightarrow u_0^2\left[\hat{\sigma}_0 + \frac{\hat{\Delta}_\mathbf{k}\hat{\Delta}_\mathbf{k}^\dagger}{(E_\mathbf{k} + \xi_\mathbf{k})^2}\right] &= \hat{\sigma}_0.
\end{aligned}$$

Breaking things up componentwise:

$$u_0^2\delta_{\alpha\beta} + \frac{\sum_\gamma[\hat{\Delta}_\mathbf{k}]_{\alpha\gamma}[\hat{\Delta}_\mathbf{k}^\dagger]_{\gamma\beta}}{(E_\mathbf{k} + \xi_\mathbf{k})^2} = \delta_{\alpha\beta} \Rightarrow u_0^2\delta_{\alpha\beta} + \frac{\frac{1}{2}\mathrm{Tr}[\hat{\Delta}_\mathbf{k}\hat{\Delta}_\mathbf{k}^\dagger]\delta_{\alpha\beta}}{(E_\mathbf{k} + \xi_\mathbf{k})^2} = \delta_{\alpha\beta}.$$

Finally we obtain:

$$u_0^2 = \frac{(E_\mathbf{k} + \xi_\mathbf{k})^2}{(E_\mathbf{k} + \xi_\mathbf{k})^2 + \frac{1}{2}\mathsf{Tr}[\widehat{\Delta}_\mathbf{k}\widehat{\Delta}_\mathbf{k}^\dagger]}$$

$$\widehat{u}_\mathbf{k} = \frac{(E_\mathbf{k} + \xi_\mathbf{k})\widehat{\sigma}_0}{\sqrt{(E_\mathbf{k} + \xi_\mathbf{k})^2 + \frac{1}{2}\mathsf{Tr}[\widehat{\Delta}_\mathbf{k}\widehat{\Delta}_\mathbf{k}^\dagger]}}$$

$$\widehat{v}_\mathbf{k} = \frac{-\widehat{\Delta}_\mathbf{k}}{\sqrt{(E_\mathbf{k} + \xi_\mathbf{k})^2 + \frac{1}{2}\mathsf{Tr}[\widehat{\Delta}_\mathbf{k}\widehat{\Delta}_\mathbf{k}^\dagger]}}.$$

We can also write the new creation/annihilation operators in terms of the old since $A_\mathbf{k} = \mathbf{U}_\mathbf{k} B_\mathbf{k}$ and $B_\mathbf{k} = \mathbf{U}_\mathbf{k}^\dagger A_\mathbf{k}$ where:

$$\mathbf{U}_\mathbf{k} = \begin{pmatrix} \widehat{u}_\mathbf{k} & \widehat{v}_\mathbf{k} \\ \widehat{v}_{-\mathbf{k}}^* & \widehat{u}_{-\mathbf{k}}^* \end{pmatrix} \Rightarrow \mathbf{U}_\mathbf{k}^\dagger = \begin{pmatrix} \widehat{u}_\mathbf{k}^\dagger & [\widehat{v}_{-\mathbf{k}}^*]^\dagger \\ \widehat{v}_\mathbf{k}^\dagger & [\widehat{u}_{-\mathbf{k}}^*]^\dagger \end{pmatrix} = \begin{pmatrix} \widehat{u}_\mathbf{k}^\dagger & [\widehat{v}_{-\mathbf{k}}^*]^\dagger \\ \widehat{v}_\mathbf{k}^\dagger & [\widehat{u}_{-\mathbf{k}}^*]^\dagger \end{pmatrix}$$

$$\mathbf{U}_\mathbf{k}^\dagger = \frac{1}{\sqrt{(E_\mathbf{k} + \xi_\mathbf{k})^2 + \frac{1}{2}\mathsf{Tr}[\widehat{\Delta}_\mathbf{k}\widehat{\Delta}_\mathbf{k}^\dagger]}} \begin{pmatrix} (E_\mathbf{k} + \xi_\mathbf{k})\widehat{\sigma}_0 & [\widehat{\Delta}_\mathbf{k}] \\ -\widehat{\Delta}_\mathbf{k}^\dagger & E_\mathbf{k} + \xi_\mathbf{k})\widehat{\sigma}_0 \end{pmatrix}$$

Writing $B_\mathbf{k} = \mathbf{U}_\mathbf{k}^\dagger A_\mathbf{k}$ componentwise:

$$b_{\mathbf{k},\alpha} = \sum_\beta \left\{ (E_\mathbf{k} + \xi_\mathbf{k})\delta_{\alpha\beta} a_{\mathbf{k},\beta} + \widehat{\Delta}_{\mathbf{k},\alpha\beta} a_{\mathbf{k},\beta}^\dagger \right\}$$

$$b_{\mathbf{k},\alpha}^\dagger = \sum_\beta \left\{ -\widehat{\Delta}_{\mathbf{k},\alpha\beta}^\dagger a_{\mathbf{k},\beta} + (E_\mathbf{k} + \xi_\mathbf{k})\delta_{\alpha\beta} a_{\mathbf{k},\beta}^\dagger \right\}$$

where $\alpha, \beta = \{\uparrow, \downarrow\}$. The b-operators depend linearly on the original electron operators $\{a, a^\dagger\}$. The represent the creation and destruction of the quasiparticles mentioned earlier. As can be seen, the action of b (or $b^\dagger$) creates an electron (by the action of $a^\dagger$ and an electron hole by the action of a. The new b-operators form the *operator* basis which diagonalize the system Hamiltonian.

Appendix B

FREQUENCY SUMMATIONS

One wishes to perform sums of the form

$$\sum_{\omega_n} \frac{1}{i\hbar\omega_n - i\alpha\hbar\nu - \eta E_1} \frac{1}{i\hbar\omega_n - \gamma E_0} = \sum_{\omega_n} h(\omega_n) \quad \alpha, \eta, \gamma = \pm 1 \tag{270}$$

Recall that the the sum above comes from products of Green functions for Fermions. Therefore the frequencies ω_n, $\omega_n + \nu$ must be Fermi frequencies. Since ω_n appears by itself in one of the terms it must be a Fermi frequency of the form $\omega_n = \pi\frac{(2n+1)}{\hbar\beta}$. Since $\omega_n + \nu$ is also a Fermi frequency it must be that ν is a Bose frequency $\left(= \pi\frac{2n}{\hbar\beta}\right)$ so that the sum remains an odd multiple of $\pi/\hbar\beta$. This is relevant in what follows.

The Fermi function has singularities at $i\omega_n$ which are just the frequencies to be summed on:

$$f(z) = \frac{1}{e^{\hbar\beta z} + 1} \tag{271}$$

$$\hbar\beta z_n = i\pi(2n+1). \tag{272}$$

From complex analysis if one takes the contour integral over a path of diverging radius R

$$\lim_{R\to\infty} \oint_{C_R} dz\, h(z) f(z) = 2\pi i \sum Res[h(z) f(z)] \tag{273}$$

(where the identification $i\omega_n \to z$ has been made) one obtains a sum over residues at all the poles of the integrand. $h(z)$ has poles at

$$z_0 = \gamma E_0/\hbar \tag{274}$$

$$z_1 = i\alpha\nu + \eta E_1/\hbar. \tag{275}$$

The denominator of $f(z)$, [namely, $q(z) = e^{\hbar\beta z} + 1$] vanishes at z_n, [$q(z_n) = 0$]; however, the first derivative of $q(z)$ is finite at z_n:

$$q'(z_n) = -\hbar\beta. \tag{276}$$

From complex analysis z_n is classed as a zero of $q(z)$ of order m=1 and can be shown to be a pole of order m=1 of $f(z)$ by taking the limit

$$\lim_{z\to z_n} (z - z_n)^m f(z) \tag{277}$$

where the limit vanishes for $m > 1$. Thus, $f(z) = 1/q(z)$ has simple poles at z_n and corresponding residues

$$Res[f(z)]_{z_n} = \lim_{z\to z_n} \left\{(z - z_n)^m f^{(m-1)}(z)\right\} \tag{278}$$

$$= -\frac{1}{\hbar\beta} \qquad \text{for m} = 1. \tag{279}$$

Since $h(z) \propto 1/z^2$, then the contour integral vanishes [by Jordan's lemma] as $R \to \infty$ leaving:

$$0 = \sum Res[h(z)f(z)] = \sum_{i\omega_n} h(i\omega_n)\left(-\frac{1}{\hbar\beta}\right) + f(z_0)Res[h(z)]_{z_0} + f(z_1)Res[h(z)]_{z_1}$$

$$\frac{1}{\hbar\beta}\sum_{i\omega_n} h(i\omega_n) = f(\gamma E_0/\hbar)\frac{1}{\gamma E_0 - i\alpha\hbar\nu - \eta E_1} + f(i\alpha\nu + \eta E_1/\hbar)\frac{1}{i\alpha\hbar\nu + \eta E_1 - \gamma E_0}$$

$$= \frac{1}{i\alpha\hbar\nu + \eta E_1 - \gamma E_0}[f(\eta E_1/\hbar) - f(\gamma E_0/\hbar)] \tag{280}$$

where $f(i\alpha\nu + \eta E_1/\hbar) = \dfrac{1}{e^{i2\alpha\pi n} e^{\beta\eta E_1} + 1} = f(\eta E_1)$ was used.

Further identities used to cast the frequency sum in final form are:

$$f(-E) = 1 - f(E).$$

Observe:

$$\begin{aligned} f(-E) + f(E) = & \\ &= \frac{1}{e^{-\beta E}+1} + \frac{1}{e^{\beta E}+1} \\ &= \frac{e^{\beta E/2}}{e^{-\beta E/2}+e^{\beta E/2}} + \frac{e^{-\beta E/2}}{e^{\beta E/2}+e^{-\beta E/2}} \\ &= 1. \end{aligned} \tag{281}$$

In the case where the frequency summation in multiplied by an overall complex number $\mathcal{Z}$

$$\mathcal{Z}\sum_{i\omega_n} h(i\omega_n) = \mathcal{Z}\frac{1}{i\alpha\hbar\nu + \eta E_1 - \gamma E_0}[f(\eta E_1/\hbar) - f(\gamma E_0/\hbar)] \tag{282}$$

then, after factoring our the sign α, the Wick's rotation $i\nu = \nu + i\delta$ yields:

$$\mathcal{Z}\sum_{i\omega_n} h(i\omega_n) =$$

$$\tfrac{1}{\alpha}[f(\eta E_1/\hbar) - f(\gamma E_0/\hbar)]\Big(\Re\{\mathcal{Z}\} + i\Im\{\mathcal{Z}\}\Big)\left[\frac{\hbar\nu + \frac{\eta}{\alpha}E_1 - \frac{\gamma}{\alpha}E_0 - i\delta}{(\hbar\nu + \frac{\eta}{\alpha}E_1 - \frac{\gamma}{\alpha}E_0)^2 + \delta^2}\right].$$

Taking $\delta \to 0$:

$$\begin{aligned} &= \tfrac{1}{\alpha}[f(\eta E_1/\hbar) - f(\gamma E_0/\hbar)]\Big(\Re\{\mathcal{Z}\} + i\Im\{\mathcal{Z}\}\Big) \\ &\qquad \times \left[\frac{1}{\hbar\nu + \frac{\eta}{\alpha}E_1 - \frac{\gamma}{\alpha}E_0} - i\pi\delta(\hbar\nu + \tfrac{\eta}{\alpha}E_1 - \tfrac{\gamma}{\alpha}E_0)\right]. \end{aligned}$$

Finally,

$$\begin{aligned} \mathcal{Z}\sum_{i\omega_n} h(i\omega_n) = \tfrac{1}{\alpha}[f(\eta E_1/\hbar) - f(\gamma E_0/\hbar)]\Bigg\{ & \\ \left[\frac{\Re\{\mathcal{Z}\}}{\hbar\nu + \frac{\eta}{\alpha}E_1 - \frac{\gamma}{\alpha}E_0} + \pi\Im\{\mathcal{Z}\}\delta(\hbar\nu + \tfrac{\eta}{\alpha}E_1 - \tfrac{\gamma}{\alpha}E_0)\right] & \\ + i\left[\frac{\Im\{\mathcal{Z}\}}{\hbar\nu + \frac{\eta}{\alpha}E_1 - \frac{\gamma}{\alpha}E_0} - \pi\Re\{\mathcal{Z}\}\delta(\hbar\nu + \tfrac{\eta}{\alpha}E_1 - \tfrac{\gamma}{\alpha}E_0)\right]\Bigg\} & \end{aligned} \tag{283}$$

Appendix C

Summation on Spin Indices

Recall the definition:

$$[\sigma_m]_{\alpha\beta} = \begin{bmatrix} \eta_{m,2} & \eta_{m,3} \\ \eta_{m,1} & -\eta_{m,2} \end{bmatrix}_{\alpha\beta}$$

$$\eta_{m,1} = \delta_{m1} + i\delta_{m2}$$

$$\eta_{m,2} = \delta_{m3}$$

$$\eta_{m,3} = \delta_{m1} - i\delta_{m2}. \tag{284}$$

The sum over indices will be carried out for

$$\sum_{\alpha\beta\gamma\delta} [\sigma_m]_{\alpha\beta}[\sigma_n]_{\gamma\delta}\,\delta_{\alpha\delta}\delta_{\beta\gamma}. \tag{285}$$

First recognize that

$$\delta_{\beta\gamma} = \begin{bmatrix} 1 & 0 \\ 0 & 1 \end{bmatrix}_{\beta\gamma}. \tag{286}$$

Substituting all the matrices into the sum:

$$\sum_{\alpha\beta\gamma\delta} \begin{bmatrix} \eta_{m,2} & \eta_{m,3} \\ \eta_{m,1} & -\eta_{m,2} \end{bmatrix}_{\alpha\beta} \begin{bmatrix} 1 & 0 \\ 0 & 1 \end{bmatrix}_{\beta\gamma} \begin{bmatrix} \eta_{n,2} & \eta_{n,3} \\ \eta_{n,1} & -\eta_{n,2} \end{bmatrix}_{\gamma\delta} \begin{bmatrix} 1 & 0 \\ 0 & 1 \end{bmatrix}_{\delta\alpha} \tag{287}$$

By the rules of matrix multiplication the *inside* indices can be dropped and the matrices multiplied out. The *outside* indices – in this case α must remain to be

summed on. This leaves the trace over the product of matrices:

$$\sum_{\alpha\beta\gamma\delta}[\boldsymbol{\sigma}_m]_{\alpha\beta}[\boldsymbol{\sigma}_n]_{\gamma\delta}\,\delta_{\alpha\delta}\delta_{\beta\gamma} = \sum_{\alpha}\left[\left[\begin{array}{cc}\eta_{m,2} & \eta_{m,3}\\ \eta_{m,1} & -\eta_{m,2}\end{array}\right]\left[\begin{array}{cc}1 & 0\\ 0 & 1\end{array}\right]\left[\begin{array}{cc}\eta_{n,2} & \eta_{n,3}\\ \eta_{n,1} & -\eta_{n,2}\end{array}\right]\left[\begin{array}{cc}1 & 0\\ 0 & 1\end{array}\right]\right]_{\alpha\alpha}$$

$$= \sum_{\alpha}\left[\left[\begin{array}{cc}\eta_{m,2} & \eta_{m,3}\\ \eta_{m,1} & -\eta_{m,2}\end{array}\right]\left[\begin{array}{cc}\eta_{n,2} & \eta_{n,3}\\ \eta_{n,1} & -\eta_{n,2}\end{array}\right]\right]_{\alpha\alpha}$$

$$= \mathsf{Tr}\left[\begin{array}{cc}\eta_{m,2}\eta_{n,2}+\eta_{m,3}\eta_{n,1} & \eta_{m,2}\eta_{n,3}-\eta_{m,3}\eta_{n,2}\\ \eta_{m,1}\eta_{n,2}-\eta_{m,2}\eta_{n,1} & \eta_{m,1}\eta_{n,3}+\eta_{m,2}\eta_{n,2}\end{array}\right]$$

$$= \eta_{m,1}\eta_{n,3}+\eta_{m,3}\eta_{n,1}+2\eta_{m,2}\eta_{n,2} = 2\,\delta_{mn} \tag{288}$$

The next sum to be performed is a bit trickier:

$$\sum_{\alpha\beta\gamma\delta}[\boldsymbol{\sigma}_m]_{\alpha\beta}[\boldsymbol{\sigma}_n]_{\gamma\delta}\,\Delta^{\dagger}_{\alpha\gamma}(-\mathbf{k}+\mathbf{q})\Delta_{\beta\delta}(\mathbf{k}). \tag{289}$$

In this case the gap parameter $\Delta_{\lambda\mu}(\mathbf{k})$ has two distinct forms depending on whether one is considering a singlet symmetry or a triplet symmetry. For the two cases one has respectively:

$$\Delta^{\mathsf{S}}_{\lambda\mu}(\mathbf{k}) = i\Delta_0 g(\mathbf{k})[\boldsymbol{\sigma}_2]_{\lambda\mu} \tag{290}$$

$$\Delta^{\mathsf{T}}_{\lambda\mu}(\mathbf{k}) = i\Delta_0[\mathbf{d}(\mathbf{k})\cdot\vec{\boldsymbol{\sigma}}\boldsymbol{\sigma}_2]_{\lambda\mu}. \tag{291}$$

Here $\boldsymbol{\sigma}_2$ is the familiar Pauli spin matrix usually associated with the $\widehat{y}$-direction:

$$\boldsymbol{\sigma}_2 = \left[\begin{array}{cc}0 & -i\\ i & 0\end{array}\right]$$

In this case the numbers $1 \leftrightarrow \widehat{x}$, $2 \leftrightarrow \widehat{y}$, $3 \leftrightarrow \widehat{z}$ are used to label axes in 3-space instead of the familiar xyz. This is because the order parameter for the triplet symmetry, $\mathbf{d}(\mathbf{k})$, exists in k-space where the axes in this space are labeled by $1, 2, 3$. These axes do not necessarily coincide with the real space axes of lattice in question, where the real space axes are labeled by x, y, z.

The composite object $\vec{\sigma}$ (perhaps more precisely referred to as a dyad) is a vector whose components are the Pauli matrices:

$$\vec{\sigma} = \sigma_1\hat{1} + \sigma_2\hat{2} + \sigma_3\hat{3} = (\sigma_1, \sigma_2, \sigma_3)$$

so that for the singlet

$$\begin{aligned}\Delta^{\mathsf{S}}(\mathbf{k}) &= i\Delta_0 g(\mathbf{k})[\sigma_2] \\ &= \Delta_0 \begin{bmatrix} 0 & g(\mathbf{k}) \\ -g(\mathbf{k}) & 0 \end{bmatrix}\end{aligned} \tag{292}$$

and for the triplet

$$\begin{aligned}\Delta^{\mathsf{T}}(\mathbf{k}) &= i\Delta_0[\mathbf{d}(\mathbf{k}) \cdot \vec{\sigma}\sigma_2] \\ &= i\Delta_0 \Big(d_{\hat{1}}(\mathbf{k})\sigma_1 + d_{\hat{2}}(\mathbf{k})\sigma_2 + d_{\hat{3}}(\mathbf{k})\sigma_3 \Big)\sigma_2 \\ &= \Delta_0 \begin{bmatrix} d_{\hat{3}}(\mathbf{k}) & d_{\hat{1}}(\mathbf{k}) - id_{\hat{2}}(\mathbf{k}) \\ d_{\hat{1}}(\mathbf{k}) + id_{\hat{2}}(\mathbf{k}) & -d_{\hat{3}}(\mathbf{k}) \end{bmatrix} i \begin{bmatrix} 0 & -i \\ i & 0 \end{bmatrix} \\ &= \Delta_0 \begin{bmatrix} -d_{\hat{1}}(\mathbf{k}) + id_{\hat{2}}(\mathbf{k}) & d_{\hat{3}}(\mathbf{k}) \\ d_{\hat{3}}(\mathbf{k}) & d_{\hat{1}}(\mathbf{k}) + id_{\hat{2}}(\mathbf{k}) \end{bmatrix}.\end{aligned} \tag{293}$$

C.1 the Singlet Case

First the sum will be performed for the singlet gap parameter. Recall from the discussion of the spin structure of paired states [see §2.2] that the use of the matrix is really a shorthand for writing down the antisymmetric spin state $|\uparrow\downarrow\rangle - |\downarrow\uparrow\rangle$ corresponding to the singlet channel. The full state–including spin and orbital components–is:

$$\Psi^{\mathsf{S}}(\mathbf{k}) = g(\mathbf{k})\otimes\big[|\uparrow\downarrow\rangle - |\downarrow\uparrow\rangle\big] \Leftrightarrow \begin{bmatrix} 0 & g(\mathbf{k}) \\ -g(\mathbf{k}) & 0 \end{bmatrix} = ig(\mathbf{k})\sigma_2.$$

Because $\Psi^{S}(\mathbf{k})$ describes fermions it must be overall antisymmetric; however, since the singlet spin channel is antisymmetric the orbital piece must be symmetric so that:

$$\Psi^{S}_{\alpha\beta}(-\mathbf{k}) = \quad \Psi^{S}_{\alpha\beta}(\mathbf{k}) \tag{294}$$

$$\Psi^{S}_{\alpha\beta}(\mathbf{k}) \quad = -\Psi^{S}_{\beta\alpha}(\mathbf{k}). \tag{295}$$

The singlet gap parameter is then given by:

$$\Delta^{S}_{\alpha\beta}(\mathbf{k}) = \Delta_0 \Psi^{S}_{\alpha\beta}(\mathbf{k}) \tag{296}$$

so that

$$\sum_{\alpha\beta\gamma\delta} [\boldsymbol{\sigma}_m]_{\alpha\beta}[\boldsymbol{\sigma}_n]_{\gamma\delta}\, \Delta^{\dagger}_{\alpha\gamma}(-\mathbf{k}+\mathbf{q})\Delta_{\beta\delta}(\mathbf{k}) =$$

$$= \sum_{\alpha\beta\gamma\delta} [\boldsymbol{\sigma}_m]_{\alpha\beta}[\boldsymbol{\sigma}_n]_{\gamma\delta} \left[\Psi^{S\dagger}(-\mathbf{k}+\mathbf{q})\right]_{\alpha\gamma} \left[\Psi^{S}(\mathbf{k})\right]_{\beta\delta}$$

$$= \sum_{\alpha\beta\gamma\delta} [\boldsymbol{\sigma}_m]_{\alpha\beta}[\boldsymbol{\sigma}^{t}_n]_{\delta\gamma} \left[\left[\Psi^{S\dagger}(-\mathbf{k}+\mathbf{q})\right]^{t}\right]_{\gamma\alpha} \left[\Psi^{S}(\mathbf{k})\right]_{\beta\delta}$$

$$= \sum_{\alpha\beta\gamma\delta} [\boldsymbol{\sigma}_m]_{\alpha\beta}[\boldsymbol{\sigma}^{t}_n]_{\delta\gamma} \left[\Psi^{S*}(-\mathbf{k}+\mathbf{q})\right]_{\gamma\alpha} \left[\Psi^{S}(\mathbf{k})\right]_{\beta\delta}$$

where the property of the matrix transpose that $\mathcal{M}_{ij} = \mathcal{M}^{t}{}_{ji}$ was applied in the second line (t here means transpose)

$$= |\Delta_0|^2 g^*(-\mathbf{k}+\mathbf{q})g(\mathbf{k}) \sum_{\alpha\beta\gamma\delta} [\boldsymbol{\sigma}_m]_{\alpha\beta} \begin{bmatrix} 0 & 1 \\ -1 & 0 \end{bmatrix}_{\beta\delta} [\boldsymbol{\sigma}^{t}_n]_{\delta\gamma} \begin{bmatrix} 0 & 1 \\ -1 & 0 \end{bmatrix}_{\gamma\alpha}$$

$$= |\Delta_0|^2 g^*(-\mathbf{k}+\mathbf{q})g(\mathbf{k}) \mathrm{Tr}\left[[\boldsymbol{\sigma}_m] \begin{bmatrix} 0 & 1 \\ -1 & 0 \end{bmatrix} [\boldsymbol{\sigma}^{t}_n] \begin{bmatrix} 0 & 1 \\ -1 & 0 \end{bmatrix}\right]$$

$$= |\Delta_0|^2 g^*(-\mathbf{k}+\mathbf{q})g(\mathbf{k}) \left[2\eta_{m,2}\eta_{n,2} + \eta_{m,1}\eta_{n,3} + \eta_{m,3}\eta_{n,1}\right]$$

$$= 2|\Delta_0|^2 g^*(-\mathbf{k}+\mathbf{q})g(\mathbf{k})\, \delta_{mn} \tag{297}$$

C.2 the Triplet Case

Next the sum will be performed for the triplet gap parameter. Again recall from the discussion of the spin structure of paired states [see §2.2] that the full triplet state–including spin and orbital components–is:

$$\Psi^{\mathsf{T}}(\mathbf{k}) = i\,\mathbf{d}(\mathbf{k})\cdot\vec{\boldsymbol{\sigma}}\boldsymbol{\sigma}_{\hat{2}} \Leftrightarrow \begin{bmatrix} -d_{\hat{1}}(\mathbf{k}) + id_{\hat{2}}(\mathbf{k}) & d_{\hat{3}}(\mathbf{k}) \\ d_{\hat{3}}(\mathbf{k}) & d_{\hat{1}}(\mathbf{k}) + id_{\hat{2}}(\mathbf{k}) \end{bmatrix}$$

Because $\Psi^{\mathsf{T}}(\mathbf{k})$ describes fermions it must again be overall antisymmetric; however, since the triplet spin channel is symmetric the orbital piece must be antisymmetric so that:

$$\Psi^{\mathsf{T}}_{\alpha\beta}(-\mathbf{k}) = -\Psi^{\mathsf{T}}_{\alpha\beta}(\mathbf{k}) \tag{298}$$

$$\Psi^{\mathsf{T}}_{\alpha\beta}(\mathbf{k}) \quad = \quad \Psi^{\mathsf{T}}_{\beta\alpha}(\mathbf{k}). \tag{299}$$

The triplet gap parameter is then given by:

$$\Delta^{\mathsf{T}}_{\alpha\beta}(\mathbf{k}) = \Delta_0\Psi^{\mathsf{T}}_{\alpha\beta}(\mathbf{k}) \tag{300}$$

so that

$$\sum_{\alpha\beta\gamma\delta}\frac{[\boldsymbol{\sigma}_m]_{\alpha\beta}[\boldsymbol{\sigma}_n]_{\gamma\delta}\,\Delta^{\dagger}_{\alpha\gamma}(-\mathbf{k}+\mathbf{q})\Delta_{\beta\delta}(\mathbf{k})}{|\Delta_0|^2} =$$

$$= \sum_{\alpha\beta\gamma\delta}[\boldsymbol{\sigma}_m]_{\alpha\beta}[\boldsymbol{\sigma}_n]_{\gamma\delta}\left[\Psi^{\mathsf{T}\dagger}(-\mathbf{k}+\mathbf{q})\right]_{\alpha\gamma}\left[\Psi^{\mathsf{T}}(\mathbf{k})\right]_{\beta\delta}$$

$$= \sum_{\alpha\beta\gamma\delta}[\boldsymbol{\sigma}_m]_{\alpha\beta}[\boldsymbol{\sigma}^{\mathsf{t}}_n]_{\delta\gamma}\left[\left[\Psi^{\mathsf{T}\dagger}(-\mathbf{k}+\mathbf{q})\right]^{\mathsf{t}}\right]_{\gamma\alpha}\left[\Psi^{\mathsf{T}}(\mathbf{k})\right]_{\beta\delta}$$

$$= \sum_{\alpha\beta\gamma\delta}[\boldsymbol{\sigma}_m]_{\alpha\beta}\left[\Psi^{\mathsf{T}}(\mathbf{k})\right]_{\beta\delta}[\boldsymbol{\sigma}^{\mathsf{t}}_n]_{\delta\gamma}\left[\Psi^{\mathsf{T}*}(-\mathbf{k}+\mathbf{q})\right]_{\gamma\alpha}$$

where the property of the matrix transpose that $\mathcal{M}_{ij} = \mathcal{M}^{\mathsf{t}}{}_{ji}$ was applied in the second line (t here means transpose); also, the factor of $|\Delta_0|^2$ has been put temporarily on the left hand side; representing the elements of $\Psi^{\mathsf{T}}(\mathbf{k})$ by ψ_i and the elements of

$\Psi^{T*}(-\mathbf{k}+\mathbf{q})$ by ϕ_j^* one has:

$$= \mathsf{Tr}\left[\begin{bmatrix} \eta_{m,2} & \eta_{m,3} \\ \eta_{m,1} & -\eta_{m,2} \end{bmatrix}\begin{bmatrix} \psi_1 & \psi_2 \\ \psi_2 & \psi_3 \end{bmatrix}\begin{bmatrix} \eta_{n,2} & \eta_{n,1} \\ \eta_{n,3} & -\eta_{n,2} \end{bmatrix}\begin{bmatrix} \phi_1^* & \phi_2^* \\ \phi_2^* & \phi_3^* \end{bmatrix}\right]$$

$$= \mathsf{Tr}\left\{\begin{bmatrix} \eta_{m,2}\psi_1 + \eta_{m,3}\psi_2 & \eta_{m,2}\psi_2 + \eta_{m,3}\psi_3 \\ \eta_{m,1}\psi_1 - \eta_{m,2}\psi_2 & \eta_{m,1}\psi_2 - \eta_{m,2}\psi_3 \end{bmatrix} \otimes \begin{bmatrix} \eta_{n,2}\phi_1^* + \eta_{n,1}\phi_2^* & \eta_{n,2}\phi_2^* + \eta_{n,1}\phi_3^* \\ \eta_{n,3}\phi_1^* - \eta_{n,2}\phi_2^* & \eta_{n,3}\phi_2^* - \eta_{n,2}\phi_3^* \end{bmatrix}\right\}$$

$$\begin{aligned} &= [\eta_{m,2}\psi_1 + \eta_{m,3}\psi_2][\eta_{n,2}\phi_1^* + \eta_{n,1}\phi_2^*] + [\eta_{m,2}\psi_2 + \eta_{m,3}\psi_3][\eta_{n,3}\phi_1^* - \eta_{n,2}\phi_2^*] \\ &+ [\eta_{m,1}\psi_1 - \eta_{m,2}\psi_2][\eta_{n,2}\phi_2^* + \eta_{n,1}\phi_3^*] + [\eta_{m,1}\psi_2 - \eta_{m,2}\psi_3][\eta_{n,3}\phi_2^* - \eta_{n,2}\phi_3^*] \end{aligned}$$

$$\begin{aligned} &= (\eta_{m,1}\eta_{n,1}\psi_1\phi_3^* + \eta_{m,3}\eta_{n,3}\psi_3\phi_1^*) + \eta_{m,2}\eta_{n,2}\,(\psi_1\phi_1^* - 2\psi_2\phi_2^* + \psi_3\phi_3^*) \\ &+ (\eta_{m,1}\eta_{n,2} + \eta_{m,2}\eta_{n,1})[\psi_1\phi_2^* - \psi_2\phi_3^*] + (\eta_{m,2}\eta_{n,3} + \eta_{m,3}\eta_{n,2})[\psi_2\phi_1^* - \psi_3\phi_2^*] \\ &+ (\eta_{m,1}\eta_{n,3} + \eta_{m,3}\eta_{n,1})[\psi_2\phi_2^*]. \end{aligned}$$

Substituting in for the η's and the ψ_i's & ϕ_j's where

$$\begin{aligned} \psi_1 &= -d_{\hat{1}} + id_{\hat{2}} & \phi_1^* &= -\widetilde{d}_{\hat{1}} - i\widetilde{d}_{\hat{2}} \\ \psi_2 &= d_{\hat{3}} & \phi_2^* &= \widetilde{d}_{\hat{3}} \\ \psi_3 &= d_{\hat{1}} + id_{\hat{2}} & \phi_3^* &= \widetilde{d}_{\hat{1}} - i\widetilde{d}_{\hat{2}} \end{aligned} \tag{301}$$

and where $d_i \doteq d_i(\mathbf{k})$ and $\widetilde{d}_j \doteq d_j^*(-\mathbf{k}+\mathbf{q})$:

$$
\begin{aligned}
(\eta_{m,1}\eta_{n,1}\psi_1\phi_3^* + \eta_{m,3}\eta_{n,3}\psi_3\phi_1^*) &= -2(\delta_{m1}\delta_{n1}d_{\widehat{1}}\widetilde{d}_{\widehat{1}} + \delta_{m2}\delta_{n2}d_{\widehat{2}}\widetilde{d}_{\widehat{2}}) \\
&\quad +2(\delta_{m1}\delta_{n1}d_{\widehat{2}}\widetilde{d}_{\widehat{2}} + \delta_{m2}\delta_{n2}d_{\widehat{1}}\widetilde{d}_{\widehat{1}}) \\
&\quad -2[\delta_{m1}\delta_{n2} + \delta_{m2}\delta_{n1}](d_{\widehat{1}}\widetilde{d}_{\widehat{2}} + d_{\widehat{2}}\widetilde{d}_{\widehat{1}})
\end{aligned}
$$

$$
\eta_{m,2}\eta_{n,2}\,(\psi_1\phi_1^* - 2\psi_2\phi_2^* + \psi_3\phi_3^*) = 2\delta_{m3}\delta_{n3}(d_{\widehat{1}}\widetilde{d}_{\widehat{1}} + d_{\widehat{2}}\widetilde{d}_{\widehat{2}} - d_{\widehat{3}}\widetilde{d}_{\widehat{3}})
$$

$$
(\eta_{m,1}\eta_{n,3} + \eta_{m,3}\eta_{n,1})\psi_2\phi_2^* = 2[\delta_{m1}\delta_{n1} + \delta_{m2}\delta_{n2}]d_{\widehat{3}}\widetilde{d}_{\widehat{3}}
$$

$$
\begin{aligned}
(\eta_{m,1}\eta_{n,2} + \eta_{m,2}\eta_{n,1})[\psi_1\phi_2^* - \psi_2\phi_3^*] &= -[\delta_{m,1}\delta_{n,3} + \delta_{m,3}\delta_{n,1}](d_{\widehat{1}}\widetilde{d}_{\widehat{3}} + d_{\widehat{3}}\widetilde{d}_{\widehat{1}}) \\
&\quad -[\delta_{m,2}\delta_{n,3} + \delta_{m,3}\delta_{n,2}](d_{\widehat{2}}\widetilde{d}_{\widehat{3}} + d_{\widehat{3}}\widetilde{d}_{\widehat{2}}) \\
&\quad +i[\delta_{m,1}\delta_{n,3} + \delta_{m,3}\delta_{n,1}](d_{\widehat{2}}\widetilde{d}_{\widehat{3}} + d_{\widehat{3}}\widetilde{d}_{\widehat{2}}) \\
&\quad -i[\delta_{m,2}\delta_{n,3} + \delta_{m,3}\delta_{n,2}](d_{\widehat{1}}\widetilde{d}_{\widehat{3}} + d_{\widehat{3}}\widetilde{d}_{\widehat{1}})
\end{aligned}
$$

$$
\begin{aligned}
(\eta_{m,2}\eta_{n,3} + \eta_{m,3}\eta_{n,2})[\psi_2\phi_1^* - \psi_3\phi_2^*] &= -[\delta_{m,1}\delta_{n,3} + \delta_{m,3}\delta_{n,1}](d_{\widehat{1}}\widetilde{d}_{\widehat{3}} + d_{\widehat{3}}\widetilde{d}_{\widehat{1}}) \\
&\quad -[\delta_{m,2}\delta_{n,3} + \delta_{m,3}\delta_{n,2}](d_{\widehat{2}}\widetilde{d}_{\widehat{3}} + d_{\widehat{3}}\widetilde{d}_{\widehat{2}}) \\
&\quad -i[\delta_{m,1}\delta_{n,3} + \delta_{m,3}\delta_{n,1}](d_{\widehat{2}}\widetilde{d}_{\widehat{3}} + d_{\widehat{3}}\widetilde{d}_{\widehat{2}}) \\
&\quad +i[\delta_{m,2}\delta_{n,3} + \delta_{m,3}\delta_{n,2}](d_{\widehat{1}}\widetilde{d}_{\widehat{3}} + d_{\widehat{3}}\widetilde{d}_{\widehat{1}}).
\end{aligned}
$$

Notice that the terms explicitly multiplied by a factor of i cancel. At this point it is natural to collect all terms multiplied by a common factor of $\delta_{mi}\delta_{nj}$ $i,j = 1,2,3$ and place these collected terms in an array ($\delta_{m1}\delta_{n1}$-terms into the 11-position, $\delta_{m1}\delta_{n2}$-terms into the 12-position, etc.):

$$\begin{bmatrix} 2[d_{\hat{2}}\tilde{d}_{\hat{2}} + d_{\hat{3}}\tilde{d}_{\hat{3}} - d_{\hat{1}}\tilde{d}_{\hat{1}}] & -2[d_{\hat{1}}\tilde{d}_{\hat{2}} + d_{\hat{2}}\tilde{d}_{\hat{1}}] & -2[d_{\hat{1}}\tilde{d}_{\hat{3}} + d_{\hat{3}}\tilde{d}_{\hat{1}}] \\ -2[d_{\hat{1}}\tilde{d}_{\hat{2}} + d_{\hat{2}}\tilde{d}_{\hat{1}}] & 2[d_{\hat{1}}\tilde{d}_{\hat{1}} + d_{\hat{3}}\tilde{d}_{\hat{3}} - d_{\hat{2}}\tilde{d}_{\hat{2}}] & -2[d_{\hat{3}}\tilde{d}_{\hat{2}} + d_{\hat{2}}\tilde{d}_{\hat{3}}] \\ -2[d_{\hat{3}}\tilde{d}_{\hat{1}} + d_{\hat{1}}\tilde{d}_{\hat{3}}] & -2[d_{\hat{2}}\tilde{d}_{\hat{3}} + d_{\hat{3}}\tilde{d}_{\hat{2}}] & 2[d_{\hat{1}}\tilde{d}_{\hat{1}} + d_{\hat{2}}\tilde{d}_{\hat{2}} - d_{\hat{3}}\tilde{d}_{\hat{3}}] \end{bmatrix} \tag{302}$$

Notice that the diagonal terms can be written in the form

$$2[\mathbf{d}\cdot\tilde{\mathbf{d}} - 2\,d_{\hat{m}}\,\tilde{d}_{\hat{m}}]$$

while the off-diagonals have the general form

$$-2[d_{\hat{m}}\,\tilde{d}_{\hat{n}} + d_{\hat{n}}\,\tilde{d}_{\hat{m}}].$$

These can be combined into

$$2[\mathbf{d}\cdot\tilde{\mathbf{d}}\,\delta_{mn} - 2[d_{\hat{m}}\,\tilde{d}_{\hat{n}} + d_{\hat{n}}\,\tilde{d}_{\hat{m}}]]. \tag{303}$$

So one ultimately obtains:

$$\sum_{\alpha\beta\gamma\delta}\frac{[\boldsymbol{\sigma}_m]_{\alpha\beta}[\boldsymbol{\sigma}_n]_{\gamma\delta}\,\Delta^{\dagger}_{\alpha\gamma}(-\mathbf{k}+\mathbf{q})\Delta_{\beta\delta}(\mathbf{k})}{|\Delta_0|^2} = 2[\mathbf{d}\cdot\tilde{\mathbf{d}}\,\delta_{mn} - 2[d_{\hat{m}}\,\tilde{d}_{\hat{n}} + d_{\hat{n}}\,\tilde{d}_{\hat{m}}]]$$

or

$$\sum_{\alpha\beta\gamma\delta}[\boldsymbol{\sigma}_m]_{\alpha\beta}[\boldsymbol{\sigma}_n]_{\gamma\delta}\,\Delta^{\dagger}_{\alpha\gamma}(-\mathbf{k}+\mathbf{q})\Delta_{\beta\delta}(\mathbf{k}) =$$

$$2|\Delta_0|^2\Big\{[\mathbf{d}^*(-\mathbf{k}+\mathbf{q})\cdot\mathbf{d}(\mathbf{k})\,\delta_{mn} - [d^*_n(-\mathbf{k}+\mathbf{q})\,d_m(\mathbf{k}) + d^*_m(-\mathbf{k}+\mathbf{q})\,d_n(\mathbf{k})]]\Big\}. \tag{304}$$

Appendix D

Symmetry Properties of the Susceptibility Tensor

D.1 the Singlet Case

Recall that the singlet pairing channel is described by a symmetric orbital piece times an antisymmetric spin piece:

$$\Delta^{S}_{\lambda\mu}(\mathbf{k}) = i\Delta_0 g(\mathbf{k})[\boldsymbol{\sigma}_2]_{\lambda\mu} \tag{305}$$

$$\boldsymbol{\sigma}_2 = \begin{bmatrix} 0 & -i \\ i & 0 \end{bmatrix} \tag{306}$$

where $g(-\mathbf{k}) = g(\mathbf{k})$ and $\Delta^{S}_{\lambda\mu}(\mathbf{k}) = -\Delta^{S}_{\mu\lambda}(\mathbf{k})$. Immediately after performing the spin sum the susceptibility has the form:

$$\chi^{S}_{mn}(\mathbf{q}, i\omega) = -2\delta_{mn}\mathcal{N}_m\mathcal{N}_n\mathbb{G}_{mn}\sum_{\mathbf{k}}\left\{\frac{|\Delta_0|^2 g^*(-\mathbf{k}+\mathbf{q})g(\mathbf{k})}{4E_{-\mathbf{k}+\mathbf{q}}E_{\mathbf{k}}}\otimes\right.$$
$$\otimes\left((1-f(E_{-\mathbf{k}+\mathbf{q}})-f(E_{\mathbf{k}}))\left[\frac{1}{i\omega+E_{-\mathbf{k}+\mathbf{q}}+E_{\mathbf{k}}}-\frac{1}{i\omega-E_{-\mathbf{k}+\mathbf{q}}-E_{\mathbf{k}}}\right]\right.$$
$$\left.+(f(E_{-\mathbf{k}+\mathbf{q}})-f(E_{\mathbf{k}}))\left[\frac{1}{i\omega+E_{-\mathbf{k}+\mathbf{q}}-E_{\mathbf{k}}}-\frac{1}{i\omega-E_{-\mathbf{k}+\mathbf{q}}+E_{\mathbf{k}}}\right]\right)$$

$$\oplus\left((1-f(E_{\mathbf{k}-\mathbf{q}})-f(E_{\mathbf{k}}))\left[\frac{u^2_{\mathbf{k}}v^2_{\mathbf{k}-\mathbf{q}}}{i\omega-E_{\mathbf{k}-\mathbf{q}}-E_{\mathbf{k}}}-\frac{u^2_{\mathbf{k}-\mathbf{q}}v^2_{\mathbf{k}}}{i\omega+E_{\mathbf{k}-\mathbf{q}}+E_{\mathbf{k}}}\right]\right.$$
$$\left.\left.+(f(E_{\mathbf{k}-\mathbf{q}})-f(E_{\mathbf{k}}))\left[\frac{u^2_{\mathbf{k}-\mathbf{q}}u^2_{\mathbf{k}}}{i\omega+E_{\mathbf{k}-\mathbf{q}}-E_{\mathbf{k}}}-\frac{v^2_{\mathbf{k}-\mathbf{q}}v^2_{\mathbf{k}}}{i\omega-E_{\mathbf{k}-\mathbf{q}}+E_{\mathbf{k}}}\right]\right)\right\}. \tag{307}$$

Noting that the sum on $\mathbf{k}$ ranges over all positive and negative values one can replace $\mathbf{k}$ with $-\mathbf{k}$ under the sum without loss of generality:

$$\chi^{S}_{mn}(\mathbf{q}, i\omega) = -2\delta_{mn}\mathcal{N}_m\mathcal{N}_n\mathbb{G}_{mn}\sum_{\mathbf{k}}\left\{\frac{|\Delta_0|^2 g^*(\mathbf{k}+\mathbf{q})g(-\mathbf{k})}{4E_{\mathbf{k}+\mathbf{q}}E_{-\mathbf{k}}}\otimes\right.$$
$$\otimes\left((1-f(E_{\mathbf{k}+\mathbf{q}})-f(E_{-\mathbf{k}}))\left[\frac{1}{i\omega+E_{\mathbf{k}+\mathbf{q}}+E_{-\mathbf{k}}}-\frac{1}{i\omega-E_{\mathbf{k}+\mathbf{q}}-E_{-\mathbf{k}}}\right]\right.$$
$$\left.+(f(E_{\mathbf{k}+\mathbf{q}})-f(E_{-\mathbf{k}}))\left[\frac{1}{i\omega+E_{\mathbf{k}+\mathbf{q}}-E_{-\mathbf{k}}}-\frac{1}{i\omega-E_{\mathbf{k}+\mathbf{q}}+E_{-\mathbf{k}}}\right]\right)$$

$$\oplus\left((1-f(E_{-\mathbf{k}-\mathbf{q}})-f(E_{-\mathbf{k}}))\left[\frac{u^2_{-\mathbf{k}}v^2_{-\mathbf{k}-\mathbf{q}}}{i\omega-E_{-\mathbf{k}-\mathbf{q}}-E_{-\mathbf{k}}}-\frac{u^2_{-\mathbf{k}-\mathbf{q}}v^2_{-\mathbf{k}}}{i\omega+E_{-\mathbf{k}-\mathbf{q}}+E_{-\mathbf{k}}}\right]\right.$$
$$\left.\left.+(f(E_{-\mathbf{k}-\mathbf{q}})-f(E_{-\mathbf{k}}))\left[\frac{u^2_{-\mathbf{k}-\mathbf{q}}u^2_{-\mathbf{k}}}{i\omega+E_{-\mathbf{k}-\mathbf{q}}-E_{-\mathbf{k}}}-\frac{v^2_{-\mathbf{k}-\mathbf{q}}v^2_{-\mathbf{k}}}{i\omega-E_{-\mathbf{k}-\mathbf{q}}+E_{-\mathbf{k}}}\right]\right)\right\}. \tag{308}$$

Using the symmetry property of the energy and the orbital function that $E_{-\mathbf{k}} = E_{\mathbf{k}}$ and $g(-\mathbf{k}) = g(\mathbf{k})$ (and the coherence factors which depend on the energy):

$$\chi^{S}_{mn}(\mathbf{q}, i\omega) = -2\delta_{mn}\mathcal{N}_m\mathcal{N}_n\mathbb{G}_{mn}\sum_{\mathbf{k}}\left\{\frac{|\Delta_0|^2 g^*(\mathbf{k}+\mathbf{q})g(\mathbf{k})}{4E_{\mathbf{k}+\mathbf{q}}E_{\mathbf{k}}}\otimes\right.$$
$$\otimes\left((1-f(E_{\mathbf{k}+\mathbf{q}})-f(E_{\mathbf{k}}))\left[\frac{1}{i\omega+E_{\mathbf{k}+\mathbf{q}}+E_{\mathbf{k}}}-\frac{1}{i\omega-E_{\mathbf{k}+\mathbf{q}}-E_{\mathbf{k}}}\right]\right.$$
$$\left.+(f(E_{\mathbf{k}+\mathbf{q}})-f(E_{\mathbf{k}}))\left[\frac{1}{i\omega+E_{\mathbf{k}+\mathbf{q}}-E_{\mathbf{k}}}-\frac{1}{i\omega-E_{\mathbf{k}+\mathbf{q}}+E_{\mathbf{k}}}\right]\right)$$

$$\oplus\left((1-f(E_{\mathbf{k}+\mathbf{q}})-f(E_{\mathbf{k}}))\left[\frac{u^2_{\mathbf{k}}v^2_{\mathbf{k}+\mathbf{q}}}{i\omega-E_{\mathbf{k}+\mathbf{q}}-E_{\mathbf{k}}}-\frac{u^2_{\mathbf{k}+\mathbf{q}}v^2_{\mathbf{k}}}{i\omega+E_{\mathbf{k}+\mathbf{q}}+E_{\mathbf{k}}}\right]\right.$$
$$\left.\left.+(f(E_{\mathbf{k}+\mathbf{q}})-f(E_{\mathbf{k}}))\left[\frac{u^2_{\mathbf{k}+\mathbf{q}}u^2_{\mathbf{k}}}{i\omega+E_{\mathbf{k}+\mathbf{q}}-E_{\mathbf{k}}}-\frac{v^2_{\mathbf{k}+\mathbf{q}}v^2_{\mathbf{k}}}{i\omega-E_{\mathbf{k}+\mathbf{q}}+E_{\mathbf{k}}}\right]\right)\right\}. \tag{309}$$

This is the final form of the singlet susceptibility that appears in the text.

D.2 the Triplet Case

Recall that the triplet pairing channel is described by an antisymmetric orbital piece times a symmetric spin piece:

$$\Delta^{\mathsf{T}}_{\lambda\mu}(\mathbf{k}) = i\Delta_0[\vec{\boldsymbol{\sigma}}\boldsymbol{\sigma}_2 \cdot \mathbf{d}(\mathbf{k})]_{\lambda\mu} \tag{310}$$

$$\boldsymbol{\sigma}_2 = \begin{bmatrix} 0 & -i \\ i & 0 \end{bmatrix} \tag{311}$$

$$\vec{\boldsymbol{\sigma}} = (\boldsymbol{\sigma}_1, \boldsymbol{\sigma}_2, \boldsymbol{\sigma}_3) = \boldsymbol{\sigma}_1\widehat{1} + \boldsymbol{\sigma}_2\widehat{2} + \boldsymbol{\sigma}_3\widehat{3} \tag{312}$$

where $\mathbf{d}(-\mathbf{k}) = -\mathbf{d}(\mathbf{k})$ and $\Delta^{\mathsf{T}}_{\lambda\mu}(\mathbf{k}) = \Delta^{\mathsf{T}}_{\mu\lambda}(\mathbf{k})$. Immediately after performing the spin sum the susceptibility has the form:

$$\begin{aligned}
\chi^{\mathsf{T}}_{mn}(\mathbf{q}, i\omega) = -\frac{1}{2}\mathcal{N}_m\mathcal{N}_n\mathbb{G}_{mn}\sum_{\mathbf{k}}\Bigg\{ & \frac{1}{E_{-\mathbf{k}+\mathbf{q}}E_{\mathbf{k}}} \otimes \\
& \otimes |\Delta_0|^2\Big[\mathbf{d}^*(-\mathbf{k}+\mathbf{q})\cdot\mathbf{d}(\mathbf{k})\delta_{mn} - [d^*_m(-\mathbf{k}+\mathbf{q})d_n(\mathbf{k}) + d^*_n(-\mathbf{k}+\mathbf{q})d_m(\mathbf{k})]\Big] \otimes \\
& \otimes\Bigg((1 - f(E_{-\mathbf{k}+\mathbf{q}}) - f(E_{\mathbf{k}}))\left[\frac{1}{i\omega + E_{-\mathbf{k}+\mathbf{q}} + E_{\mathbf{k}}} - \frac{1}{i\omega - E_{-\mathbf{k}+\mathbf{q}} - E_{\mathbf{k}}}\right] \\
& +(f(E_{-\mathbf{k}+\mathbf{q}}) - f(E_{\mathbf{k}}))\left[\frac{1}{i\omega + E_{-\mathbf{k}+\mathbf{q}} - E_{\mathbf{k}}} - \frac{1}{i\omega - E_{-\mathbf{k}+\mathbf{q}} + E_{\mathbf{k}}}\right]\Bigg) \\
\oplus\ -4\delta_{mn}\Bigg(& (1 - f(E_{-\mathbf{k}+\mathbf{q}}) - f(E_{\mathbf{k}}))\left[\frac{u^2_{\mathbf{k}}v^2_{-\mathbf{k}+\mathbf{q}}}{i\omega - E_{-\mathbf{k}+\mathbf{q}} - E_{\mathbf{k}}} - \frac{u^2_{-\mathbf{k}+\mathbf{q}}v^2_{\mathbf{k}}}{i\omega + E_{-\mathbf{k}+\mathbf{q}} + E_{\mathbf{k}}}\right] \\
& +(f(E_{-\mathbf{k}+\mathbf{q}}) - f(E_{\mathbf{k}}))\left[\frac{u^2_{-\mathbf{k}+\mathbf{q}}u^2_{\mathbf{k}}}{i\omega + E_{-\mathbf{k}+\mathbf{q}} - E_{\mathbf{k}}} - \frac{v^2_{-\mathbf{k}+\mathbf{q}}v^2_{\mathbf{k}}}{i\omega - E_{-\mathbf{k}+\mathbf{q}} + E_{\mathbf{k}}}\right]\Bigg) \Bigg\}.
\end{aligned} \tag{313}$$

Noting that the sum on $\mathbf{k}$ ranges over all positive and negative values one can replace $\mathbf{k}$ with $-\mathbf{k}$ under the sum without loss of generality:

$$\chi^{\mathsf{T}}_{mn}(\mathbf{q}, i\omega) = -\frac{1}{2}\mathcal{N}_m\mathcal{N}_n\mathbb{G}_{mn}\sum_{\mathbf{k}}\left\{\frac{1}{E_{\mathbf{k+q}}E_{-\mathbf{k}}}\otimes\right.$$
$$\otimes|\Delta_0|^2\Big[\mathbf{d}^*(\mathbf{k}+\mathbf{q})\cdot\mathbf{d}(-\mathbf{k})\delta_{mn} - [d^*_m(\mathbf{k}+\mathbf{q})d_n(-\mathbf{k}) + d^*_n(\mathbf{k}+\mathbf{q})d_m(-\mathbf{k})]\Big]\otimes$$
$$\otimes\Bigg((1-f(E_{\mathbf{k+q}})-f(E_{-\mathbf{k}}))\left[\frac{1}{i\omega+E_{\mathbf{k+q}}+E_{-\mathbf{k}}}-\frac{1}{i\omega-E_{\mathbf{k+q}}-E_{-\mathbf{k}}}\right]$$
$$+(f(E_{\mathbf{k+q}})-f(E_{-\mathbf{k}}))\left[\frac{1}{i\omega+E_{\mathbf{k+q}}-E_{-\mathbf{k}}}-\frac{1}{i\omega-E_{\mathbf{k+q}}+E_{-\mathbf{k}}}\right]\Bigg)$$

$$\oplus\ -4\delta_{mn}\Bigg((1-f(E_{\mathbf{k+q}})-f(E_{-\mathbf{k}}))\left[\frac{u^2_{-\mathbf{k}}v^2_{\mathbf{k+q}}}{i\omega-E_{\mathbf{k+q}}-E_{-\mathbf{k}}}-\frac{u^2_{\mathbf{k+q}}v^2_{-\mathbf{k}}}{i\omega+E_{\mathbf{k+q}}+E_{-\mathbf{k}}}\right]$$
$$\left.+(f(E_{\mathbf{k+q}})-f(E_{-\mathbf{k}}))\left[\frac{u^2_{\mathbf{k+q}}u^2_{-\mathbf{k}}}{i\omega+E_{\mathbf{k+q}}-E_{-\mathbf{k}}}-\frac{v^2_{\mathbf{k+q}}v^2_{-\mathbf{k}}}{i\omega-E_{\mathbf{k+q}}+E_{-\mathbf{k}}}\right]\Bigg)\right\}. \tag{314}$$

Using the symmetry property of the energy and antisymmetry of the orbital piece that $E_{-\mathbf{k}} = E_{\mathbf{k}}$ (and the coherence factors which depend on the energy) and $\mathbf{d}(-\mathbf{k}) =$

$-\mathbf{d}(\mathbf{k})$:

$$\chi^{\mathsf{T}}_{mn}(\mathbf{q},i\omega) = \frac{1}{2}\mathcal{N}_m\mathcal{N}_n\mathbb{G}_{mn}\sum_{\mathbf{k}}\Bigg\{\frac{1}{E_{\mathbf{k+q}}E_{\mathbf{k}}}\otimes$$
$$\otimes|\Delta_0|^2\Big[\mathbf{d}^*(\mathbf{k}+\mathbf{q})\cdot\mathbf{d}(\mathbf{k})\delta_{mn} - [d^*_m(\mathbf{k}+\mathbf{q})d_n(\mathbf{k}) + d^*_n(\mathbf{k}+\mathbf{q})d_m(\mathbf{k})]\Big]\otimes$$
$$\otimes\Bigg((1-f(E_{\mathbf{k+q}})-f(E_{\mathbf{k}}))\left[\frac{1}{i\omega+E_{\mathbf{k+q}}+E_{\mathbf{k}}}-\frac{1}{i\omega-E_{\mathbf{k+q}}-E_{\mathbf{k}}}\right]$$
$$+(f(E_{\mathbf{k+q}})-f(E_{\mathbf{k}}))\left[\frac{1}{i\omega+E_{\mathbf{k+q}}-E_{\mathbf{k}}}-\frac{1}{i\omega-E_{\mathbf{k+q}}+E_{\mathbf{k}}}\right]\Bigg)$$

$$\oplus\ -4\delta_{mn}\Bigg((1-f(E_{\mathbf{k+q}})-f(E_{\mathbf{k}}))\left[\frac{u^2_{\mathbf{k}}v^2_{\mathbf{k+q}}}{i\omega-E_{\mathbf{k+q}}-E_{\mathbf{k}}}-\frac{u^2_{\mathbf{k+q}}v^2_{\mathbf{k}}}{i\omega+E_{\mathbf{k+q}}+E_{\mathbf{k}}}\right]$$
$$+(f(E_{\mathbf{k+q}})-f(E_{\mathbf{k}}))\left[\frac{u^2_{\mathbf{k+q}}u^2_{\mathbf{k}}}{i\omega+E_{\mathbf{k+q}}-E_{\mathbf{k}}}-\frac{v^2_{\mathbf{k+q}}v^2_{\mathbf{k}}}{i\omega-E_{\mathbf{k+q}}+E_{\mathbf{k}}}\right]\Bigg)\quad\Bigg\}. \tag{315}$$

D.3 the Nonunitary Triplet Case

Recall the Green matrices and the order parameter out of which the nonunitary triplet susceptibility is comprised:

$$\widehat{\Delta}^{\mathsf{G}}_{\mathsf{J}}(\mathbf{k}) = \Big|\mathbf{m}(\mathbf{k})\Big|\boldsymbol{\sigma}_0 - \mathsf{J}\,\mathbf{m}(\mathbf{k})\cdot\vec{\boldsymbol{\sigma}} \tag{316}$$

$$\widehat{\Delta}^{\mathsf{F}}_{\mathsf{J}}(\mathbf{k}) = i\Delta_0[\mathring{\mathbf{D}}_{\mathsf{J}}(\mathbf{k})\cdot\vec{\boldsymbol{\sigma}}\boldsymbol{\sigma}_2] \tag{317}$$

$$\mathring{\mathbf{D}}_{\mathsf{J}}(\mathbf{k}) \doteq \Delta_0\Big[\Big|\mathbf{m}(\mathbf{k})\Big|\mathbf{d}(\mathbf{k}) + i\mathsf{J}\,\mathbf{m}(\mathbf{k})\times\mathbf{d}(\mathbf{k})\Big] \tag{318}$$

$$\mathbf{m}(\mathbf{k}) = i|\Delta_0|^2\mathbf{d}(\mathbf{k})\times\mathbf{d}^*(\mathbf{k}). \tag{319}$$

The order parameter is odd for a triplet: $\mathbf{d}(-\mathbf{k}) = -\mathbf{d}(\mathbf{k})$. Consequently, $\mathring{\mathbf{D}}_{\mathsf{J}}(-\mathbf{k}) = -\mathring{\mathbf{D}}_{\mathsf{J}}(\mathbf{k})$. However, because the magnetic term $\mathbf{m}(\mathbf{k})$ is constructed out of a product of order parameters, it is even:

$$\mathbf{m}(-\mathbf{k}) = i|\Delta_0|^2\mathbf{d}(-\mathbf{k})\times\mathbf{d}^*(-\mathbf{k}) = (-)^2i|\Delta_0|^2\mathbf{d}(\mathbf{k})\times\mathbf{d}^*(\mathbf{k}) = \mathbf{m}(\mathbf{k}).$$

Furthermore, as shown at the beginning of the section for the nonunitary susceptibility $\mathbf{m}(\mathbf{k})$ is real. As a result:

$$\widehat{\Delta}^{G}_{J}(-\mathbf{k}) = \widehat{\Delta}^{G}_{J}(\mathbf{k}) \tag{320}$$

$$\widehat{\Delta}^{F}_{J}(-\mathbf{k}) = -\widehat{\Delta}^{F}_{J}(\mathbf{k}) \tag{321}$$

$$\mathring{\mathbf{D}}_{J}(-\mathbf{k}) = -\mathring{\mathbf{D}}_{J}(\mathbf{k}) \tag{322}$$

$$\mathbf{m}(-\mathbf{k}) = \mathbf{m}(\mathbf{k}). \tag{323}$$

The energy and coherence factors remain even:

$$E_{-\mathbf{k},J} = \sqrt{\xi^2_{-\mathbf{k}} + |\Delta_0 \mathbf{d}(-\mathbf{k})|^2 + J|\mathbf{m}(-\mathbf{k})|} = E_{\mathbf{k},J} \tag{324}$$

$$u^2_{-\mathbf{k},J} = u^2_{\mathbf{k},J} \tag{325}$$

$$v^2_{-\mathbf{k},J} = v^2_{\mathbf{k},J}. \tag{326}$$

Recall that $\xi_{\mathbf{k}} = \epsilon_{\mathbf{k}} - \mu$ was defined in the introduction and seen to be even in its argument. Under the sum on $\mathbf{k}$ the tensors $\Pi^{I}_{\alpha\beta\gamma\delta}(\mathbf{k},\mathbf{q},i\omega)$ and $\Pi^{II}_{\alpha\beta\gamma\delta}(\mathbf{k},\mathbf{q},i\omega)$ originally have the form:

$$\sum_{\mathbf{k}} \Pi^{I}_{\alpha\beta\gamma\delta}(\mathbf{k},\mathbf{q},i\omega) = \sum_{\mathsf{J},\mathsf{H}=\pm 1} \sum_{\mathbf{k}} \frac{\Delta^{\mathsf{G}}_{\mathsf{J},\delta\alpha}(\mathbf{k}-\mathbf{q})\Delta^{\mathsf{G}}_{\mathcal{H},\beta\gamma}(\mathbf{k})}{4|\mathbf{m}(\mathbf{k}-\mathbf{q})|\cdot|\mathbf{m}(\mathbf{k})|}\otimes$$
$$\otimes\Bigg\{(1-f(E_{\mathbf{k}-\mathbf{q}})-f(E_{\mathbf{k}}))\left[\frac{u^2_{\mathbf{k}}v^2_{\mathbf{k}-\mathbf{q}}}{i\omega-E_{\mathbf{k}-\mathbf{q}}-E_{\mathbf{k}}}-\frac{u^2_{\mathbf{k}-\mathbf{q}}v^2_{\mathbf{k}}}{i\omega+E_{\mathbf{k}-\mathbf{q}}+E_{\mathbf{k}}}\right]$$
$$+(f(E_{\mathbf{k}-\mathbf{q}})-f(E_{\mathbf{k}}))\left[\frac{u^2_{\mathbf{k}-\mathbf{q}}u^2_{\mathbf{k}}}{i\omega+E_{\mathbf{k}-\mathbf{q}}-E_{\mathbf{k}}}-\frac{v^2_{\mathbf{k}-\mathbf{q}}v^2_{\mathbf{k}}}{i\omega-E_{\mathbf{k}-\mathbf{q}}+E_{\mathbf{k}}}\right]\Bigg\}. \qquad (327)$$

and

$$\sum_{\mathbf{k}} \Pi^{II}_{\alpha\beta\gamma\delta}(\mathbf{k},\mathbf{q},i\omega) = \sum_{\mathsf{J},\mathsf{H}=\pm 1} \sum_{\mathbf{k}} \frac{\Delta^{\mathsf{F}\dagger}_{\mathsf{J},\alpha\gamma}(-\mathbf{k}+\mathbf{q})\Delta^{\mathsf{F}}_{\mathcal{H},\beta\delta}(\mathbf{k})}{16|\mathbf{m}(-\mathbf{k}+\mathbf{q})|\cdot|\mathbf{m}(\mathbf{k})|E_{-\mathbf{k}+\mathbf{q},\mathsf{J}}E_{\mathbf{k},\mathcal{H}}}\otimes$$
$$\otimes\Bigg\{(1-f(E_{-\mathbf{k}+\mathbf{q}})-f(E_{\mathbf{k}}))\left[\frac{1}{i\omega+E_{-\mathbf{k}+\mathbf{q}}+E_{\mathbf{k}}}-\frac{1}{i\omega-E_{-\mathbf{k}+\mathbf{q}}-E_{\mathbf{k}}}\right]$$
$$+(f(E_{-\mathbf{k}+\mathbf{q}})-f(E_{\mathbf{k}}))\left[\frac{1}{i\omega+E_{-\mathbf{k}+\mathbf{q}}-E_{\mathbf{k}}}-\frac{1}{i\omega-E_{-\mathbf{k}+\mathbf{q}}+E_{\mathbf{k}}}\right]\Bigg\} \qquad (328)$$

Taking $\mathbf{k}\to-\mathbf{k}$ on the right hand side and using the evenness of the energy and coherence factors ($E_{-\mathbf{k}}=E_{\mathbf{k}}$):

$$\sum_{\mathbf{k}} \Pi^{II}_{\alpha\beta\gamma\delta}(\mathbf{k},\mathbf{q},i\omega) = \sum_{\mathsf{J},\mathsf{H}=\pm 1} \sum_{\mathbf{k}} \frac{\Delta^{\mathsf{F}\dagger}_{\mathsf{J},\alpha\gamma}(\mathbf{k}+\mathbf{q})\Delta^{\mathsf{F}}_{\mathcal{H},\beta\delta}(-\mathbf{k})}{16|\mathbf{m}(\mathbf{k}+\mathbf{q})|\cdot|\mathbf{m}(\mathbf{k})|E_{\mathbf{k}+\mathbf{q},\mathsf{J}}E_{-\mathbf{k},\mathcal{H}}}\otimes$$
$$\otimes\Bigg\{(1-f(E_{\mathbf{k}+\mathbf{q}})-f(E_{\mathbf{k}}))\left[\frac{1}{i\omega+E_{\mathbf{k}+\mathbf{q}}+E_{\mathbf{k}}}-\frac{1}{i\omega-E_{\mathbf{k}+\mathbf{q}}-E_{\mathbf{k}}}\right]$$
$$+(f(E_{\mathbf{k}+\mathbf{q}})-f(E_{\mathbf{k}}))\left[\frac{1}{i\omega+E_{\mathbf{k}+\mathbf{q}}-E_{\mathbf{k}}}-\frac{1}{i\omega-E_{\mathbf{k}+\mathbf{q}}+E_{\mathbf{k}}}\right]\Bigg\} \qquad (329)$$

and

$$\sum_{\mathbf{k}} \Pi^{I}_{\alpha\beta\gamma\delta}(\mathbf{k},\mathbf{q},i\omega) = \sum_{\mathsf{J},\mathsf{H}=\pm 1} \sum_{\mathbf{k}} \frac{\Delta^{\mathsf{G}}_{\mathsf{J},\delta\alpha}(-\mathbf{k}-\mathbf{q})\Delta^{\mathsf{G}}_{\mathcal{H},\beta\gamma}(-\mathbf{k})}{4|\mathbf{m}(\mathbf{k}+\mathbf{q})|\cdot|\mathbf{m}(\mathbf{k})|}\otimes$$
$$\otimes\Bigg\{(1-f(E_{\mathbf{k}+\mathbf{q}})-f(E_{\mathbf{k}}))\left[\frac{u^2_{\mathbf{k}}v^2_{\mathbf{k}+\mathbf{q}}}{i\omega-E_{\mathbf{k}+\mathbf{q}}-E_{\mathbf{k}}}-\frac{u^2_{\mathbf{k}+\mathbf{q}}v^2_{\mathbf{k}}}{i\omega+E_{\mathbf{k}+\mathbf{q}}+E_{\mathbf{k}}}\right]$$
$$+(f(E_{\mathbf{k}+\mathbf{q}})-f(E_{\mathbf{k}}))\left[\frac{u^2_{\mathbf{k}+\mathbf{q}}u^2_{\mathbf{k}}}{i\omega+E_{\mathbf{k}+\mathbf{q}}-E_{\mathbf{k}}}-\frac{v^2_{\mathbf{k}+\mathbf{q}}v^2_{\mathbf{k}}}{i\omega-E_{\mathbf{k}+\mathbf{q}}+E_{\mathbf{k}}}\right]\Bigg\}. \qquad (330)$$

Recall that $\Delta^{\mathsf{G}}_{\mathsf{J},\delta\alpha}(\mathbf{k})$ is even while $\Delta^{\mathsf{F}}_{\mathsf{J},\delta\alpha}(\mathbf{k})$ is odd:

$$\sum_{\mathbf{k}} \Pi^{II}_{\alpha\beta\gamma\delta}(\mathbf{k},\mathbf{q},i\omega) = -\sum_{\mathsf{J},\mathsf{H}=\pm 1} \sum_{\mathbf{k}} \frac{\Delta^{\mathsf{F}\dagger}_{\mathsf{J},\alpha\gamma}(\mathbf{k}+\mathbf{q})\Delta^{\mathsf{F}}_{\mathcal{H},\beta\delta}(\mathbf{k})}{16|\mathbf{m}(\mathbf{k}+\mathbf{q})|\cdot|\mathbf{m}(\mathbf{k})|E_{\mathbf{k}+\mathbf{q},\mathsf{J}}E_{-\mathbf{k},\mathcal{H}}}\otimes$$
$$\otimes\Bigg\{(1-f(E_{\mathbf{k}+\mathbf{q}})-f(E_{\mathbf{k}}))\left[\frac{1}{i\omega+E_{\mathbf{k}+\mathbf{q}}+E_{\mathbf{k}}}-\frac{1}{i\omega-E_{\mathbf{k}+\mathbf{q}}-E_{\mathbf{k}}}\right]$$
$$+(f(E_{\mathbf{k}+\mathbf{q}})-f(E_{\mathbf{k}}))\left[\frac{1}{i\omega+E_{\mathbf{k}+\mathbf{q}}-E_{\mathbf{k}}}-\frac{1}{i\omega-E_{\mathbf{k}+\mathbf{q}}+E_{\mathbf{k}}}\right]\Bigg\} \qquad (331)$$

and

$$\sum_{\mathbf{k}} \Pi^{I}_{\alpha\beta\gamma\delta}(\mathbf{k},\mathbf{q},i\omega) = \sum_{\mathsf{J},\mathsf{H}=\pm 1} \sum_{\mathbf{k}} \frac{\Delta^{\mathsf{G}}_{\mathsf{J},\delta\alpha}(\mathbf{k}+\mathbf{q})\Delta^{\mathsf{G}}_{\mathcal{H},\beta\gamma}(\mathbf{k})}{4|\mathbf{m}(\mathbf{k}+\mathbf{q})|\cdot|\mathbf{m}(\mathbf{k})|}\otimes$$
$$\otimes\Bigg\{(1-f(E_{\mathbf{k}+\mathbf{q}})-f(E_{\mathbf{k}}))\left[\frac{u^2_{\mathbf{k}}v^2_{\mathbf{k}+\mathbf{q}}}{i\omega-E_{\mathbf{k}+\mathbf{q}}-E_{\mathbf{k}}}-\frac{u^2_{\mathbf{k}+\mathbf{q}}v^2_{\mathbf{k}}}{i\omega+E_{\mathbf{k}+\mathbf{q}}+E_{\mathbf{k}}}\right]$$
$$+(f(E_{\mathbf{k}+\mathbf{q}})-f(E_{\mathbf{k}}))\left[\frac{u^2_{\mathbf{k}+\mathbf{q}}u^2_{\mathbf{k}}}{i\omega+E_{\mathbf{k}+\mathbf{q}}-E_{\mathbf{k}}}-\frac{v^2_{\mathbf{k}+\mathbf{q}}v^2_{\mathbf{k}}}{i\omega-E_{\mathbf{k}+\mathbf{q}}+E_{\mathbf{k}}}\right]\Bigg\}. \qquad (332)$$

Thus, Eqs. 246 and 245 are obtained. Note that $|\mathbf{m}(\mathbf{k}+\mathbf{q})|\cdot|\mathbf{m}(\mathbf{k})|$ means simply to multiply the magnitudes of the m-vectors while $\mathbf{m}(\mathbf{k}+\mathbf{q})\cdot\mathbf{m}(\mathbf{k})$ means to take their inner product.

Also, observe the explicit, overall minus sign appearing in front of the terms in $\sum_{\mathbf{k}} \Pi^{II}_{\alpha\beta\gamma\delta}(\mathbf{k},\mathbf{q},i\omega)$.

Appendix E

Special Limits

It is worthwhile to investigate some special limits of the general unitary electron spin susceptibility. The limits to be investigated are:

- the Uniform Dynamical Susceptibility, $\chi_{mn}(\mathbf{q} \to \mathbf{0}, \omega)$;
- the Nonuniform Static Susceptibility, $\chi_{mn}(\mathbf{q}, \omega \to 0)$;
- the Uniform Static Susceptibility, $\chi_{mn}(\mathbf{q} \to \mathbf{0}, \omega \to 0)$.

In the discussions accompanying the special limits below, two very important scale factors are the characteristic length $l_{\mathbf{mag}}(\sim 1/q)$ over which the applied perturbing field varies, and the coherence length $\xi_{\mathbf{0}}$ which characterizes the size of the Cooper pairs in the sample. A useful identity (obtained with the help of l'Hopital's rule) to keep in mind which appears in the limit of $\mathbf{q} \to \mathbf{0}$ is:

$$\begin{aligned}
\lim_{\mathbf{q}\to\mathbf{0}} \frac{f(E_{\mathbf{k+q}}) - f(E_{\mathbf{k}})}{E_{\mathbf{k+q}} - E_{\mathbf{k}}} &= \lim_{\mathbf{q}\to\mathbf{0}} \frac{\frac{\delta}{\delta \mathbf{q}} f(E_{\mathbf{k+q}})}{\frac{\delta}{\delta \mathbf{q}} E_{\mathbf{k+q}}} \\
&= \lim_{\mathbf{q}\to\mathbf{0}} \frac{[\partial f(E_{\mathbf{k+q}})/\partial E_{\mathbf{k+q}}] \frac{\delta}{\delta \mathbf{q}} E_{\mathbf{k+q}}}{\frac{\delta}{\delta \mathbf{q}} E_{\mathbf{k+q}}} \\
&= \frac{\partial f(E_{\mathbf{k}})}{\partial E_{\mathbf{k}}}
\end{aligned}$$

E.1 The Singlet Uniform Dynamical Spin Susceptibility: $\chi^{S}_{mn}(\mathbf{q} \to \mathbf{0}, \omega)$

Beginning with the singlet case the first limit to consider is:

$$\chi^{S}_{mn}(\mathbf{0}, \omega) = \lim_{\mathbf{q}\to\mathbf{0}} \chi^{S}_{mn}(\mathbf{q}, \omega).$$

This limit corresponds to the application of a uniform, external, a.c. magnetic field of frequency ω. In this limit $l_{\mathbf{mag}} \gg \xi_{\mathbf{0}}$. The Cooper pairs in the sample see a spatially uniform applied field. Alternatively, since the field varies over a relatively large distance (compared to $\xi_{\mathbf{0}}$), the field sees singlet pairs of spin s=0. For very weak fields (i.e., $H \ll H_{c_2}$) the singlet pair (having spin s=0) does not respond to the applied field.

This result is born out in Eqs. 161 and 162 by holding ω finite while setting $\mathbf{q} = \mathbf{0}$:

$$\chi^{S}_{mn}(\mathbf{0}, \omega) = \lim_{\mathbf{q}\to\mathbf{0}} \chi^{S}_{mn}(\mathbf{q}, \omega) \equiv 0 \tag{333}$$

in the zero T limit. Obviously, as the field strength is increased, some of the spin pairs will break. These excitations are now able to respond to the applied field and grow in number until $H = H_{c_2}$. At this point all the spin pairs are broken and the normal state response is observed.

E.2 The Singlet Nonuniform Static Spin Susceptibility: $\chi^{S}_{mn}(\mathbf{q}, \omega \to 0)$

The next limit to consider is:

$$\chi^{S}_{mn}(\mathbf{q}, 0) = \lim_{\omega\to 0} \chi^{S}_{mn}(\mathbf{q}, \omega).$$

From Eq. 161 we have:

$$\Re\Big[\chi^{\mathsf{S}}_{mn}(\mathbf{q},\omega=0)\Big] = -2\delta_{mn}\,\mathbb{G}_{mn}\sum_{\mathbf{k}}\Bigg\{ \frac{(u^2_{\mathbf{k+q}}u^2_{\mathbf{k}} + v^2_{\mathbf{k+q}}v^2_{\mathbf{k}} + 2u_{\mathbf{k}}v_{\mathbf{k}}u_{\mathbf{k+q}}v_{\mathbf{k+q}})[f(E_{\mathbf{k+q}}) - f(E_{\mathbf{k}})]}{E_{\mathbf{k+q}} - E_{\mathbf{k}}} - \frac{(u^2_{\mathbf{k}}v^2_{\mathbf{k+q}} + u^2_{\mathbf{k+q}}v^2_{\mathbf{k}} - 2u_{\mathbf{k}}v_{\mathbf{k}}u_{\mathbf{k+q}}v_{\mathbf{k+q}})[1 - f(E_{\mathbf{k+q}}) - f(E_{\mathbf{k}})]}{E_{\mathbf{k+q}} + E_{\mathbf{k}}}\Bigg\} \tag{334}$$

and from Eq. 162 we have:

$$\Im\Big[\chi^{\mathsf{S}}_{mn}(\mathbf{q},\omega=0)\Big] = 2\pi\,\delta_{mn}\,\mathbb{G}_{mn}\sum_{\mathbf{k}}\Big\{ (u^2_{\mathbf{k}}v^2_{\mathbf{k+q}} - u^2_{\mathbf{k+q}}v^2_{\mathbf{k}})[1 - f(E_{\mathbf{k+q}}) - f(E_{\mathbf{k}})]\delta(E_{\mathbf{k+q}} + E_{\mathbf{k}})\Big\} \tag{335}$$

Notice that when $\omega \to 0$ that the first two terms in Eq. 162 give rise to a term of the form:

$$(u^2_{\mathbf{k}}u^2_{\mathbf{k+q}} - v^2_{\mathbf{k}}v^2_{\mathbf{k+q}})[f(E_{\mathbf{k+q}}) - f(E_{\mathbf{k}})]\delta(E_{\mathbf{k+q}} - E_{\mathbf{k}}).$$

so that when $E_{\mathbf{k+q}} \neq E_{\mathbf{k}}$ the delta function vanishes and when $E_{\mathbf{k+q}} = E_{\mathbf{k}}$ the Fermi function cancel so that this term vanishes identically and does not contribute in the limit $\omega \to 0$.

This limit corresponds to the application of a static magnetic field to the system. The field can have some spatial modulation $\mathbf{q}$.

E.3 The Singlet Uniform Static Spin Susceptibility: $\chi^{\mathsf{S}}_{mn}(\mathbf{q}\to\mathbf{0},\omega\to 0)$

The last limit corresponds to the uniform static spin susceptibility $\chi^{\mathsf{S}}_{mn}(\mathbf{0},0)$. This limit is found by taking the limit $\mathbf{q}\to\mathbf{0}$ in Eqs. 334 and 335.

$$\chi^{\mathsf{S}}_{mn}(\mathbf{q}=0,\omega=0) = \lim_{\mathbf{q}\to\mathbf{0}}\Big\{\lim_{\omega\to 0}\chi^{\mathsf{S}}_{mn}(\mathbf{q},\omega)\Big\} \tag{336}$$

or

$$\chi^{S}_{mn}(\mathbf{0},0) = \lim_{\mathbf{q}\to\mathbf{0}} \chi^{S}_{mn}(\mathbf{q},0). \tag{337}$$

Upon setting $\mathbf{q} = \mathbf{0}$ in Eqs. 334 and 335: in Eq. 334 the ratio of the Fermi functions to the excitation energies goes to 0/0 in the first term, so that the identity can be applied here; the second term in Eq. 334 term vanishes (the coherence factors cancel); Eq. 335 vanishes completely (the Fermi functions cancel in the first term while the coherence factors cancel in the second term):

$$\begin{aligned}\chi^{S}_{mn}(0,0) = \Re\left[\chi^{S}_{mn}(\mathbf{0},0)\right] &= -2\delta_{mn}\,\mathbb{G}_{mn}\sum_{\mathbf{k}}\lim_{\mathbf{q}\to\mathbf{0}}\Bigg\{ \\ &\qquad (u^4_{\mathbf{k}} + v^4_{\mathbf{k}} + 2u^2_{\mathbf{k}}v^2_{\mathbf{k}})\frac{[\partial f(E_{\mathbf{k}+\mathbf{q}})/\partial E_{\mathbf{k}+\mathbf{q}}]\frac{\delta}{\delta\mathbf{q}}E_{\mathbf{k}+\mathbf{q}}}{\frac{\delta}{\delta\mathbf{q}}E_{\mathbf{k}+\mathbf{q}}}\Bigg\} \\ &= -2\delta_{mn}\,\mathbb{G}_{mn}\sum_{\mathbf{k}}\left\{(u^4_{\mathbf{k}} + v^4_{\mathbf{k}} + 2u^2_{\mathbf{k}}v^2_{\mathbf{k}})\frac{\partial f(E_{\mathbf{k}})}{\partial E_{\mathbf{k}}}\right\}\end{aligned} \tag{338}$$

and using the definition of the coherence factors

$$u^2_{\mathbf{k}} = \frac{1}{2}\left(1 + \frac{\xi_{\mathbf{k}}}{E_{\mathbf{k}}}\right) \qquad v^2_{\mathbf{k}} = \frac{1}{2}\left(1 - \frac{\xi_{\mathbf{k}}}{E_{\mathbf{k}}}\right)$$

$$\chi^{S}_{mn}(\mathbf{0},0) = -2\delta_{mn}\,\mathbb{G}_{mn}\sum_{\mathbf{k}}\frac{\partial f(E_{\mathbf{k}})}{\partial E_{\mathbf{k}}}. \tag{339}$$

This limit corresponds to the application of a time independent, uniform magnetic field. In this case, spins paired in the singlet channel $(|\uparrow\downarrow\rangle - |\downarrow\uparrow\rangle)/\sqrt{2}$ do not respond readily to the perturbing field at $T = 0$. In this case $l_{\mathsf{mag}} \gg \xi_0$. Again the spatial variation of the external field is much larger than the coherence length of the Cooper pairs. The field *sees* pairs having spin s=0 and does not couple strongly to the pairs for low field $H \ll H_{c_2}$.

However, as the temperature is increased, thermal fluctuations can break pairs and allow the quasiparticles to respond to the field. As the temperature is increased further, more and more quasiparticles are excited out of the superconducting ground

state and are able to respond to the external field.

In the following sections the same considerations are made for the case of triplet pairing.

E.4 The Triplet Uniform Dynamical Spin Susceptibility: $\chi^{\mathsf{T}}_{mn}(\mathbf{q}\to\mathbf{0},\omega)$

The first limit to consider is:

$$\chi^{\mathsf{T}}_{mn}(\mathbf{0},\omega)=\lim_{\mathbf{q}\to\mathbf{0}}\ \chi^{\mathsf{T}}_{mn}(\mathbf{q},\omega).$$

This limit is readily obtained from Eqs. 163 and 164. Note that:

$$\lim_{\mathbf{q}\to\mathbf{0}}\mathcal{D}_{mn}(\mathbf{k},\mathbf{q})=\mathcal{D}_{mn}(\mathbf{k},\mathbf{0})=|\mathbf{d}^*(\mathbf{k})|^2\delta_{mn}-[d^*_m(\mathbf{k})d_n(\mathbf{k})+d^*_n(\mathbf{k})d_m(\mathbf{k})] \tag{340}$$

so that

$$\lim_{\mathbf{q}\to\mathbf{0}}\mathcal{D}_{mn}(\mathbf{k},\mathbf{q})=\Re\Big[\mathcal{D}_{mn}(\mathbf{k},\mathbf{0})\Big]\qquad\qquad \Im\Big[\mathcal{D}_{mn}(\mathbf{k},\mathbf{0})\Big]=0 \tag{341}$$

and

$$\begin{aligned}\Re\Big[\chi^{\mathsf{T}}_{mn}(\mathbf{0},\omega)\Big]=\frac{1}{2}\mathbb{G}_{mn}\sum_{\mathbf{k}}\Bigg\{&\\ &+|\Delta_0|^2\frac{[1-2f(E_{\mathbf{k}})]}{E^2_{\mathbf{k}}}\left(\frac{\Re\Big[\mathcal{D}_{mn}(\mathbf{k},\mathbf{0})\Big]}{\hbar\omega+2E_{\mathbf{k}}}-\frac{\Re\Big[\mathcal{D}_{mn}(\mathbf{k},\mathbf{0})\Big]}{\hbar\omega-2E_{\mathbf{k}}}\right)\\ &-4\delta_{mn}\left((1-2f(E_{\mathbf{k}}))\left[\frac{u^2_{\mathbf{k}}v^2_{\mathbf{k}}}{\hbar\omega-2E_{\mathbf{k}}}-\frac{u^2_{\mathbf{k}}v^2_{\mathbf{k}}}{\hbar\omega+2E_{\mathbf{k}}}\right]\right)\quad\Bigg\}.\end{aligned}$$

Simplifying further and using $u^2_{\mathbf{k}}v^2_{\mathbf{k}}=\dfrac{|\Delta_0\mathbf{d}(\mathbf{k})|^2}{4E^2_{\mathbf{k}}}$ and the definition of $\mathcal{D}_{mn}(\mathbf{k},\mathbf{0})$:

$$\begin{aligned}\Re\Big[\chi^{\mathsf{T}}_{mn}(\mathbf{0},\omega)\Big]=\frac{1}{2}\mathbb{G}_{mn}|\Delta_0|^2\sum_{\mathbf{k}}\Bigg\{&[1-2f(E_{\mathbf{k}})]\otimes\\ &\otimes\frac{2|\mathbf{d}(\mathbf{k})|^2\delta_{mn}-[d^*_m(\mathbf{k})d_n(\mathbf{k})+d^*_n(\mathbf{k})d_m(\mathbf{k})]}{E^2_{\mathbf{k}}}\left(\frac{1}{\hbar\omega+2E_{\mathbf{k}}}-\frac{1}{\hbar\omega-2E_{\mathbf{k}}}\right)\Bigg\}.\end{aligned} \tag{342}$$

For the imaginary part of the susceptibility:

$$\Im\Big[\chi^{\mathsf{T}}_{mn}(\mathbf{0},\omega)\Big] = \frac{\pi}{2}\mathbb{G}_{mn}|\Delta_0|^2\sum_{\mathbf{k}}\Big\{[1-2f(E_{\mathbf{k}})]\otimes$$
$$\otimes\frac{2|\mathbf{d}(\mathbf{k})|^2\delta_{mn}-[d^*_m(\mathbf{k})d_n(\mathbf{k})+d^*_n(\mathbf{k})d_m(\mathbf{k})]}{E^2_{\mathbf{k}}}\Big(\delta(\hbar\omega-2E_{\mathbf{k}})-\delta(\hbar\omega+2E_{\mathbf{k}})\Big)\quad\Big\}.$$

Observe the symmetry properties of the $\mathbf{q}=\mathbf{0}$ triplet susceptibility. The real part contains the divisors $(\hbar\omega\pm E_{\mathbf{k}})$ while the imaginary part contains the delta functions:

$$\Re\Big[\chi^{\mathsf{T}}_{mn}(\mathbf{0},-\omega)\Big] = \Big[\Re\chi^{\mathsf{T}}_{mn}(\mathbf{0},\omega)\Big] \tag{343}$$

$$\Im\Big[\chi^{\mathsf{T}}_{mn}(\mathbf{0},-\omega)\Big] = -\Im\Big[\chi^{\mathsf{T}}_{mn}(\mathbf{0},\omega)\Big]. \tag{344}$$

E.5 The Triplet Nonuniform Static Spin Susceptibility: $\chi^{\mathsf{T}}_{mn}(\mathbf{q},\omega\to 0)$

The next limit to consider is:

$$\chi^{\mathsf{T}}_{mn}(\mathbf{q},0) = \lim_{\omega\to 0}\ \chi^{\mathsf{T}}_{mn}(\mathbf{q},\omega).$$

From Eq. 163 one has:

$$\begin{aligned}\Re\Big[\chi^{\mathsf{T}}_{mn}(\mathbf{q},0)\Big] = \frac{1}{2}\mathbb{G}_{mn}\sum_{\mathbf{k}}\Big\{&\\ &2|\Delta_0|^2\frac{[f(E_{\mathbf{k}+\mathbf{q}})-f(E_{\mathbf{k}})]}{E_{\mathbf{k}+\mathbf{q}}E_{\mathbf{k}}}\frac{\Re\Big[\mathcal{D}_{mn}(\mathbf{k},\mathbf{q})\Big]}{E_{\mathbf{k}+\mathbf{q}}-E_{\mathbf{k}}}\\ &+2|\Delta_0|^2\frac{[1-f(E_{\mathbf{k}+\mathbf{q}})-f(E_{\mathbf{k}})]}{E_{\mathbf{k}+\mathbf{q}}E_{\mathbf{k}}}\frac{\Re\Big[\mathcal{D}_{mn}(\mathbf{k},\mathbf{q})\Big]}{E_{\mathbf{k}+\mathbf{q}}+E_{\mathbf{k}}}\\ &-4\delta_{mn}\Bigg(-(1-f(E_{\mathbf{k}+\mathbf{q}})-f(E_{\mathbf{k}}))\left[\frac{u^2_{\mathbf{k}}v^2_{\mathbf{k}+\mathbf{q}}+u^2_{\mathbf{k}+\mathbf{q}}v^2_{\mathbf{k}}}{E_{\mathbf{k}+\mathbf{q}}+E_{\mathbf{k}}}\right]\\ &+(f(E_{\mathbf{k}+\mathbf{q}})-f(E_{\mathbf{k}}))\left[\frac{u^2_{\mathbf{k}+\mathbf{q}}u^2_{\mathbf{k}}+v^2_{\mathbf{k}+\mathbf{q}}v^2_{\mathbf{k}}}{E_{\mathbf{k}+\mathbf{q}}-E_{\mathbf{k}}}\right]\Bigg)\quad\Big\}\end{aligned} \tag{345}$$

For the imaginary part using Eq. 164 one has:

$$\Im\left[\chi^{\mathsf{T}}_{mn}(\mathbf{q},0)\right] = \frac{1}{2}\mathbb{G}_{mn}\sum_{\mathbf{k}}\Big\{$$
$$2|\Delta_0|^2\frac{[f(E_{\mathbf{k}+\mathbf{q}})-f(E_{\mathbf{k}})]}{E_{\mathbf{k}+\mathbf{q}}E_{\mathbf{k}}}\frac{\Im\left[\mathcal{D}_{mn}(\mathbf{k},\mathbf{q})\right]}{E_{\mathbf{k}+\mathbf{q}}-E_{\mathbf{k}}}$$
$$+2|\Delta_0|^2\frac{[1-f(E_{\mathbf{k}+\mathbf{q}})-f(E_{\mathbf{k}})]}{E_{\mathbf{k}+\mathbf{q}}E_{\mathbf{k}}}\frac{\Im\left[\mathcal{D}_{mn}(\mathbf{k},\mathbf{q})\right]}{E_{\mathbf{k}+\mathbf{q}}+E_{\mathbf{k}}}$$
$$-4\pi\delta_{mn}(1-f(E_{\mathbf{k}+\mathbf{q}})-f(E_{\mathbf{k}}))\left[-u^2_{\mathbf{k}}v^2_{\mathbf{k}+\mathbf{q}}+u^2_{\mathbf{k}+\mathbf{q}}v^2_{\mathbf{k}}\right]\delta(E_{\mathbf{k}+\mathbf{q}}+E_{\mathbf{k}})\quad\Big\} \tag{346}$$

When $\omega \to 0$ the last term of Eq. 164 gives rise to a term of the form

$$(f(E_{\mathbf{k}+\mathbf{q}})-f(E_{\mathbf{k}}))\left[-u^2_{\mathbf{k}+\mathbf{q}}u^2_{\mathbf{k}}+v^2_{\mathbf{k}+\mathbf{q}}v^2_{\mathbf{k}}\right]\delta(E_{\mathbf{k}+\mathbf{q}}-E_{\mathbf{k}}).$$

Observe in this limit, however, that when $E_{\mathbf{k}+\mathbf{q}} \neq E_{\mathbf{k}}$ that the delta function vanishes and when $E_{\mathbf{k}+\mathbf{q}} = E_{\mathbf{k}}$ that the Fermi functions cancel so that this term vanishes identically.

Because the delta function is symmetric in its argument the second & fourth and the sixth & eighth terms in both real and imaginary parts of the susceptibility canceled upon setting $\omega = 0$. Note that the third term contains the factor $\delta(E_{\mathbf{k}+\mathbf{q}}+E_{\mathbf{k}})$. Since $E_{\mathbf{k}+\mathbf{q}}, E_{\mathbf{k}} \geq 0$, this term contributes only when $E_{\mathbf{k}+\mathbf{q}} = E_{\mathbf{k}} \equiv 0$.

In the BCS regime where there is a well defined Fermi surface (defined by $\epsilon_{\mathbf{k}} = \mu$) the momentum states of $\mathbf{k_1} = \mathbf{k}$ and $\mathbf{k_2} = \mathbf{k}+\mathbf{q}$ are momentum states of equal energy that are connected by the vector $\mathbf{q}$. To see this observe that when $E = 0$ that:

$$0 = E_{\mathbf{k}} = \sqrt{\xi^2_{\mathbf{k}} + \tfrac{1}{2}\mathsf{Tr}|\Delta_{\mathbf{k}}|^2}.$$

The two terms $\xi^2_{\mathbf{k}}$ and $\frac{1}{2}\mathsf{Tr}|\Delta_{\mathbf{k}}|^2$ are positive definite and so must vanish independently so that. Then

$$\xi^2_{\mathbf{k}} = 0 = (\epsilon_{\mathbf{k}}-\mu)^2$$

and $\mathbf{k}$ resides on the Fermi surface.

Furthermore since the energy $\frac{1}{2}\mathrm{Tr}|\Delta_{\mathbf{k}}|^2$ must also vanish. This implies that in the BCS limit this term contributes only for gapless symmetries (i.e., for symmetries of the order parameter where $\Delta_{mn}(\mathbf{k})$ vanishes in some places on the Fermi surface).

Altogether, only $\mathbf{k}$-states that reside on the Fermi surface contribute to this term and only for gapless symmetries. The exact same discussion follows for the entire imaginary part of the singlet susceptibility in the $\omega = 0$ limit, Eq. 335, which also contains a factor of $\delta(E_{\mathbf{k}+\mathbf{q}} + E_{\mathbf{k}})$.

E.6 The Triplet Uniform Static Spin Susceptibility: $\chi^{\mathsf{T}}_{mn}(\mathbf{q} \to \mathbf{0}, \omega \to 0)$

The last limit is the limit of the uniform spin susceptibility $\chi^{\mathsf{T}}_{mn}(\mathbf{0}, 0)$. This limit is found by taking the limit $\mathbf{q} \to \mathbf{0}$ in Eqs. 345 and 346.

$$\chi^{\mathsf{T}}_{mn}(\mathbf{0}, 0) = \lim_{\mathbf{q}\to\mathbf{0}} \chi^{\mathsf{T}}_{mn}(\mathbf{q}, 0).$$

From Eq. 345 one has:

$$\begin{aligned}\Re\left[\chi^{\mathsf{T}}_{mn}(\mathbf{0}, 0)\right] = \frac{1}{2}\mathbb{G}_{mn} \sum_{\mathbf{k}} \Bigg\{ & \\ & 2|\Delta_0|^2 \frac{\mathcal{D}_{mn}(\mathbf{k}, \mathbf{0})}{E^2_{\mathbf{k}}} \left(\frac{\partial f(E_{\mathbf{k}})}{\partial E_{\mathbf{k}}} + \frac{1 - 2f(E_{\mathbf{k}})}{2E_{\mathbf{k}}} \right) \\ & + 4\delta_{mn} \left(u^2_{\mathbf{k}} v^2_{\mathbf{k}} \frac{1 - 2f(E_{\mathbf{k}})}{E_{\mathbf{k}}} - (u^4_{\mathbf{k}} + v^4_{\mathbf{k}}) \frac{\partial f(E_{\mathbf{k}})}{\partial E_{\mathbf{k}}} \right) \quad \Bigg\}\end{aligned}$$

Substituting in for the coherence factors and using the identity for $u_{\mathbf{k}}^2 v_{\mathbf{k}}^2$:

$$\begin{aligned}\Re\Big[\chi_{mn}^{\mathsf{T}}(\mathbf{0},0)\Big] =& \frac{1}{2}\mathbb{G}_{mn}\sum_{\mathbf{k}}\Bigg\{ \\ & 2|\Delta_0|^2\frac{\mathcal{D}_{mn}(\mathbf{k},\mathbf{0})}{E_{\mathbf{k}}^2}\left(\frac{\partial f(E_{\mathbf{k}})}{\partial E_{\mathbf{k}}}+\frac{1-2f(E_{\mathbf{k}})}{2E_{\mathbf{k}}}\right) \\ & +4\delta_{mn}\left(\frac{|\Delta_0\mathbf{d}(\mathbf{k})|^2}{4E_{\mathbf{k}}^2}\left[\frac{1-2f(E_{\mathbf{k}})}{E_{\mathbf{k}}}\right]-\frac{1}{2}\left[1+\frac{\xi_{\mathbf{k}}^2}{E_{\mathbf{k}}^2}\right]\frac{\partial f(E_{\mathbf{k}})}{\partial E_{\mathbf{k}}}\right)\Bigg\}\end{aligned}$$

then using $\xi_{\mathbf{k}}^2 = E_{\mathbf{k}}^2 - |\Delta_0\mathbf{d}(\mathbf{k})|^2$

$$\begin{aligned}\Re\Big[\chi_{mn}^{\mathsf{T}}(\mathbf{0},0)\Big] =& \mathbb{G}_{mn}\sum_{\mathbf{k}}\Bigg\{ \\ & |\Delta_0|^2\frac{2|\mathbf{d}(\mathbf{k})|^2\delta_{mn}-[d_m^*(\mathbf{k})d_n(\mathbf{k})+d_n^*(\mathbf{k})d_m(\mathbf{k})]}{E_{\mathbf{k}}^2}\left(\frac{\partial f(E_{\mathbf{k}})}{\partial E_{\mathbf{k}}}+\frac{1-2f(E_{\mathbf{k}})}{2E_{\mathbf{k}}}\right) \\ & -2\delta_{mn}\frac{\partial f(E_{\mathbf{k}})}{\partial E_{\mathbf{k}}}\Bigg\}.\end{aligned}$$

From Eq. 346 one has:

$$\Im\Big[\chi_{mn}^{\mathsf{T}}(\mathbf{0},0)\Big] = 0 \tag{347}$$

The first two terms carrying $\Im\Big[\mathcal{D}_{mn}(\mathbf{k},\mathbf{0})\Big]$ vanish. The coherence factors cancel in the third term and the Fermi functions cancel in the fourth.

Appendix F

The Critical Frequencies

This section is the result of a collaboration with Robert Cherng. The main point of this section is to show how the critical frequencies that characterize both the uniform triplet susceptibility and the quasiparticle density of states was derived. The two quantities of interest have the respective forms:

$$\Im\left[\chi^{\mathsf{T}}_{mn}(\mathbf{0},\omega)\right] = 2\hbar|\omega|\mathrm{sgn}(\omega)\frac{\pi|\Delta_0|^2}{(2\pi)^3}\mathbb{G}_{mn}\frac{[1-2f(\hbar\omega/2)]}{(\hbar\omega)^2}\otimes \\ \otimes \sum_{j\,=\,1,2}\int dydz\;\Delta^2_{x_{js}}\frac{\Theta(D_{\mathsf{sym}}(y,z,\omega))}{\left|\sin(x_j)\sqrt{D_{\mathsf{sym}}(y,z,\omega)}\right|} \tag{348}$$

with

$$\Delta^2_{x_{js}} = \Big(A^2\sin^2(x_j)[\delta_{mn}-\delta_{m1}\delta_{n1}] + B^2\sin^2(y)[\delta_{mn}-\delta_{m2}\delta_{n2}] + C^2\sin^2(z)[\delta_{mn}-\delta_{m3}\delta_{n3}]\Big)$$

and

$$\mathcal{N}(\omega) = \frac{1}{2}\frac{1}{(2\pi)^3}\sum_{js}\int dydz\;\Big(|\hbar\omega| + \xi_{x_{js}}\Big)\frac{\cdot\Theta(D_{\mathsf{sym}}(y,z,\omega))}{|\sin(x_{js})\sqrt{D_{\mathsf{sym}}(y,z,\omega)}|} \tag{349}$$

It should be noted that $D_{\mathsf{sym}}(y,z,\omega_0)$ and $|\sin(x_{js})|$ are functions whose form depends on the symmetry of the order parameter. To ensure the reality of these quantities one must have

$$D_{\mathsf{sym}}(y,z,\omega) \;\geq\; 0 \tag{350}$$

$$|\cos(x_{js})| \;\leq\; 1 \tag{351}$$

where $|\sin(x_{js})| = \sqrt{1-\cos^2(x_{js})}$.

The analysis can be broken into two regimes: the low frequency and high frequency. The low frequency special points come from the function $D_{\mathsf{sym}}(y,z,\omega)$, $\mathsf{sym}=\{S,P,D\}$. More specifically, the condition that $D_{\mathsf{sym}}(y,z,\omega) \geq 0$ is used to find a further condtion on the allowed frequency:

$$D_{\mathsf{sym}}(y,z,\omega) \geq 0 \longrightarrow (\hbar\omega_0)^2 \geq G(y,z). \tag{352}$$

The expression states that for a given state (y,z) in **k**-space (actually **r**-space) the smallest the frequency $\hbar\omega_0$ can be, such that the state still contributes to $\mathcal{N}(\omega)$ or $\Im\left[\chi^{\mathsf{T}}_{mn}(\mathbf{0},\omega)\right]$, is $G(y,z)$. The special points of $G(y,z)$ are found. These points appear as kinks and extrema in the plots of Eqs. 348 & 349.

The high frequency points are derived using the fact that $|\sin(x_{js})| = \sqrt{1-\cos^2(x_{js})}$ is real $\left\{x_{js} = x_{js}(y,z,\omega_0)\right\}$. $|\cos(x_{js})|$ is defined in terms of an algebraic function which is unbounded in magnitude as $|\omega_0| \to \infty$; however, since cosine is bounded to have magnitude no greater than 1 the frequencies for which $|\cos(x_{js})| = 1$ define cut-off frequencies at the top of the energy band. Expressions 348 and 349 vanish above these frequencies.

In practice the maximal values of the expression $(\hbar\omega_0)^2 = E^2_{x_{js}}$ are found by first applying the fact that

$$\cos(x_{js})\Big|_{\hbar\omega_{0,\max}} = \pm 1 \tag{353}$$

$$\sin(x_{js})\Big|_{\hbar\omega_{0,\max}} = 0 \tag{354}$$

and then solving for the maximal values of $\hbar\omega_0$.

F.1 Low Frequency

For small frequency (i.e., $|\hbar\omega_0| \sim \omega_{0,\min}$) and assuming the quasi-one-dimensional condition ($t_x \gg t_y \gg t_z$)

$$0.2 < |\sin(x_{js})| < 0.4$$

and $|\sin(x_{js})|$ varies slowly over the entire Brillouin zone for all symmetries considered. This can be seen by considering the form of the function $D_{\mathsf{sym}}(y,z,\omega)$ on which $|\sin(x_{js})|$ depends through $\sqrt{1-\cos^2(x_{js})}$:

$$\cos(x_{js}) = \frac{-t_x f(y,z) + (-)^j \sqrt{D_{\mathsf{sym}}(y,z,\omega)}}{t_x^2 - g_{\mathsf{sym}}^2(y,z)} \tag{355}$$

$$f(y,z) = t_x \cos(x) + t_y \cos(y) + t_z \cos(z) - \mu. \tag{356}$$

$D_{\mathsf{sym}}(y,z,\omega)$ has the general form

$$D_{\mathsf{sym}}(y,z,\omega) = (\hbar\omega_0)^2 - h_{\mathsf{sym}}(y,z) \tag{357}$$

where $g_{\mathsf{sym}}(y,z)$ and $h_{\mathsf{sym}}(y,z)$ are labels for the symmetry dependent functional dependencies of $\cos(x_{js})$ and $D_{\mathsf{sym}}(y,z,\omega)$. In the very low frequency limit (i.e., $|\omega| \sim \omega_{\min}$) the number of momentum states (y,z) for which $D_{\mathsf{sym}}(y,z,\omega) \geq 0$ is small and y,z are restricted to be near certain values [for the symmetries considers these value are typically $y,z = \pm\pi$ and $y,z = 0,\pm\pi$.

Thus one can ignore $|\sin(x_{js})|$ and treat it as a constant in the low frequency limit and just consider the behavior of $D_{\mathsf{sym}}(y,z,\omega)$ in deriving the low frequency points. In particular $D_{\mathsf{sym}}(y,z,\omega) = 0$ generates bounding curves which define the regions in **k**-space that contribute to the quantities of interest. From $D_{\mathsf{sym}}(y,z,\omega) = 0$ one obtains an expression for the frequency

$$(\hbar\omega)_0^2(y,z) = G(y,z). \tag{358}$$

The task is then to find the special points (y, z) of $G(y, z)$. Plugging these points back into $G(y, z)$ yields the critical frequencies. Specific features of $\mathcal{N}(\omega)$ can be related to the values of these frequencies once found. Of note is the fact that the values of these critical frequencies correspond to changes in the geometry of the contributing regions in **k**-space (where these regions are defined by $D_{\mathsf{sym}}(y, z, \omega) \geq 0$ and bounded by $D_{\mathsf{sym}}(y, z, \omega) = 0$).

Specifically, it is observed that there exists a minimum $\hbar\omega_0$ below which the quantities of interest vanish. There are also kinks in the plots of these quantities (i.e., discontinuities in their first derivatives). Expressions for these critical frequency values are obtained for the gapped symmetries P_{x+y+z} & S and the gapless symmetries P_{y+z}, & D_{xy} symmetries.

Also, please bear in mind two facts: regarding the imaginary part of the uniform spin susceptibility in the low frequency regime only the result for the P symmetries are applicable (the susceptibility vanishes for the singlet S and D symmetries). Also, $\hbar\omega_0 = \hbar\omega/2$ when relating the following results to the susceptibility and $\hbar\omega_0 = \hbar\omega$ when relating the following results to the DOS.

F.1.1 The Gapped Symmetries

F.1.1.1 P_{x+y+z} Symmetry

The order parameter of the P_{x+y+z} symmetry has the general form $\Delta_{\mathbf{r}}^2 = \Delta_{\mathbf{0}}^2[A^2\sin^2(x) + B^2\sin^2(y) + C^2\sin^2(z)]$ (where $A^2 + B^2 + C^2 = 2$). Then $D_{P_{x+y+z}}(y, z, \omega)$ and the

corresponding expression for frequency are given by:

$$D_{P_{x+y+z}}(y,z,\omega) = A^2{\Delta_0}^2 f^2(y,z) + K\{(\hbar\omega_0)^2 - {\Delta_0}^2[A^2 + B^2\sin^2(y) + C^2\sin^2(z)]\} \geq 0 \tag{359}$$

$$(\hbar\omega_0)^2 = A_2\Delta_0^2\left[1 - \frac{f^2(y,z)}{K}\right] + K\left[B^2\cos^2(y) + C^2\cos^2(z)\right] \doteq G(y,z) \tag{360}$$

where $f(y,z) = t_y\cos(y) + t_z\cos(z) - \mu$ and $K = t_x^2 - A^2{\Delta_0}^2$. Solving for the special points:

$$\nabla G = \mathbf{0} = \begin{bmatrix} \dfrac{\partial G}{\partial y} \\ \\ \dfrac{\partial G}{\partial z} \end{bmatrix} = \left\{ \begin{array}{l} 2\Delta_0^2\sin(y)\left[\left(\dfrac{A^2t_y^2}{K} + B^2\right) + A^2t_y\dfrac{(t_z\cos(z) - \mu)}{K}\right] \\ \\ 2\Delta_0^2\sin(z)\left[\left(\dfrac{A^2t_z^2}{K} + C^2\right) + A^2t_z\dfrac{(t_y\cos(y) - \mu)}{K}\right] \end{array} \right\}$$

If one has $\sin(y), \sin(z) = 0$ which gives rise to the points $y, z = \{0, \pm\pi\}$ and the corresponding critical frequencies:

$$(\hbar\omega_{0,\min})^2 = A^2{\Delta_0}^2\left[1 - \frac{(\mu + t_y + t_z)^2}{t_x^2 - A^2{\Delta_0}^2}\right] \tag{361}$$

$$(\hbar\omega_{0,1})^2 = A^2{\Delta_0}^2\left[1 - \frac{(\mu + t_y - t_z)^2}{t_x^2 - A^2{\Delta_0}^2}\right] \tag{362}$$

$$(\hbar\omega_{0,2})^2 = A^2{\Delta_0}^2\left[1 - \frac{(\mu - t_y + t_z)^2}{t_x^2 - A^2{\Delta_0}^2}\right] \tag{363}$$

$$(\hbar\omega_{0,3})^2 = A^2{\Delta_0}^2\left[1 - \frac{(\mu - t_y - t_z)^2}{t_x^2 - A^2{\Delta_0}^2}\right]. \tag{364}$$

Then if one has $\sin(z) = 0 \neq \sin(y)$ the points $z = \{0, \pm\pi\}$ and from $\partial G/\partial y$

$$\cos(y) = -A^2t_y\frac{(t_z\cos(z) - \mu)}{A^2t_y^2 + KB^2} = -A^2t_y\frac{(\pm t_z - \mu)}{A^2t_y^2 + KB^2}$$

which produces the frequencies:

$$(\hbar\omega_{0,4})^2 = {\Delta_0}^2[A^2 + B^2] - \Delta_0^2A^2B^2\frac{(\mu + t_z)^2}{A^2t_y^2 + KB^2} \tag{365}$$

$$(\hbar\omega_{0,5})^2 = {\Delta_0}^2[A^2 + B^2] - \Delta_0^2A^2B^2\frac{(\mu - t_z)^2}{A^2t_y^2 + KB^2}. \tag{366}$$

Alternatively, if one has $\sin(y) = 0 \neq \sin(z)$ the points $y = \{0, \pm\pi\}$ and from $\partial G/\partial z$

$$\cos(z) = -A^2 t_z \frac{(t_y \cos(y) - \mu)}{A^2 t_z^2 + KC^2} = -A^2 t_z \frac{(\pm t_y - \mu)}{A^2 t_z^2 + KC^2}$$

which produces the frequencies:

$$(\hbar\omega_{0,6})^2 = {\Delta_0}^2[A^2 + C^2] - \Delta_0^2 A^2 C^2 \frac{(\mu + t_y)^2}{A^2 t_z^2 + KC^2} \tag{367}$$

$$(\hbar\omega_{0,7})^2 = {\Delta_0}^2[A^2 + C^2] - \Delta_0^2 A^2 C^2 \frac{(\mu - t_y)^2}{A^2 t_z^2 + KC^2}. \tag{368}$$

Lastly, it may be that $y, z \neq \{0, \pm\pi\}$. From $\partial G/\partial y$ and $\partial G/\partial z$ one obtains:

$$\cos(y) = A^2 C^2 \frac{t_y \mu}{A^2[t_z^2 B^2 + t_y^2 C^2] + B^2 C^2 K} \tag{369}$$

$$\cos(z) = A^2 B^2 \frac{t_z \mu}{A^2[t_z^2 B^2 + t_y^2 C^2] + B^2 C^2 K} \tag{370}$$

which yield:

$$(\hbar\omega_{0,8})^2 = \Delta_0^2[A^2 + B^2 + C^2] - \Delta_0^2 A^2 B^2 C^2 \frac{\mu^2}{A^2[t_z^2 B^2 + t_y^2 C^2] + B^2 C^2 K}. \tag{371}$$

At this point it is important to note that these nine frequencies correspond to the general P_{x+y+z} symmetry for which $A, B, C \neq 0$. Had the same analysis been performed for just the P_x symmetry with $B, C = 0$ then only the first four frequencies would be obtained. Performing the analysis for the P_{x+y} symmetry with $C = 0$ [P_{x+z} symmetry with $B = 0$] then first four frequencies plus $(\hbar\omega_{0,4})^2$ & $(\hbar\omega_{0,5})^2$ [$(\hbar\omega_{0,6})^2$ & $(\hbar\omega_{0,7})^2$] would be obtained.

F.1.1.2 S Symmetry

S symmetry has $\Delta_{\mathbf{r}}^2 = {\Delta_0}^2$ with $D(y, z, \omega)$ having the form:

$$D(y, z, \omega) = t_x^2[(\hbar\omega_0)^2 - {\Delta_0}^2] \geq 0 \tag{372}$$

$$\Rightarrow (\hbar\omega_0)^2 \geq {\Delta_0}^2 \tag{373}$$

Clearly this is a gapped symmetry since for no region of k-space contributes to $\mathcal{N}(\omega)$ for $|\hbar\omega_0| < |\Delta_0|$. However, the entire Brillouin zone contributes for $|\hbar\omega_0| \geq |\Delta_0|$. This yields only one critical value $|\hbar\omega_0| = |\Delta_0|$.

F.1.2 The Gapless Symmetries

F.1.2.1 P_{y+z} Symmetry

The P_{y+z} symmetry has $\Delta_r^2 = {\Delta_0}^2[B^2\sin^2(y) + c^2\sin^2(z)]$. $D_{P_{y+z}}(y,z,\omega)$ has the form:

$$D_{P_{y+z}}(y,z,\omega) = t_x^2\left((\hbar\omega_0)^2 - t_x^2{\Delta_0}^2[B^2\sin^2(y) + c^2\sin^2(z)]\right) \geq 0 \qquad (374)$$

$D_{P_{y+z}}(y,z,\omega) = 0$ generates bounding curves which define the regions in k-space that contribute. From $D_{P_{y+z}}(y,z,\omega) = 0$ one obtains an expression for the frequency:

$$(\hbar\omega_0)^2 = G(y,z) \qquad (375)$$

with $G(y,z) \doteq B^2\sin^2(y) + C^2\sin^2(z)$. The special points of G are:

$$\nabla G = 0 = \begin{bmatrix} B^2\sin(2y) \\ C^2\sin(2z) \end{bmatrix} \qquad (376)$$

where the gradient vanishes for $y,z = \left\{0, \pm\frac{\pi}{2}, \pm\pi\right\}$. This yields four values of $\hbar\omega_0$:

$$(\hbar\omega_{0,\min})^2 = 0 \qquad (377)$$

$$(\hbar\omega_{0,1})^2 = {\Delta_0}^2B^2 \qquad (378)$$

$$(\hbar\omega_{0,2})^2 = {\Delta_0}^2C^2 \qquad (379)$$

$$(\hbar\omega_{0,3})^2 = {\Delta_0}^2[B^2 + C^2] \qquad (380)$$

For $C = 0$ (or $B = 0$) one obtains the P_y (P_z) case. In this case, instead of pockets of initial contributions one has bands at the middle and edges of the 1^{st} B.Z. that extend across the $\widehat{3}$ ($\widehat{2}$) directions in k-space. For $(\hbar\omega_0)^2 > (\hbar\omega_{0,3})^2$, the entire Brillouin zone contributes to $\mathcal{N}(\omega)$.

F.1.2.2 D_{xy} Symmetry

The D_{xy} symmetry has $\Delta_r^2 = {\Delta_0}^2\sin^2(x)\sin^2(y)$ with $D_{D_{xy}}(y,z,\omega)$ having the form:

$$D_{D_{xy}}(y,z,\omega) = {\Delta_0}^2\sin^2(y)f^2(y,z) + K(y)[(\hbar\omega_0)^2 - {\Delta_0}^2\sin^2(y)] \geq 0 \qquad (381)$$

$$\hbar\omega_0^2(y,z) = {\Delta_0}^2\sin^2(y)\left[1 - \frac{f^2(y,z)}{K(y)}\right] \qquad (382)$$

Where $f(y,z) = t_y \cos(y) + t_z \cos(z) - \mu$ and $K(y) = t_x^2 - {\Delta_0}^2 \sin^2(y)$. Since $|t_x| \gg |\Delta_0|$, the variation of $K(y)$ is negligible: $K(y) \approx t_x^2$. Using this approximation, we define

$$(\hbar\omega_0)^2 \approx \sin^2(y)\left[1 - \frac{f^2(y,z)}{t_x^2}\right] \doteq G(y,z) \tag{383}$$

which yields the following special points:

$$\nabla G = \mathbf{0} = \left\{ \begin{array}{c} \frac{\partial G}{\partial y} \\ \\ \frac{\partial G}{\partial z} \end{array} \right\} = \left[\begin{array}{c} 2\sin(y)\left\{\cos(y)\left[1 - \frac{f^2(y,z)}{t_x^2}\right] + \sin^2(y)\frac{t_y f(y,z)}{t_x^2}\right\} \\ \\ 2\sin^2(y)\sin(z)\frac{t_z f(y,z)}{t_x^2} \end{array} \right]$$

One has $\sin(y) = 0$, $\sin(z) = 0$ (so that $\hbar\omega_{0,\min} = 0$ is one of the frequencies) and a cubic equation for $\cos(y)$ from the expression in brackets for $\frac{\partial G}{\partial y}$:

$$-2\alpha^2\cos^3(y) - 3\alpha\beta\cos^2(y) + [1 + \alpha^2 - \beta^2]\cos(y) + \alpha\beta = 0 \tag{384}$$

where $\alpha = \frac{t_y}{t_x}$, $\beta = \frac{t_z\cos(z) - \mu}{t_x}$ $z = \{0, \pm\pi\}$. We solve for the roots of Eq. 384 satisfying $|\cos(y)| \leq 1$ as follows:

$$\cos(\theta) = \beta(\alpha^2 - 1)\left(\frac{3}{2 + 2\alpha^2 + \beta^2}\right)^{\frac{3}{2}} \tag{385}$$

$$\cos(y) = \frac{1}{\alpha}\left[\sqrt{\frac{2 + 2\alpha^2 + \beta^2}{3}}\cos\left(\frac{\theta + 4\pi}{3}\right) - \frac{\beta}{2}\right] \tag{386}$$

This yields three distinct $\hbar\omega_0$ values:

$$(\hbar\omega_{0,\min})^2 = 0 \tag{387}$$

$$(\hbar\omega_{0,1})^2 \approx A^2B^2{\Delta_0}^2[1 - \cos^2(y_1)]\{1 - [\alpha\cos(y_1) + \beta_1]^2\} \tag{388}$$

$$(\hbar\omega_{0,2})^2 \approx A^2B^2{\Delta_0}^2[1 - \cos^2(y_2)]\{1 - [\alpha\cos(y_2) + \beta_2]^2\} \tag{389}$$

Where $\alpha = \frac{t_y}{t_x}$, $\beta_1 = \frac{t_z - \mu}{t_x}$, $\beta_2 = \frac{-t_z - \mu}{t_x}$ and $\cos(y_1)$ is given by equation 386 with $\beta = \beta_1$ while $\cos(y_2)$ is given by the same equation with $\beta = \beta_2$.

The qualitative behavior for the D_{xy} symmetry is approximately the same as in the P_y case except at high $\hbar\omega_0$.

The symmetry is also gapless since $\omega_{0,\min} = 0$.

F.2 High Frequency

In the high frequency limit $|\hbar\omega| \gg \Delta_0$ the value of the DOS and uniform electron spin susceptibility is moderated by the $|\sin(x_j)|$ factor which appears in the integrals Eq. 348 and Eq. 349. This is because of how $\sin(x_j)$ is defined:

$$\begin{aligned} \left|\sin(x_{jS})\right| &= \sqrt{1-\cos^2(x_{jS})} \\ \cos(x_{jS}) &= \frac{-t_x f(y,z) + (-)^j \sqrt{D_{\mathsf{sym}}(y,z,\omega)}}{t_x^2 - g_{\mathsf{sym}}^2(y,z)} \end{aligned} \tag{390}$$

Inspection of $D_{\mathsf{sym}}(y,z,\omega_0)$ in the previous section shows that it grows without bound as ω_0 grows. However, sine and cosine are to be bounded in magnitude by 1. As $|\sin(x)|$ is given by the right hand side of the expression above, an upper bound on the magnitude of ω_0 must be imposed. This upper bound, $\omega_{\max}$, on frequency corresponds to the maximum value of the energy $E_{\mathbf{r},\omega_0}$ and leads to the condition $\mathcal{N}(\omega_0 > \omega_{\max}) \equiv 0$, $\Im\left[\chi^{\mathsf{T}}_{mn}(\mathbf{0},\omega_0 > \omega_{\max})\right] \equiv 0$.

Although not shown, a plot of the of the quantities of interest for the individual $j = 1$ and $j = 2$ terms reveals a sharp cut-off frequency whose location depends on j: there can be two cut-offs $\omega_{\max,j=1}$ and $\omega_{\max,j=2}$. The analysis of these cut-offs will reveal that

$$\hbar\omega_{0,\max,j=1} = 2|t_x + t_y + t_z + \mu| \tag{391}$$

$$\hbar\omega_{0,\max,j=2} = 2|t_x + t_y + t_z - \mu|. \tag{392}$$

While the DOS and susceptibility are continuous over most of the interval $[|\Delta_0|, \omega_{\mathbf{0},\max,j=1}]$ they have a discontinuity in their first derivative at $\omega_{0,\max,j=2} = |t_x + t_y + t_z - \mu|/\hbar$ where the $j = 2$ term stops contributing to the integral. They continue to decrease smoothly in value until $\omega = \omega_{0,\max,j=1}$ where it vanishes and experiences another discontinuity in the first derivative.

The analysis to find the high frequency cut-offs $\hbar\omega_{\mathbf{0}}, \max, j = 1$ & $\hbar\omega_{\mathbf{0}}, \max, j = 2$ is now undertaken. Again these frequencies correspond to the maximum of the excitation energy

$$E_{\mathbf{r}}^2 = (t_x \cos(x) + t_y \cos(y) + t_z \cos(z) - \mu)^2 + |\Delta_{\mathbf{r}}|^2. \tag{393}$$

Earlier it was seen that the uniform triplet susceptibility and the DOS are written in their most general form in terms of a three dimensional integral (in **k**-space) which is first integrated along the x direction. For the symmetries discussed, sym=$\{S, P, D\}$, $\cos(x)$ has the general form

$$\cos(x_{js}) = \frac{-t_x f(y,z) + (-)^j \sqrt{D_{\mathsf{sym}}(y,z,\omega)}}{t_x^2 - g_{\mathsf{sym}}^2(y,z)} \tag{394}$$

$$f(y,z) = t_x \cos(x) + t_y \cos(y) + t_z \cos(z) - \mu \tag{395}$$

$$D_{\mathsf{sym}}(y,z,\omega) = (\hbar\omega_{\mathbf{0}})^2 - h_{\mathsf{sym}}(y,z) \tag{396}$$

where $g_{\mathsf{sym}}(y,z)$ and $h_{\mathsf{sym}}(y,z)$ are labels for the symmetry dependent functional dependencies of $\cos(x_{js})$ and $D_{\mathsf{sym}}(y,z,\omega)$. The point is that $D_{\mathsf{sym}}(y,z,\omega)$, and the right hand side of $\cos(x_{js})$ are unbounded as $\hbar\omega \to \infty$. However, depending on whether $j = 1$ or 2 there are frequencies for which the right hand side of $\cos(x_{js})$ equals one in magnitude.

So it is desirable to maximize the function

$$(\hbar\omega_{\mathbf{0}})^2 = (t_x \cos(x_{js}) + t_y \cos(y) + t_z \cos(z) - \mu)^2 + |\Delta_{\mathbf{r}}|^2 \tag{397}$$

under the constraint that $\cos(x_{jS}) = \alpha = \pm 1$ so that

$$(\hbar\omega_0)^2 \to (\alpha t_x + t_y\cos(y) + t_z\cos(z) - \mu)^2 + \delta_{S,\text{sym}}\Delta_0^2 + \delta_{D,\text{sym}}\Delta_0^2\sin^2(x_{jS})\sin^2(y) + \delta_{P,\text{sym}}\Delta_0^2[A^2\alpha^2 + B^2\sin^2(y) + C^2\sin^2(z)]$$

and using the fact that when $|\cos(x)| = 1$, $\sin(x) = 0$:

$$(\hbar\omega_0)^2 = (\alpha t_x + t_y\cos(y) + t_z\cos(z) - \mu)^2 + \delta_{S,\text{sym}}\Delta_0^2 + \delta_{P,\text{sym}}\Delta_0^2[A^2\alpha^2 + B^2\sin^2(y) + C^2\sin^2(z)] \tag{398}$$

First note that depending whether sym $= \{S, P, D\}$ the appropriate form of the gap function contributes. Secondly, the gap for the D symmetry has vanished under the constraint so that $(\hbar\omega_0)^2$ differs by only a constant between the S and D symmetries.

Maximizing:

$$\left\{\begin{array}{c} \frac{\partial(\hbar\omega_0)^2}{\partial y} \\ \\ \frac{\partial(\hbar\omega_0)^2}{\partial z} \end{array}\right\} = \left[\begin{array}{l} -2\sin(y)\left[t_y(\alpha t_x + (t_z\cos(z) - \mu)) + (t_y^2 - \delta_{P,\text{sym}}B^2\Delta_0^2)\cos(y)\right] \\ \\ -2\sin(z)\left[t_z(\alpha t_x + (t_y\cos(y) - \mu)) + (t_z^2 - \delta_{P,\text{sym}}C^2\Delta_0^2)\cos(z)\right] \end{array}\right] \equiv 0$$

with zeros at:

$$y, z = \{0, \pm\pi\}$$

$$\left\{\ \cos(y) = -\frac{C^2t_y[\alpha t_x - \mu]}{B^2t_z^2 + C^2t_y^2 - B^2C^2\Delta_0^2},\quad \cos(z) = -\frac{B^2t_z[\alpha t_x - \mu]}{B^2t_z^2 + C^2t_y^2 - B^2C^2\Delta_0^2}\ \right\}$$

where the second set of zeros apply only to the P symmetry. Using the fact that $|\mu| \sim |t_x| \gg |t_y| \gg |t_z|$ the second derivate test shows that the point $(y, z) = (0, 0)$ maximizes $(\hbar\omega_0)^2$ when $\alpha = 1$ and $(y, z) = (\pi, \pi)$ maximizes $(\hbar\omega_0)^2$ when $\alpha = -1$ yielding:

$$(\hbar\omega_{0,\text{max},j=1})^2 = (t_x + t_y + t_z + \mu)^2 + \delta_{\text{sym},S}\Delta_0^2 \quad \alpha = -1 \tag{399}$$

$$(\hbar\omega_{0,\text{max},j=2})^2 = (t_x + t_y + t_z - \mu)^2 + \delta_{\text{sym},S}\Delta_0^2 \quad \alpha = 1 \tag{400}$$

One may make the association of $\alpha = -1$ with $j = 1$ and $\alpha = 1$ with $j = 2$ by considering the form of $\cos(x_{jS})$. Using the fact that $|\mu| \sim |t_x| \gg |t_y| \gg |t_z|$

$$-t_x f(y,z) = t_x(\mu - t_y \cos(y) - t_z \cos(z)) > 0$$

which is positive definite since $\mathrm{sgn}(t_x) = \mathrm{sgn}(\mu)$. If $j = 1$ the numerator of $\cos(x_{jS})$ can be positive for small frequency but as $(\hbar\omega_0)^2$ grows, $\cos(x_{jS})$ goes negative; however, if $j = 2$ $\cos(x_{jS})$ is positive definite and reaches the value 1 before the $j = 1$ root reaches -1. Therefore, $(\hbar\omega_{0,\mathrm{max},j=1})^2 > (\hbar\omega_{0,\mathrm{max},j=2})^2$.

Bibliography

[1] *For an illustration see* T. Ishiguro and K. Yamaji, *Organic Superconductors*, pages 36-37, (Springer-Verlag, Berlin, 1990).

[2] I. J. Lee, M. J. Naughton, G. M. Danner, and P. M. Chaikin, Phys. Rev. Lett. **78**, 3555 (1997).

[3] S. Belin and K. Behnia, Phys. Rev. Lett. **79**, 2125 (1997).

[4] I. J. Lee, D. S. Chow, W. G. Clark, J. Strouse, M. J. Naughton, P. M. Chaikin, and S. E. Brown, (private communication with Lee, pending publication of data)

[5] *The Pauli paramagnetic limit is discussed in* A. M. Clogston, *Phys. Rev. Lett.* **9**, 266 (1962); B. S. Chandrasekhar, *Appl. Phys. Lett.* **1**, 7 (1962).

[6] B. S. Chandrasekhar, Appl. Phys. Lett. **1**, 7 (1962).

[7] Y. Hasegawa and H. Fukuyama, J. Phys. Soc. Jpn. **56**, 877 (1987).

[8] K. B. Efetov and A. I. Larkin, Sov. Phys. JETP **41**, 76 (1975).

[9] A. A. Abrikosov, *J. Low Temp. Phys.* **53**, 359 (1983).

[10] L. P. Gorkov and D. Jerome, J. Phys. (Paris) Lett. **46**, L643 (1985).

[11] A. G. Lebed, JETP Lett. **44**, 114 (1986)

[12] L. N. Burlachkov et al., Europhys. Lett. **4**, 941 (1987).

[13] N. Dupuis, G. Montambaux, and C. A. R. Sá de Melo, Phys. Rev. Lett. **70**, 2613 (1993).

[14] C. D. Vaccarella and C. A. R. Sá de Melo, Phys. Rev. B **64**, 212504 (2001)

[15] B. Lussier, B. Ellman and L. Taillefer, Phys. Rev. Lett. **73,** 3294 (1994).

[16] M. Tinkham, *Introduction to Superconductivity*, 2nd ed., McGraw-Hill Publ. (1996)

[17] L. N. Cooper, Phys. Rev. **104**, 1189 (1956)

[18] G. D. Maham, *Many-Particle Physics*, 2nd ed., Plenum Publ. (1990)

[19] V. P. Mineev and K.V. Samokhin, *Introduction to Unconventional Superconductivity*, Gordan and Breech Publ. (1999)

[20] M. Sigrist and K. Ueda, Rev. Mod. Phys. **63**, No.2, 239 (1991)

[21] C. P. Slichter, *Principles of Magnetic Resonance*, 2nd. Ed., Springer Verlag Publ. (1978)